The Origins of Electrical Discharge Patterns in the Main Olfactory Bulb of the Rat.

Jayne R. Bramley

A dissertation submitted to the University of Edinburgh for the degree of Doctor of Philosophy

July 2000

Declaration

The studies outlined in this thesis were undertaken in the Department of Biomedical Sciences, University Medical School, Edinburgh under the supervision of Professor Gareth Leng. This dissertation has not been submitted for any other qualification at any other university. All of the work contained in this thesis was performed by the author unless indicated otherwise.

Jayne R. Bramley

July, 2000

ACKNOWLEDGEMENTS.

I would like to thank my supervisors Professor Gareth Leng and Professor John Russell for all their help and guidance throughout my three years in Edinburgh and I thank everybody in the laboratory for making my time in Edinburgh such an enjoyable experience.

Many thanks go to Dr Mayank Dutia and Dr Alex Johnston for all their invaluable advice, and expertise of *in vitro* electrophysiology. I am grateful to Dr Colin Brown for his assistance in the surgical preparation of morphine tolerant animals, and to Dr Alex Bailey for his assistance with intracardial perfusions and Fos immunocytochemistry. Thanks to the occupants of the postgraduate office; Ped Srisawat, Arleta Reif-Marganiec, Jack Somponpun and others for their friendship. Special thanks go to Dina Sidhva and Sorapun Vorapon, for being brilliant flatmates; and even better cooks, and to Gail Valler, Jill Edwards and Dr Sinéad Scullion for always being there with a supporting shoulder.

A big thank you to David, for his tireless patience and support from across the ocean, and finally, I must thank my parents and grandparents for all their love and encouragement; I could not have done it without them.

I dedicate this thesis to my Grandfather
who has been a tremendous source of knowledge
and inspiration throughout my life.

Following his advice I have kept smiling
through this challenging time.

AChE	acetylcholine esterase
aCSF	artificial cerebrospinal fluid
AMPA	α-amino-3-hydroxy-5-methyl-4-isoxazole propionic acid
AOB	accessory olfactory bulb
APV	D-2-amino-5-phosphonovalerate
b/w	body weight
cAMP	cyclic adenosine monophosphate
CNQX	6-Cyano-7-nitroquinoxaline-2,3-dione
CNS	central nervous system
DAB	diaminobenzidine
EFP	evoked field potential
EPL	external plexiform layer
EPSP	excitatory post synaptic potential
FG	Fluoro-Gold
GABA	gamma aminobutyric acid
GAD	glutamic acid decarboxylase
GTP	guanosine triphosphate
h	hours
HDB	horizontal limb of the diagonal band
ICC	immunocytochemistry
i.c.v.	intracerebroventricular
i.d.	inner diameter
INTH	interspike interval time histogram
i.p.	intraperitoneal
IPSP	inhibitory post synaptic potential
IPSC	inhibitory post synaptic current
i.v.	intravenous
LHRH	luteinizing hormone-releasing hormone
LOT	lateral olfactory tract

MCL	mitral cell layer
Met-ENK	methionine-enkephalin
MOB	main olfactory bulb
MOR	morphine sulphate
mRNA	messenger ribonucleic acid
NLX	Naloxone
NMDA	N-methyl-D-aspartate
NSS	normal sheep serum
o.d.	outer diameter
ON	olfactory nerve
p	probability
PB	phosphate buffer
PB-T	phosphate buffer with Triton
Pir	piriform cortex
PVN	paraventricular nucleus
S.E.M.	standard error of the mean
SON	supraoptic nucleus
TEA	tetraethylammonium chloride
TTX	tetrodotoxin

Landmark discoveries made in the olfactory bulb have formed the basis of much of our understanding of other brain regions. In fact, it was in the olfactory bulb that the first example of a dendrodentritic synapse in the mammalian central nervous system was found. The olfactory bulb is rich in a diverse selection of neurotransmitters, and with the bonus that the bulb is relatively easy to access, it provides an excellent model in which to study neural networks.

The aim of this PhD project was to study the neural pathway that is thought to connect the olfactory bulb to the supraoptic nucleus of the hypothalamus. To understand the input to the supraoptic nucleus from the olfactory system we sought to determine the discharge frequency and firing pattern of the output neurones, mitral cells. The electrical activity of single neurones was recorded extracellularly from the olfactory bulb of anaesthetised rats. Mitral cells were identified electrophysiologically by antidromic activation following stimulation of the lateral olfactory tract and observation of bulbar field potentials. It became apparent that the mitral cells consistently showed a spontaneous patterned discharge that has not been previously reported and we have described this pattern in terms of three separate levels of bursting behaviour.

What we have termed the 'gross' phasic pattern was displayed by all mitral cells and consisted of a characteristic slow, cyclic firing pattern with peaks of activity occurring with a constant periodicity, burst lengths lasted for approximately two minutes with equal periods of quiescence separating the bursts. Some mitral cells (53%) show distinct silent periods between bursts of high activity others (47%) simply show a reduced rate of activity between bursts. Auto-correlation plots show that within this overall phasic pattern is a respiratory driven bursting activity, the activity of mitral cells increases during the inspiratory phase as air is drawn over the olfactory receptors in the nasal mucosa. Plotting the instantaneous frequency of mitral cell activity reveals the third bursting pattern, exhibited by 57% of mitral cells recorded. This shows that during each long burst of activity the mitral cell fires at

two distinct frequencies, the lower frequency is in the range 0-50Hz and the high frequency firing is in the range 100-250Hz. In 84% of the bursts that showed two distinct firing frequencies there was a delay in the onset of the higher frequency mode, at the start of each peak of activity. Mitral cells have been shown to be capable of initiating and propagating action potentials from their distal dendrites, as well as from the conventional initiation site at the soma-axon hillock region. It is proposed in this thesis that the high frequency firing mode described might be generated in the mitral cell dendrites.

The mitral cell is involved in complex interactions with both neighbouring mitral cells and granule cells that provide for lateral and reciprocal inhibition respectively. Granule cells are the most numerous of the various types of interneurone in the bulb and their firing pattern was found to be non-phasic and at only one frequency mode. Following stimulation of the lateral olfactory tract mitral cells exhibited a period of inhibition following the stimulus pulse. This is consistent with the general consensus that upon activation, mitral cells activate granule cells, which in turn feedback to inhibit the mitral cells (reciprocal inhibition). Extracellular recordings of mitral cell activity were also made in a slice preparation of the olfactory bulb. It was discovered that *in vitro* the mitral cells did not discharge in a slow, phasic pattern and the high frequency firing seen *in vivo* was not evident. During the slice preparation many of the long lateral dendrites of the mitral cells are unavoidably removed and this may disturb the local interactions and thereby alter the discharge pattern.

Once the discharge pattern of olfactory neurones was determined these parameters were then used as a basis for the stimulation of the lateral olfactory tract and the effect on supraoptic neurone activity determined by studying the distribution of Fos-positive cells. Two stimulation protocols were used both were strong stimuli applied unilaterally, in different formats. The first was a short burst at a high frequency to mimic an acute, strong output from the olfactory bulb and the second

was a prolonged stimulation used to disrupt the output discharge pattern. The literature suggests that the connection between the olfactory bulb and the supraoptic nucleus is unilateral, monosynaptic and terminates in the ventro-lateral dendritic region of the supraoptic nucleus. Following prolonged stimulation of the lateral olfactory tract there was a significant increase ($p<0.01$) in Fos expression in the supraoptic nucleus on both the ipsilateral and contralateral sides which suggests that the pathway between the olfactory bulb and the supraoptic nucleus may be more complex than initially thought. Areas of the brain known to receive strong olfactory input, such as the piriform cortex, showed a unilateral increase in Fos expression following the brief pulse of stimulation.

Administration of morphine during parturition interrupts the progress of parturition by inhibiting oxytocin release. The olfactory bulb is highly active at the time of parturition and shows dense expression of mu- and kappa opioid receptors, and so the possibility that morphine may impair oxytocin release in part by blocking the input from the olfactory bulb was considered. The effect of morphine and its antagonist, naloxone on the discharge pattern of mitral cells was studied in both the *in vivo* and *in vitro* preparations. *In vivo* morphine was seen to have a subtle effect in that it inhibited the high frequency firing but did not significantly alter the overall firing rate or periodicity of bursts, this effect was irreversible. However, *in vitro* morphine fully inhibited mitral cell activity which returned to pre-morphine rates following the administration of naloxone. The discrepancy between the two sets of data may be a dose issue. *In vivo* the drugs were administered via an intravenous route which may have led to a reduced concentration of the drug evoking a response from the mitral cells compared to the concentration of the drug that the mitral cells in vitro were exposed to. It may also be due to the reduced local circuitary of the mitral cell in the *in vitro* preparation, causing the mitral cell to become more susceptible to the effects of morphine.

Chapter 1

General Introduction

1.1 An overview of the olfactory system

The olfactory sensory system is split into two major divisions, the vomeronasal and olfactory pathways that are functionally and anatomically distinct. The sensory receptors of the vomeronasal system are located in the vomeronasal organ that is encased in a cartilaginous capsule at the base of the nasal septum and which opens via a duct into the nasal cavity. The receptors of the olfactory pathway are found in the mucosa of the nasal epithelium. The vomeronasal receptor neurones possess apical microvilli, whereas the main olfactory receptors have cilia at their receptive area on the epithelium. The vomeronasal system is involved in the detection of pheromones, and the main olfactory pathway detects environmental cues. Both types of chemosensory receptor send axons, grouped in distinct fasicles, up the nasal cavity where they bundle together to form the vomeronasal and olfactory nerves. The nerve fibres penetrate the cribiform plate and terminate in the olfactory lobes, located at the rostral pole of the telencephalon.

The olfactory bulb is split into two parts, the main olfactory bulb (MOB) and the accessory olfactory bulb (AOB). The vomeronasal nerves run between the main olfactory lobes and enter the AOB at the posterior dorsal aspect of the MOB, terminating exclusively in the AOB. Whereas the olfactory nerves terminate solely in the MOB. Odour information is processed via the AOB in parallel with the main olfactory system. The cytoarchitecture and synaptic organisation are very similar between the two parts of the bulb, although the laminar organisation in the AOB is less distinct.

A major difference between the MOB and the AOB is their projection sites: the AOB projects to regions of the amygdala that do not receive afferents from the MOB. These amygdaloid nuclei in turn project to the medial preoptic area and the medial hypothalamus, regions of the central nervous system that are implicated in the regulation and modulation of reproduction and aggression. The output of the AOB is

to the medial anterior, medial posterior, and posterior cortical nuclei of the amygdala. From here the output from the AOB is directed to the basal forebrain via the stria terminalis and ventral pathways terminating in regions such as the bed nucleus of the stria terminalis, medial preoptic area, ventromedial hypothalamus, and the mammillary complex (Kevetter and Winnans, 1981b). The accessory pathway is thought to be involved in the perception of chemical stimuli of a social nature. These stimuli have the potential to; induce hormonal changes, affect the success of pregnancy, alter the course of puberty, modulate female cyclicity and ovulation, elicit courtship and attraction and modulate reproductive behaviour and aggression (Keverne, 1995).

Projections from the MOB to the amygdala consist of pathways to the anterior cortical and posterolateral cortical nuclei. Efferents from these parts of the amygdala are much more extensive than in the vomeronasal system, projecting to the mediobasal hypothalamus and the bed nucleus of the stria terminalis (in different regions to the vomeronasal connections) via the stria terminalis. The MOB also sends efferents to the amygdalo-hippocampal area and the primary olfactory cortex. The primary olfactory cortex is easily differentiated from the thicker and structurally more complex neocortical areas around it. The olfactory cortex has relatively little radial or columnar organisation and relies on its associational areas, a collection of structures including the piriform cortex, the anterior olfactory nucleus, the entorhinal cortex, the infralimbic cortex and the olfactory tubercle, for the processessing of olfactory information. There are regional differences in the projection from the MOB, the ventral portion projects more heavily to the medial and posterior parts of the olfactory tubercle than does the dorsal part of the bulb. The cortical regions that are involved in the olfactory and accessory olfactory systems are shown in figure 1.1.

One projection from the olfactory amygdala that may be particularly important is to the vomeronasal parts of the amygdala. This is the first point in the

vomeronasal pathway where ascending olfactory information can interact with vomeronasal inputs (Kevetter and Winnans, 1981a). Electrophysiological evidence suggests that single cells in this region receive inputs from both chemosensory systems (Licht and Meredith, 1985).

Figure 1.1. Schematic diagrams to show the areas that comprise the olfactory cortex and the pathway from the olfactory bulb to these associational areas.

A) Maps of the olfactory and accessory olfactory cortical areas, drawn on the ventral surface of the brain (in the centre) and on an 'unfolded' equal surface area projection of the cortex (right). The margins of the lateral olfactory tract are indicated by the dashed line (adapted from; Neurobiology of Taste and Smell, Finger and Silver, 1987).

Abbreviations: Al (v/d/v), agranular insular cortex (ventral/dorsal/posterior); AOB, accessory olfactory bulb; AON (d/e/l/m/vp), anterior olfactory nucleus (dorsal/external/lateral/medial/ventroposterior); Coa, anterior cortical nucleus of the amygdala; Cop, posterior cortical nucleus of the amygdala; DLEA, dorsolateral entorhinal area; DPC, dorsal peduncular cortex; IL, infralimbic cortex; LEA, lateral entorhinal area; LOT, lateral olfactory tract; Me, medial nucleus of the amygdala; NLOT, nucleus of the lateral olfactory tract; OB, olfactory bulb; OT, olfactory tubercle; PAC, periamygdaloid cortex; PC(a/p) piriform cortex (anterior/posterior); Pr, perirhinal area; TT(v/t), tenia tecta (ventral/dorsal); VLEA, ventrolateral entorhinal area; VMEA, ventromedial entorhinal area;

B) Diagram of the olfactory pathway in the rodent and its main connections with central systems (taken from Halász and Shepherd, 1983).

Abbreviations: AON, anterior olfactory cortex; AM, amygdala; g, granule cell; GL, glomerular layer; EPL, external plexiform layer; HIPPO, hippocampus; HYPO, hypothalamus; m, mitral cell; on, olfactory nerves; OT, olfactory tubercle; PC, piriform cortex; pg, periglomerular cell; SEP-DB, region of septum and diagonal band; TER, transitional entorhinal cortex; THAL, thalamus.

[A]

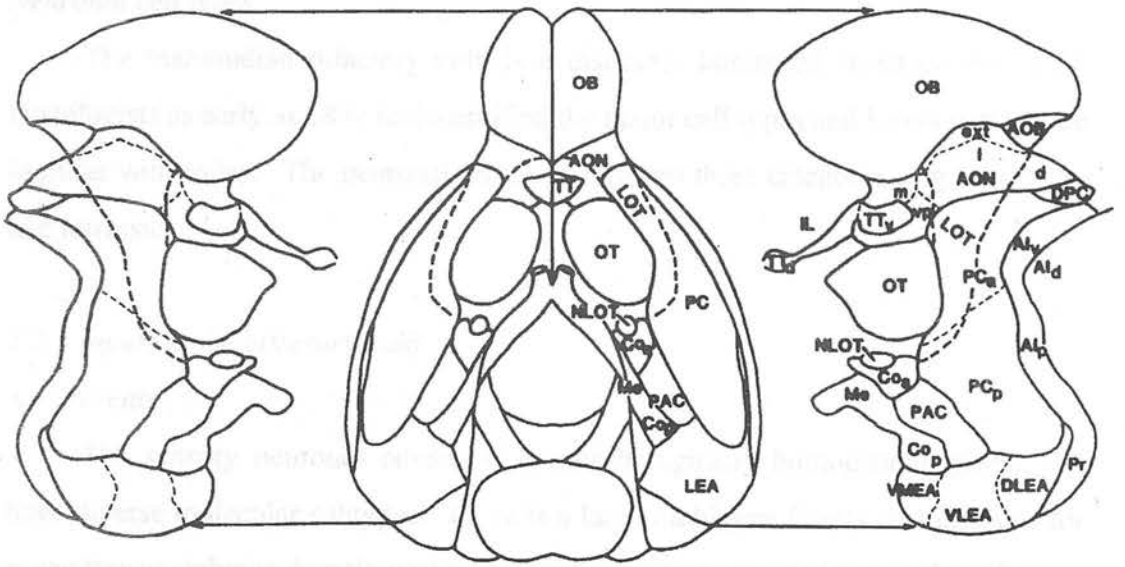
OB
AON
TT
LOT
OT
PC
NLOT
Co
Me
PAC
LEA
OB
AOB
ext
AON
d
DPC
m
TT
vm
IL
LOT
OT
PC
NLOT
Co
Me
PAC
PC
Co
VMEA
DLEA
VLEA
Pr

[B]

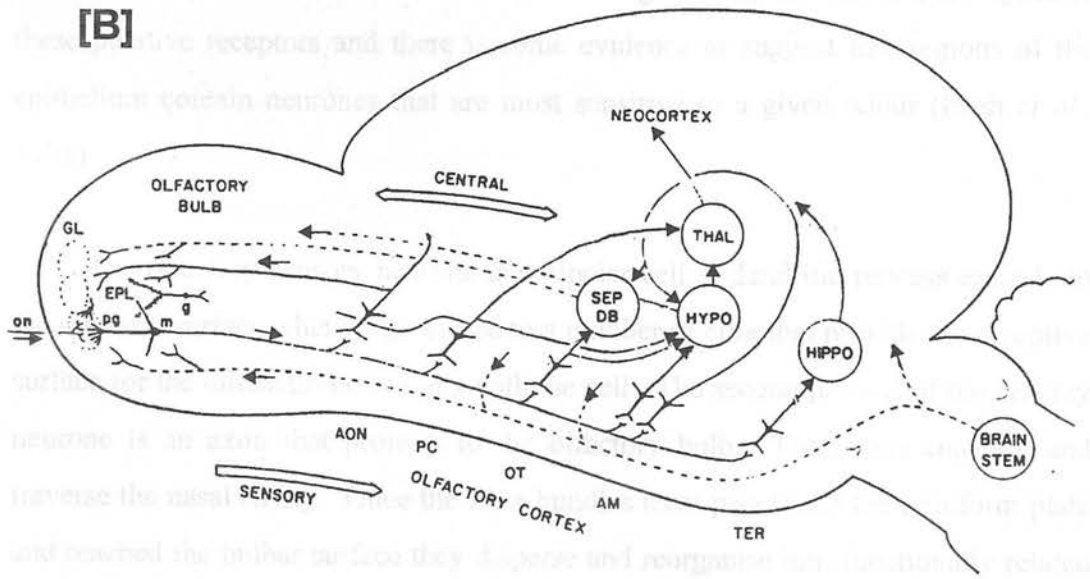
NEOCORTEX
OLFACTORY BULB
CENTRAL
GL
EPL
pg
m
g
on
THAL
SEP DB
HYPO
HIPPO
BRAIN STEM
AON
PC
OT
AM
SENSORY
OLFACTORY CORTEX
TER

1.2 Organisation of the olfactory bulb

Neuronal cell types

The mammalian olfactory bulb is a distinctly laminated structure (fig. 1.2). Histologists as early as 1891 had identified the major cell types and layers that we are familiar with today. The neuronal elements fall into three categories: input, output, and intrinsic.

1.2.1 Inputs to the olfactory bulb

A) Afferents

The sensory neurones consist of a morphologically homogenous group, but have diverse molecular subtypes. There is a large multigene family that encodes for seven transmembrane domain proteins, whose expression is restricted to the olfactory epithelium. Eighteen different members of this family of proteins have been cloned (Buck and Axel, 1991) and it is thought that these are likely to encode individual odourant receptors. Individual neurones are thought to express one or a few types of these putative receptors and there is some evidence to suggest that regions of the epithelium contain neurones that are most sensitive to a given odour (Ezeh *et al.*, 1995).

The olfactory sensory neurone is a bipolar cell; a dendritic process extends to the mucosal surface where it gives rise to a number of cilia that provide the receptive surface for the interaction of odours with the cell. The second process of the sensory neurone is an axon that projects to the olfactory bulb. The axons coalesce and traverse the nasal cavity. Once the fibre bundles have penetrated the cribiform plate and reached the bulbar surface they disperse and reorganise into functionally related subsets (Treloar *et al.*, 1996). *In situ* hybridisation studies have shown that the mRNA for a given olfactory receptor can be found in one or a few glomeruli (Mombaerts *et al.*, 1996). This does not exclude the possibility that a glomerulus contains terminals from neurones expressing differing receptor subtypes (Treloar *et*

al., 1996), but it does suggest that the reorganised axon bundles converge on specific glomerular targets. An important feature of the sensory neurones within the olfactory system is their continuous renewal from stem cells in the epithelium throughout adult life (Graziadei and Monti-Graziadei, 1979). The specificity of synaptic connections in the glomeruli is maintained despite this constant turnover of the sensory terminals, (Singer *et al*, 1995).

Exposure of isolated cilia from rat olfactory epithelium to various odourants leads to the rapid activation of adenyl cyclase and increased levels of cAMP in the dendritic membranes of olfactory sensory neurones (Pace *et al.*, 1985; Sklar *et al.*, 1986; Breer *et al.*, 1990; Boekhoff *et al.*, 1990). The activation of adenyl cyclase is dependent on GTP and is therefore likely to be mediated by G-proteins. Elevations in cAMP are thought to initiate the depolarisation of olfactory neurones by activation of a cation permeable channel that allows for alterations in the membrane potential (Nakamura and Gold, 1987).

B) Centrifugal inputs

The olfactory bulb receives numerous centrifugal inputs and is under extensive and highly differentiated control by the brain. Extensive connections are made by fibres from the anterior olfactory nucleus, and also by axon collaterals from pyramidal neurones in the olfactory cortex, all of which terminate within the granule cell layer. Furthermore, there is evidence that these centrifugal afferents terminate in distinct sublaminae of the granule cell layer (Davis and Macrides, 1981). Axons from the rostral regions of the piriform cortex terminate on the superficial layer of granule cells, whereas more caudal regions send afferents to the deep portion of the granule cell layer. Electrophysiological evidence indicates that projections from the piriform cortex form excitatory synapses onto granule cells and result in inhibition of mitral/tufted cells. Centrifugal afferents also arise from: the nucleus of the horizontal limb of the diagonal band; the locus coeruleus and; the raphe nucleus all of which

terminate within both the granule cell layer and the periglomerular regions of the glomerular layer (Shipley et al., 1985; Nickell and Shipley 1993).

In addition to these centrifugal inputs there is a topographically organised mitral/tufted cell projection to the pars externa of the anterior olfactory nucleus, whose cells project via the anterior commisure to a region of the contralateral bulb homotopic to the region of the ipsilateral bulb from which they received their input. Corresponding regions of the two bulbs can thus indirectly influence and receive feedback from each other. Activation of these commissural pathways by electrical stimulation of the anterior olfactory nucleus or the contralateral olfactory bulb produces strong inhibitory effects on mitral/tufted cells, this inhibition is mediated through granule cells. A second bilateral pathway involves olfactory information being transferred to the contralateral hemisphere at the level of the piriform cortex. The piriform cortex is divided into three major layers according to Price (1973). The commissural fibres from the piriform cortex are largely restricted in their origin to layer IIb of the anterior part of the piriform cortex and in their termination on the contralateral side to the posterior part of the piriform cortex and adjacent olfactory cortical areas (Haberly and Price, 1978).

1.2.2 Output from the olfactory bulb

The output from the olfactory bulb is carried by the axons of the "principal neurones", the mitral and tufted cells. The mitral/tufted cell primary dendrite provides the exclusive pathway from receptor input (in the glomeruli) to olfactory output in the efferent projection of the olfactory bulb.

A) Mitral cells

In fish and amphibia, the principal neurones are relatively undifferentiated. In reptiles, birds, and mammals, however, mitral cell bodies lie in a thin layer (1-2 cells thick) 200-400 μm deep to the glomerular layer. Mitral cells have the largest cell

bodies and nuclei in the bulb, ranging up to 30μm in diameter and have a characteristic pyramidal shape. The primary dendrite is directed radially outwards towards the glomeruli where it terminates in a distal tuft. Each mitral cell also gives rise to several secondary dendrites; these are laterally directed and terminate within the external plexiform layer (EPL). The primary and secondary dendrites have generally smooth surfaces thus mitral cells are "aspiny" neurones.

In mammals subtypes of mitral cells have been identified based on the branching pattern of their secondary dendrites (Orona *et al.*, 1984). Following the iontophoretic injection of horseradish peroxidase at various depths in the EPL of the rat olfactory bulb two classes of mitral cell were described. The first, Type I mitral cells, send their secondary dendrites into the deepest region of the EPL whereas, type II mitral cells send their secondary dendrites further, into the middle region of the EPL.

The mitral cell axons proceed to the depths of the olfactory bulb, through the granule cell layer, and then pass caudally to gather at the posterolateral surface to form the lateral olfactory tract (LOT). The fibres from the accessory olfactory bulb collect into the accessory olfactory tract, which runs with the LOT but is distinct from it. Within the bulb, the axons give off recurrent collaterals, injections of horseradish peroxidase show that the collaterals remain within the granule layer and internal plexiform layer (Orona *et al.*, 1984). A further distinction between the two types of mitral cell is the extent to which their axons form collaterals. Type I mitral cells have very few axon collaterals in the granule cell layer and none were seen in the internal plexiform layer, whereas Type II mitral cells have extensive axonal branching in the internal plexiform layer and upper granule cell layer.

B) Tufted cells

Output cells similar to mitral cells, but which have somata distributed throughout the EPL rather than in a defined cell body layer, are called "tufted cells". The tufted cells have also been shown to be a heterogeneous group and are classified into subsets according to the location of their somata in the EPL. The EPL has been divided into three zones, or sublaminae: external, middle, and internal; with external being underneath the glomerular layer and internal next to the mitral cell layer (Haberly and Price, 1977; Macrides and Schneider, 1982; Orona *et al.*, 1984).

The main population, middle tufted cells, lie as their name suggests in the middle of the EPL and have a slightly smaller cell body than mitral cells of 15-20 μm in diameter. The primary dendrite terminates as a "tuft" of branches in a glomerulus, and the axon collaterals are mostly confined within the internal plexiform layer and granule cell layer. A large proportion of axons joins the LOT but have different projection patterns to the central olfactory areas than mitral cells (Haberly and Price, 1977). Mitral cells are retrogradely labelled from all parts of the olfactory cortex following the injection of horseradish peroxidase. However, the ratio of labelled tufted cells to mitral cells greatly decreases as injections are made into caudal olfactory cortex regions suggesting that the axons of tufted cells terminate in the rostral part of the olfactory cortex.

External tufted cell somata are found in the glomerular layer and have the shortest secondary dendrites; the length of the secondary dendrites increases progressively with the depth of the cell body in the EPL. Hence Type I mitral cells have the longest secondary dendrites, reaching round almost half the circumference of the EPL. External tufted cells give off extensive axon collaterals in the internal plexiform layer and granule cell layer; some send an axon into the LOT, whereas others do not and are therefore considered to be intrinsic neurones.

The internal tufted cells have somata in the deep EPL close to the border with the mitral cell layer. In the rabbit olfactory bulb several investigators (Kishi *et al.*, 1982; Mori *et al.*, 1983) described mitral cells and what they termed 'displaced' mitral cells. These so-called "displaced mitral" cells may well have been the internal tufted cells described in the rat by Orona *et al.*, (1984). These are distinguished from Type II mitral cells in that their soma lie distinctly above the mitral cell layer.

1.2.3 Intrinsic neurones of the olfactory bulb

A) Periglomerular cells

The "periglomerular cells" are mostly found at the deep border of the glomerular layer, surrounding the glomeruli. These neurones have small cell bodies (8-10μm in diameter) and send a dendritic tuft into one (sometimes two) glomeruli. The dendritic branches intermingle with the terminals of olfactory axons and the branches of mitral and tufted cells. The branching axons of periglomerular cells take a lateral course and terminate in or around neighbouring glomeruli, suggesting that they are involved in interglomerular communication (Pinching and Powell, 1971a and 1971b).

The periglomerular cell falls into the category of 'short-axon cell' because its axon remains within the olfactory bulb. Morphologically the periglomerular cells seem to be a homogenous group but biochemical subtypes containing different transmitters have been found (Halasz *et al.*, 1977). Many glomerular cells have been immunocytochemically shown to contain glutamic acid decarboxylase, an enzyme involved in the production of GABA. However, a population of periglomerular cells were found to contain tyrosine hydroxylase, the dopamine synthesising enzyme, in their somata and dendrites.

B) Granule cells

Granule cells are small (8-10μm in diameter) and are by far the most numerous cell type in the bulb. The cell bodies lie in broad sheets below the internal plexiform layer and their dendrites radiate upwards and ramify in the EPL, but do not enter the glomeruli. There is also a deep process that branches sparingly in the granule cell layer. Electron microscopic studies suggest that these are dendrites, judged by their fine structural features (Price and Powell, 1970b). Hence, granule cells exhibit a bipolar orientation of their dendrites and lack an axon. A characteristic feature of granule cells is the spines (or gemmules) that cover the dendritic processes. Gap junctions are found between adjacent perikarya in the granule cell layer (Pasternostro *et al.*, 1995). Lucifer yellow injections into single granule cells result in the staining of small subsets of adjacent cells. These findings suggest that granule cells may be organised into syncytial subsets.

Extracellular injections of horseradish peroxidase were used to identify two types of granule cell in rodents, (Orona *et al.*, 1983). Injections in the EPL resulted in filled mitral/tufted cells as well as granule cell dendrites. These labelled somata were arranged in a cylindrical region extending from the EPL perpendicularly into the granule cell layer, the radius of this cylinder rarely exceeded 160μm. Injections into the granule cell layer at different depths revealed dendrites that extended to varying levels in the EPL. Injections made deep in the granule cell layer labelled granule cells with dendritic processes extending into only the deep portion of the EPL. Conversely, superficial granule cell layer injections labelled many granule cells with dendrites that extended across the entire EPL. These dendrites had very few or no spines in the deep EPL but were covered with many spines once they reached the superficial layer of the EPL where they branched extensively. Very few cells had dendritic ramifications in the middle of the EPL or with ramification in both the superficial as well as deep EPL.

Struble and Walters (1982) also reported two subpopulations of granule cells, differentiated by light microscopy. Following staining of tissue from rat olfactory bulbs with Bouin's solution and embedded in glycomethacrylate, 'light' and 'dark' granule cells were observed. Within the granule cell layer the light granule cells were not evenly distributed; almost 70% of them were found in the deeper half of the granule cell layer. Furthermore, the light granule cells tended to have thicker, more complex basal dendrites than the dark granule cells. This distribution of granule cell dendrites and the location of mitral/tufted cell secondary dendrites in the EPL suggest that the deep granule cells predominantly influence the secondary dendrites of Type I mitral cells in the deep EPL. Whereas the superficial granule cells influence the more superficial secondary dendrites of Type II mitral cells and the subclasses of tufted cells.

Terminations of the projections, running through the anterior commisure from the pars externa, are found in the superficial layers of the granule cell layer in the contralateral bulb. However, the projections from medial and ventral parts of the anterior olfactory nucleus terminate both in the deep zone of the granule layer and in the glomerular layer. This segregation by layer of extrinsic inputs to the granule cells is in keeping with the idea that two distinct populations of granule cells are involved in local circuits and output pathways, working in parallel with each other.

C) Short-axon cells

Short-axon cells are intrinsic interneurones and form a diverse group that is the most widely distributed, found throughout the granule, periglomerular and external plexiform layers. Although, they are represented sparingly in the external plexiform layer and are found more frequently in the glomerular layer. They are scattered throughout the granule cell layer, in relatively small numbers, and consist of several subtypes with dendritic trees of variable extent and orientation providing pathways

for both horizontal and vertical interconnections in the deeper layers of the bulb (Schneider and Macrides, 1978).

Short-axon cells do not receive olfactory nerve inputs nor do they make synaptic contact with mitral/tufted dendrites, although they may receive some mitral/tufted axon synapses (Price and Powell, 1970c; Pinching and Powell, 1971a), they are involved primarily in interglomerular loops within the glomerular layer. Short-axon cell dendrites are contacted by the axons of periglomerular cells and they in turn, send axons to contact the extraglomerular dendrites of adjacent periglomerular cells. Short-axon cells are also connected axodendritically with other members of their class. The spatial extent of the axons of these cells appears smaller than that of the periglomerular cells (about 2-3 glomerular widths). The axons of superficial short-axon cells can reach all levels of the external plexiform layer as well as the periglomerular region. Thus, they have the potential to influence cells of other layers whilst receiving their input from the interneurones of the periglomerular region only.

1.3 Laminar distribution of neuronal cell types

The main olfactory bulb is composed of five distinct laminae containing the cell types described in the previous section that are specific for each layer (fig. 1.2).

1.3.1 Glomerular layer (GL)

This layer is comprised of the olfactory glomeruli, large spherical structures up to 200μm or more in diameter, which are the most characteristic feature of the olfactory bulb in all vertebrates. The glomeruli are surrounded by glial sheaths that separate them from surrounding neuronal somata. The glomeruli themselves contain no neuronal cell bodies, their mass is made up largely of olfactory nerve terminals and the dendrites of the principal neurones (mitral/tufted cells) and interneurones (periglomerular and short-axon cells). No cells in the granule cell layer send

dendrites into the glomeruli. There is a degree of variation in the coronal plane of the number of glomeruli present in the glomerular layer, with fewer glomeruli in the dorsal and ventral sectors.

The axons of the olfactory nerve do not branch or synapse until they reach the bulb where they terminate exclusively in the glomeruli. However, the ratio of glomeruli to primary receptor axons is very small hence, there is a huge convergence of axons onto individual glomeruli which are clearly demarcated within the layer. Recent studies using an olfactory marker protein driven LacZ reporter to mark subsets of receptors showed that some glomeruli were only partially labelled (Treloar *et al.*, 1996). This suggests that the input to some glomeruli may be heterogeneous. Once inside the glomeruli the olfactory nerve terminals ramify extensively and make axodendritic synapses onto the dendritic processes of the relay neurones (mitral and tufted cells) and the intrinsic neurones (periglomerular cells) (Pinching and Powell, 1971b). Activity in one glomerulus can affect other glomeruli through interglomerular connections provided by the periglomerular cell.

1.3.2 External plexiform layer (EPL)

This layer consists mainly of mitral cell primary dendrites that are coursing upward toward the glomeruli and a great number of lateral dendrites belonging to both mitral/tufted cells and granule cells. The mitral cells have long, branching, lateral dendrites that can reach lengths of up to 800-1000μm. These dendrites are orientated horizontally to the axis of the primary dendrite and terminate within the EPL.

The dominant type of synaptic interaction is a pair of reciprocal contacts between the secondary dendrite of a mitral/tufted cell and the spine of a granule cell dendrite. These were the first dendrodendritic synapses identified in the nervous system (Rall *et al.*, 1966). In the reciprocal pair, the mitral-to-granule synapse is

Type 1 (excitatory) whereas, the granule-to-mitral synapse is Type 2 (inhibitory) (Price and Powell, 1970a). Over 80% of all synapses in the EPL are involved in such reciprocal pairs. If we consider that there are up to 100 granule cells for each mitral cell, and each granule cell has 50-100 spines in the EPL (Greer, 1987; Mori, 1987) it is obvious that these dendrodendritic microcircuits provide for extremely powerful interactions with the mitral cells.

At the level of output control in the EPL each type of principal neurone is dominated by different subpopulations of granule cells: superficial granule cells control superficial and middle tufted cells, and deep granule cells control mitral cells. In addition to synapses made by the dendrites, the EPL also contains axon terminals from intrinsic short axon cells and centrifugal fibres (the locus coeruleus and horizontal limb of the diagonal band). These axon terminals make Type 1 synapses predominately on the presynaptic granule spines (Price and Powell, 1970a); no contacts have been seen on the mitral cell dendrites.

1.3.3 Mitral cell layer (MCL)

The mitral cell layer consists of a narrow band (2-3 cells wide) of mitral cell bodies. The size of mitral cell bodies varies in the coronal plane but not the rostrocaudal plane (Panhuber *et al.*, 1985). The larger cells are located in the lateral and medial sections of the layer with smaller mitral cells found in the dorsal and ventral sections. This variation in size of the mitral cells has also been noted by Smithson *et al.* (1989) who reported the presence of large and petite mitral cells in the mitral cell layer following the retrograde labelling of mitral cells.

The mitral cell sends its primary dendrite to the glomerular layer where it forms a tuft within the glomerulus and synapses with the primary olfactory nerve axons. The mitral cell also exhibits extensive secondary dendrites that can reach

lengths of 400-500μm, travelling almost the circumference of the bulb and are situated within the EPL.

1.3.4 Internal plexiform layer (IPL)

Between the mitral cell layer and the granule cell layer is a narrow layer relatively free of cell bodies - the internal plexiform layer. This layer mainly consists of a huge number of granule cell dendrites passing through on their way to the EPL. Some axons and dendritic processes of short-axon cells and terminations of centrifugal fibres are also found in this region. The external tufted cells send their axons into the internal plexiform layer where they form a dense tract and travel within this layer to the opposite side of the same bulb where they terminate on the apical branches of granule cells. Hence the activity on one side of the bulb can influence the activity on the opposite side of the same bulb.

1.3.5 Granule cell layer (GCL)

This layer contains the somata of many of the bulbar interneurones: the granule cells and the short-axon cells. In the granule cell layer axon terminals are found on both the shafts and spines of the granule cell dendrites. Price and Powell (1970a) showed that these axon terminals derive from both intrinsic (axon collaterals of mitral/tufted cells and the axons of deep short-axon cells) and centrifugal inputs. As already mentioned, certain centrifugal afferents terminate in distinct sublaminae of the granule cell layer. Fibres from the pars medialis of the anterior olfactory nucleus terminate in the deep half of the granule cell layer; while the pars posterior, ventralis, dorsalis and lateralis of the anterior olfactory nucleus terminate in the superficial granule cell layer.

It should be noted that all of the synaptic connections in which the granule cell takes part are orientated toward the granule cell, with the sole exception of the dendrodendritic synapses from the granule spines onto the mitral dendrites in the

EPL. The latter are therefore the only output avenue from the granule cell. Due to these diverse synaptic connections the granule cell has been described by Shepherd as "an interneuron par excellence for local and intrinsic neuronal integration" (G. M Shepherd, 1972).

Figure 1.2. Schematic diagrams to illustrate the laminar distribution of the principal output cells and the various types of interneurone found in the main olfactory bulb. **A**) The localisation of the two subclasses of mitral cell (Type I and II) with their different branching pattern of secondary dendrites in the external plexiform layer and also, the position of tufted cell somata in the three sublaminae of the external plexiform layer. Glomeruli are depicted as circles with broken lines, into which the terminals of the olfactory nerve arborise and contact the dendritic tufts of mitral and tufted cells. Axon collaterals are shown in the granule cell layer, the axons of mitral and middle/internal tufted cells form the lateral olfactory tract. **B**) The same arrangement of layers, this time showing the distribution of the different classes of intrinsic interneurone found in the olfactory bulb. Dashed lines indicate the presence of centrifugal fibres and their termination sites within the olfactory bulb layers.

Abbreviations: EPL, external plexiform layer; G, granule cell; GCL, granule cell layer; GL, glomerular layer; IPL, internal plexiform layer; LOT, lateral olfactory tract; M, mitral cell; MCL, mitral cell layer; ON, olfactory nerve; Pg, periglomerular cell; SA, short-axon cell; Td, tufted cell.

(Modified from; the Synaptic Organisation of the Brain, 4th Edition, edited by Gordon M. Shepherd, 1998).

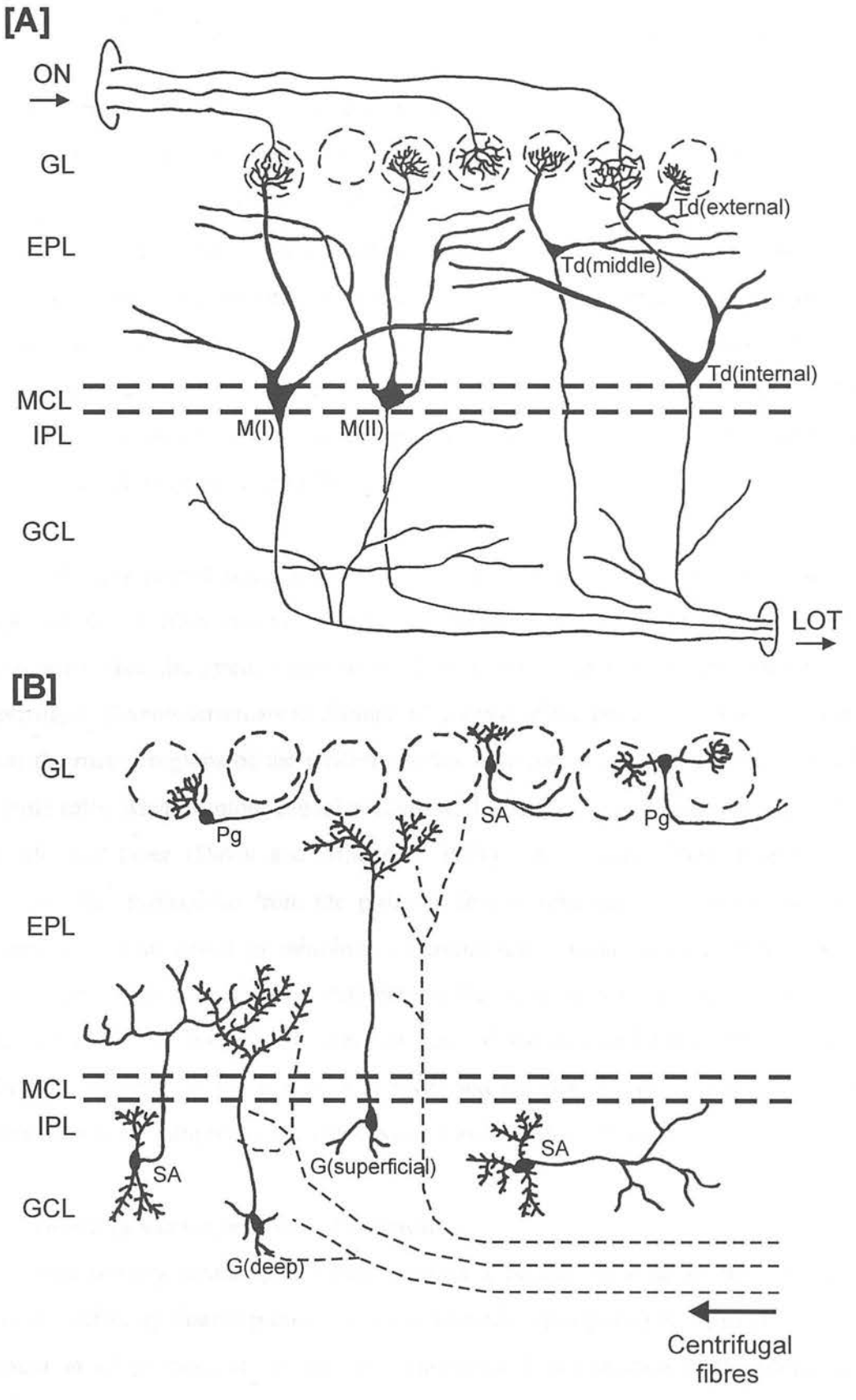
[A]
ON
GL
EPL
MCL
IPL
GCL
M(I)
M(II)
Td(external)
Td(middle)
Td(internal)
LOT
[B]
GL
EPL
MCL
IPL
GCL
Pg
SA
Pg
SA
SA
G(superficial)
G(deep)
Centrifugal
fibres

1.4 Neurotransmitters in the olfactory bulb

There have been several comprehensive reviews concerning the neurochemistry of the olfactory bulb including Halasz and Shepherd (1983) and Shipley and Ennis (1996). These describe the large variety of neuroactive substances released by the bulbar neurones and centrifugal fibres. A summary diagram, figure 1.3, illustrates the wide variety of substances released at synaptic contacts between the different cell types found in the olfactory bulb of the rat. Centrifugal afferents to the olfactory bulb are very dense, come from multiple sources and play important roles in regulating neural excitability in the bulb.

Olfactory-related afferents arise from the anterior olfactory nucleus and also by axon collaterals from pyramidal neurones in the piriform cortex, all of which terminate within the granule cell layer. Furthermore, there is evidence that these centrifugal afferents terminate in distinct sublaminae of the granule cell layer. Axons from the rostral regions of the piriform cortex terminate on the superficial layer of granule cells, whereas more caudal regions send afferents to the deep portion of the granule cell layer (Davis and Macrides, 1981). Electrophysiological evidence indicates that projections from the piriform cortex form excitatory synapses onto granule cells and result in inhibition of mitral/tufted cells (Nicoll, 1971). The subcortical modulatory afferents originate in the brain stem (locus coeruleus/raphe nucleus) and basal forebrain (horizontal limb of the diagonal band) all of which terminate within both the granule cell layer and the periglomerular regions of the glomerular layer (Shipley et al., 1985; Nickell and Shipley 1993).

1.4.1 Olfactory marker protein and carnosine

The sensory olfactory neurones contain a peptide specific to the olfactory system, "olfactory marker protein", first discovered by Margolis (1972) in mice. It is present in all portions of the sensory neurones and is restricted to the glomeruli within the olfactory bulb. It is only present in functionally mature sensory cells and

not the stem cells of the neuroepithelium. Although the olfactory marker protein is localised exclusively to the receptor cells and their processes, this distinct localisation seems to be dependent on a 'normally' functioning bulb. Treatment of the olfactory lobe with zinc sulphate eliminated the olfactory marker protein, which recovered in parallel with morphological signs of regeneration (Margolis *et al.*, 1974).

The olfactory bulb also contains a high concentration of a dipeptide of histidine, carnosine (Margolis *et al.*, 1986). Electrophysiology experiments show that the olfactory axons are excitatory, but neither olfactory marker protein nor carnosine has been shown to be neuroactive at this synapse. Application of exogenous carnosine to the bulbar surface of the gecko olfactory bulb, (Tonosaki and Shibuya, 1979) or microionophoresis to the mitral cell region in rat (MacLeod and Straughan, 1979), frog and turtle preparations (Nicoll *et al.*, 1980) did not produce the expected excitation of mitral cells.

1.4.2 Glutamate

The presence of glutamate in the olfactory bulb was first discovered in the rat by Popov *et al.* (1967), (c.f. Halasz and Shepherd, (1983)). The laminar distribution of glutamate was studied by two groups, Nadi *et al.* (1980) and Godfrey *et al.* (1980) who both found a relatively uniform distribution of glutamate throughout the layers of the bulb with slightly higher levels in the glomerular/external plexiform layer.

In the glomerular layer

The destruction of the olfactory chemoreceptors in the nasal epithelium by the application of zinc sulphate had no effect on the glutamate content of the olfactory bulb. In addition, glutamate uptake in the olfactory bulb was little affected by ablation of the nasal epithelium (Margolis *et al*, 1974) providing circumstantial indications that glutamate is not a transmitter in the olfactory nerves. However, more

recent evidence obtained by using a combination of electron microscopy and immunocytochemistry has revealed that glutamate is co-localised with carnosine in axon terminals of the rat olfactory nerves (Sassoe-Pognetto *et al.*, 1993). Furthermore, in a hemisected preparation of the turtle olfactory bulb Berkowicz *et al.* (1994) demonstrated that the depolarising potential evoked by olfactory nerve stimulation consists of two components, which are differentially blocked by the glutamate receptor antagonists AP5 and DNQX. Similar results were found in the rat olfactory bulb slice (Ennis *et al.*, 1996). Thus, the electrophysiological data indicates that both NMDA and non-NMDA glutamate receptors mediate the response seen in mitral cells following orthodromic activation.

It has recently been shown that lesioning the rat olfactory mucosa with a solution of zinc sulphate first causes a transient up-regulation followed by a reduction in the mRNA expression of metabotropic glutamate receptor 1a (mGluR1a) within the glomeruli of the olfactory bulb Ferraris *et al.* (1997) and Casabona *et al.* (1998). This supports the view that glutamate participates in the physiology of synaptic transmission between the olfactory nerve and the principal neurones of the olfactory bulb. The discrepancy from the study by Marglolis et al. (1974) may be due to the fact that other subtypes of mGluR are found in the olfactory bulb specifically the mGluR2 receptor in the external plexiform layer where it is associated with the pre-synaptic sites of granule cell spines (Kaba et al., 1994) and is involved in the dendrodendritic interactions with mitral cells. Hence, ablation of the olfactory epithelium may produce a subtle effect in the overall glutamate content of the olfactory bulb that was not uncovered in the earlier experiments.

In the external plexiform layer

In ionophoretic studies Baumgarten *et al.* (1963) found that some units within the olfactory bulb were excited and some inhibited by glutamate. Nicoll (1971) showed the major effect of glutamate, in the isolated turtle preparation, to be

inhibition of mitral cell firing. At first this seemed somewhat paradoxical, since the action of glutamate in other regions of the central nervous system was strongly excitatory. However, with the additional information on the circuitry between the mitral and granule cell, it was realised that this effect of glutamate was mediated by the reciprocal synapse between the two cell types. Thus, it was suggested that the site of action of glutamate in these experiments be on the granule cell gemmules, and that excitation of these leads to activation of the inhibitory synapses onto the mitral cell dendrites. The subtype of glutamate receptor present on the granule cell spines has been shown to be mGluR2 (Kaba *et al.*, 1994). Jahr and Nicoll, (1982b) made intracellular recordings from the turtle olfactory bulb slice to show that glutamate does indeed enhance the release of GABA from granule cells.

The first studies to look at the release of glutamate within the olfactory bulb were carried out by Yamamoto and Matsui (1976) using a slice preparation of guinea-pig cortex. Stimulation of the LOT resulted in an increase in the release of radio-labelled glutamate ([^{14}C]Glu) from the slice. In low-Ca^{2+} medium the glutamate efflux induced by LOT stimulation dropped to one-third of control values. Furthermore, in the guinea-pig slice preparation Bradford and Richards (1976) found that high frequency stimulation of the LOT (50Hz for 10min) caused increased Ca^{2+}-dependent release of glutamate, but not aspartate. The candidacy of glutamate as the transmitter of the output synapses from the presynaptic mitral cell soma-dendrites has been strengthened by the finding of NMDA receptors in the external plexiform layer (Cotman *et al.*, 1987).

1.4.3 γ-aminobutyrate (GABA)

A variety of techniques have been used to look at the laminar distribution of GABA sites of activity. Analysis of GAD and GABA trans-aminase activity (Austin *et al*, 1979) has been carried out on micro-dissected layers of the bulb. The distribution of GABA, determined by measuring the levels of GAD activity, across

the layers can be characterised by a bell-shape curve, peaking in the EPL (Graham *et al.*, 1973; Austin *et al.*, 1979). This was supported by immunohistochemical studies (Ribak *et al*, 1977; 1981), which showed that the highest concentration of GABA or GABA-related compounds were to be found in regions where granule cell bodies and their synaptic terminals are located. At the electron-microscope level the presence of GAD was revealed in most of the granule cells, in their dendrites and the gemmules that synapse with the lateral dendrites of mitral cells in the EPL. In the glomerular layer many periglomerular cells and their processes also showed GAD activity, while mitral, tufted and short-axon cells did not. Further support was given by autoradiographic studies using a [^{3}H]GABA label; results showed a high density of silver grains over the granule cell dendritic gemmules in the EPL. Using a quantitative grain analysis method the labelling was found to be 11-fold higher than the minimal grain density over mitral cell dendrites (Halasz *et al*, 1981). Some periglomerular cells and their dendrites contain GAD, as well as take up GABA (Ribak *et al.*, 1977). In rabbit olfactory bulb slice preparations, GABA-activated whole-cell currents and single-channel currents recorded from periglomerular cells show $GABA_A$ receptor properties (Bufler *et al.*, 1992b).

Nicoll (1970) showed that in the cat, mitral cell activity was depressed with the ionophoretic application of GABA and picrotoxin was seen to block this inhibitory effect of GABA. In a series of experiments by Tonosaki and Shibuya (1979), rather than by electrical stimulation, the mitral cells of the gecko olfactory bulb were stimulated by an odour (amyl acetate). Under this stimulation protocol, the exposed surface of the bulb was superfused with GABA, which resulted in a decrease in the odour-evoked and spontaneous activities of mitral cells. When the bulb was superfused with GABA together with bicuculline, GABA had no effect. The ionophoretic application of GABA into the EPL had similar effects as the superfused GABA, but was not effective when applied to the glomerular layer only. This

supports the theory that GABA plays an exclusive role as the transmitter in the region of the peripheral processes of granule cells.

Yu *et al.* (1993) found conflicting results when testing the effect of bicuculline (a $GABA_A$ antagonist) on the spontaneous firing activity of mitral cells, *in vivo* in the rat. They found that 75% of the cells tested responded with an increase in their firing rate however, 19% showed a decreased firing rate after the infusion of bicuculline, and the remaining 6% showed no detectable change in their spontaneous firing rate. The effect of bicuculline on the post-stimulus inhibition experienced by mitral cells following stimulation of the LOT was also studied. Again, inconsistent effects of bicuculline were found; 67% showed a decreased duration of inhibition following the stimulus pulse, 22% showed an increase in the inhibitory period and the remaining cells showed no change in the duration of post stimulus inhibition. Hence, mitral cells show heterogeneity in both their spontaneous firing patterns and their response to bicuculline.

1.4.4 Glycine

Evidence for glycine as a transmitter in the olfactory bulb has recently been obtained, glycine was found to evoke chloride-mediated membrane currents in rabbit olfactory bulb slices (Bufler *et al.*, 1992a) and to have powerful inhibitory effects on both mitral/tufted cells and granule cells in culture (Trombley and Shepherd, 1994). Immunoreactivity for monoclonal antibodies against glycine and glycine receptors has been found in the EPL and around mitral cell bodies (van den Pol and Gorcs, 1988). *In situ* hybridisation experiments have shown that the $\alpha 3$ glycine receptor subunit is present in the olfactory bulb (Malioso *et al.*, 1991). Thus, the olfactory bulb has emerged as one of the best examples that a role for glycine as a neurotransmitter exists in the brain as well as the spinal cord.

1.4.5 Dopamine

The first definitive study of glomerular transmitters showed, by histofluorescence and EM autoradiography, that some periglomerular cells are positive for dopamine synthesising enzymes (Halasz *et al.*, 1977). The dopamine is transneuronally regulated; degeneration and regeneration of olfactory nerves following olfactory nerve transection are paralleled by a decrease and increase of dopamine levels in the olfactory bulb (Baker *et al.,* 1983). It is generally accepted that most tufted cells share the same neurotransmitters at their dendritic and axonal output synapses with mitral cells, however, some tufted cells appear to be dopaminergic (Halasz *et al.*, 1977).

1.4.6 Serotonin (5-HT)

The presence of serotonin (5-hydroxy-tryptamine, 5-HT) fibres was first localised within the olfactory bulb by Dahlström *et al.* (1965) using fluorescent microscopy. A small number of fine terminals were reported in the outer granule layer, however, no fluorescent cell bodies were seen in the bulb, suggesting that the origin of the 5-HT fibres was extrabulbar. Fluoresence has also been observed within the glomerular layer (Broadwell and Jacobowitz, 1976) indicating the presence of serotonergic fibres within this layer. Dahlstrom and Fuxe (1964) using fluorescent microscopy identified the raphe as one of the main sources for the 5-HT projection to the olfactory bulb. This was confirmed by several groups using retrograde labelling techniques: DeOlmos *et al.* (1978) injected horseradish peroxidase into the olfactory bulb, and Araneda *et al.* (1980) injected radioactive labelled 5-HT. The same pathway was labelled in the anterograde direction and suggested areas of activity in the glomerular layer and to a much lesser extent in the EPL (Halaris *et al.*, 1976). It has already been noted in discussion of the glomerular layer that 5-HT fibres terminate within the glomeruli, thus permitting the brainstem to have a direct influence at the initial level of olfactory signal processing.

Ionophoretic studies have indicated an inhibitory action of serotonin on mitral cell activity (Bloom *et al.*, 1971).

1.4.7 Noradrenaline

Immunohistochemical visualisation has demonstrated the presence of noradrenergic fibres in the rat olfactory bulb. The presence of dopamine-B-hydroxylase (DBH), an enzyme which accurately parallels the noradrenaline content of a region, was visualised and fibres were found mostly within the granule cell layer (Halasz *et al.*, 1983). Under the electron microscope labelled nerve terminals were seen to contact dendrites or dendritic spines thought to belong to the granule cells (Halasz *et al.*, 1978). The origin of the noradrenergic fibres is the locus coeruleus in the brainstem. Using retrograde tracing techniques Shipley *et al.* (1985) estimated that 40% of all the fibres that emerge from the locus coeruleus are directed towards the olfactory bulb.

The noradrenergic afferents from the locus coeruleus have been shown to increase mitral cell firing (Jahr and Nicoll, 1982; Jiang *et al.*, 1993). By incubating the bulbar surface with radioactively labelled noradrenaline, Brennels (1974) demonstrated that upon electrical stimulation of the LOT there was a selective increase in the release of radioactivity. This release was dependent on Ca^{2+}, and the intensity, duration and frequency of stimulation. Ionophoresis of noradrenaline into the mitral cell area regularly increased the spontaneous firing of unitary spikes recorded from mitral cells (Bloom *et al.*, 1964; McLennan, 1971). Noradrenaline is thought to inhibit excitatory transmission from mitral cell to granule cells via presynaptic, α_2 receptors Trombley and Shepherd, (1993). The mechanism appears to involve reduction of a Ca^{2+} conductance in the presynaptic terminal (Trombley, 1992).

1.4.8 Acetylcholine

Acetylcholine was the first putative transmitter identified in the olfactory bulb (Koelle, 1954), determined by the localisation of acetylcholine esterase (AChE), the enzyme that hydrolyses acetylcholine in order to terminate its action at the synapse. Based on AChE staining, cholinergic fibres were found to originate in the reticular area and in the nucleus of the diagonal band (Shute and Lewis, 1967). These projections were confirmed by Wenk *et al.* (1977) who made unilateral lesions of the lateral preoptic area, and demonstrated a decrease in cholinesterase activity in regions of the olfactory system. The cholinergic fibres are distributed relatively evenly through the laminae, with highest levels in the EPL (Rotter, 1977). Ionophoresis of ACh *in vivo* has a mostly depressant effect on mitral cell firing (Bloom *et al.*, 1971; Nickell and Shipley, 1988).

1.4.8 Additional neurotransmitters

Other neuroactive substances employed within the olfactory bulb include Substance P, enkephalins, somatostatin, and lutenising hormone-releasing hormone.

Substance P

With immunocytochemistry, Substance P fluorescent fibres were first recognised in the peripheral olfactory system (the nasal mucosa) of rats (Hökfelt *et al.*, 1975). Ljungdahl *et al.* (1978) observed labelled nerve terminals of Substance P fibres throughout all layers of the rat olfactory bulb. Later, Inagaki *et al.* (1982 (rat); 1981 (frog)) recognised intrabulbar Substance P-positive cell bodies in addition to labelled fibres. The majority of Substance P-immunoreactive cells were found in the glomerular layer, with a few labelled cells in the mitral and granule cell layers. The PAP method, complemented by Golgi studies, showed labelled external tufted cells and their dendritic processes, in the glomerular neuropil, unlabelled olfactory nerve fibres were seen in synaptic contact with the HRP-labelled external tufted cell dendrites (Burd *et al.*, 1982).

Enkephalins

Herkenham and Pert (1982) described a predominance of [^{3}H] naloxone receptors within the glomeruli and external plexiform layer of the main and accessory olfactory bulb of the rat. Enkephalin-like immunoreactivity has been shown in a relatively high number of periglomerular cells and granule cells, and a few short-axon cells. Immunoreactive fibres were reported to be present in all layers of the olfactory bulb, with the exception of the olfactory nerve and the periventricular layer of the rat. The latter observation would suggest that there were no centrifugal enkephalin-containing fibres in the rat. In contrast, Davis *et al.* (1982) described Met-ENK-immunoreactive fibres in the bulbar portions of the anterior commissure of the hamster. This finding is supported by the result of unilateral bulbectomy in the mouse; there is a significant fall in opiate receptors in the remaining olfactory bulb (Hirsch and Margolis, 1980). Peripheral deafferentiation did not affect the endogenous level of Met-ENK (Margolis, 1981).

Nicoll *et al.* (1980) studied the electrophysiological consequences of application of a stable enkephalin analogue (D-Ala-Met5-enkephalinamide) onto the bulbar neurones. They found that it attenuated the IPSPs, particularly those generated by direct depolarisation of the mitral cells, and this action could be reversed by the application of naloxone.

Luteinising hormone-releasing hormone

The first evidence of LHRH-immunoreactivity in the olfactory bulb of hamsters was provided by Hoffman *et al.* (1979), LHRH fibres were observed in the glomerular layer, external plexiform layer and the granule cell layer. Two systems of LHRH fibres have been described in the main olfactory bulb (Jennes and Stumpf, 1980; Phillips *et al.*, 1980), one that originates from the septal and diagonal band area and terminates in the granule cell layer of the olfactory bulb, the other derives

from more rostral areas of the olfactory system and supplies mostly the olfactory nerve and glomerular layers of the posterior olfactory bulb.

Somatostatin

Finley *et al.* (1981) mapped the rat brain with the PAP technique in order to reveal somatostatin immunoreactivity in nerve elements. They found the only neuronal cell bodies of the olfactory lobe reacting with somatostatin antibody to be located within the accessory olfactory nucleus, the olfactory tubercle and piriform cortex. Positively stained fibres were also present in the nucleus and tract of the diagonal band. Davis *et al.* (1982) described somatostatin-positive somata in the deep granule layer of the hamster olfactory bulb. These cells were relatively few in number and resembled deep short-axon cells. They also described somatostatin immunoreactive central fibres running in the anterior commissure.

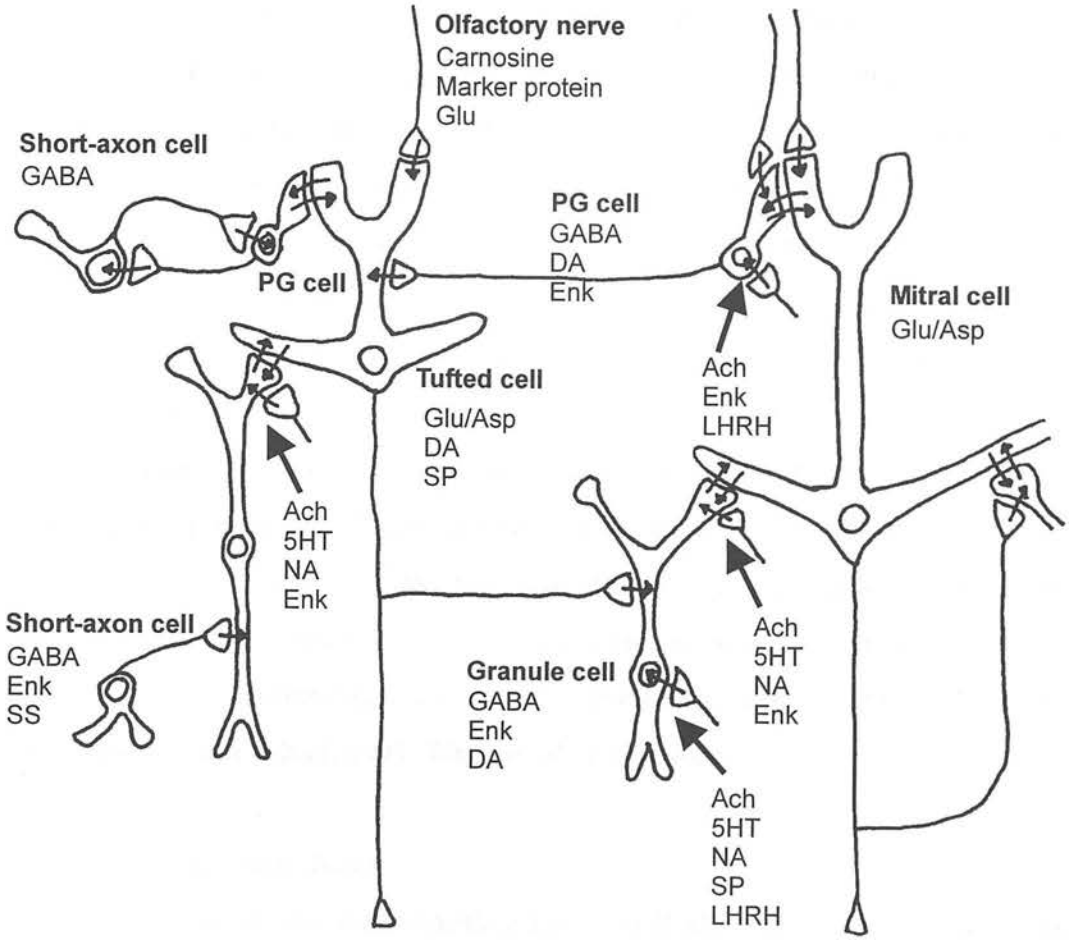

Figure 1.3. Schematic drawing illustrating the neuroactive substances released at synapses within the olfactory bulb. Large arrows indicate that the substance is released from the terminals of a centrifugal fibre. Abbreviations: GABA, gamma-aminobutyrate acid; NA, noradrenaline; ACh, acetylcholine; Glu, glutamate; Asp, aspartate; DA, dopamine; Enk, enkephalins; SP, substance P; LHRH, luteinising hormone-realising hormone; 5HT, serotonin; SS, somatostatin.

1.5 Synaptic actions

Synaptic circuits in the vertebrate olfactory bulb have been analysed in several types of preparation. First were *in vivo* experiments with anaesthetised animals, particularly rabbit, rat, and salamander. The separation of input and output pathways, in the olfactory nerves and lateral olfactory tract respectively, enabled these studies to identify the basic types of synaptic actions and synaptic circuits, as well as permit analysis of these circuits during odour stimulation. The next step was the introduction of isolated preparations. The first of these was the isolated olfactory bulb of the turtle (Mori *et al.*, 1981c) which enabled exhaustive studies to be carried out on synaptic excitation by olfactory axons and synaptic inhibition by the dendrodendritic synapses. More recently, a mammalian slice preparation has been developed (Nickell *et al.*, 1996) that provides for adequate preservation of the olfactory bulb microcircuits. Finally, cell cultures were introduced as a means of analysing the pharmacology of specific excitatory and inhibitory synapses (Bischofberger and Schild, 1995: Wang *et al.*, 1996a,b).

1.5.1 Orthodromic stimulation

Experiments on the isolated turtle olfactory bulb show that a single shock to the olfactory nerve gives rise to a series of synaptic potentials (two excitatory and two inhibitory) in the mitral cell, these potentials are graded in amplitude with stimulus strength (Mori *et al.*, 1981b). The excitatory potentials are linked to the glomerular response and when the inhibitory potentials are blocked by the application of bicuculline, a prolonged excitatory potential is seen. When unopposed by inhibition this excitatory post-synaptic potential (EPSP) renders the mitral cell hyperexcitable so that it responds with a burst of impulses (Nowycky *et al.*, 1981b). With sufficiently strong impulses an action potential is generated at the cell body, this is generated by both Na^+ and Ca^{2+} currents (Mori *et al.*, 1981a; Jahr and Nicoll, 1982b).

Similarly, intracellular recordings were made in a mammalian preparation, the rat olfactory bulb slice (Chen and Shepherd, 1997; Nickell *et al.*, 1996). A bipolar stimulating electrode was positioned in the olfactory nerve layer, (situated above the glomerular layer) slightly rostral to the recording electrode. Upon electric stimulation a long lasting (200ms-5s) EPSP occurred, the amplitude of which was graded with stimulus intensity, strong stimulation would result in a discharge of action potentials. It was discovered that not all mitral cells responded in the same way to olfactory nerve stimulation, some responded only with a period of hyperpolarisation, which was not preceded by an EPSP.

The neurotransmitter involved in synaptic transmission between the olfactory nerve and mitral cells has been identified as glutamate (Berkowicz *et al.*, 1994). The nature of the neurotransmitter employed at the olfactory nerve-to-mitral cell synapse was also investigated in the rat olfactory bulb slice (Chen and Shepherd, 1997). The NMDA receptor antagonist APV reduced the amplitude as well as the late component of the EPSP, leaving its rising phase unaffected. The non-NMDA receptor anatagonist CNQX suppressed both the early and late components of the EPSP. In the presence of both antagonists the synaptic transmission between the olfactory nerve and mitral cells was completely blocked.

5.2 Antidromic stimulation

Mitral cells

By contrast, when a single shock to the LOT resulting in antidromic stimulation of the mitral cell, the response lacks the excitatory potentials described for orthodromic activation in the turtle whole-bulb preparation (Mori et al., 1981b). However, inhibitory potentials similar to those seen in the orthodromic activation are present. This is to be expected if these inhibitory potentials are generated in the secondary dendrites of the mitral cell by the actions of granule cells. The brief period of antidromic impulse invasion is followed by a long period during which

many mitral cells are inhibited. In extracellular recordings the inhibition is seen as a suppression of the spike response to a second or test antidromic volley (Phillips *et al.*, 1963). The test spike fails even when the first volley is subthreshold for the axon of the unit under study, indicating that the suppression is not due to mitral cell refractoriness but rather to synaptic inhibition. With strong shocks the inhibition is quite powerful and long lasting, with durations of up to several hundred milliseconds. The inhibition has also been described as an interruption of spontaneously firing spikes (Green *et al.*, 1962). Intracellular recordings show that the period of inhibition corresponds to a hyperpolarisation of the mitral cell membrane (Nicoll, 1969; Yamamoto *et al.*, 1963).

Nickell *et al.* (1996) found that mitral cells, in the rat olfactory bulb slice, displayed spontaneous high-amplitude extracellular spikes, similar to the "giant mitral spikes" reported in the *in vivo* rabbit (Shepherd, 1963). Amplitudes of up to 73mV peak-to-peak have been reported in the rabbit (Phillips *et al.*, 1963) without significant shift in the d-c base line, indicating that the recording tip remains in an extracellular position. The 'giant' spikes recorded *in vivo* sometimes have an inflection on the initial phase (Shepherd, 1963). Using conventional techniques of paired antidromic volleys it has been shown that the inflection indicates that the spike has two components corresponding to the A and B spikes in motorneurones and other central neurones (Coombs *et al.*, 1957; Fuortes *et al.*, 1957). In addition to the A and B spikes, a small spike preceding the A spike has been reported at short testing intervals, this has been termed as the M spike and is thought to occur in the first node of the myelinated axon. This all indicates that the antidromic impulse invades successive regions or types of excitable membrane in a sequence very similar to that in other large central relay neurones.

In the rat olfactory bulb slice Chen and Shepherd (1997) stimulated the LOT by placing a bipolar stimulating electrode at a site where the mitral cell axons gather to

form the tract, within the bulb slice. An antidromic impulse was generated which was characteristically followed by a depolarisation rather than a hyperpolarisation. The antidromic EPSP generally lasted for a much briefer duration and had a smaller amplitude than the EPSP generated by orthodromic stimulation. It has been suggested that this depolarisation is as a result of mitral cell autoexcitation. A similar phenomenon has been described in the *in vivo* rabbit (Nicoll, 1971). There are no anatomically identified excitatory synapses onto the mitral cell dendrites apart from the synapses with olfactory nerve terminals within the glomeruli (Kosaka *et al.*, 1997; Pinching and Powell, 1971a). However, there is evidence in the turtle olfactory bulb that these dendrites are excited by glutamate, the transmitter that the mitral cells themselves release (Nicoll and Jahr, 1982).

Aroniadou-Anderjaska *et al.* (1999) investigated whether the release of glutamate from the mitral cell dendrites was capable of exciting the parent cell and neighbouring mitral cells in the mammalian main olfactory bulb. Intracellular recordings were made from a slice preparation of the rat olfactory bulb, maintained in medium containing bicuculline metchloride, a $GABA_A$ receptor antagonist, to reduce inhibition by granule cells, and low Mg^{2+}, to facilitate the activation of NMDA receptors. The response of mitral cells to a single shock to the olfactory nerve was a prolonged depolarisation (duration 200->800ms), preceded by a spike, both of these olfactory nerve evoked components were blocked by the application of the NMDA receptor antagonist APV. This would suggest that glutamate released from the dendrites of the activated (parent) cell either directly activates NMDA receptors on the parent cell or excites neighbouring cells, which act back on the parent cell. This may contribute to the prolonged response of mitral cells when the apical dendrites are depolarised by synaptic input from the olfactory nerve.

Granule cells

Intracellular micropipettes were used to fill granule cells with horseradish peroxidase and also to record the response of these interneurones to stimulation of the LOT (Mori and Kishi, 1982). Recordings were confirmed as being from granule cells by histological verification of the location of stained soma and the branching patterns of the associated dendrites. They reported similar subclasses of granule cells as Orona *et al.* (1983), with deep and superficial groups of granule cells. Following the LOT stimulation, granule cells showed a depolarisation with a hump on the falling phase. When a conditioning LOT volley was applied 20ms before the testing pulse, the test response was markedly depressed. In some granule cells, the depolarisation was followed by a prolonged hyperpolarisation.

The fact that the granule cell lacks an axon implies that it may not generate impulses or may not generate them in the usual manner. If it does not generate impulses, extracellular unit recordings will not be obtainable. With extracellular recording techniques, unitary spikes in the granule cell layer are infrequently encountered. This is in sharp contrast to the large numbers of granule cells and the dense packing of their cell bodies in this layer. The infrequent encounters might be due to the very small size of the granule cell bodies, but using similar techniques, recordings from periglomerular cells (which have comparably small cell bodies) spikes are seen very frequently (Shepherd, 1963a; 1971). The periglomerular cells possess short axons, whereas the granule cells do not, this could indicate that spikes recorded from the granule cell layer are related to the short-axon cells scattered throughout the layer.

Bufler *et al.* (1993) made patch-clamp recordings from granule cells in rabbit (aged between one and ten days) olfactory bulb slices. They found that an action potential could not be evoked upon depolarisation of the granule cell. Under identical experimental conditions action potentials were readily elicited in other cell

types of the rabbit olfactory bulb (Bufler *et al*, 1992b). Upon depolarisation (under voltage-clamp), an outward current developed which consisted of a transient and sustained component, but no fast inward current could be elicited. It was suggested that these results supported the classic interpretation (Shepherd, 1972) of the granule cell function as inhibitory, non-spiking interneurones.

However, several groups have clearly demonstrated granule cell spikes (Wellis and Scott, 1990; Jahr and Nicoll, 1982b; Mori and Kishi, 1982). Granule cell spikes would probably provide for a more extensive output of the granule cell than would a passive, non-spiking granule cell. It has been suggested that the granule cell spike may be necessary for evoking significant self-inhibition in the mitral cells. The apparent passive nature (i.e. non-spiking) of the granule cell might be due to experimental conditions, including anaesthesia, and the composition of buffers used in isolated bulb preparations (Nowycky *et al.*, 1981a,b; Jahr and Nicoll, 1982a,b). In the case of Bufler et al. (1993) the lack of granule cell spikes may have been due to the young age of the animals, the granule cells described may not have been functionally mature and possibly behave differently from granule cells found in the adult.

Wellis and Scott (1990) confirmed the findings of Mori and Kishi (1982) and reported that electrical stimulation of the LOT, as well as orthodromic stimulation of the olfactory nerve layer, induced a response by granule cells. The responses to stimulation of either site were similar and consisted of a depolarising excitatory postsynaptic potential (approximately 30ms in duration) that produced single or multiple action potentials followed by a long hyperpolarisation (~180ms in duration). Reduction of the stimulus intensity below spike threshold produced an EPSP alone.

1.5.3 Recurrent inhibition

A wealth of information has been gathered concerning the reciprocal relationship between the mitral and granule cells. The dendrodentritic reciprocal synapse was first discovered by Rall *et al.* (1966) and was the first of its type found in the mammalian CNS. This was achieved using a computational model constructed from data obtained in intracellular and extracellular unit recordings (Phillips *et al.*, 1963; Shepherd, 1963a). The model was used to identify precisely the timing and placement of the synaptic potentials recorded. The results indicated that the backward spreading impulse in the mitral secondary dendrites is appropriately timed and placed to make these dendrites the presynaptic elements for synaptic excitation of the granule spines. The EPSP in the granule cell spines in turn is appropriately timed and placed to mediate the long-lasting inhibition of the mitral cells.

The depolarisation of the mitral cell dendrite, by spread of an antidromic or orthodromic impulse from the cell body, activates the excitatory synapse onto the granule spine. The EPSP in the spine activates the inhibitory synapse back onto the mitral dendrite. This causes a hyperpolarising IPSP in the mitral dendrite, which suppresses the excitability of the mitral cell until the inhibitory action has worn off. It has been suggested that this sequence of dendrodendritic interactions may provide the basis for the generation of rhythmic activity in the olfactory bulb (Rall and Shepherd, 1968; Freeman, 1975). The generation of the impulse at the soma-axon hillock, with backspread into the dendrites during both orthodromic and antidromic activation was in accord with the classical model of the functional organisation of the neurone. Both actively and passively spreading impulses were tested and found to be adequate for extensively invading the mitral secondary dendrites (Rall and Shepherd, 1968).

The theoretical model was tested physiologically using the isolated turtle brain preparation, which allows for the preservation of intrinsic circuits, by Jahr and Nicoll

(1982b). The presynaptic role of mitral cell dendrites was verified by injecting a mitral cell with a depolarising current resulting in a fast spike followed by a slow IPSP. Tetrodotoxin (TTX) was added to the bathing medium to block Na^+ conductance, this caused the cell to respond with a smaller, slower spike, presumably due to Ca^{2+} conductance. The spike was still followed by the slow IPSP. When bicuculline was also added to the bath, the cell still responded with a spike but the IPSP was eliminated, because the only active mitral cell was the one injected, this experiment shows several critical features: the mitral cell soma-dendrites act as a presynaptic terminal to the granule cell; the circuit is recurrent onto the injected cell; and the inhibitory transmitter is GABA.

This has been supported by experiments in the rat olfactory bulb slice in which the afterhyperpolarisation was abolished by the addition of bicuculline methiodide to the bathing medium, in the presence of TTX (Isaacson and Strowbridge, 1998). The hyperpolarising potential was also blocked by the application of Cd^{2+}, an inorganic Ca^{2+} channel antagonist. Together, these results indicate that the evoked IPSC is mediated by $GABA_A$ receptors and that dendrodendritic inhibition requires voltage-gated Ca^{2+} channels. The release of glutamate from conventional axonal synapses requires strong depolarisation to open high-threshold Ca^{2+} channels that control exocytocis (Dunlap *et al.*, 1995). If a similar mechanism is involved in the olfactory bulb, the propagation of high-amplitude action potentials through the dendrites may be required to activate local Ca^{2+} channels. The dendrites of the mitral cell have been shown to be capable of propagating action potentials with high amplitude and fast timecourse (Isaacson and Strowbridge, 1998; Bischofberger and Jonas, 1997).

Ca^{2+} currents

Mitral cells in a culture preparation were loaded with the fluorescent Ca^{2+} indicator Oregon Green and a single action potential evoked in the mitral cell by the application of a high K^+ solution (Bischofberger and Schlid, 1995). A photodiode

was used to monitor the changes in fluorescence in various locations of the mitral cell following activation, Ca^{2+} transients were seen to occur in the soma, primary and secondary dendrites as well as the distal dendritic tuft.

In most axonal presynaptic terminals only Ca^{2+} chelators with very rapid binding kinetics, such as BAPTA (1,2-bis(2-aminophenoxy)ethane-N,N,N',N'-tetraacetic acid) can completely suppress neurotransmitter release (Adler *et al.*, 1991). By contrast, Ca^{2+} chelators with similar binding affinities but slower binding kinetics such as EGTA, (ethyleneglycol-bis(-aminoethylether)-N,N,N',N'-tetraacetic acid) have little effect on single evoked synaptic responses. This may indicate that the Ca^{2+} channels are very close to the sites of exocytosis, since only chelators with very rapid kinetics are able to intercept Ca^{2+} ions before they are able to trigger transmitter release. In mitral cells, dendrodentritic responses to single voltage steps were virtually absent in the presence of BAPTA. By comparison, mitral cells treated with a similar concentration of EGTA displayed reliable but diminished dendrodendritic inhibition. This suggests that the Ca^{2+} channels that trigger glutamate release are relatively close to the proteins that control exocytocis.

The next step was to look at the subtypes of Ca^{2+} channel involved. Nifedipine, a blocker of L-type Ca^{2+} channels, had no effect on dendrodentritic inhibition. Although at high concentrations nickel is non-specific, at low concentrations it selectively blocks T- and R-type channels (Avery and Johnston, 1996; Randall and Tsien, 1997). Again, nickel only caused a slight reduction in the inhibitory response, indicating that neither T- nor R-type channels were involved. The application of ω-conotoxin GVIA, blocker of N-type channels, reduced dendrodendritic inhibition. Increasing concentrations did not result in a greater reduction in the inhibitory response. However, the inhibition was reduced dramatically with the application of ω-conotoxin MVIIC, which at high concentrations blocks both N- and P/Q type Ca^{2+}

channels. Taken together, these results point to P/Q-type Ca^{2+} channels as being the dominant classes that mediate dendrodendritic inhibition.

1.5.5 Lateral inhibition

The secondary dendrites of mitral cells extend across large regions of the olfactory bulb hence; the influence of a single mitral cell can be extended further, since single granule cells contact multiple mitral cells. This has been suggested to form the basis for lateral inhibition within the olfactory bulb, which is believed to play an important role in odour discrimination (Yokoi *et al.*, 1995; Brennan and Keverne, 1997). Simultaneous recordings of two mitral cells, in rat olfactory bulb slices, were used to determine the extent to which lateral inhibition occurred (Isaacson and Strowbridge, 1998). A depolarising voltage step applied to a mitral cell (cell 1) caused dendrodentritic self-inhibition and also evoked an IPSC in a nearby mitral cell (cell 2). Thus, the release of glutamate from the dendrites of cell 1, due to the voltage step, evoked GABA release that then acted on and inhibited an unstimulated cell, cell 2. The application of APV blocked the self-inhibition of cell 1 and also abolished the lateral inhibition recorded in cell 2. There was partial recovery of both responses following APV washout. These manipulations were performed in the presence of TTX, demonstrating that, in the absence of sodium-dependent action potentials, lateral inhibition could be mediated solely through dendritic interactions between mitral and granule cells.

1.6 Dendritic properties of mitral cells

Sites of impulse initiation.

Simultaneous dendritic and somatic whole-cell recordings from mitral cells in rat olfactory bulb slices have shown that the primary dendrites are capable of the active propagation of action potentials (Bischofberger and Jonas, 1997; Isaacson and Strowbridge, 1998). Irrespective of whether the depolarising current injection was performed at the soma or the distal dendrite, the dendritic action potential lagged

behind the somatic action potential in all recordings. This suggests that the action potential was initiated near the soma and propagated back into the dendrite. The large amplitude and fast timecourse of the action potential was conserved during back propagation into the dendrite, unlike the case with cortical pyramidal neurones (Stuart and Sackmann, 1994). With the addition of the Na^+ channel blocker TTX to the bathing medium, the amplitude of the dendritic action potential was reduced, indicating that voltage-activated Na^+ channels support the back propagation of action potentials into the dendrites. Furthermore, the application of the K^+ channel blocker, tetraethylammonium chloride (TEA), to the bathing medium markedly prolonged the timecourse of the dendritic action potential. Hence, the active propagation of action potentials with large amplitude and rapid repolarisation are supported by the presence of voltage-gated Na^+ and K^+ channels in the membrane of the primary dendrite.

Classical models of impulse initiation dictate that the impulse always arises in the soma-axon hillock region with back propagation through excitable dendrites. However, more recently it has been proposed that the dendrites are sufficiently excitable to initiate impulses that propagate forward along the dendrite towards the soma. An elegant example of the latter has been demonstrated in rat olfactory bulb slices using dual whole-cell recordings at the soma region and distal primary dendrite whilst electrically stimulating the olfactory nerve (Chen *et al.*, 1997). A single shock to the olfactory nerve evoked an EPSP that was consistently larger at the distal recording site, in accordance with the synaptic input being confined to the distal glomerular tuft. When the olfactory nerve stimuli were weak, action potentials were evoked first at the soma and later at the distal dendritic recording site, consistent with the classical theory. However, as the stimulus intensity increased the initial site of action potential initiation shifted to the distal primary dendrite, followed by an action potential at the soma recording site. Both the somatic and dendritic impulses evoked by current pulse injection were blocked by TTX, indicating that these fast action potentials depend on the activation of voltage-gated Na^+ channels.

Similar mechanisms have been described in hippocampal pyramidal cells (Turner *et al.*, 1991). During low intensity synaptic input, action potentials are initiated in the initial segment and invade the dendrites secondarily. With larger inputs, the trigger site as shifted to the dendrite, with subsequent invasion of the soma. The increased stimulus intensity leading to higher levels of synaptic excitation presumably corresponds to stronger odour stimulation, which *in vivo* elicits large amplitude slow potentials across the glomeruli, and large amplitude EPSPs giving rise to burst responses in mitral cells (Wellis and Scott, 1987).

In addition to being dependent on the intensity of synaptic input the impulse initiation site was also influenced by inhibitory input. During weak olfactory nerve (ON) stimulation, the somatically initiated impulse could be blocked by hyperpolarising the somatic membrane, or by an IPSP elicited by a single shock to the EPL. Under moderate ON stimulation hyperpolarisation of the soma membrane caused the site of impulse initiation to shift from the soma to the distal primary dendrite, the same result was obtained by an EPL-evoked IPSP. The IPSP was always larger at the soma than at the distal primary dendrite, due to the passive spread of the IPSP from the dendrodendritic synapses located at the lateral secondary dendrites and soma. This shows that in a range of EPSP amplitude where the impulse is usually initiated in the soma region, proximal inhibitory input can shift the impulse origin for the same EPSP to the distal dendrite and change the direction of impulse propagation in the dendrite from backward to forward.

Thus, it appears that both the excitatory synaptic input at the distal dendritic tuft and the granule cell inhibition via dendrodendritic synapses close to the soma can influence the site of impulse initiation and direction of impulse propagation. This provides a means by which the mitral cell can overcome inhibition at the soma, ensuring that the distal tuft continues to actively respond to excitatory input despite the shutdown of impulse output in the axon. Even under these conditions, the

dendritic impulses could allow for local Ca^{2+} influx, enabling the distal dendrites to continue to be involved in local processes such as dendritic release of transmitters. These mechanisms are likely to play an important role in sensory responses under physiological conditions.

Fast pre-potentials

Chen *et al.* (1997) noticed a further feature of the somatic action potential, a fast prepotential, a classic indicator of distal dendritic excitability first shown in hippocampal pyramidal cells (Spencer and Kandel, 1961). In the case of hippocampal neurones the fast prepotential was described as being an "abrupt potential step which sometimes appears at the foot of hippocampal neurone spikes. It is a relatively small potential change, being about one-third as large as the A spike" (Spencer and Kandel, 1961). The term "fast prepotential" is used to distinguish it from slower prespike potentials that occur in the hippocampal neurone during antidromic and orthodromic stimulation (Kandel *et al.*, 1961). In their experiments, Spencer and Kandel (1961) made intracellular recordings of hippocampal neurones in anaesthetised adult cats. They found that spike generation occurred both with and without the prepotential however, there was nothing corresponding to a fast prepotential in either the antidromic spike or in the directly evoked spike. Since Spencer and Kandel (1961) were unable to demonstrate the fast prepotential during antidromic activation, it was thought unlikely that the fast prepotentials arose from the axon, as is the case for M spikes in motoreurones (Brock *et al.*, 1953; Coombs *et al.*, 1955). It is difficult, on theoretical grounds, to account for activation of spike-like responses in either the axon or the soma under conditions of soma hyperpolarisation, because this hyperpolarisation would prevent soma and dendritic synapses from discharging an axonal or somatic spike generator. A trigger zone in the axon might be discharged during soma hyperpolarisation if there were sufficient synapses on the initial segment to produce critical axon depolarisation. No such axo-axonal synapses have been described for hippocampal neurones, therefore by a process of elimination, it appears

that the most likely site of origin of the fast prepotential is neither in the axon nor the soma, but probably at some point within the dendritic tree of these cells. Due to the small amplitude of the fast prepotentials it seems reasonable to presume that the active membrane responsible for the fast prepotential does not extend to the soma and that probably a passive area of membrane lies in between.

In a separate study Chen and Shepherd (1997), whilst stimulating the olfactory nerve in olfactory bulb slices, again noticed the presence of fast prepotentials when recording from mitral cells. In most cases this prepotential triggered a full sized action potential, but in some instances it appeared in isolation. The prepotentials displayed a short duration and all-or-nothing nature, indicating that they were due to impulse activity rather than synaptic potentials. The isolated prepotential resisted large hyperpolarising currents, suggesting that it was initiated at a location electrotonically remote from the recording site at the soma. The small amplitude and resistance to soma membrane hyperpolarisation suggest that this fast pre-potential may be generated in a distal portion of the primary dendrite, possibly in the dendritic tuft within the glomerulus.

1.7 Olfactory coding

Functional units

The basic logic underlying olfactory sensory perception has remained elusive. The inference that the glomerulus represents a functional unit has been drawn on the basis of its rather discretely organised input and the punctuate distribution of glomerular activation in response to odours. The 2-deoxyglucose (2DG) autoradiographic method first showed how a map of metabolic activity, induced in neurones by sensory stimulation, could provide information about spatial distribution of activity across the glomeruli (Sharp *et al.*, 1975; 1977; Stewart *et al.*, 1979; Jourdan *et al.*, 1982). The patterns of activity tend to be bilaterally symmetrical and differ with different odours. The patterns for a given odour occur in the same

glomerular domain in different animals; the weakest odour concentrations elicit activity in one or a few glomeruli, reflecting input from the olfactory cells with the highest-affinity receptors for that odour. Whereas, the strongest stimuli elicit activity more widely within a domain, reflecting input from cells with lower-affinity receptors. A study using Ca^{2+} sensitive dyes in the zebrafish has clearly demonstrated the different patterns of glomerular activation related to different amino acid stimuli. The properties of these patterns are virtually identical to those from the 2DG studies in mammals (Friedrich and Korsching, 1996). Activation of individual identified glomeruli (Teicher *et al.*, 1980; Lancet *et al.*, 1982) has supported a variety of anatomical and molecular evidence that the glomerulus is a functional unit in the processing of odour stimuli.

Electrophysiological studies have been performed in rabbits to analyse the responses of mitral cells to stimulation with a homologous series of odour compounds (Mori *et al.*, 1992). The recordings were made from functionally identified regions of the glomerular sheet allowing for the systematic analysis of responses to wide range of chemically related compounds. The spectrum of odour molecules that can activate a given mitral cell was called the cells 'molecular receptive range (MRR)'. The mitral cells all showed narrow MRRs, with responses to only two or three neighbours in a given series of compounds from C2 to C12. These results provide the first evidence that odours are mapped spatially in the olfactory bulb.

With the evidence that the fundamental units of odour information are sets of odour determinants processed by individual glomeruli, Yokoi *et al.* (1995) tested for the role of the dendrodentritic microcircuits in processing that information. It was noted in the previous paragraph that the response of a mitral cell to a homologous series is limited to 2-3 neighbouring members of the series. A characteristic finding was that the members immediately adjacent to these compounds elicited inhibition of

the mitral cell. This appears to be analogous to the contrast enhancement that characterises the receptive field properties of cells in other systems. Instead of spatial contrast to enhance edge discrimination between light and dark fields as in the visual system, it involves the molecular determinant contrast to enhance detection between differing odours. Application of bicuculline abolished the inhibition, indicating that it is mediated by $GABA_A$ receptors, further evidence suggested that this GABAergic inhibition is mediated by the interactions of granule cells with the mitral/tufted cells (Yokoi *et al.*, 1995)

The experiments outlined provide the most direct evidence that a critical role of the dendrodendritic *lateral inhibition* of mitral cells by granule cells is to enhance contrast between the activity of mitral cells transmitting information about different odour stimuli. In view of the evidence for the action of the glomerulus as a functional unit, it is reasonable to hypothesise that the contrast enhancement occurs between mitral cells relaying information from different glomeruli. These mechanisms are likely to play a critical role in the ability to carry out odour discrimination.

Anatomical units

Intracellular injection of Lucifer Yellow has revealed neuronal dye coupling in the developing rat olfactory bulb (Paternostro *et al.*, 1995). The dye-filled primary dendrites of mitral cells were seen to extend through the EPL and ramify into glomerular tufts. The dye-coupled cell groups comprised discrete clusters of mitral cells and underlying columns of granule cells. The number of dye-filled granule cells was significantly increased in P30 rats compared to P20, and the distribution of filled granule cells also showed age related differences. At P10, most filled granule cells were found 60-140 μm below the mitral cell layer, whereas at P30 the majority of granule cells were found much closer to the mitral cell layer, 0-60μm beneath. There was no evidence for dye-coupled neurones following injections of Lucifer

Yellow into the extracellular space near the mitral cell layer, suggesting that the dye coupling required a cell-to-cell pathway. The immunocytochemical localisation of the gap junction protein, Cx43, is found in high concentration within the olfactory bulb. In the glomerular layer, Cx43-like immunoreactivity (Cx43-LI) was scattered throughout the glomeruli both inside and out. Considerably less Cx43-LI was found in the external and internal plexiform layers and weaker still was the staining in the mitral and granule cell layers (associated with cell body profiles). At the electron microscopic level, adjacent perikaryal membranes of mitral-to-granule and mitral-to-mitral cells established typical gap junctions. Gap junctions between neurones are thought to form functional networks of cells exhibiting co-ordinated activity patterns. However, the study concentrated on the developing olfactory bulb and did not address the question of how prominent this neuronal coupling is in the adult olfactory bulb.

1.8 Olfactory learning

The dendrodentritic synaptic microcircuit has emerged as an attractive model for examining the factors underlying plasticity at single synapses. Olfactory learning is not restricted to early development, since it has been shown that adult female mice learn the odour of an impregnating male. If she is subsequently exposed to a male from a different strain to the stud male, the pregnancy is blocked due to reduction of LH and impairment of ovarian steroidogenesis necessary for supporting pregnancy. This phenomenon is known as the "Bruce effect" (Bruce, 1959), where the female has formed an olfactory memory for the stud male.

Selective destruction of the vomeronasal organ prevented pregnancy block in mice but ZnSO4- induced damage of the olfactory epithelium did not (Lloyd-Thomas and Keverne, 1982). This strongly suggests that the effect is mediated via the vomeronasal system and its connections to the accessory olfactory bulb. The anaesthetic lignocaine was infused locally at the first two relays in the accessory

pathway, i.e. the AOB and the medial amgydala (Kaba *et al.*, 1989). When infused into the AOB recognition did not occur and the stud male blocked his own fertilisation. However, infusion into the medial amygdala did not prevent memory formation and only strange males blocked the pregnancy. These results indicate that the memory formation occurs in the AOB itself, the first relay in the pathway. There is a critical period over which this imprint is formed. If a female mouse is immediately removed after mating and then returned to the stud male 6h later, the pregnancy is blocked (Rosser and Keverne, 1985). Therefore, not only does recognition require mating but also a critical period after mating spent with the stud male, in order for subsequent recognition. Once formed, the memory lasts for 30-50 days (Brennan *et al.*, 1990).

Noradrenergic projections to the AOB have been implicated in the recognition process (Keverne and De La Riva, 1982). Selective lesions, using infusions of the neurotoxin 6-hydroxy-dopamine (6-OHDA), which acts to severely depletes the AOB of noradrenaline (> 70%), prevents memory formation for the stud male. Mating induces a significant increase in noradrenaline turnover in the MOB and AOB but not in the cortex of the mouse (Brennan *et al.*, 1990). The increased activity lasts for up to 4h after mating, correlating with the exposure time to pheromones required for memory formation. At 48h after mating the female is re-exposed to the stud male and there is no increase in noradrenaline turnover, implying that increased activity in noradrenaline terminals is not necessary for memory recall.

Intracellular recordings in the turtle olfactory bulb (Jahr and Nicoll, 1982a) show that noradrenaline reduces the inhibition exerted by granule cells on the mitral cell. This leads to sustained excitation of mitral cells. This effect can be mimicked by the application of a GABA antagonist such as bicuculline. In theory, if the inhibition of mitral cells is prevented by bicuculline for a period of 4h a memory trace should be formed without mating taking place. This hypothesis was tested by

Kaba *et al.* (1989) who found that an olfactory memory was formed, but it was not entirely specific. At least one other strain as well as the stud male was recognised, making this a more general recognition. These results could be due to the GABA blockade releasing inhibition on all mitral cells whereas noradrenaline release may activate only a subset of mitral cells.

Similar mechanisms have been implicated in a different recognition process. Olfactory cues from infants play an important role in enabling the inexperienced mother to recognise the offspring at parturition and facilitate the onset of maternal behaviours. It has also been revealed that there is a potential for increased sensitivity to certain odours at certain critical periods in an animal's life. A good example of this is seen in the sheep: before parturition, relatively few neurones in a given region of the bulb respond to lamb odours, but after parturition many more neurones can be found to be responsive to lamb odours in that same region. This is correlated with massive increases in bulbar transmitter release, where higher levels of glutamate and GABA (released from intrinsic neurones), and acetylcholine and noradrenaline (released from centrifugal terminals) have been measured (Kendrick *et al.*, 1992).

Summary

The output from the olfactory bulb is carried by the axons of the "principal neurones", the mitral and tufted cells. The mitral/tufted cell primary dendrite provides the exclusive pathway from receptor input (in the glomeruli) to olfactory output in the efferent projection of the olfactory bulb. Local neural circuits and centrifugal afferents that terminate within the granule cell layer of the olfactory bulb influence the activity of mitral/tufted cells. Furthermore, interactions between subpopulations of both the output neurones and principal interneurones provide multiple pathways for the processing of olfactory information and this information is transferred between ipsilateral and contralateral hemispheres resulting in a complex and highly organised system through which odourant information is processed.

Outline of thesis

A neural connection exists between the olfactory bulb and the supraoptic nucleus of the hypothalamus and this pathway has been shown to be active at the time of parturition (Meddle *et al.*, 1998). The projection from the olfactory bulb to the supraoptic nucleus is via the lateral olfactory tract, which is formed from the axons of the principal neurones the mitral and tufted cells.

This thesis set out to confirm the connection between the olfactory bulb and the supraoptic nucleus by electrically stimulating the lateral olfactory tract and studying the distribution of Fos-positive cells. Two different stimulation protocols were used to determine whether the nature of lateral olfactory tract activation was important in the excitation of supraoptic neurones. Extracellular recordings were made *in vivo* to characterise the spontaneous discharge patterns of the olfactory neurones and to study the effect of lateral olfactory tract stimulation on these firing patterns.

Administration of morphine during parturition interrupts the progress of parturition by inhibiting oxytocin release. The olfactory bulb shows dense expression of mu- and kappa opioid receptors, and so the possibility that morphine may impair oxytocin release in part by blocking the input from the olfactory bulb that is active during parturition was considered. The effects of morphine and of a selective kappa antagonist on the spontaneous activity of mitral cells *in vivo* and *in vitro* were therefore tested to assess the likely impact of morphine on output activity of the bulb.

Chapter 2

General Materials and Methods

2.1 Animals

Female Sprague Dawley rats, body weights 250-350g (Bantin and Kingman, UK) were used in all *in vivo* experiments; rats with weights of 50-150g were used for *in vitro* experiments. Animals were randomly taken at different stages of their oestrous cycles. The rats were housed under controlled conditions, ambient temperature 21-23°C with a 12h light/12h dark cycle, food (standard breeder diet, Bantin and Kingman, UK) and water *ad libitum*. Rats were acclimatised for 1-2 weeks after arrival before use in experiments.

2.2 Anaesthesia

Urethane

For non-recovery experiments rats were anaesthetised with urethane (ethyl carbamate; 25% weight/volume solution, Sigma, UK). A single intraperitoneal (i.p.) dose of 1.25g/kg produced the required level of anaesthesia for the duration of the experiments.

Xylocaine

To supplement non-recovery anaesthesia, Xylocaine 2% (Lignocaine hydrochloride BP, Astra pharmaceuticals Ltd, UK) was applied sub-cutaneously at sites of surgery.

Halothane

A gaseous mixture of 5% halothane BP (May and Baker, U.K.), oxygen (47.5%: BOC, Glasgow Ltd) and nitrous oxide (47.5%: BOC, Glasgow Ltd) was delivered from an anaesthetic machine with the flow rate set at 600ml/min. The anaesthetic agent was allowed to accumulate in a perspex container into which the rat was placed for administration of the initial dose. Anaesthesia was maintained throughout surgery by inhalation from a sealed perspex box, attached to a stereotaxic frame with separate delivery/extraction tubing.

Sagatal

For non-recovery experiments involving the immunocytochemical processing of tissue for Fos, Sagatal BP (sodium pentobarbitone, 60mg/ml; Rhone Merrieux Ltd, Harlow, U.K.) was used in preference to urethane due to the effect of urethane inducing c-*fos* expression. A single i.p. dose of 60mg/kg produced the required level of anaesthesia and this was maintained by additional i.p. doses of 0.1-0.2ml as required. This was the anaesthetic agent used to terminate an experiment, administered as either an i.v. or i.p. overdose injection.

2.3 Surgical Preparation

2.3.1 Cannulation of the jugular vein

Cannulae tubing (1.0mm o.d, 0.5mm i.d; Altec, UK) cut into approximately 15cm lengths were connected to 1ml polypropylene syringes (Steriseal, Worcestershire, UK) and filled with 0.9% saline. The tip of the cannula was cut at an angle of 45° to aid insertion into the blood vessel. The rat was placed on its back and a small horizontal incision was made to one side of the midline of the neck. The skin was gently pulled away from the edge of the incision by inserting the closed blades of a pair of scissors and slowly opening them to expose the underlying musculature. A pair of blunt forceps was used to tease apart the musculature and connective tissue, revealing the branches of the jugular vein.

Sharp forceps were used to remove fatty tissue and two silk ligatures (EP2; Davis and Geck, Lancashire, UK) were placed around the major trunk of the vein. The distal ligature was tightened to prevent venous return. A small incision was made proximal to this ligature and the cannula inserted approximately 2cm into the length of the vein. If blood could be drawn back, the proximal ligature was tightened to secure the cannula in place and prevent blood loss. The wound was closed with 3-4 sutures (EP2).

2.3.2 Dorsal surgery

Following the cannulation of the jugular vein ear bars were fitted and the rat positioned in a stereotaxic frame. A midline incision was made and the underlying tissue scraped clear of the skull surface. The stimulating electrode was placed above bregma and using the vernier scale the electrode was moved 4.0mm lateral and 3.2mm anterior to be positioned over the LOT (Paxinos and Watson, 1997). These co-ordinates were thought to be a reasonable distance from the olfactory lobe thereby preventing direct spread of electrical current from the stimulation site into the area which we were recording from. It is also the point at which the LOT is at its broadest.

A hole was drilled (round 3 burr) at this site and the dura carefully removed to allow easy penetration of the stimulating electrode. In all *in vivo* experiments a side-by-side bipolar stimulating electrode was used (Clark Electromedical Instruments, UK). The stimulating electrode was lowered until it was seen to bend slightly, indicating it had reached the ventral surface of the skull. The electrode was subsequently raised 0.5mm to be positioned within the LOT.

A larger area of skull was removed, using the drill, over the ipsilateral olfactory lobe, the position of the olfactory lobe was judged by observing the suture lines on the rostral portion of the skull surface. The dura was carefully removed in a small area of the exposed olfactory bulb to prevent breaking the electrode tip when inserting the electrode into the bulb. If a large area of the dura was lifted away, the tissue tended to vibrate due to the blood pressure and result in unstable recordings.

2.3.3 Morphine dependence and tolerance

Morphine sulphate BP (The Royal Infirmary, Edinburgh) was dissolved in sterile water and filtered (Millex-GV, 0.22μm filter unit; Millipore Corp., USA) to give a stock solution of 50mg/ml. The osmotic mini-pump (1μl/h, Alzet 2001; Alza

Corp.,USA) was filled with the stock solution and left to prime in sterile 0.9% saline overnight at room temperature. The remaining stock solution was used to make dilutions of 20mg/ml and 10mg/ml, which were contained in eppendorfs and stored at 4°C. The infusion assembly consisted of a stainless steel cannula made from a 1cm length of 21 gauge tubing bent at 90° 4.5mm from its tip and bevelled at 45°. This was attached to an 18cm length of coiled polythene tubing (1.2mm o.d., 0.76 i.d.; Portex Ltd, Kent, UK) and stored in 70% alcohol.

Female Sprague-Dawley rats were anaesthetised with 5% halothane, body weights recorded, and the scalp shaved. The rats were placed in a stereotaxic frame and the level of anaesthesia maintained throughout the surgical procedure. A longitudinal midline scalp incision was made and the sub-cutaneous tissue scraped clear of the skull surface. The needlepoint attached to the stereotaxic frame was lowered to the point of bregma and then lambda to ensure the skull was level. Using lthe Vernier scale the needlepoint was moved 3.0mm posterior and 2.0mm right lateral relative to bregma and the surface marked with a 23-gauge needle. A 1.0mm diameter hole was drilled (round 2 burr) at this site for the insertion of the infusion cannula. Two 1.3mm holes were drilled (round 3 burr) clear of the cannula hole to hold two stainless steel support screws (3.2mm x 10 BA).

The infusion set-up was filled with 40µl of the 20mg/ml solution and 40µl of the 10mg/ml solution, separated by a 1µl air bubble. The 100µl Hamilton syringe (Sigma, UK) was left connected to the infusion tubing supported by a retort stand and the whole assembly was positioned close to the skull. The infusion cannula was inserted vertically through the guide hole so that its tip lay in the right lateral cerebral ventricle, 4.0mm below the skull surface. The cannula was fixed into position by a mound of dental acrylic (Simplex Rapid; Associated Dental Products Ltd, Swindon, UK) bonded to the two stainless steel screws which were anchored to the skull. Care

was taken to prevent the dental acrylic from covering bregma, as this was needed as a reference point in the next stage of the experiment. A pouch was produced in the subscapular space and the mini-pump placed subcutaneously. The Hamilton syringe was detached from the infusion tubing and the cannula connected to the mini-pump. The wound was closed with 3-4 sutures. The animal would receive increasing doses of morphine sulphate over the next 5 days (10μg/h for 40h, 20μg/h for 40h and 50μg/h for 40h), increasing the degree of tolerance (Bicknell *et al.*, 1988).

2.3.4 In vitro slice preparation

Female Sprague Dawley rats (50-150g) were anaesthetised with halothane (placed in a sealed perspex container with a piece of cotton wool soaked with halothane). A sufficient level of anaesthesia was determined by a lack of the limb withdrawal reflex to a paw pinch. Once anaesthetised, the rats body weights were recorded and then they were decapitated using a small animal guillotine. The head was cleared of musculature and skin and a rapid craniotomy was performed. The skull was cut in half (coronally) and the remaining bone removed with fine bone rongeurs. The forebrain and olfactory bulbs were quickly and carefully removed and placed in aerated (95% O_2, 5% CO_2 gaseous mixture, BOC, Glasgow Ltd, UK) ice cold artificial cerebrospinal fluid (aCSF). The aCSF medium comprised of (in mM); NaCl 124, KCl 3, NaH_2PO_4 1.25, $CaCl_2$ 2, $MgSO_4$ 1.3, $NaHCO_3$ 26 and D(+)-glucose 10 (Chen and Shepherd, 1997). All the above chemicals were obtained from Sigma, UK.

The tissue was placed on a cold dissecting stage and the brain was cut along the midline to separate the olfactory lobes. The tissue block was trimmed so that a small part of the forebrain remained attached to the bulb to provide support during the cutting process. The ventral surface of the bulb was fixed to the advancing stage with cyanoacrylate glue (Permabond, UK) and immersed in a reservoir of ice cold medium. It took no longer than five minutes to reach this stage from decapitation.

The reservoir was secured in position in the Vibroslice (Campden Instruments, Loughborough, UK) and approximately 1mm was trimmed off the dorsal surface of the bulb. Successive slices of olfactory bulb were cut in a horizontal plane at a thickness of 400μm and placed into aerated ice cold medium.

The slices were floated onto a moistened fine bristle paintbrush and transferred to the ramp of an Haas type interface recording chamber (fig. 2.1), that was positioned on an anti-vibration table. The slice lay on a fine mesh in the recording chamber with its undersurface in contact with aCSF delivered to (and removed from) the chamber at a rate of 1.5ml/min by means of a 2-channel peristaltic pump (Gilson, France). The effluent was drained into a waste flask, it was not recycled. Conditions inside the chamber were kept at 33±0.2°C and the slice was continuously perfused with aCSF. A continuous stream of 95% O2 and 5% CO2 gas saturated with water vapour was passed over the slice to provide the tissue with oxygen and keep it moist. A fine strand of cotton wool was carefully placed over the slice, this helped draw the medium over the surface of the slice and prevent the slice drying out. Slices were left to incubate in the chamber for at least an hour before recording commenced.

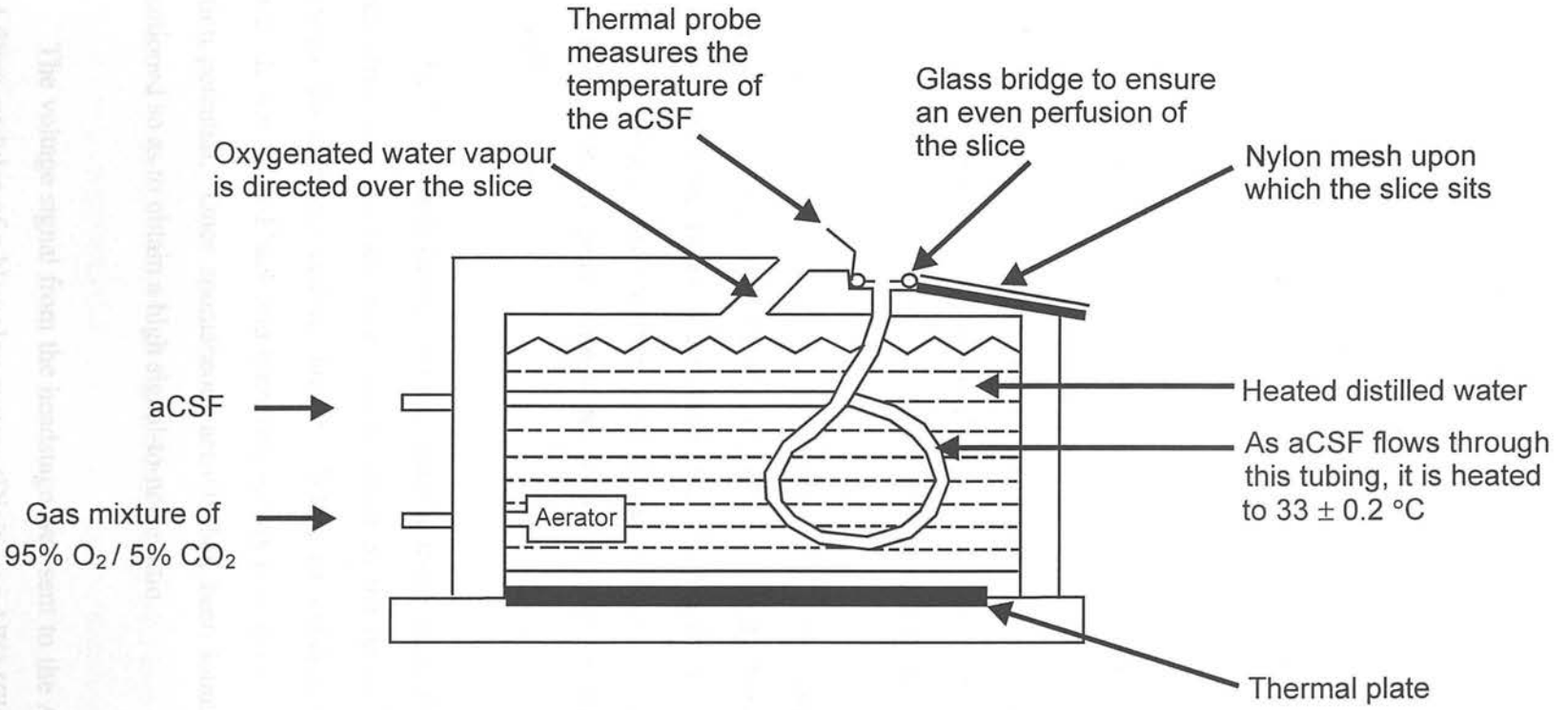

Figure 2.1. Schematic diagram of the Haas type interface chamber. The olfactory bulb slices were placed on the nylon mesh of the ramp and superfused with aCSF and oxygenated water vapour and maintained at a temperature of 33 ± 0.2°C during the *in vitro* recordings.

2.4 Recording extracellular activity

2.4.1 In vivo experiments

Recording electrodes were made from glass capillary tubing (1.5mm o.d x 0.86mm i.d, Clark Electromedical Instruments, UK) and produced using a microelectrode puller (Narishge, Japan). The electrodes were filled with physiological saline (0.9% NaCl) using an electrode filler (World Precision Instruments Inc., USA). The electrode tips were gently wiped before being positioned in the arm of the hydraulic micro-drive (David Kopf Instruments, USA), giving them a resistance of approximately (20-40)MΩ. A silver wire connected to the headstage of the Neurolog system (Digitimer Ltd) was inserted into the shaft of the microelectrode. The tip of the electrode was placed on the surface of the bulb under visual control using a binocular dissecting microscope (Zeiss, Germany).

The stimulator (Grass Medical Instruments, USA) was programmed to deliver a biphasic pulse at a frequency of 0.5Hz (unless stated otherwise) to the stimulating electrode which was positioned in the LOT. The amplitude of the current pulse was controlled using constant current units (Grass Medical Instruments); the amplitude was 1mA peak to peak, unless the antidromic spike exhibited an all-or-none threshold potential.

The microelectrode was lowered into the tissue using the remote control of the micro-drive and the field potentials observed as the tip of the electrode advanced through the different cellular layers. When an antidromic spike was seen the electrode was moved back and forth very slowly to attempt to pick up a spontaneous action potential. Once spontaneous activity had been found the electrode tip was positioned so as to obtain a high signal-to-noise ratio.

The voltage signal from the headstage was sent to the AC preamp (x100 gain) and filter modules of a Neurolog system (Digitimer, UK) (filtering of the signal was

kept to a minimum: low frequency cut-off, 500Hz; high frequency cut-off, wide band; 50Hz notch activated). The amplified and filtered signal was viewed on a storage oscilloscope (Gould, UK) and fed to the spike processor (Digitimer, UK). The spike processor controlled the audio amplifier and also the trigger level, the trigger level was essentially a window with an upper and lower limit. The amplitude of an extracellular action potential needed to be greater than the lower limit (set so as to exclude background noise) but less than the upper limit (set to exclude the stimulus pulse or sudden noise).

A pulse was triggered each time the action potential appeared in the window and these were fed to a CED 1401 Plus analogue-to-digital (A/D) interface (Cambridge Electronic Design, UK) linked to a PC (Akhter, 486). The recording was viewed on-line using the Spike2 capture programme and analysed off-line using the Spike2 for Windows programme (Cambridge Electronic Design, 1996).

2.4.2 In vitro experiments

Extracellular recording electrodes were made from glass capillary tubing (1.5mm o.d x 0.86 i.d) and pulled on a microelectrode puller (Palmer, BioScience, Washington). The electrodes were filled with 2M sodium gluconate using an electrode filler and all air bubbles were removed by gently tapping the capillary tubing. Electrode tips were gently wiped before being inserted into a perspex microelectrode holder (which contained a silver/silver chloride wire) and attached to the headstage of the Axoclamp 2B amplifier, this gave them a resistance in the range of 15-20MΩ. The chamber was illuminated by a fibre optic light source (Flexilux, Germany). Electrodes were lowered under visual control using a binocular dissecting microscope (Wild M3 Heerbrugg, Kent, UK) into the mitral cell layer of the olfactory bulb this was clearly visible as a dark, translucent band in the slice.

The microelectrode was advanced into the tissue using a hydraulic micromanipulator (Intracel, UK) until a spontaneous extracellular action potential was encountered which appeared over and above the background noise and increased in amplitude as the microelectrode approached the cell. The microelectrode tip was positioned so as to obtain a high signal-to-noise ratio with an extracellular action potential of sufficient amplitude that could be easily discriminated. The voltage (x10 gain) signal from an Axoclamp 2B (Axon Instruments, USA) was delivered to a Neurolog system (Digitimer, UK) containing a filters module (low frequency cut-off 500Hz; high frequency cut-off 5000Hz; 50Hz notch activated), a high gain (x100) AC amplifier and an audio amplifier. The extracellular signal, filtered and amplified, was monitored on a storage oscilloscope (Gould, UK) and fed to a spike triggering module of the Neurolog system. To distinguish the extracellular action potential from the background noise the trigger level was set to a level of amplitude greater than that of the background noise but below that of the extracellular action potential. A TTL pulse was triggered each time the action potential crossed the discriminated level and these were fed to a CED 1401 Plus analogue-to-digital (A/D) interface (Cambridge Electronic Design, UK) linked to a PC (Dell, Pentium II) running a spike collection programme (Spike2, Cambridge Electronic Design).

Aliquots (500µl) of stock solutions for the drugs used were made up in distilled water and frozen until used. The test solutions of each drug were made up by diluting the stock solution in oxygenated aCSF immediately before use, and applied to the slices by switching the perfusion inlet to the appropriate reservoir containing the drug.

2.5 Retrograde labelling

A 1% solution of a fluorescent retrograde tracer (Fluoro-Gold, Fluorchrome Inc., USA) was prepared in double distilled water. The solution was contained in an eppendorf, covered with foil to protect from light and stored at 4°C. Rats received an

initial dose of anaesthetic by being placed in a perspex box into which 5% halothane flowed. The anaesthetic was delivered in a gaseous mixture of nitrous oxide and oxygen at a flow rate of 600ml/min. The percentage of halothane in the gaseous mixture could be varied between 0 and 5%, enabling the experimenter to keep the rat in a desirable state of anaesthesia.

Once the rat had reached a sufficient level of anaesthesia it was removed from the box, its body weight recorded and scalp shaved. The rat was then transferred to a stereotaxic frame and the level of anaesthesia maintained throughout the surgical procedure. An incision was made along the midline of the scalp and the connective tissue scraped away to expose the surface of the skull. A needle point attached to the arm of the frame was lowered to bregma and then lambda to ensure the skull was level. Injection sites were located by measuring co-ordinates from bregma (Paxinos and Watson, 1997), SON 0.9mm posterior, 1.9mm lateral and 9.0mm dorsoventrally, amygdala region 3.8mm posterior, 4.0mm lateral and 9.0mm dorsoventrally. Each rat received a unilateral injection of Fluoro-Gold (FG) into either the vicinity of the SON or the amgydala region. A 1.0mm hole was made using a dental drill (round 2 burr) and a guide cannula attached to the arm of the frame was lowered to the required depth. An electrode filler was attached to a 25µl Hamilton syringe containing the FG solution. The electrode filler had been cut so that it was just seen to exit the guide cannula, this was to prevent the tracer from being drawn up the cannula rather than being ejected into the brain tissue. The electrode filler was inserted into the guide cannula and the syringe clamped into position. A volume of 1µl FG was injected and then the guide cannula was withdrawn very slowly over a period of 30min to minimise uptake of tracer by damaged fibres of passage.

Once the guide cannula had been removed the wound was closed with 3-4 sutures (EP 2). Following surgery rats were placed into a clean cage, quickly recovered from the anaesthetic and were seen to roam the cage 10min after surgery.

A survival time of 2-7 days is recommended for transport of the tracer (Fluorochome Inc.), after which the rats were used in further experiments.

2.6 Intracardial perfusion

Rats were administered a lethal dose of Sagatal (approximately 0.7-0.8ml), when the rat failed to respond to pinching of the toe it was considered ready for perfusion. An incision was made through the abdomen wall just below the rib cage and the diaphragm cut to expose the beating heart. The thoracic cavity was opened up by cutting through the rib cage on either side of the heart; the cut rib flap was folded headward and clamped in position. A blunt hypodermic needle (15-gauge) was inserted upward through the left ventricle until it was visualised approximately 5mm inside the ascending aorta. A nick was made in the right atrium to allow an escape route for the blood and perfusion fluid.

The perfusion system consists of a 15-gauge needle connected to a length of tubing that is looped into a peristaltic pump; the other end of the tubing is placed into a flask containing the perfusion solution. The rat was perfused with heparinised saline (5000IU heparin (Multiparin, CP Pharmaceuticals Ltd, UK) in 1L of 0.9% saline) until the effluent became clear. The pump was stopped and the fixative (4% paraformaldehyde in 0.1M phosphate buffer) introduced into the perfusion line, approximately 400ml were passed through the rat. When the fixative entered the animal, twitching of the muscles occurred indicating the perfusion was proceeding correctly and the limbs started to stiffen.

Once the fixation process had been completed, the brain was carefully removed from the skull and post-fixed overnight in a solution of 4% paraformaldehyde (Sigma, UK) and 15% sucrose. The brain was then transferred to a solution of 30% sucrose in 0.1M phosphate buffer for 24h or until the brain had sunk. The sucrose

acts as a cryoprotectant and prevents fracturing of the tissue when it is frozen. The brains were placed on tinfoil and frozen on powdered dry ice, and stored at -70°C.

2.7 Fos Immunocytochemistry (ICC)

The expression of Fos, the protein product of the immediate-early gene c-*fos*, is used extensively as an indicator of neuronal activation (Hoffman *et al*, 1993). The unlabelled antibody peroxidase anti-peroxidase (PAP) method was developed by Sternberger *et al.* (1986) to overcome the inherent background caused by non-specific binding, thereby increasing sensitivity of direct labelled antibody methods. The availability of secondary antibodies pre-complexed to peroxidase has led to further development of this method. The primary antibody is specifically raised against the desired protein antigen. The secondary antibody functions immunologically by attaching to the primary antibody, as it has two identical binding sites, one reacts with the secondary site of the primary antibody, the second is conjugated to the marker, typically horseradish peroxidase. The label is produced by a chemical reaction in which hydrogen peroxidase is the substrate and 3,3'-diaminobenzidine (DAB) is the electron donor, to yield a brown insoluble product. An N-terminally selected rabbit polyclonal anti-Fos (c-*fos* Ab-2, Oncogene Sciences, Cambridge Bioscience, UK) antibody was raised to a peptide that corresponds to residues 4-17 of human Fos and reacts with human and rodent cellular forms of Fos. Part of the N-terminal of the Fos protein has little homology to Fos related antigens and, therefore, this antibody has a high specificity and will not recognise these related antigens.

In our methodology, we use the glucose oxidase-diaminobenzidine-nickel intensified method developed by Shu *et al.* (1988) to visualise the Fos expressed as a result of electrical stimulation of the lateral olfactory tract. This method has a greater sensitivity and results in a more intense staining of the Fos protein compared to the direct hydrogen peroxide/diaminobenzidine method previously used. Glucose

oxidase and glucose act as the substrate and DAB is the electron donor. This chemical reaction yields more electrons per peroxidase molecule and therefore, more reaction product is deposited around the peroxidase complex. In the presence of nickel, the DAB chromogen turns black, therefore, a darker and denser product is deposited around each bound antibody complex. Fos is located discretely in the nucleus and when labelled by this method, appear as densely labelled purple/black nuclei, which are easily visualised by light microscopy.

2.7.1 Processing tissue for Fos ICC

Day 1

Fos ICC was performed on free-floating tissue, sectioned using a freezing slide microtome (Leica, UK) at an optimal temperature of -21 to -22 °C. Coronal brain sections were cut (52μm) and collected in petri dishes of phosphate buffer (PB). Sections were washed in a solution of phosphate buffer and 0.2% Triton X-100 (PB-T) for 3x10min to remove excess fixative/cryoprotectant. Triton X-100 is a detergent that acts to breakdown cell membranes allowing for a greater penetration by the hydrogen peroxide block and eventually the primary antibody. During all washing and incubation steps, the sections were gently agitated on a rotational shaker table (Edmund Bühler, Germany). Sections were given a 5min wash in PB prior to the blocking of endogenous peroxidase using the methanol solution. Again, the sections are washed with PB-T (3x10min) and non-specific staining blocked with a wash (1x30min) in the pre-incubation buffer that contains 1% normal sheep serum. The sections were left to incubate in the primary antibody solution (Ab-2 Fos) at 1:1000 dilution in PB-T, for an optimum of 36h at 4°C.

Day 3

The sections were washed in PB-T (3x10min) to remove excess antibody and thereby prevent over-staining of the tissue. The antibody:antigen complex was located using the Vector Stain Elite Kit (Vector Labs, UK). The sections were left to

incubate for 1h in a solution of biotinylated anti-rabbit immunoglobulin, normal goat serum and PB-T at room temperature. Following this initial incubation the sections were washed with PB-T and then incubated for a further 1h in a solution containing Avidin DH, biotinylated horseradish peroxidase and PB-T, at room temperature. This solution was made at least 30min prior to incubation with the tissue to allow time for the formation of the avidin-biotinylated horseradish peroxidase complex. The sections were rinsed in PB-T (2x10min) and 0.1M acetate buffer (1x15min) before the final visualisation steps.

For visualisation of the reaction product, the glucose oxidase-Ni DAB method was used, which has been shown to yield high specific staining with a low background. The DAB solution was prepared and the glucose oxidase added to the mixture immediately prior to use. The sections were carefully monitored throughout the reaction process to ensure control sections remained white while regions of experimental interest developed a black/purple staining. When the desired level of staining had been reached the reaction was terminated by washing the sections in 0.1M sodium acetate (1x15min). The sections were rinsed in PB and stored in petri dishes at 4°C until mounted onto gelatine-subbed slides. The tissue was dehydrated by immersing the slides in ethanol at 70% (5min), 90% (5min), 95% (5min), 100% (10min) and 100% (1min) and then cleared in xylene (BDH). The slides were cover-slipped using either DePeX mountant (BDH) or fluoromount (BDH) if the sections contained fluorescence.

2.7.2 Materials

Heparinised saline

Heparinised saline (5 IU/ml) was prepared by adding 1ml of a 5000 units/ml heparin solution (Multiparin, CP Pharmaceutical Ltd., Wrexham, UK) to 1,000 ml physiological saline (0.9% w/v Sodium Chloride in double distilled water).

4% Paraformaldehyde in 0.1M PB

1.15% w/v Disodium Hydrogen Orthophosphate 2-hydrate ($Na_2HPO_4.2H_2O$ AnalaR; BDH)

0.272% w/v Sodium Dihydrogen Orthophosphate 1-hydrate ($NaH_2PO_4.H_2O$ AnalaR; BDH)

4.0% w/v Paraformaldehyde (CH_2O, Sigma)

This solution was then adjusted to pH 7.3-7.4 with 1M HCL or 1M NaOH

Phosphate buffer (PB)

Stock solution (1M) was prepared in double distilled water (ddH_2O) and contained:

11.5% w/v Disodium Hydrogen Orthophosphate 2-hydrate ($Na_2HPO_4.2H_2O$ AnalaR; BDH)

2.72% w/v Sodium Dihydrogen Orthophosphate 1-hydrate ($NaH_2PO_4.H_2O$ AnalaR; BDH)

This solution was then adjusted to pH 7.3-7.4 with 1M HCL or 1M NaOH

The stock solution was diluted 1:10 in ddH_2O to give the 0.1M PB

Washing solution (PB-T)

0.2% v/v Triton X-100 in 0.1M PB

Hydrogen Peroxide solution

0.1M PB contained:

20% v/v Methanol (CH_3 OH AnalaR; BDH)

0.3% w/v Hydrogen Peroxide (H_2O_2 AnalaR; BDH)

Pre-incubation buffer

0.1M PB contained:

0.3% v/v Triton X-100

1% v/v Normal Sheep Serum (NSS) (Scottish Antibody Production Unit, UK)

Primary antibody

Rabbit anti-Fos (c-fos Ab-2, Oncogene Sciences, Cambridge Bioscience, UK) diluted (1:1000) (1µl/ml) in pre-incubation buffer

Secondary antibody

Goat anti-rabbit IgG-peroxidase complex (Vectastain Elite ABC Kit, Vector Labs, UK) diluted (1:100) (10µl/ml) in 0.1M PB-T and 3% v/v normal goat serum

Avidin-biotinylated horseradish peroxidase complex (ABC)

Avidin DH and biotinylated horseradish peroxidase complex (Vector Stain Elite Kit, Vector Labs, UK) each diluted (1:50) (20µl/ml) in 0.1M PB-T.

This solution was left to incubate for at least 30min prior to use

Acetate buffer (0.2M)

1.64% w/v Sodium Acetate Anhydrous ($CH_3.COONa$; BDH)

This solution was prepared in ddH_2O and adjusted to pH6.0 using acetic acid

Visualisation solution

Acetate buffer containing:

0.4% w/v Glucose ($C_6H_{12}0_6$ AnalaR; BDH)

0.08% w/v Ammonium Chloride (NH_4Cl AnalaR; BDH)

0.003% w/v Glucose Oxidase (b-D-glucose: oxygen 1-oxidoreductase; EC 1.1.3.4, $O(CHOH)_4CHCH_2OH$, type VII-S from *Aspergillus niger*; Sigma)

2.5% w/v Di-Ammonium Nickel (II) Sulphate 6-hydrate [$(NH_4)_2SO_4.NiSO_4.6H_20$ (AnalaR; BDH)]

0.025% Diaminobenzidine (DAB) (3,3',4,4'-Tetraaminobiphenyl, tetrahydrochloride, $C_{12}H_{14}N_4.4HCl$; Sigma)

To prepare 100ml of the visualisation solution: nickel sulphate, glucose and ammonium chloride were dissolved in 50ml of 0.2M acetate buffer and DAB was

dissolved in 50ml of ddH_2O. After the nickel and DAB solutions were mixed well and filtered the glucose oxidase was added immediately prior to use.

Chrome alum gelatine

1% w/vol. gelatine powder (BDH)

0.1% chromic potassium sulphate (BDH)

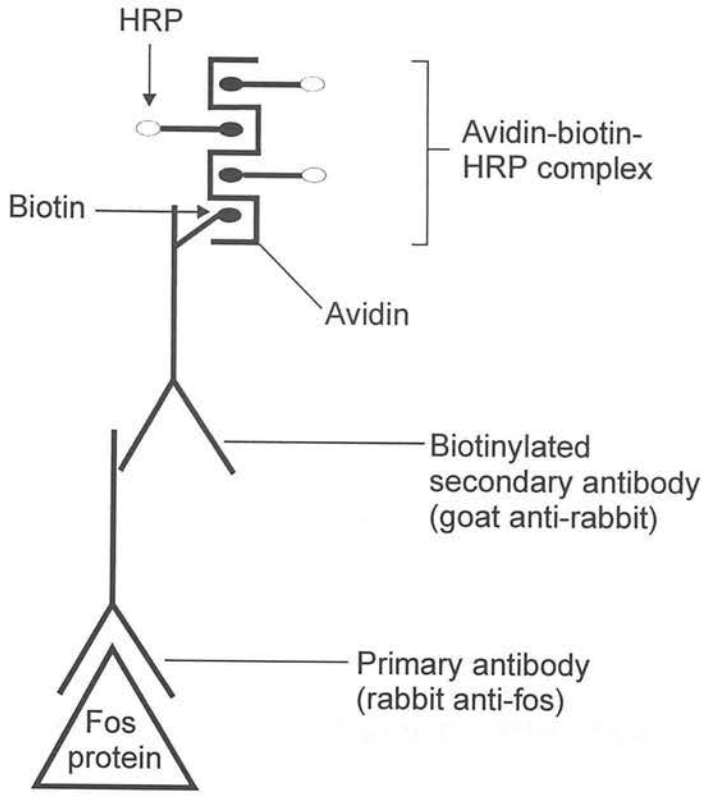

Figure 2.2. Diagram to show the complex formed during the ABC method of immunocytochemical localisation of Fos protein in rat brain sections. Firstly, the sections are incubated, for an optimum of 36h, with a primary antibody raised against the antigen (Fos protein). This primary antibody is developed in the rabbit, the second incubation involves an antibody that is raised against rabbit immunoglobulins (in the goat), and the secondary antibody is labelled with biotin (black circles). An avidin-biotin-horseradish peroxidase complex is prepared and time given to allow saturation of the complex before it is applied to the tissue. This complex recognises and binds to the biotin labelled secondary antibody. The final step is the visualisation step, in our methodology we used the glucose oxidase-diaminobenzidine-nickel intensified method. The reaction product is deposited round the peroxidase molecules (white circles), in the presence of nickel the diaminobenzidine chromagen turns black, creating an easily distinguishable marker of Fos-positive cells. Abbreviations: HRP, Horseradish peroxidase.

Chapter 3

Firing Characteristics of Olfactory Bulb Neurones

3.1 INTRODUCTION

Despite the wealth of study on the olfactory bulb, there has been surprisingly little attention paid to the basic discharge characteristics of the output cells *in vivo*. Before considering the effect of electrical stimulation of the output cells on target cells, it is essential first to consider what frequency or pattern of stimulation provides an effective increase above spontaneous ongoing activity.

3.1.1 Mitral cell discharge patterns

Yu *et al.* (1993) described the spontaneous firing patterns of mitral cells recorded *in vivo* from urethane anaesthetised rats. Units were located by the reversal in polarity of the field potential evoked from the stimulation of the LOT, which is a convenient electrophysiological marker for the mitral cell body layer. Cells were identified antidromically as mitral cells and at the end of pontamine sky blue dye was ejected from the electrode and the cells were histologically verified as being in the mitral cell body layer. The latencies to antidromic activation ranged from 1.0 to 2.2ms (mean = 1.9ms) and the spontaneous firing rates were in the range 5-15Hz. Three spontaneous firing patterns were observed: a) high frequency bursts with relatively long silent periods between successive bursts; b) high frequency bursts not clearly separated by silent periods; and c) continuous firing cells. These differences in firing patterns could not be explained by the influence of nasal airflow, as the experiments were performed on rats with tracheal cannulations.

Reinhardt *et al.* (1981) studied the firing characteristics of olfactory bulb neurones in the miniature pig. The pigs were anaesthetised with Halothane and the mitral cell layer was localised with reference to the zero-isopotential of the evoked field. They concluded that the firing pattern of olfactory bulb cells in the pig is complex, often phasic and unrelated to respiration or sniffing. From the mitral cells recorded the mean latency of antidromic spikes was 2.6ms ± 0.17 (S.E.M.) and approximately 30% displayed a firing pattern consisting of alternating periods of

activity and inactivity. The median burst duration was 2.3 min (range 0.1-16 min), and the median interval between bursts was 2.1 min (range 0.13-12.9 min). They also found that four of the orthodromically-driven cells, which had variable latencies to antidromic stimulation, displayed this phasic discharge pattern.

Motokizawa and Ogawa (1997) recorded from mitral cells in cats anaesthetised with an initial dose of ketamine hydrochloride and maintained under anaesthesia with intravenous urethane-chloralose. Cells were identified as being mitral/tufted cells, following antidromic stimulation of the LOT and from the shape of the evoked field potential. At the end of recordings an anodal d.c current was passed through the recording electrode to mark the site of penetration. The spontaneous activities of mitral cells were classified into four types; three on the basis of the distribution of interspike intervals (INTH) and the fourth as a silent type. The silent type was defined as being responsive to stimulation of the LOT, but with silent periods greater than 1min between successive spikes. The INTH groups were as follows: a) bimodal b) skewed and c) symmetric. The mean interspike interval varying as a function of the spontaneous discharge type, being 112 ± 147ms, 45 ± 48ms and 63 ± 51ms (mean ± standard deviation) respectively. Approximately 90% of the mitral/tufted cells showed either bimodal or skewed distribution, no difference in this distribution was seen in cats under tracheal or nasal respiration. Mitral/tufted cells of the cat olfactory bulb, which showed bimodal and skewed distributions at high frequency, were characterised by a strong tendency to fire in bursts. Mitral/tufted cells occasionally displayed a cluster of spikes synchronised with the respiratory cycle, but the number of unsynchronised units was much greater than that of synchronised units.

To look at the effect of nasal airflow on the discharge pattern of the output neurones the olfactory epithelium was destroyed using zinc sulphate. The mitral/tufted cells retained burst activity but none of these bursts were synchronised

with respiration. The influence of centrifugal fibres on the burst discharge was examined by disconnecting the olfactory bulbs from the telencephalon by surgical lesion of the olfactory peduncle at the border between the bulb and the LOT. The occurrence of burst discharge was confirmed in 60% of units under tracheal respiration and in 70% of units under nasal respiration. The destruction of the olfactory epithelium and disconnection of the olfactory bulb from the hemisphere did not produce a significant change in the frequency distribution of mitral cell firing patterns.

3.1.2 Oscillatory behaviour

In a slice preparation of the rat olfactory bulb, Chen and Shepherd (1997) noticed that the membrane potential of the mitral cell had a subthreshold oscillation (in the range 20-40Hz), which alternates with epochs of clustered action potentials. A computational model developed by Wang (1993) looks at the ionic basis for the generation of intrinsic 40Hz oscillations in neuronal networks. It was postulated that the interplay between a slowly inactivating potassium current and a persistent sodium current was able to produce intrinsic membrane potential oscillation at a frequency of 35-55Hz, with epochs of clustered action potentials, a phenomenon described by Chen and Shepherd (1997) in their olfactory bulb slice. It would seem that the membrane potential oscillation is due to interaction among ion conductances and is therefore an intrinsic membrane property.

However, another theory as to the origin of the oscillation of mitral cell activity is explained by the reciprocal dendrodendritic synapses between mitral cell secondary dendrites and granule cell spines. Through these reciprocal synapses, depolarisation of mitral cells (driven by excitatory input) can activate inhibitory granule cells, which in turn hyperpolarise the mitral cells; this hyperpolarisation attenuates the excitability of the granule cells, causing disinhibition in the mitral cells, i.e. depolarising the mitral cells again (Rall and Shepherd, 1968). Such a cycle

may repeat giving rise to oscillatory activity within the synaptic circuit rather than in individual neurones. It is still unclear which mechanism dominates in the production of the subthreshold oscillation seen in rat mitral cells.

3.1.3 Discharge patterns of granule cells

Much less information has been gathered for the granule cell. Intracellular recordings of granule cell activity by Wellis and Scott (1990) in the rat *in vivo* show that 75% of granule cells exhibited excitatory responses to odourant stimulation (one was found to be inhibited, the remaining cells recorded were not responsive). The rats were anaesthetised with a barbiturate agent and fitted with two tracheal cannulae, one for respiration and the other to control nasal airflow. Stimulating electrodes were positioned over the LOT to activate granule cells via the dendrodendritic synapse and produce the field potential, and an array of seven electrodes was positioned over the olfactory nerve layer far rostral to the recording site for orthodromic stimulation. The response of each cell to both antidromic and orthodromic stimulation was tested before being exposed to an odour.

Odours could produce spiking responses that either occurred after every sniff, the number of spikes produced by each sniff of odour at a particular concentration remained constant and the number of spikes produced was concentration-dependent, or rapidly habituated to the stimulus and only responded after the first sniff. Other granule cells, although capable of spiking in response to electrical stimulation, only showed a depolarisation that did not evoke spikes to odour stimulation. These depolarisations were transient with each sniff or prolonged over a series of sniffs. The odour response latencies of granule cells were found to be relatively constant, beginning approximately 200ms after the onset of the artificial sniff. Increasing stimulus concentration produced shorter latencies. The physiological differences may be related to the morphological differences between the two types of granule

cell found in the granule cell layer. Spiking odour responses were found superficial to most non-spiking responses.

AIMS

The primary aim in this section of the study was to make extracellular unit recordings, *in vivo*, from neurones with cell bodies in the mitral and granule cell layers of the main olfactory bulb, and to establish the spontaneous firing characteristics of recorded cells. Field potentials generated by cell population activity following stimulation of the LOT were used to aid discrimination of the different layers. The LOT is formed by the axons of the output neurones, mitral/tufted cells, so stimulation of the tract results in the antidromic activation of these neurones. The mitral/tufted cells are involved in dendrodentritic reciprocal synapses with granule cells in the external plexiform layer hence, stimulation of the tract would be expected to influence the interneurones of the granule cell layer. To this end, the affect of LOT stimulation on the firing rate and discharge pattern of bulbar neurones was investigated.

It has been suggested that the activity of mitral/tufted cells is influenced by a diverse range of extrabulbar factors such as: air intake cycles (Onoda and Mori, 1980; Motokizawa, 1996; Philpot *et al.*, 1997); ambient odours (Scott and Aaron, 1976; Wilson and Leon, 1987; Buonviso and Chaput, 1990; Kashiwadani *et al.*, 1999); and centrifugal innervation from structures in the forebrain (Nickell and Shipley, 1988; Kunze *et al.*, 1991;) and brainstem (Shipley *et al.*, 1985; Jiang *et al.*, 1996; Okutani *et al.*, 1998). The degree to which these factors influence the discharge pattern of olfactory neurones was studied by removing the source of such factors and recording the unit activity of mitral cells in a slice preparation of the olfactory bulb and comparing the results with those seen *in vivo*.

3.2 METHODS

3.2.1 Surgical preparation

In most respects the methodology employed was as detailed in Chapter 2. Briefly, adult female Sprague-Dawley rats (250 - 350g) were anaesthetised with urethane (i.p. 1.25g/kg body weight) and a jugular cannula inserted. Anaesthesia poses a potentially important influence on olfactory bulb circuits. It has been demonstrated in chronic recordings from rabbits that pentobarbital anaesthesia can change the regularity of neural firing in the bulb, without greatly altering the response form (Stewart and Scott, 1976). It was demonstrated that urethane did not dramatically change the test response (only a weak facilitation) to a pair of pulses delivered to the LOT, compared with the response in the unanaesthetised rat (in the latter case a midcollicular brain stem section was performed). However, when testing rats anaesthetised with barbiturate the test response to the paired-shock stimulation was greatly diminished, also, a single dose of urethane provides a long period of stable anaesthesia (approximately 12h), thus urethane was chosen for these experiments. The rats were placed in a stereotaxic frame and fixed into position using ear bars. Dorsal surgery was performed and the stimulating electrode positioned within the LOT and the recording electrode lowered into the dorsally exposed, ipsilateral main olfactory bulb (fig. 3.1).

3.2.2 Verification of stimulation site

In initial experiments the position of the stimulating electrode was verified by removing the brain following completion of the experiment and fixing it in 4% paraformaldehyde. Sucrose was added to the fixative solution (to act as a cryoprotectant) along with potassium ferrocyanide and potassium ferricyanide (BDH). The brains were then left in this solution for two days, a procedure that stains the tract yellow. The brain was cut on a freezing slide microtome and the sections (52μm) were mounted on gelatine subbed slides. The slides were cover-slipped using DPX mountant and viewed using a binocular microscope under a low

objective (x10); photomicrographs (fig. 3.2) were taken using a Leica macroscope and camera system. The brain section in the photomicrograph is faint due to the tissue not being counterstained however, the tract is still clear.

3.2.3 Experimental design

Stimulation of the LOT consisted of a biphasic pulse; width 0.1ms, at a frequency of 0.5Hz (fig. 3.1). Evoked field potentials were used as an indication of recording depth. The mitral cell layer is identified by the isopotential (fig. 3.3B) and the granule cell layer is recognised by the distinct positive phase as the second component of the field potential (fig. 3.3C). Antidromic identification of mitral cells required that the cell responded to the stimulation with a constant latency spike furthermore, the stimulus-evoked spike was required to collide with a spontaneous spike (fig. 3.4). In the double recordings electrodes were placed into a dual headstage and positioned so that the tips were close together (approximately 100μm apart). Each electrode was controlled by a separate remote micromanipulator. One electrode was moved into the proximity of a mitral cell before the second electrode was moved in an attempt to minimise disturbance to recordings.

3.2.4 Data analysis

Data was analysed offline using the Spike2 analysis programme (Cambridge Electronic Design, 1986). Oscilloscope traces were printed online and scanned into a PC (Dell, Pentium) at a later date. The firing rate of cells was used as the measure of cell activity. When a cell displayed phasic activity the length of the burst and inter burst time were also calculated.

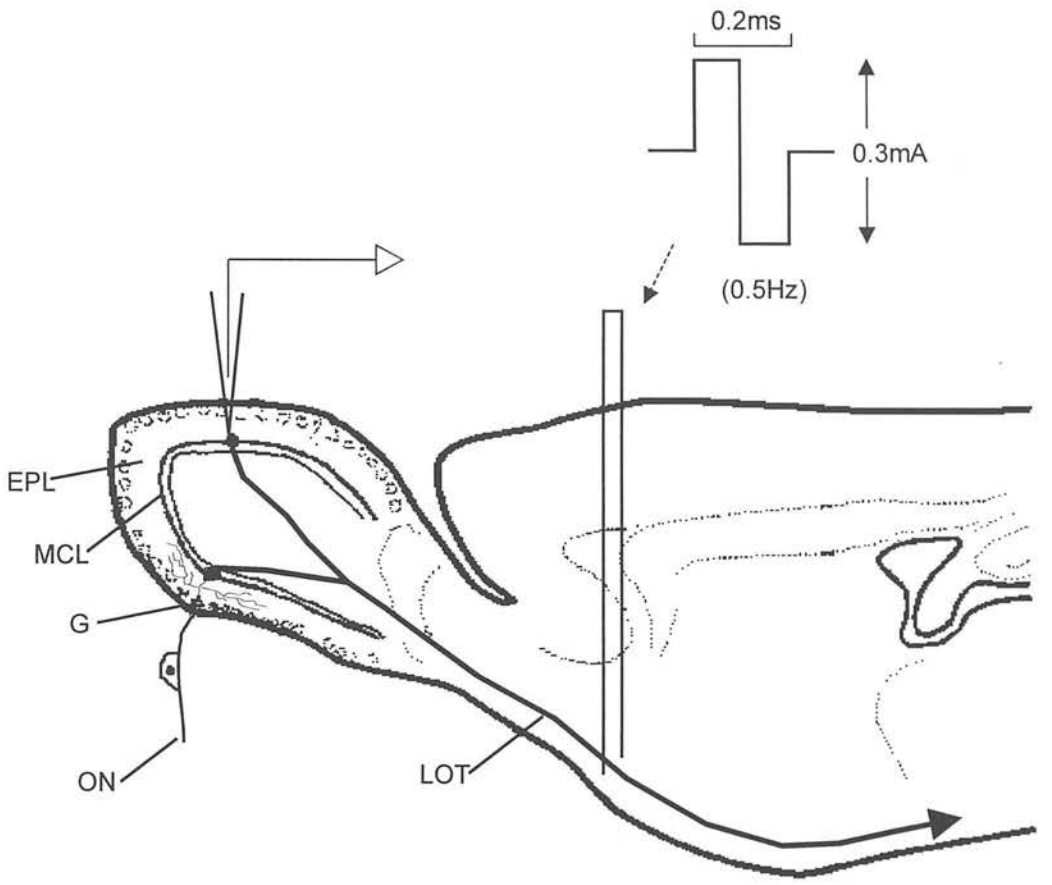

Figure 3.1. Schematic diagram illustrating the position of the stimulating and recording electrodes for the antidromic identification of mitral cells and the generation of bulbar field potentials. Extracellular recordings were made from cells located in the mitral cell and granule cell layers of the dorsally exposed main olfactory bulb. A stimulating electrode was positioned within the LOT for the antidromic activation of mitral cells and to evoke field potentials to aid discrimination of cellular layers. The parameters of the stimulation are indicated. Abbreviations: EPL, (external plexiform layer); G, (glomerulus); LOT, (lateral olfactory tract); MCL, (mitral cell layer); ON, (olfactory nerve).

Figure 3.2. Serial coronal reconstruction of rat brain, based on the atlas of Paxinos and Watson (1997) showing the accepted electrode positions within the lateral olfactory tract (LOT). The co-ordinate of each section (mm anterior to bregma) is indicated in the top right of each section. The inset photograph of a 52μm brain section stained with potassium ferrocyanide and potassium ferricyanide shows an electrode tract in the LOT.

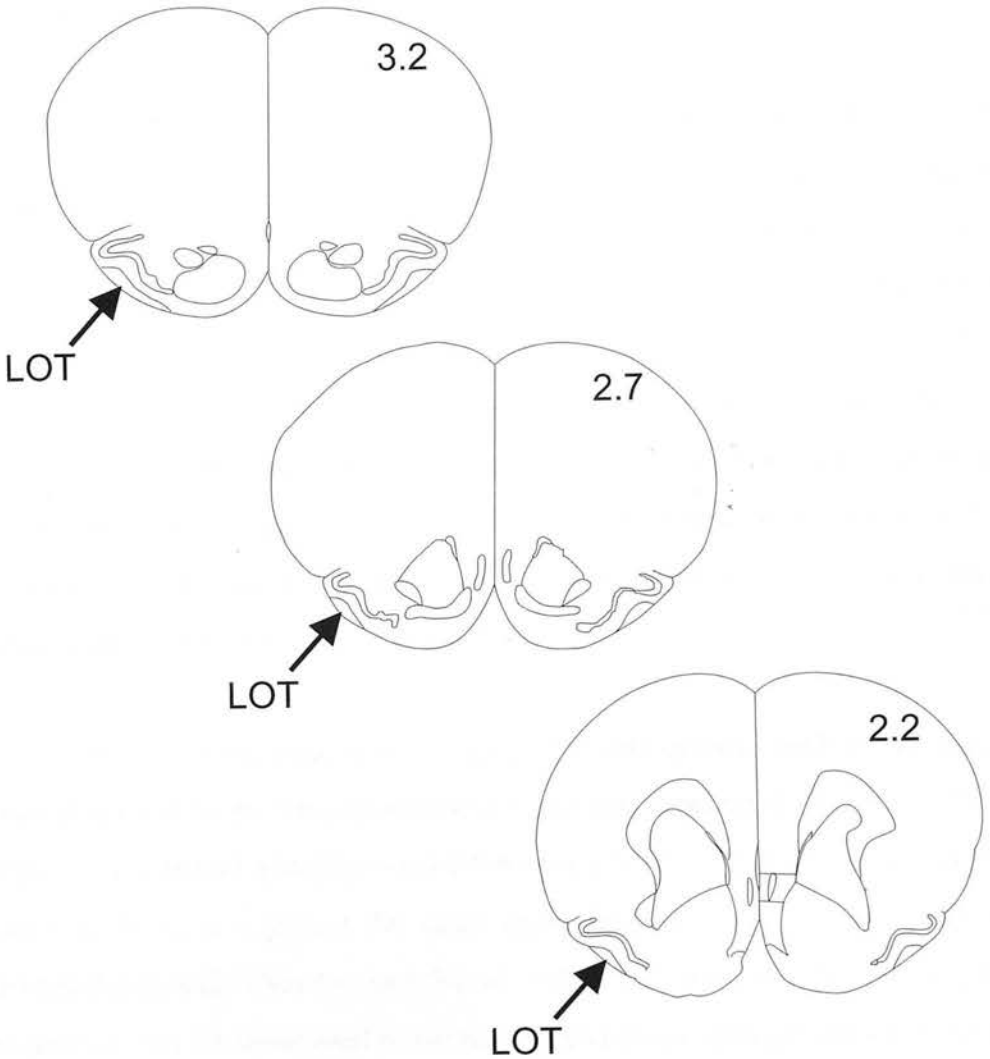

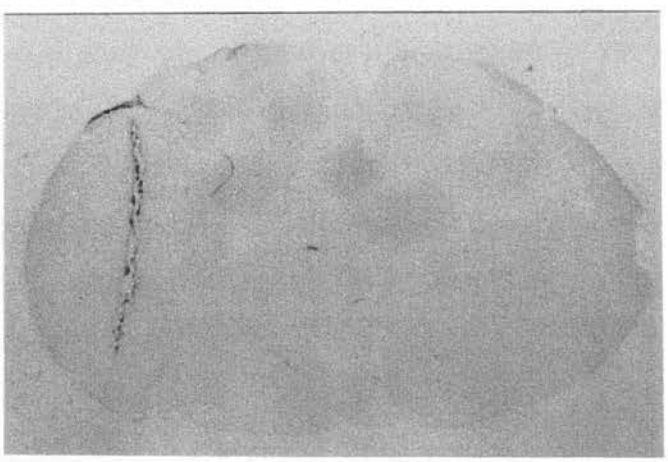

2mm

3.3 RESULTS

3.3.1. Electrical activity

Data are presented for 137 olfactory neurones recorded extracellularly from 50 rats. Eighty-nine cells were antidromically identified as mitral cells showing onset latencies for antidromic activation in a range of 1.0ms to 5.8ms (mean ± S.E.M. = 2.72 ± 0.19ms) (fig. 3.4) with a threshold stimulus intensity for production of an antidromic spike between 0.1mA and 0.5mA (mean ± S.E.M. = 0.3 ± 0.06mA). These cells were all recorded from the depth of the olfactory bulb where the isopotential was seen (fig. 3.3B). Cells localised within the granule cell layer (n=39) did not show a constant latency response to stimulation of the LOT and were recorded from the region of olfactory bulb that displayed the evoked field potential characteristic of the granule cell layer (fig. 3.3C).

Spikes recorded from mitral cells (15%) and granule cells (5%) showed a distinctive notch in the descending phase of the action potential (fig. 3.5). The peak height of the notched waveform varied between 0.7mV and 2.5mV (mean ± S.E.M. = 1.26 ± 0.19mV, n = 9) and the spike width (measured at 1/3 amplitude) varied between 0.3ms and 1.0ms (mean ± S.E.M. = 0.64 ± 0.11ms, n = 9). The position of the notch during the downward phase was not consistent amongst the spikes recorded however, the notch was more frequently seen at the bottom of the repolarising phase. All other spikes were positively directed in a biphasic waveform displaying peak heights of between 0.3mV and 2.4mV (mean ± S.E.M. = 1.18 ± 0.13mV, n = 29) and spike widths of between 0.3ms and 1.0ms (mean ± S.E.M. = 0.57 ± 0.04ms, n = 29). The width was measured at 1/3 amplitude rather than 1/2 amplitude in order to compare results with spike widths measured at 1/3 amplitude for magnocellular cells of the SON (Mason and Leng, 1984).

All mitral cells displayed a phasic firing pattern with either distinct silent periods between peaks of activity or were continuously active with periods of

decreased activity between peaks of high firing. Forty-seven cells showed a spontaneous, phasic firing pattern containing silent periods (fig. 3.6A), these neurones fired with an intra-burst firing rate between 7.1spikes/s and 27.7spikes/s (mean ± S.E.M. =14.26 ± 1.1spikes/s) and an activity quotient of 21%-77% (mean ± S.E.M. = 50 ± 3%). Periods of activity occurred at a relatively constant periodicity, mean burst length between 50.20s-302.70s (mean ± S.E.M. =121.72 ± 10.11s) and an inter-burst time in the range of 39.05s-251.13s (mean ± S.E.M. = 128.64 ± 11.49s). The remaining cells (n=42) were phasically firing but with no clear silent periods between peaks of high activity (fig. 3.6B), displaying a mean firing rate of between 3.38-31.32 spikes/s (mean ± S.E.M. = 13.04 ± 1.45 spikes/s). Again, the bursts of increased activity occurred with a relatively constant periodicity, mean burst length in a range of 26.64-291.85s (mean ± S.E.M. = 102.80 ± 6.57s) and an inter-burst time in the range of 13.04-273.51s (mean ± S.E.M. = 62.77 ± 8.19s). A small number of cells (n=9) displayed phasic firing patterns similar to those described for mitral cells, but could not be antidromically identified. All the cells recorded from the granule cell layer, as indicated by the shape of the evoked field potential, showed a constant rate of firing in the range of 2.23-21.36s (mean ± S.E.M. = 10.64 ± 0.1 spikes/s). There were no periodic increases in the firing rate as was seen in the mitral cells (fig. 3.6C).

3.3.2 Periodicity of olfactory neurone firing

Several analytical methods were used to breakdown the firing patterns into their constituent components, thereby providing a better understanding of the electrical activity of olfactory bulb neurones.

3.3.2.1 Event correlation histograms

An event correlation shows the likelihood of an event occurring before or after an event that has been set as the trigger for a sweep of analysis. In this type of histogram the trigger event is a spontaneous spike that performs a sweep of analysis

over a specified time period before and after it has occurred. Each spike generates a sweep of analysis; a spike that falls within a sweep is not ignored hence there is an overlapping of analysis periods. The sweeps are accumulated to produce the histogram, the larger a count in a bin the greater the probability of finding an event at that time delay. The correlation of a spike with itself at time zero is ignored. This is known as an auto-correlation histogram.

Auto-correlation histograms constructed from a 5min period of mitral cell spontaneous activity show how regularly the bursts of activity occur. Eighty-two of the eighty-nine mitral cells recorded were analysed with auto-correlation histograms (the seven not tested did not have a sufficiently long period of spontaneous activity). The example in figure 3.7 is of a single mitral cell, with all auto-correlation plots taken from the same period of spontaneous activity of this cell. On the largest timescale with sweeps of activity covering a period of 250s either side of each individual spike, it is clear that this is a phasic cell without defined periods of silence between the peaks of activity. The histogram indicates that there is an increased probability of the cell firing at a time delay of 100s, this then starts to decline again after about 200s. This suggests that the cell is firing in bursts of activity that last for 100s and is then relatively quiet for 100s before the proceeding burst.

Equivalent histograms were constructed for granule cells (thirty two of the thirty nine granule cells recorded were analysed, again the cells not tested did not have a sufficiently long period of spontaneous activity from which the histogram could be constructed). The auto-correlation of granule cell activity over a long timescale shows a very different picture. The number of events in successive bins does not alter greatly over the 250s time period, there is approximately a 20% fall in the number of events between 1 and 200s. This indicates that there is a slightly lower probability of spikes occurring at longer time intervals from a spike but not variable enough to constitute phasic activity.

On a smaller timescale of the autocorrelation histogram, a sweep of analysis covering an 8s-time period, there are a further series of peaks evident in the histograms of both cell types. The peaks of activity are highly regular and were well defined in both mitral (n=60/82) and granule cells (n=19/32), in the remaining cells it was difficult to discriminate the peaks. In the histograms where the peaks are easily discernible it can be seen that three peaks occur in a two-second-time period. In the final set of histograms shown in figure 3.7 the timescale is in the millisecond range and a distinct peak of activity occurs between time zero and 10ms in the mitral cell histogram that is absent from the granule cell histogram.

3.3.2.2 Dual recordings

To determine whether the gross phasic discharge pattern of mitral cells described was a global phenomenon throughout the bulb or if it was due to local circuits the firing pattern of two individual mitral cells were recorded simultaneously. To look at the correlation between the phasic activity of mitral cells dual recordings (n=6) of two individual cells were made from six rats. By lowering the recording electrode dorsoventrally it passes through the mitral cell layer twice and in the dual recordings the two cells were not always from the same layer. It was found that the bursting activity between two mitral cells was only loosely correlated. Only one of the six pairs of phasically firing mitral cells showed any consistent synchrony in their bursts (fig 3.8A) both of these cells were recorded from the superficial mitral cell layer. Cross-correlation histograms (fig. 3.9) were constructed from 900s of cell activity a period incorporating three bursts from each cell. The histograms were drawn at two time-scales, the largest time-scale (250s either side of zero) correlates the bursts of activity whilst the smaller time-scale (1.5s either side of zero) correlates the spike activity between the two different cells. The pair of mitral cells that appears to fire bursts of activity at the same time; at the largest time-scale it can be seen that one cell is lagging behind the other (lag time = 26.3s). Even though there is a slight lag time between the two mitral cells they both have peaks of activity and

troughs within the same period of time. At the shorter time-scale the correlation of the cells firing spikes is slightly out of phase.

The other pairs of cells exhibited bursts that drifted in and out of synchrony occasionally firing a burst at the same time. In the example shown in figure 3.8B both mitral cells were again recorded from the superficial mitral cell layer. Cross-correlation histograms constructed for this pair of mitral cells over a 900s period incorporates 4 bursts from one cell and three bursts from the second cell. The resulting histograms are shown in figure 3.9B; at the largest time-scale one cell is lagging the other over a slightly longer time period (37.4s) than that described for the pair of mitral cells in 3.9[A]. Unlike the two mitral cells that appear to fire bursts of activity at the same time, at the largest time-scale this pair of mitral cells do not peak and trough within the same time period. Whilst one cell displays a peak of activity the other shows a trough. At the shorter time-scale there is no correlation between the two cells, demonstrated by the flat lines of the histogram.

3.3.2.3 Fourier transforms

Fourier analysis is a mathematical procedure used to determine the collection of sinewaves (differing in frequency and amplitude) that is contained within, and makes up the wave pattern under consideration. The analysis procedure requires the number of bins in the histogram to be a power of two in the range 16 to 4096. The bin width in the histograms is 0.1s and 256 bins were used for the analysis, therefore a period of 25.6s of auto-correlation data for each cell type was studied. The mean of the individual Fourier transforms for mitral (n = 58) and granule cells (n = 32) (fig. 3.10) show the range of frequencies at which sinusoids occur and are displayed on the ordinate axis; the amplitude of the sinusoids is represented on the abscissa. Prominent sinusoids within the wave occur as peaks of high amplitude against a background 'noise' level.

Both mitral and granule cell plots show prominent peaks around a relative frequency of 38. This suggests that within a 25.6s period a cycle of a sine wave occurs thirty eight times, this calculates as a frequency of 1.48Hz and agrees well with the peaks seen in the auto-correlation histogram that occur with a frequency of three in 2s (1.5Hz). These peaks are thought to be due to an influence by respiration, the peaks seen in the Fourier transform close to a relative frequency of 40 are probably due to variations in the respiratory rate (the mean respiratory rate was measured as being 89 breaths/min). The plot for mitral cells shows two further peaks, at frequencies of 2.4Hz and 2.9Hz that may have been caused by skipped breaths.

Figure 3.11 shows the spontaneous activity of mitral and granule cells over a short time period (2.5s) and demonstrates the bursting nature of the olfactory neurones. Both cell types under the respiratory influence fire groups of spikes that result in the auto-correlation plots and Fourier transforms already described. The mitral cells show an additional bursting nature in that within the clusters of spikes are successive spikes with very short intervals (< 10ms). This second form of bursting behaviour displayed by mitral cells is clearly evident in the interspike interval histograms of their spontaneous activity (fig. 3.12).

3.3.3 Interspike interval distributions

A useful method of investigating spike distribution in individual neurones is to plot the intervals between successive spikes in a frequency histogram, with ranges of interspike intervals on the ordinate axis and the occurrence of that interval range on the abscissa. This is known as an interspike interval histogram (INTH).

Interspike interval histograms generated from 5min periods of spontaneous activity from different mitral cells show two patterns of spike distribution, 57% of mitral cells recorded displayed a bimodal INTH; the remaining 43% showed one

frequency mode (fig. 3.12). The modal interspike intervals for the bimodal mitral cells varied from 3ms to 8ms (mean ± S.E.M. = 5.2 ± 0.2ms) for the first mode and between 12ms and 38ms (mean ± S.E.M. = 20.3 ± 1.03ms) for the second mode. The cells that displayed one mode in the interspike interval histograms showed modal interspike intervals in a range between 5ms and 56ms (mean ± S.E.M. = 23.2 ± 1.9ms). The skew of the histograms varied between 0.5 and 10.5 (mean ± S.E.M. = 3.2 ± 0.31).

Cells recorded from the granule cell layer did not display the bimodal firing frequency described for the mitral cells. There are fewer events in the interval periods between zero and 10ms, the interval period over which the high frequency mode occurs. Events that do occur in this period do not form a distinct mode. The INTH for granule cells show modal interspike intervals of 4ms to 62ms (mean ± S.E.M. = 21.2 ± 2.9ms). The skew of the histograms for these cells was in the range of 0.1 to 5.3 (mean ± S.E.M. = 1.86 ± 0.24). Bar charts show the range of values for the mean and modal interspike intervals of the two cell groups and also the skew of the interspike interval distribution (fig. 3.14). A comparison of the relationship between the modal interspike interval and the mean interspike interval for mitral and granule cells (fig.3.15) shows that although there is some degree of overlap between the two cell types, mitral cells more frequently display spike distributions with short duration mean and modal interspike intervals.

3.3.4 'Poisson' distributions

The tail of the histograms (the time period between 30 and 40ms) of mean interspike intervals for the two different mitral cell distributions and for granule cells were fitted with an exponential curve (fig. 3.13). If spikes are generated by a random (Poisson) process then the interspike interval distribution should be an approximate 'Poisson' distribution - described by the area under a negative exponential curve. Both of the mitral cell distributions and the granule cell distribution follow an

exponential decay from intervals of 20ms (this is the peak of the histogram and the peak of the second mode in bimodal mitral cells) and longer intervals thereafter. The number of spikes that occur at shorter intervals than 20ms in the single mode mitral cell and granule cell distribution are below the exponential curve, whereas the first mode of the bimodal mitral cells occurs well above the exponential curve. This indicates that spikes that occur within 20ms or less from each other have an influence over proceeding spikes and firing is not randomised. Once the distribution begins to follow the exponential curve then the firing can be described as random, with no influence over cell activity. This is further demonstrated in hazard plots of mitral and granule cell activity.

In exponential decay the time taken to decay to half the initial amount present is called the half-life. It does not depend on the initial amount present and is determined solely by the rate constant of decay. The half-life was measured from the histograms by reading the value on the x-axis that corresponded to half the value on the y-axis at which the curve intercepted. The granule cell distribution showed a half-life of 18ms; the mitral cell (one mode distribution) of 20ms and the mitral cell (bimodal distribution) of 18ms.

3.3.5 Hazard functions

Hazard functions of the mean interspike intervals give the probability of cell firing per millisecond after a spike (at time 0), given that another spike has not occurred earlier and is a measure of excitability. Thus, it offers a demonstration of the time over which the preceding spike has an influence over the cell firing again. The point at which the distributions plateau indicates that the preceding spike no longer has any influence on cell firing. Hazard functions are constructed by analysing the interspike interval histograms that are arranged in 1ms bins. The hazard is calculated for each bin of data by dividing the number of events in that bin

by (the total number of events in the histogram minus total number of events that have occurred previous to the bin under analysis).

Hazard functions have been constructed for both mitral (n = 44) and granule cells (n = 25) (fig. 3.16) the mitral cell plot is composed from the two plots labelled i) and ii) which are the two different interval distributions displayed by mitral cells. Immediately after an action potential firing is minimal for both cell types and this represents the period of post-spike hyperpolarisation. After this initial period the probability of firing increases above the plateau line (between 15 and 45ms) indicative of a depolarising after potential. The hazard function of the mitral cell population differs from the granule cell population in that there are two peaks of increased probability above the plateau line; the additional peak in the mitral cell plot occurs between 4 and 10ms. Once a plateau level has been reached the probability of firing is the same for both cell types and from this point on, the preceding spike no longer has an influence over cell firing. This point should correspond to the point in the exponential curve at which the distribution begins to follow an exponential rate of decay i.e. random firing of spikes since the preceding spike no longer has any influence over cell firing. There is a slight discrepancy in the numbers here (at intervals of approximately 20ms in the exponential fits and at intervals of approximately 40ms in the hazard plots). This is caused by the exponential curves 'sagging' slightly, they do not give a perfect fit to the tail of the distribution (fig. 3.12).

3.3.5 Instantaneous frequency

When the ratemeter recordings of mitral cell activity (from mitral cells that display bimodal interval distributions) are re-drawn as instantaneous frequency plots (1/interspike interval) the two firing frequencies are seen to occur in each burst of activity (fig. 3.17). Furthermore, there is a clear separation of the two frequency modes; the low frequency is in a range of 0-50 Hz and the high frequency is in a

range of 100-250Hz, with a band of little activity clearly demarcating the two frequencies. On closer inspection, in 84% of phasic periods of activity there is a delay in the range of 8.82s to 128.77s (mean ± S.E.M. = 30.9 ± 2.48s) before the high frequency component becomes apparent. Without plotting the instantaneous frequency histogram it is not obvious that the cell is firing at two different frequencies since there is very little change in the mean firing rate during the burst. Oscilloscope traces of spontaneous spikes show that the bursts consist of 2-6 spikes, the peak height decreasing with each spike in the burst. This phenomenon has not been observed in granule cell recordings.

Figure 3.3. Evoked field potentials (EFPs) recorded from: [A] the external plexiform layer; [B] the mitral cell layer and; [C] the granule cell layer of the main olfactory bulb during stimulation of the LOT. The field potential for each layer consists of three components that represent current sources and sinks. Notice the reversal of polarity of field potential components. An isopotential occurs at the level of the mitral cell layer. Abbreviations: EPL, (external plexiform layer); GCL, (granule cell layer); MCL, (mitral cell layer).

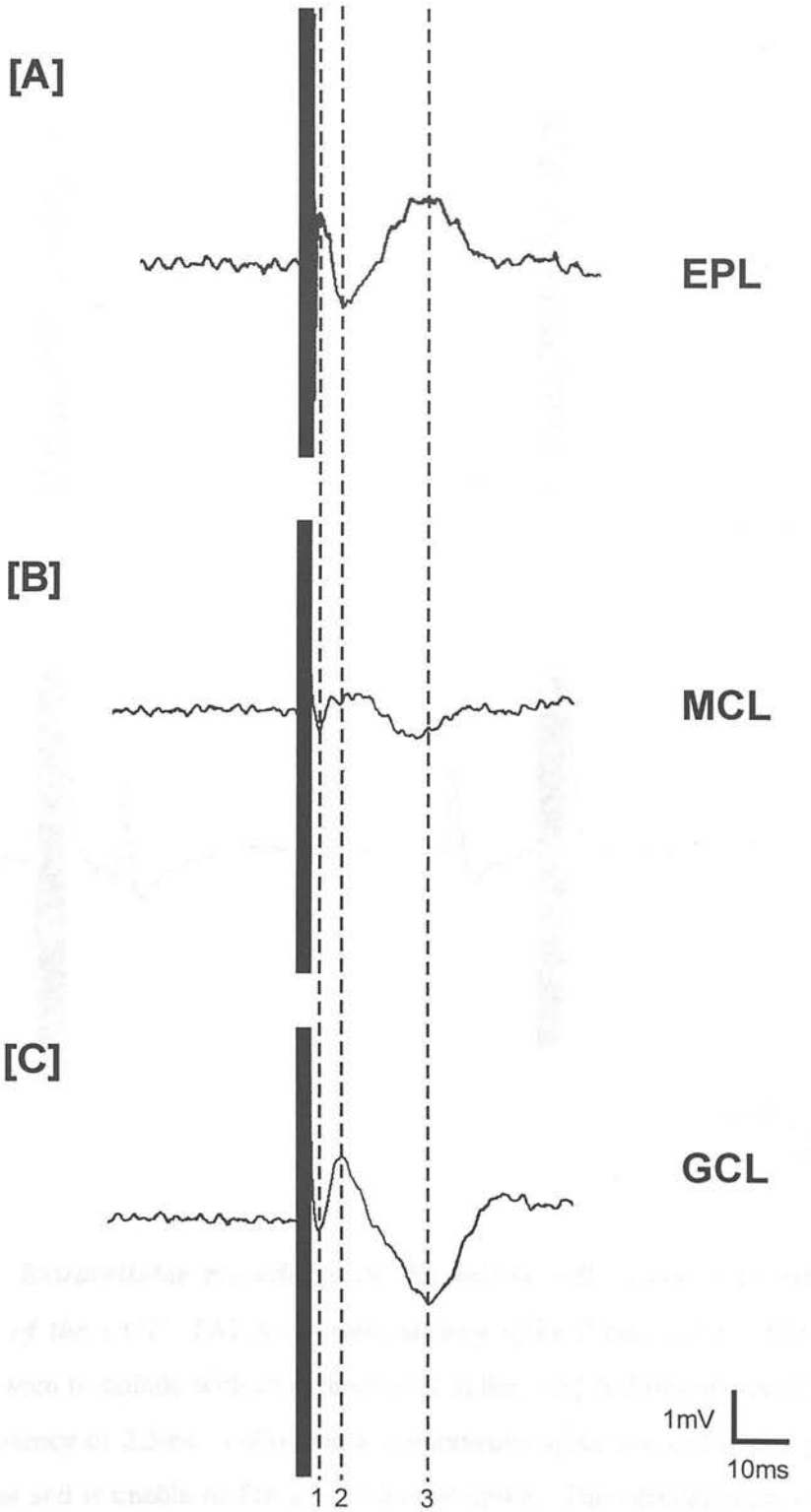
[A]
EPL
[B]
MCL
[C]
GCL
1mV
10ms
1
2
3

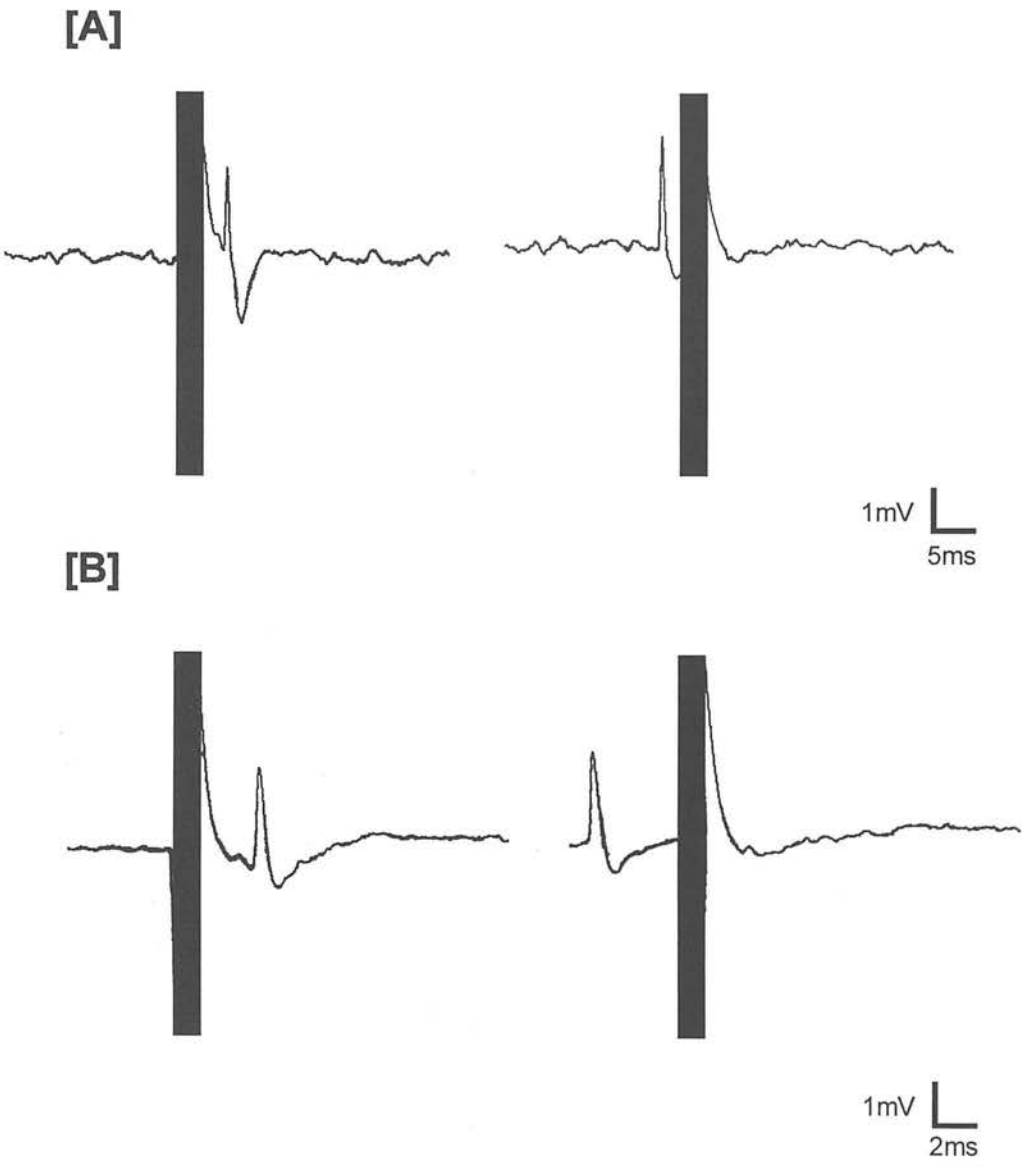

Figure 3.4. Extracellular recordings of the mitral cell response to antidromic stimulation of the LOT. [A] A constant latency spike (5ms) follows the stimulus pulse and is seen to collide with an orthodromic spike. [B] A different mitral cell with a constant latency of 2.5ms. Following a spontaneous spike this cell is in a period of refractoriness and is unable to fire an antidromic spike. The vertical black bars mask the stimulus artifacts.

Figure 3.5. Diagram illustrating the 'notched' and biphasic waveforms recorded from olfactory bulb neurones. [A]-[C] examples of the notched waveform taken from recordings of mitral cells and [D] trace of a notched waveform obtained from a granule cell. Notice the 'notch' occurs during the repolarising phase of the action potential. [E]-[F] are examples of the biphasic waveform, notice that the degree of after-hyperpolarisation is different in the two waveforms. Both spikes are taken from mitral cell recordings. [G] A schematic drawing of a spike illustrating the measurements made for spike height and width.

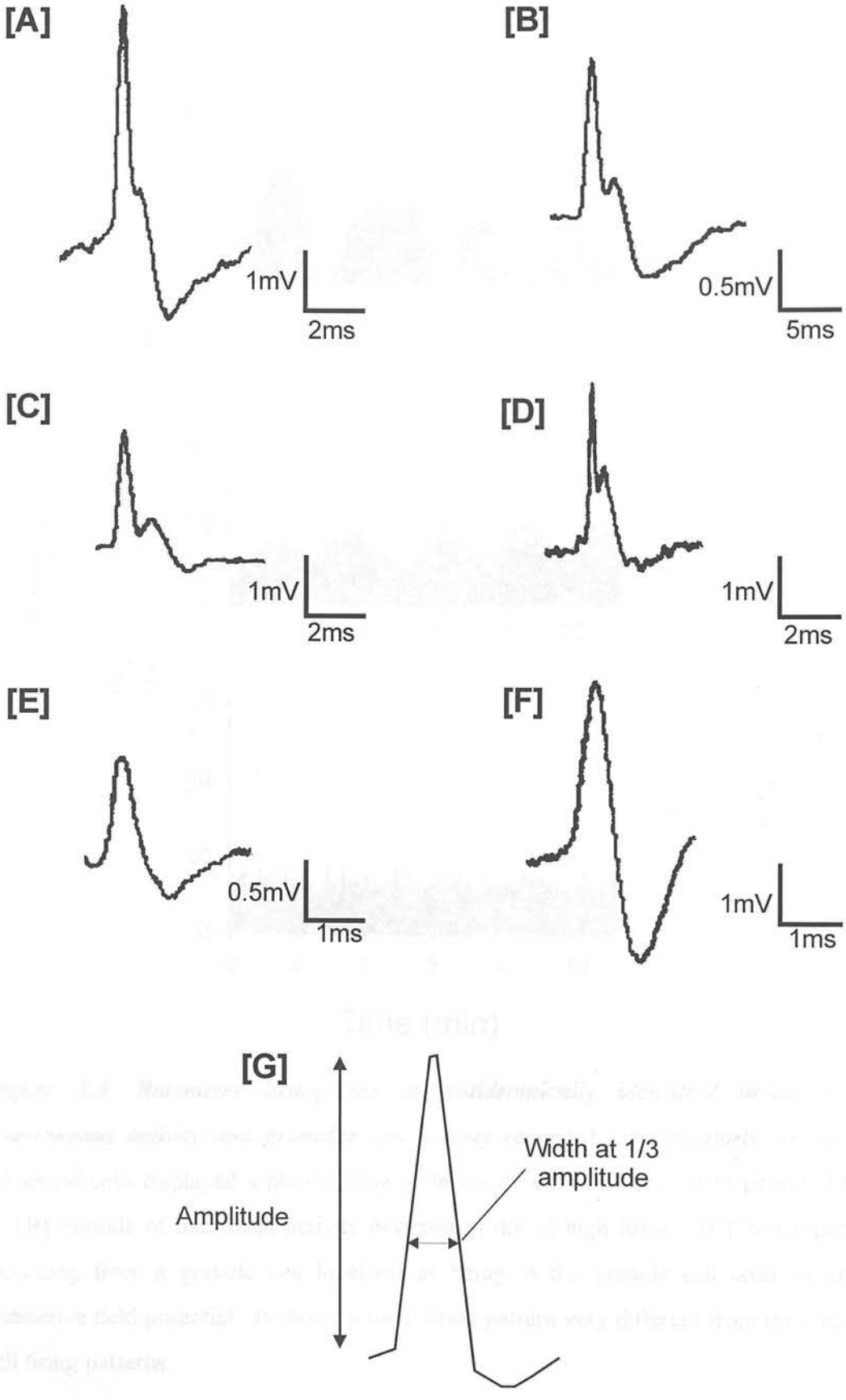
[A]
1mV
2ms
[B]
0.5mV
5ms
[C]
1mV
2ms
[D]
1mV
2ms
[E]
0.5mV
1ms
[F]
1mV
1ms
[G]
Amplitude
Width at 1/3
amplitude

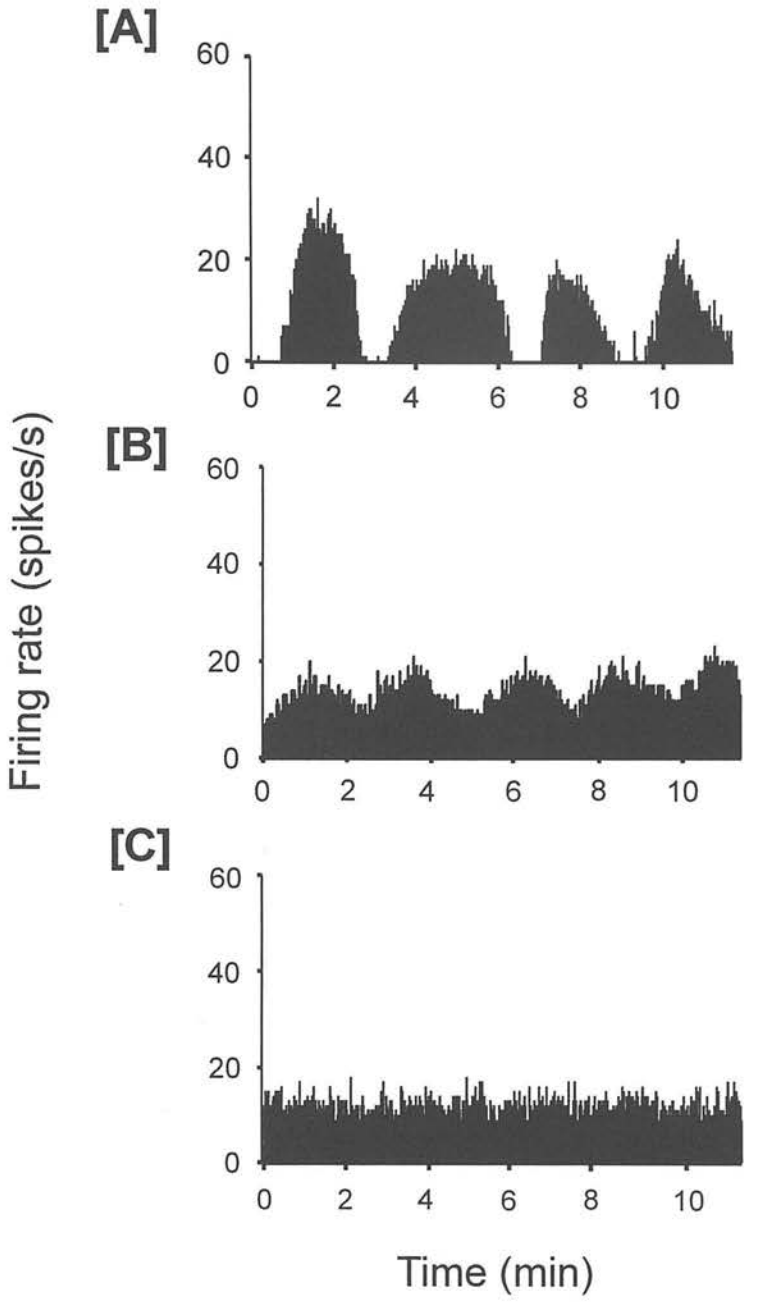

Figure 3.6. Ratemeter histograms of antidromically identified mitral cell spontaneous activity and granular cell activity recorded extracellularly, in vivo. All mitral cells displayed a phasic firing pattern with either distinct silent periods [A] or [B] periods of decreased activity between peaks of high firing. [C] Is a typical recording from a granule cell localised as being in the granule cell layer by the distinctive field potential. It shows a tonic firing pattern very different from the mitral cell firing patterns.

Figure 3.7. Auto-correlation plots of a 5min period of mitral cell and granule cell spontaneous activity. A total of eighty-two mitral cells and thirty-two granule cells were analysed, the cells shown in this figure are representative of the population and all histograms are taken from a single mitral and granule cell. [A] Auto-correlation plot shows the regularity of the bursts of mitral cell activity and the absence of this phasic pattern in the granule cell. [B] The same auto-correlation plot as shown in [A] re-drawn on a shorter timescale. A further series of peaks are evident for both cell types (73% of mitral cells and 59% of granule cells) these are thought to be due to the respiratory influence on the firing rate of olfactory bulb neurones. [C] Auto-correlation plots in the millisecond range show a large peak of activity between zero and 10ms for the mitral cell, which is missing in the granule cell plot.

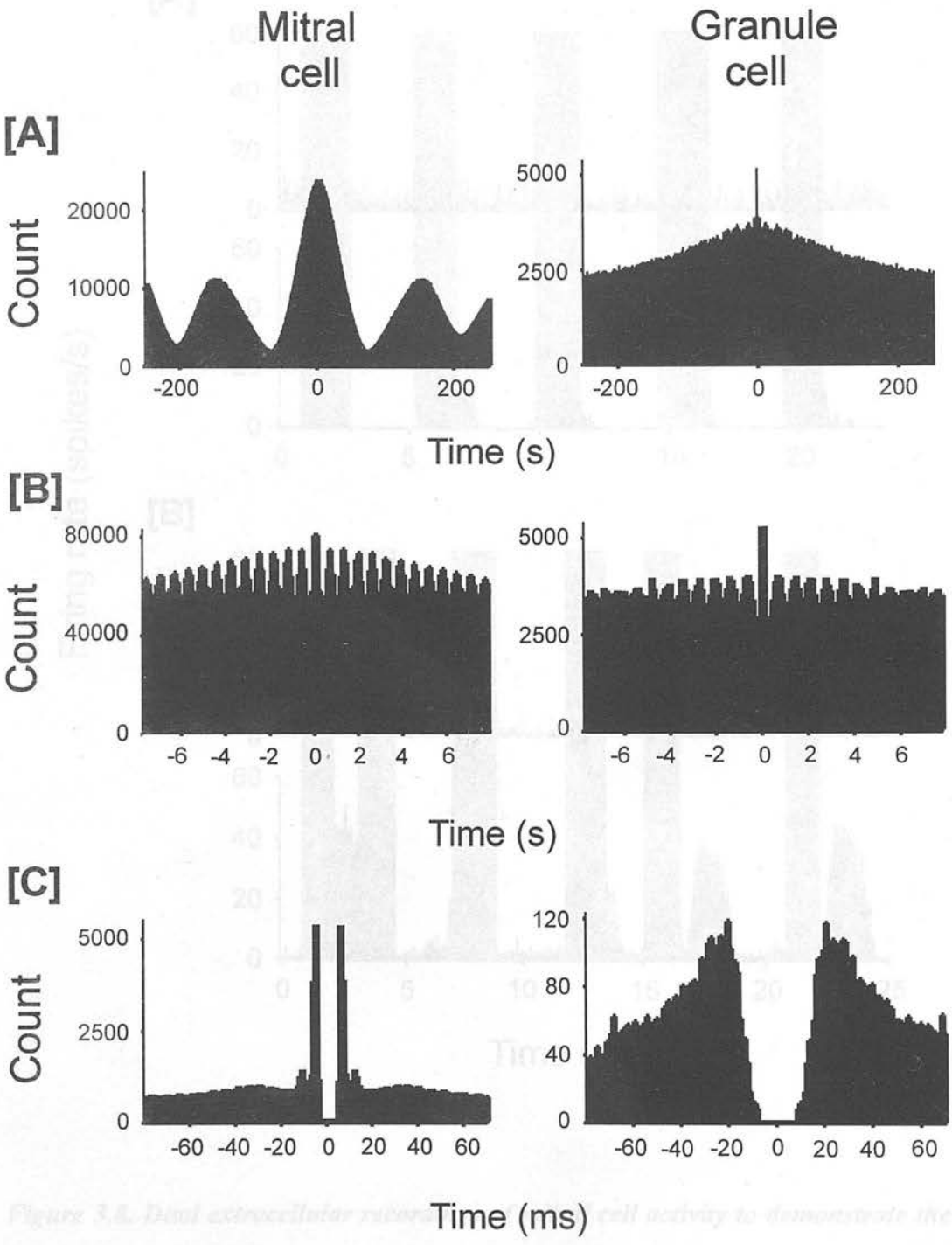
Mitral cell
Granule cell
[A]
Count
20000
10000
0
-200
0
200
5000
2500
0
-200
0
200
Time (s)
[B]
Count
80000
40000
0
-6 -4 -2 0 2 4 6
5000
2500
0
-6 -4 -2 0 2 4 6
Time (s)
[C]
Count
5000
2500
0
-60 -40 -20 0 20 40 60
120
80
40
0
-60 -40 -20 0 20 40 60
Time (ms)

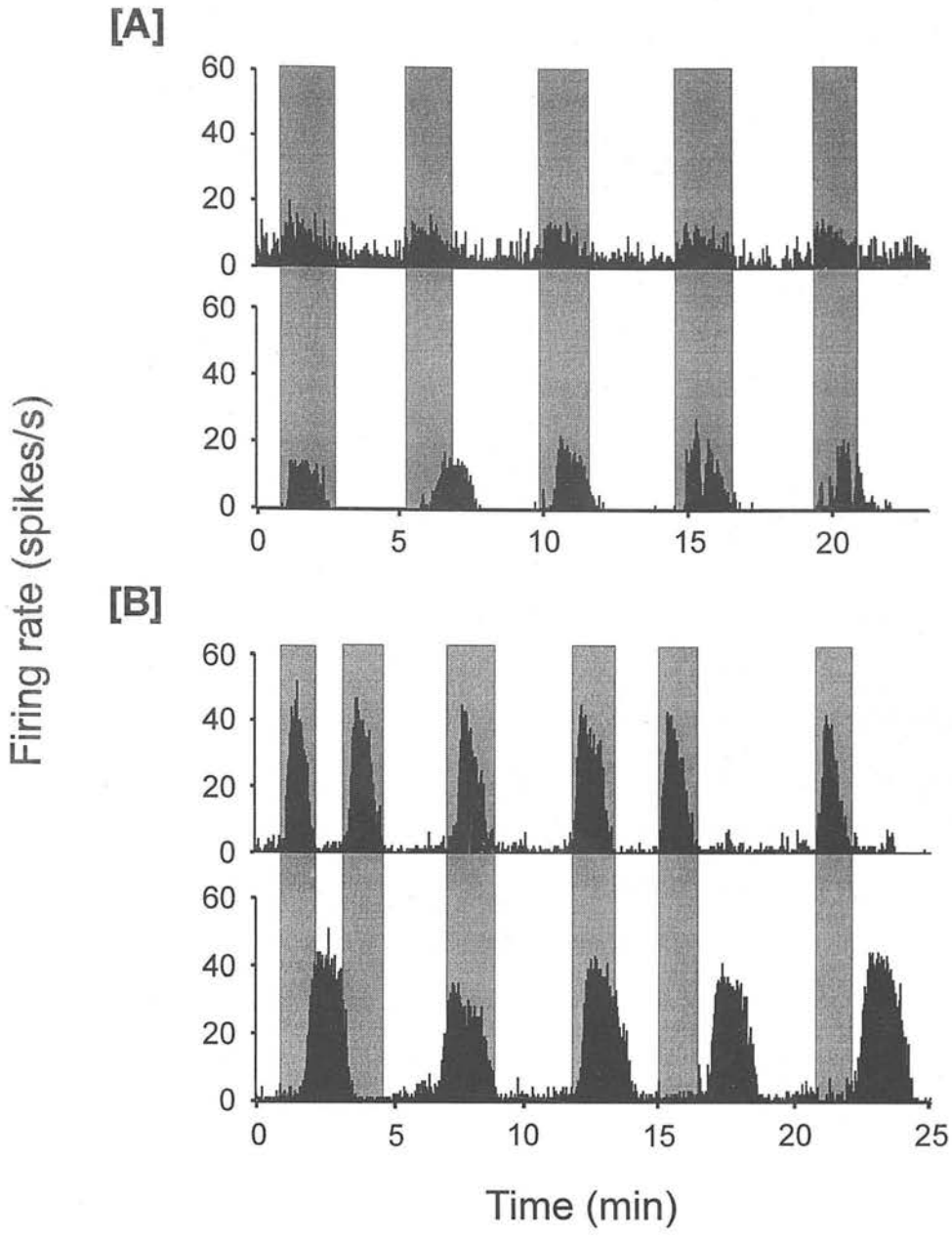

Figure 3.8. Dual extracellular recordings of mitral cell activity to demonstrate the degree of synchrony in mitral cell firing. [A] Two mitral cells both recorded from the dorsal mitral cell layer in which 80% of bursting activity occurs at the same time and, [B] a pair of mitral cells which are also located in the dorsal mitral cell layer and only occasionally exhibit bursts of activity at the same time period, drifting in and out of synchrony.

Figure 3.9. Cross-correlation histograms of [A] the pair of mitral cells that appear to have synchronous bursts of activity (previously shown in fig. 3.8A) and, [B] the pair of mitral cells that fire bursts of activity that drift in and out of synchrony (shown in fig. 3.8B). The histograms are plotted at two different time scales; the larger time-scale shows the degree of synchrony between the bursts of activity and the shorter time-scale shows the synchrony in spike arrivals. It is clear that in both pairs of mitral cells one cell is lagging the other, but the lag time in [A] is shorter than in [B] (26.3s and 37.4s respectively). Also, in [A] the peaks and troughs of activity occur within the same period of time whereas [B] whilst one cell has a peak of activity the other displays a trough. At the shorter timescale the difference in synchrony is more obvious, again [A] shows a lag time between cells firing spikes however [B] shows flat lines indicating no synchrony between the cells.

[A]

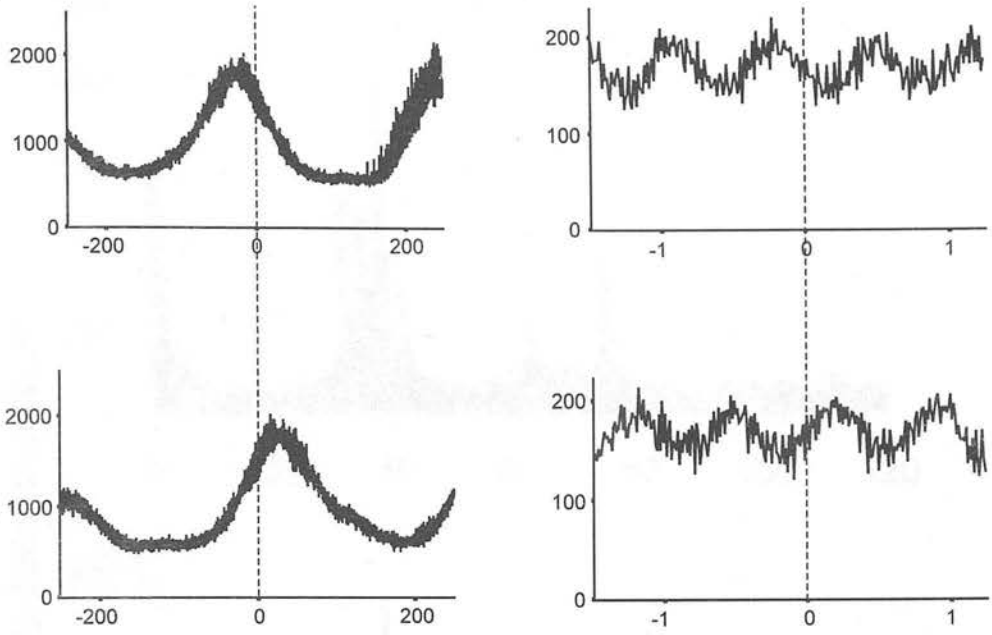
2000
1000
0
-200
0
200
200
100
0
-1
0
1
2000
1000
0
-200
0
200
200
100
0
-1
0
1

[B]

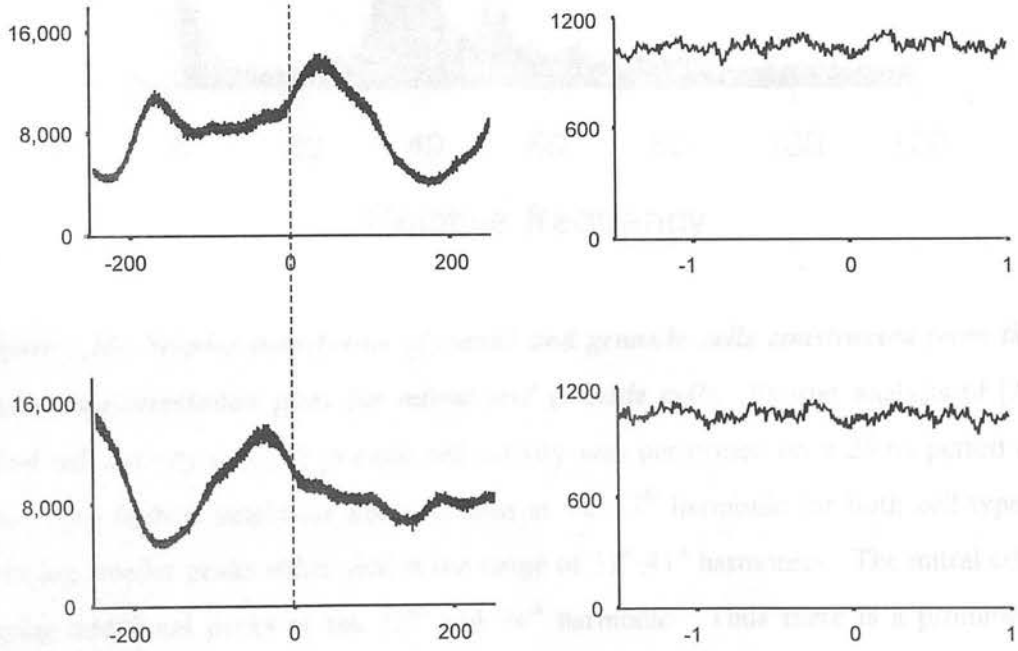
16,000
8,000
0
-200
0
200
1200
600
0
-1
0
1
16,000
8,000
0
-200
0
200
1200
600
0
-1
0
1

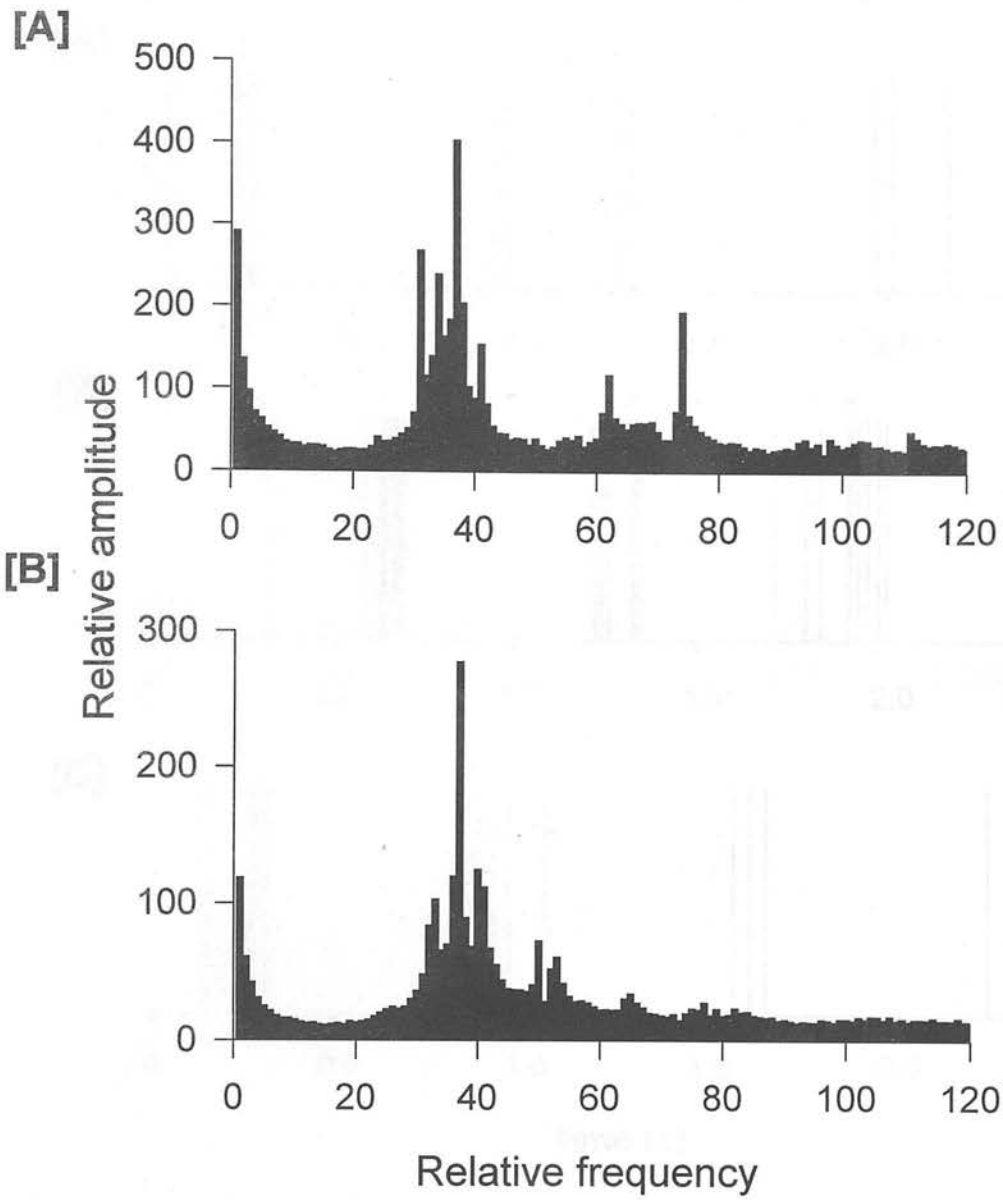

Figure 3.10. Fourier transforms of mitral and granule cells constructed from the mean auto-correlation plots for mitral and granule cells. Fourier analysis of [A] mitral cell activity and [B] granule cell activity was performed on a 25.6s period of data. The highest amplitude peaks is seen at the 37th harmonic for both cell types, there are smaller peaks either side in the range of 31st-41st harmonics. The mitral cells display additional peaks at the 62nd and 74th harmonic. Thus there is a prominent sinewave occurring 37 times in a 25.6s time period (1.4Hz).

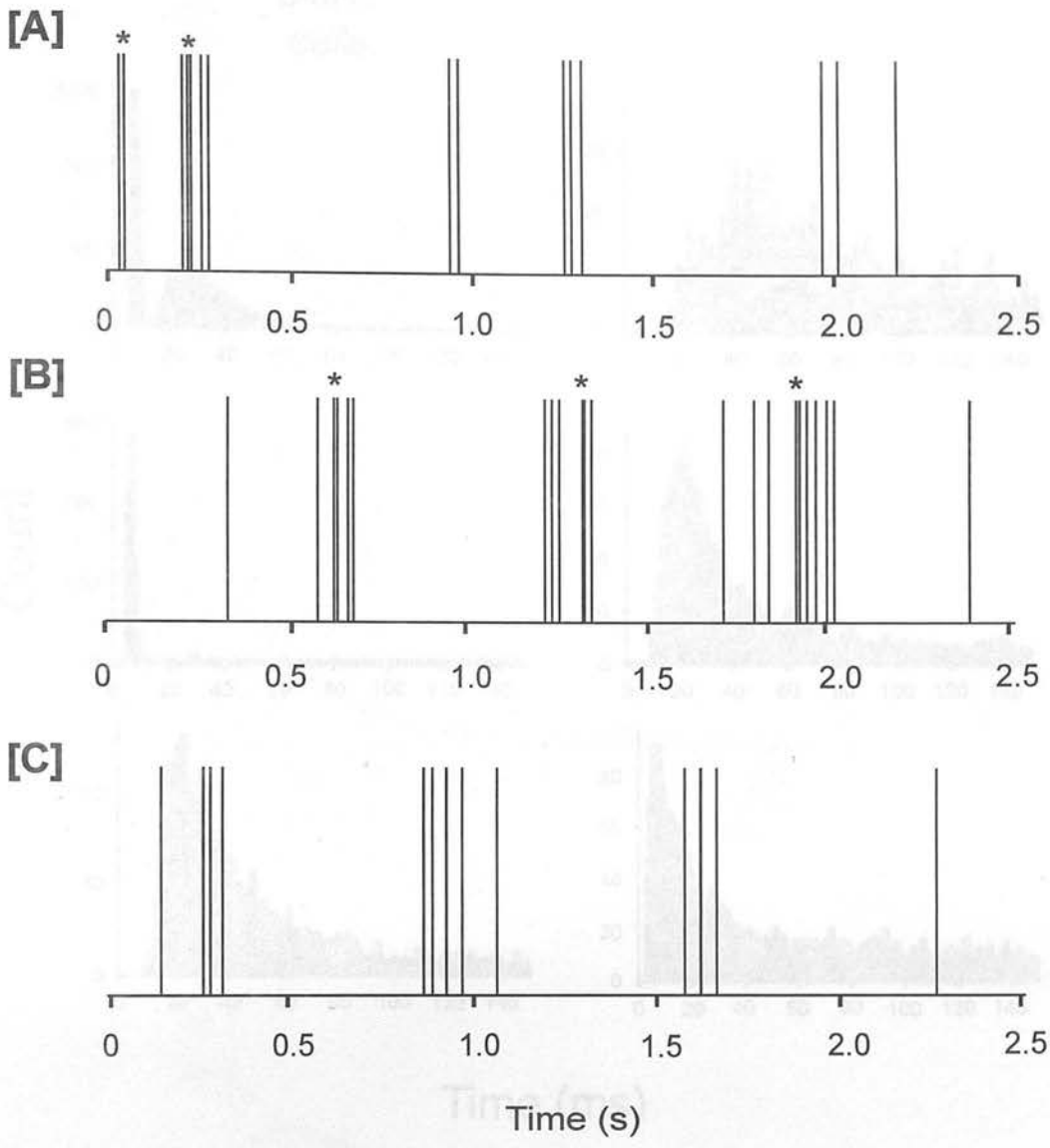

Figure 3.11. The pattern of spontaneous activity [A]-[B] recorded from two different mitral cells, which were classified as bimodal, and [C] one granule cell. Notice the varying number of spikes in each burst even for an individual cell. Also, notice that there are two degrees of bursting within the timescale shown, there are three groups of spikes (which is also seen in granule cells and is due to the respiratory influence on olfactory neurone firing) and within each group there are spikes which occur in quick succession of each other (*).

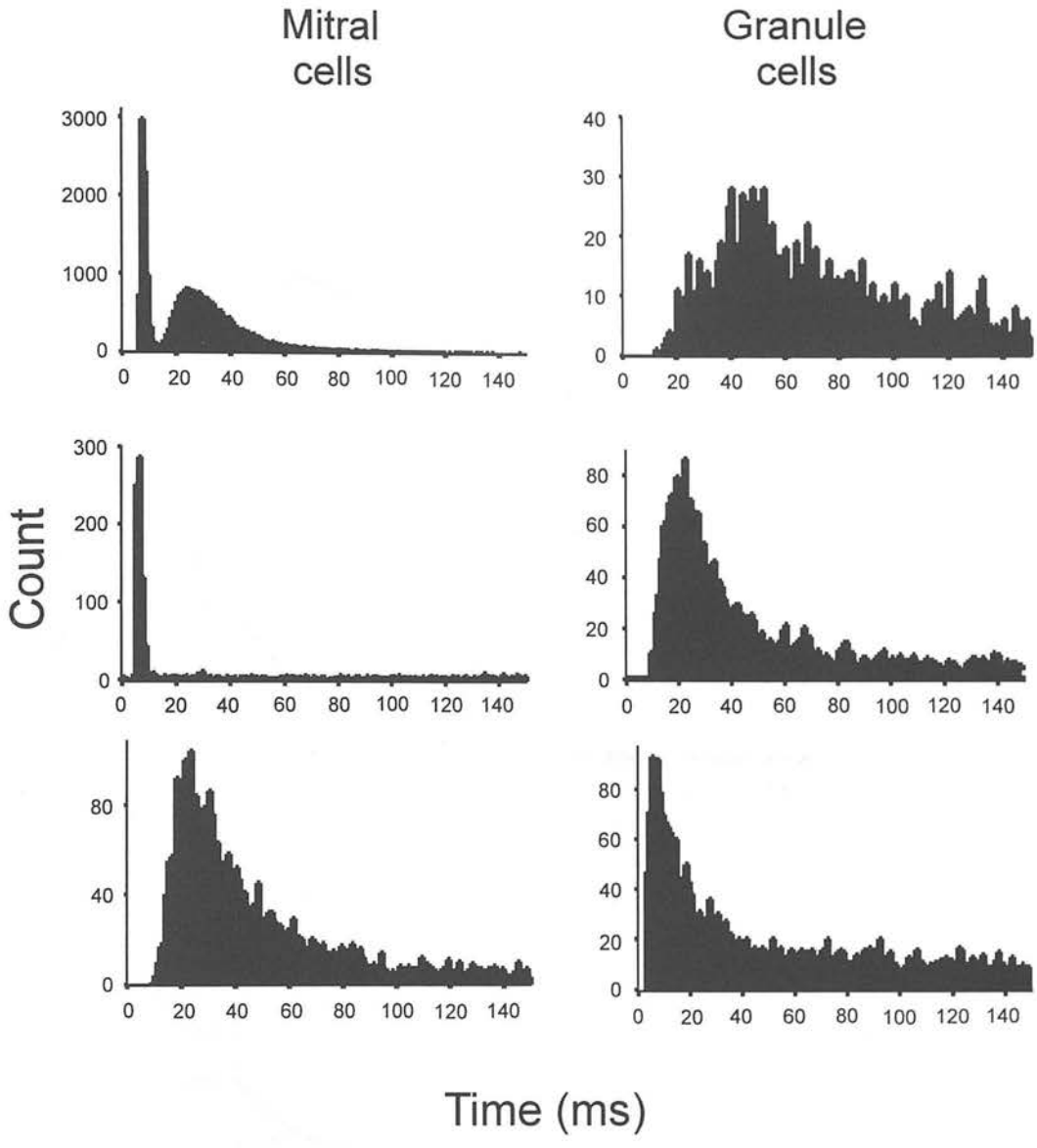

Figure 3.12. Interspike interval histograms of the spontaneous activity of three antidromically identified mitral cells (left) and three granule cells (right) recorded during a 5min period. The interspike intervals varied from 1ms to 400ms in length but the histograms are curtailed at 150ms, (bin width = 1ms). Mitral cells (57%) displayed a bimodal firing pattern not seen in granule cells.

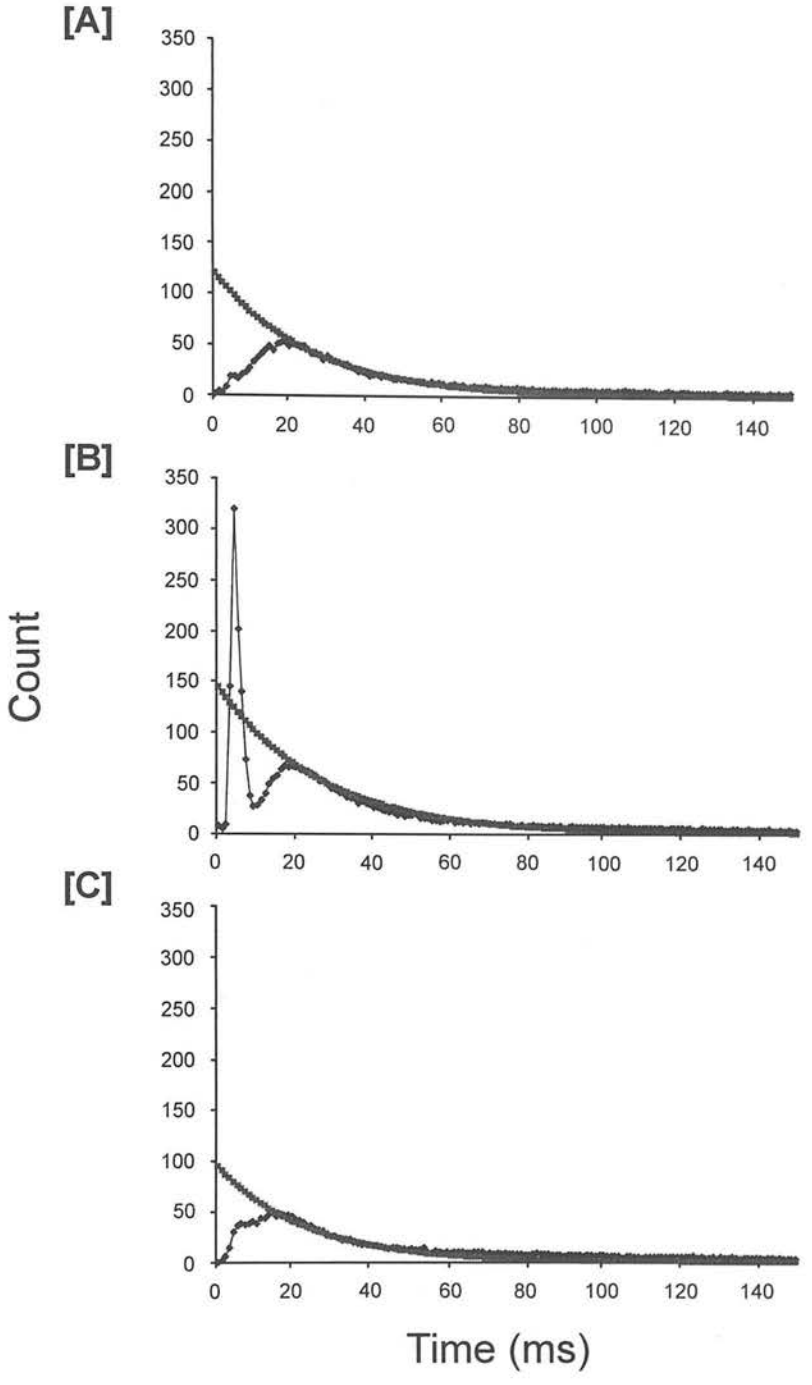

Figure 3.13. Interspike interval histograms of the mean intervals for [A] mitral cells with one mode of firing [B] mitral cells with two modes of firing and [C] granule cells. All three histograms have an exponential curve fitted to the tail of the distribution. Notice from the three histograms that it is only the peak of the high frequency mode from the bimodally firing mitral cells that occurs above the line of the exponential.

Figure 3.14. Histograms of: [A] the modal interspike interval; [B] the mean interspike interval and; [C] the skew, for mitral cells n = 64 (grey bars) and granule cells n = 34 (black bars). Notice there is a degree of overlapping between the two cell groups in both modal and mean interspike intervals. In [A] the mitral cells form two distinct groups whereas the granule cells, although they do exhibit small modal interspike intervals, they are not divided into two groups. In [B] the distribution of mean intervals for mitral cells is more skewed than that for granule cells and [C] indicates that histograms of mitral cell activity are more likely to exhibit high skewness than those of granule cells.

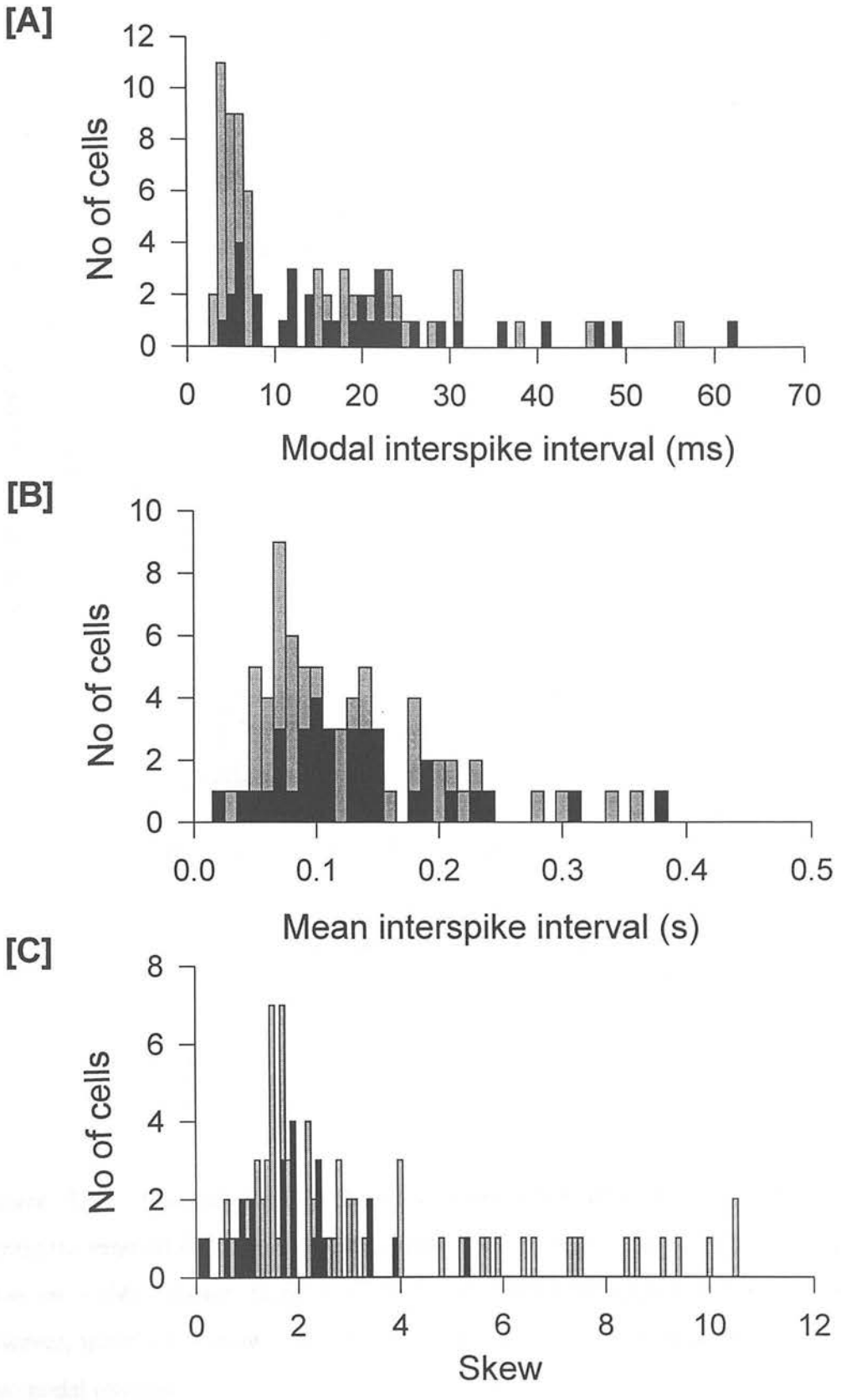
[A]
No of cells
0
2
4
6
8
10
12
0
10
20
30
40
50
60
70
Modal interspike interval (ms)
[B]
No of cells
0
2
4
6
8
10
0.0
0.1
0.2
0.3
0.4
0.5
Mean interspike interval (s)
[C]
No of cells
0
2
4
6
8
0
2
4
6
8
10
12
Skew

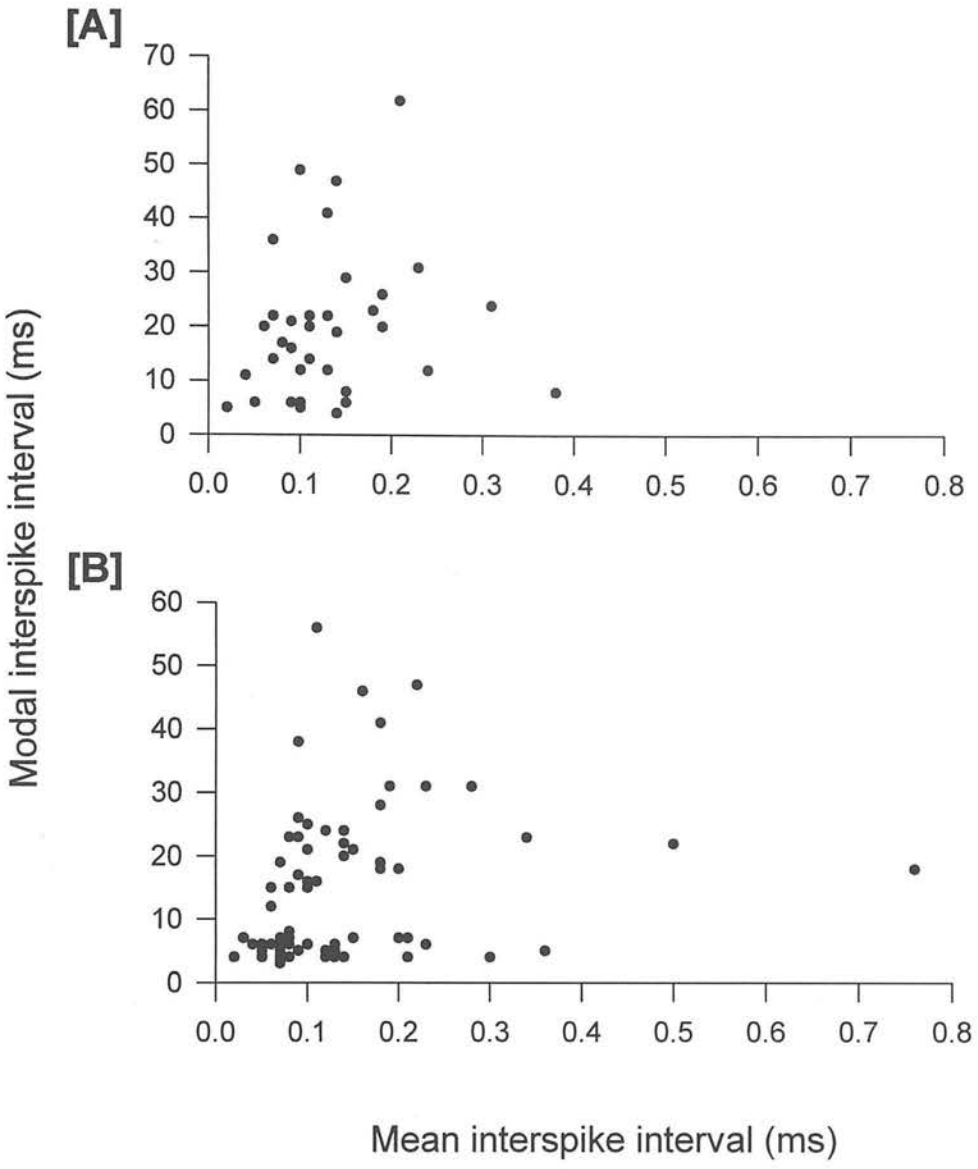

Figure 3.15. The relationship between mean interspike interval and modal interspike interval for cells in the [A] granule cell layer (n = 34) and [B] mitral cell layer (n = 64). Again, there is a degree of overlap between the two cell types however, mitral cells show a greater propensity to display low mean intervals with low modal intervals.

Figure 3.16. Hazard functions of the mean interspike intervals for [A] granule cells (n = 25) and [B] mitral cells (n = 44). The hazard function of cell activity gives the probability of cell firing per millisecond after a spike (at time 0), given that another spike has not occurred earlier and is a measure of excitability, providing a clear indication of the time period over which the after-effects of a spike influence further firing. The hazard functions shown in this figure have been truncated once a plateau level has been reached. Achievement of a plateau level by a given time indicates that by this time, the preceding spike is having no further significant effect on the excitability of the cell. Plotting the hazard function for granule cells [A] shows that immediately after an action potential firing within 10ms of a spike is minimal and the probability increases between 10 and 35ms before it reaches a plateau. In the case of mitral cells [B] immediately after an action potential firing is minimal however, the probability is increased within 4-10ms after a preceding spike. The probability falls away again and then increases between 15-40ms following a spike and reaches a plateau level at approximately the same time as seen for the granule cells. The overall hazard function for mitral cells is composed from the hazard functions shown in (i) and (ii) showing the two different spike distributions exhibited by mitral cells (one mode; n = 22 and two modes; n = 22). Error bars show the standard error of the mean.

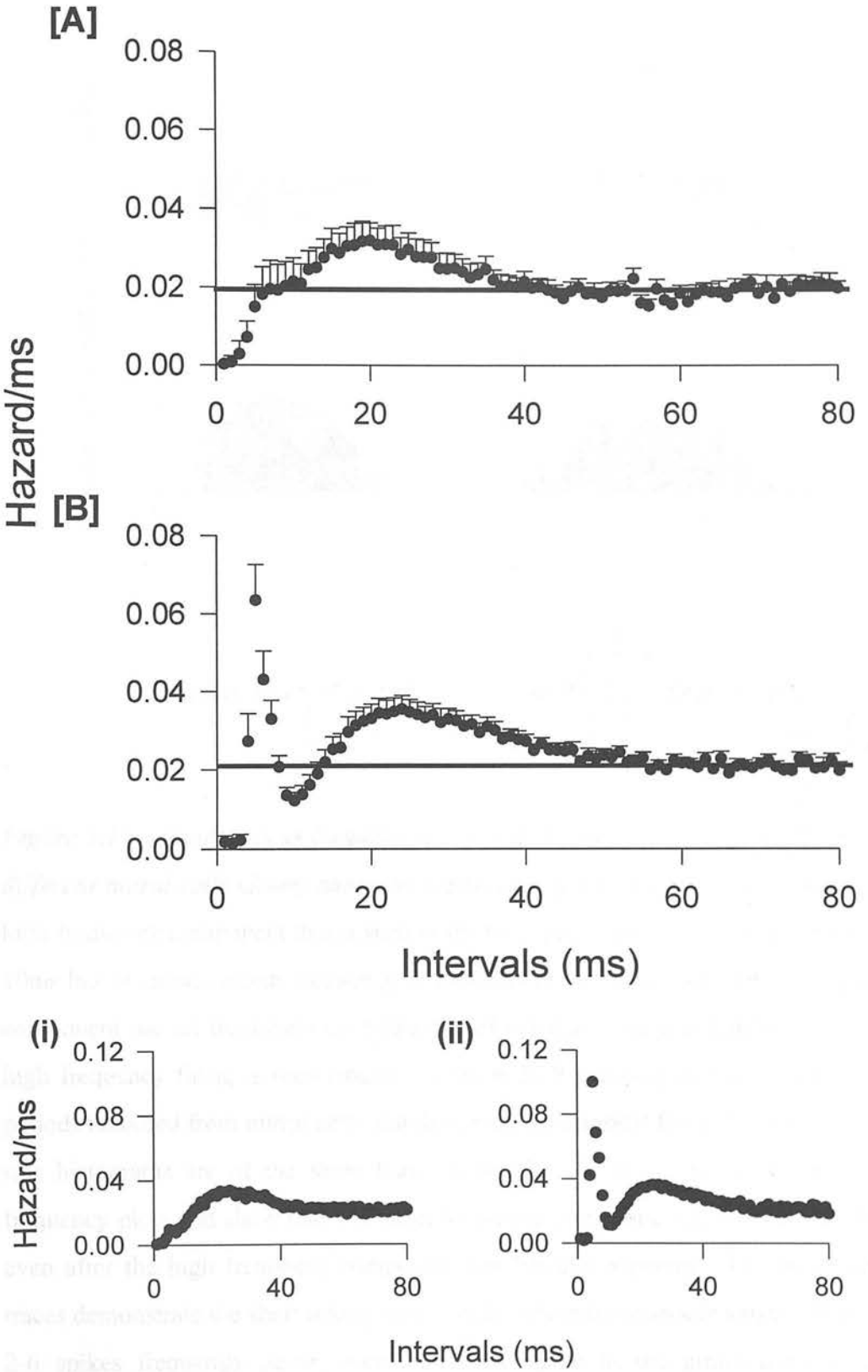
[A]
0.08
0.06
0.04
0.02
0.00
0
20
40
60
80
Hazard/ms
[B]
0.08
0.06
0.04
0.02
0.00
0
20
40
60
80
Intervals (ms)

(i)
(ii)
0.12
0.08
0.04
0.00
0
40
80
Hazard/ms
Intervals (ms)

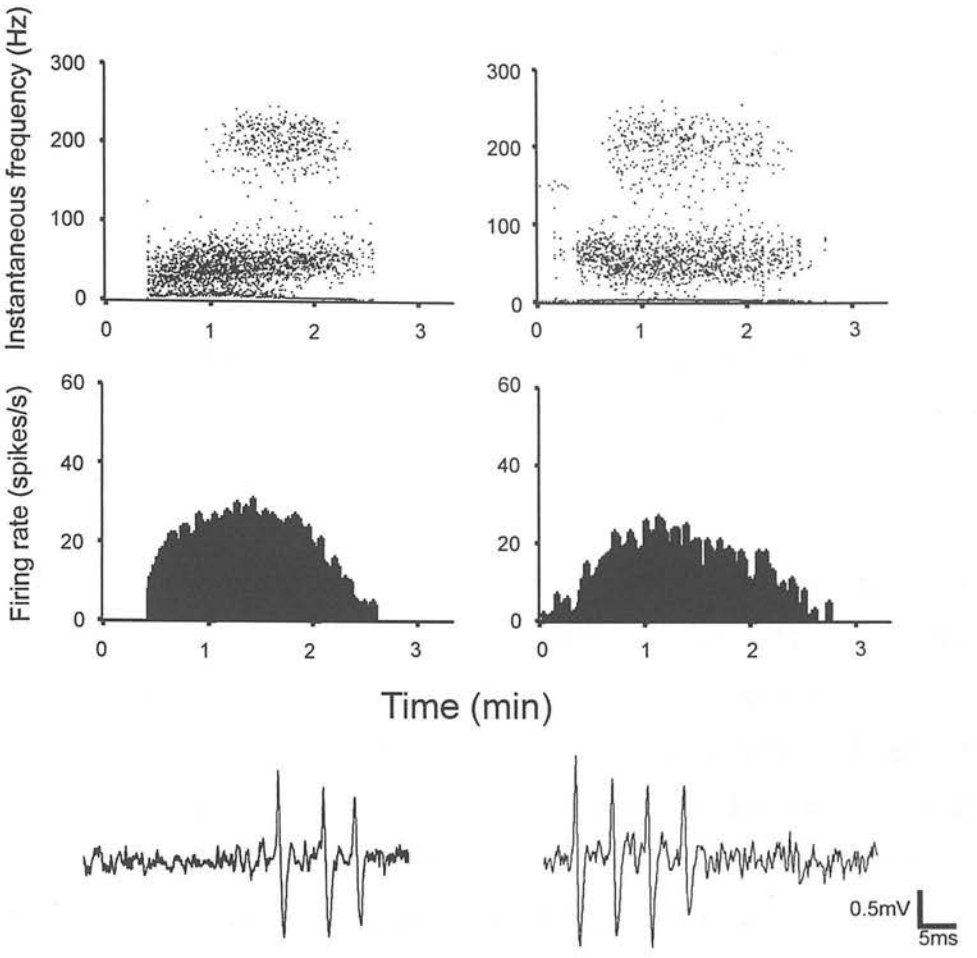

Figure 3.17. Instantaneous frequency (1/interspike interval) histograms from two different mitral cells clearly show the separation of the two modes of firing. The high frequency component that is seen in the interspike intervals to occur between 4-10ms has an instantaneous frequency of 100-250Hz and the second, lower frequency component has an instantaneous frequency of 0-80Hz. There is a delay before the high frequency firing is seen (mean ± s.e.m = 30.9 ± 2.48s) in 84% of the phasic periods recorded from mitral cells that displayed the bimodal firing distribution. The rate histograms are of the same burst of activity as shown in the instantaneous frequency plots and show that the mean frequency does not change during the burst even after the high frequency component has become apparent. The oscilloscope traces demonstrate the short interspike intervals between successive spikes. Bursts of 2-6 spikes frequently occur, each successive spike in the group decreasing in amplitude.

3.3.6 LOT stimulation

A peri-stimulus time histogram (PSTH) is similar to an event correlation, in that it uses a trigger to initiate a sweep of analysis, but unlike the auto-correlation plots, if a trigger event falls within a sweep it is ignored. The sweeps are accumulated to form the histogram; time periods before and after the trigger are shown on the ordinate axis and the number of events at a particular time period shown on the abscissa.

Mitral cell activity was inhibited by the stimulus pulse in all cases (fig. 3.19D), periods of inhibition lasted between 40ms and 120ms (mean ± S.E.M. = 50 ± 9ms). This period of inhibition incorporates the post-spike hyperpolarisation and inhibition induced by the granule cell circuitry. This is further demonstrated in figure 3.18 which shows the difference between the period of inhibition that follows a spike during spontaneous firing (3.18C) and the period of inhibition in mitral cell firing that follows a stimulatory pulse to the LOT (3.18B). The period of inhibition following the stimulus pulse is two-fold longer than the period of inhibition caused by the post-spike hyperpolarisation indicating that stimulation of the LOT induces a synaptically mediated inhibition of mitral cell activity.

Cells recorded from the granule cell layer gave a mixed response to stimulation of the LOT (fig. 3.19A-C), 36% responded with a period of excitation that occurred between 20ms and 40ms after the stimulus pulse and lasted for between 15ms and 50ms (mean ± S.E.M. = 25 ± 5.5ms). The remaining cells were either non-responsive (41%) or showed a period of suppressed activity (10%), no granule cells were inhibited fully as in the mitral cell group.

The population response of both cell types to stimulation of the LOT is shown in figure 3.20; the graphs show the sum of individual histograms rather than the mean. The granule cell plot shows that in addition to the period of excitation

described above there is also an orthodromic activation of the granule cells (exhibited by 13% of granule cells recorded). The second period of granule cell activation is seen to correlate with the period of inhibition shown by the mitral cell population.

By doubling the intensity of the stimulus pulse it is possible to cause the antidromic spike to repeatedly fail (fig. 3.21). During stimulation with the intensity close to threshold the antidromic spike is present following each stimulus pulse however, once the intensity is increased the spike fails 60% of the time. This demonstrates the increased inhibition exerted on the recorded mitral cell, as the strength of the stimulus is increased a larger population of mitral cells are activated thereby increasing the degree of lateral inhibition experienced by the recorded cell.

Furthermore, when a spontaneous spike is used as the trigger for a stimulus pulse to be delivered to the LOT (constant-collision protocol) the bursting activity of the cell is disrupted (fig. 3.22). In 'constant-collision' the stimulus immediately follows a spontaneous action potential, hence the antidromic spike is extinguished by collision with the spontaneous, orthodromic spike, and so antidromic invasion of the cell body of the recorded neurone does not occur. Accordingly, changes in the activity of the recorded neurone that follow such shocks may be attributed to the antidromic invasion of neurones in synaptic contact with the recorded unit. Comparing the PSTHs of activity during single pulse stimulation and constant-collision stimulation the latter shows a prolonged inhibition of mitral cell activity. This is because in the constant-collision protocol the stimulus occurs after the spike leading to a delayed activation of inhibitory collaterals relative to the time of the spike resulting in a longer post-spike silence.

When a double-pulse protocol is applied to a mitral cell and the interval between conditioning and test pulses varied, the antidromic spike is seen to fail at certain inter-pulse widths (fig. 3.23). With a 4ms gap between stimulus pulses the

mitral cell did not fail to fire an antidromic spike. However, gaps of between 7 and 24ms caused the spike after the second pulse to occasionally fail, with an inter-pulse gap of 15ms it failed consistently. At longer time intervals between stimuli (25-55ms) the second spike was always present. This stimulation protocol gives an indication of the time periods over which the mitral cell is experiencing inhibition at the level of the soma from axon collaterals and granule cell circuitry.

3.3.7 In vitro recordings of mitral cell activity

The mitral cell layer was clearly visible under the dissecting microscope as a narrow translucent band and because of the pre-dominance of mitral cell somata in this layer along with their large dimensions, it was highly probable that neurones recorded in this area would be mitral cells. Extracellular recordings from mitral cells (n=45) in the slice preparation of the olfactory bulb did not reveal similar firing patterns as seen *in vivo*. The firing patterns of spontaneous activity seen *in vitro* (fig. 3.24) did not display the long bursts of activity separated by periods of silence or quiescence as seen in the phasic mitral cells nor did the discharge pattern look similar to patterns recorded from granule cells *in vivo*. Only three of the cells displayed the periodic firing similar to the phasic mitral cells recorded *in vivo*, but the periods of activity were on a much shorter timescale. The mean firing rate varied from 2.8-14.3spikes/s (mean ± S.E.M. = 7.5 ± 0.8 spikes/s). Mitral cells (11%) recorded *in vitro* showed a notch in the descending phase of the action potential, similar to the waveform seen in mitral cells recorded *in vivo*.

Following the construction of INTHs from 5min periods of mitral cell spontaneous activity (fig. 3.25A) two cells were found to display a bimodal firing frequency however, the first peak is not in the same range as the high frequency mode seen *in vivo*. The first mode occurs between 20 and 40ms (*in vivo* this was found between zero and 10ms) and the second mode is found between 50 and 80ms (*in vivo* this occurred between 15 and 40ms). The majority (71%) showed a skewed

distribution. The hazard function plot of the mean interspike intervals for all mitral cells recorded *in vitro* is shown in figure 3.25B. There is a difference between the hazard plots for cells recorded *in vivo* and cells recorded *in vitro*. *In vitro* the hazard function does not rise above the plateau line indicating that there is no depolarising potential, instead the hyperpolarising potential is prolonged. The probability reaches a plateau at 40ms which is similar to the plot for cells recorded *in vivo* however, the probability of cell firing at the plateau level is slightly higher for the cells recorded *in vitro* (0.03 compared to 0.02 *in vivo*).

Figure 3.18. Peri-stimulus histograms constructed from periods of mitral cell activity under [B] stimulation of the LOT and [C] spontaneous firing. The ratemeter recording [A] shows data from an individual mitral cell and the time periods sampled in the histograms are indicated by arrows. Using stimulatory pulses as the trigger event results in the histogram shown in [B] whereas the histogram shown in [C] is constructed by using spontaneous spikes as the trigger for a sweep of analysis. Notice the period of inhibition following stimulation of the LOT is two-fold longer than the inhibition that occurs after a spike this represents activation of the granule cell circuitry resulting in an additional period of inhibition following the post-spike hyperpolarisation demonstrated in [C].

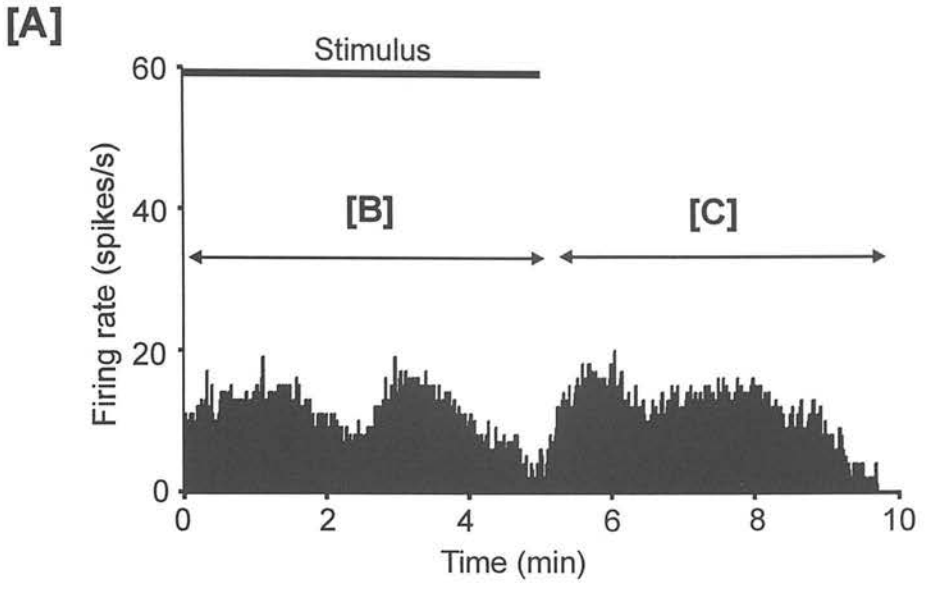
[A]
Stimulus
60
40
20
0
Firing rate (spikes/s)
[B]
[C]
0
2
4
6
8
10
Time (min)

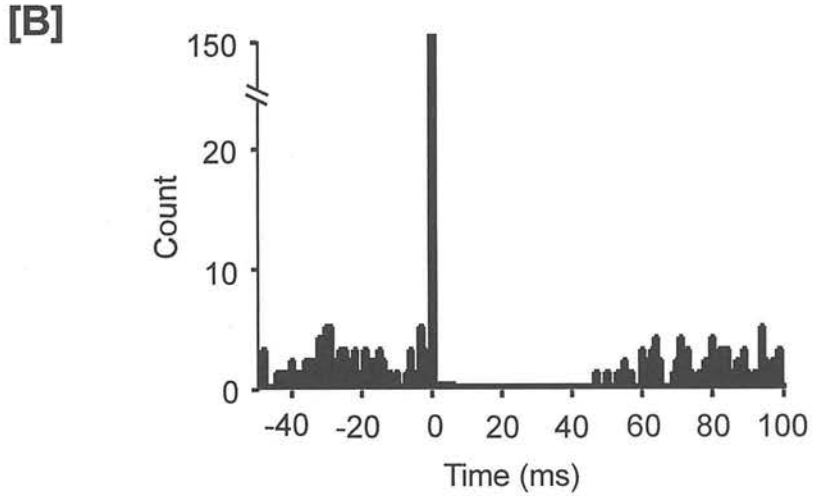
[B]
150
20
10
0
Count
-40
-20
0
20
40
60
80
100
Time (ms)

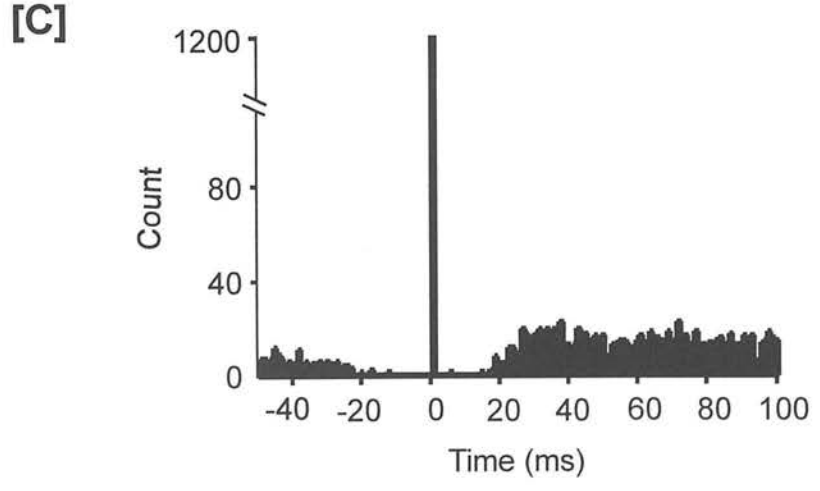
[C]
1200
80
40
0
Count
-40
-20
0
20
40
60
80
100
Time (ms)

Figure 3.19. [A]-[C] Peri-stimulus histograms of individual cells from the granule cell layer showing the variation in response to stimulation of the LOT and for comparison the peri-stimulus histogram of an individual mitral cell response is shown in [D]. From thirty-four granule cells fourteen displayed a period of excitation after stimulation of the LOT; sixteen were found to be non-responsive and the remaining four cells exhibited a period of suppressed activity (none were fully inhibited). All mitral cells recorded showed a period of post-stimulus inhibition, note that the antidromic spike has been truncated.

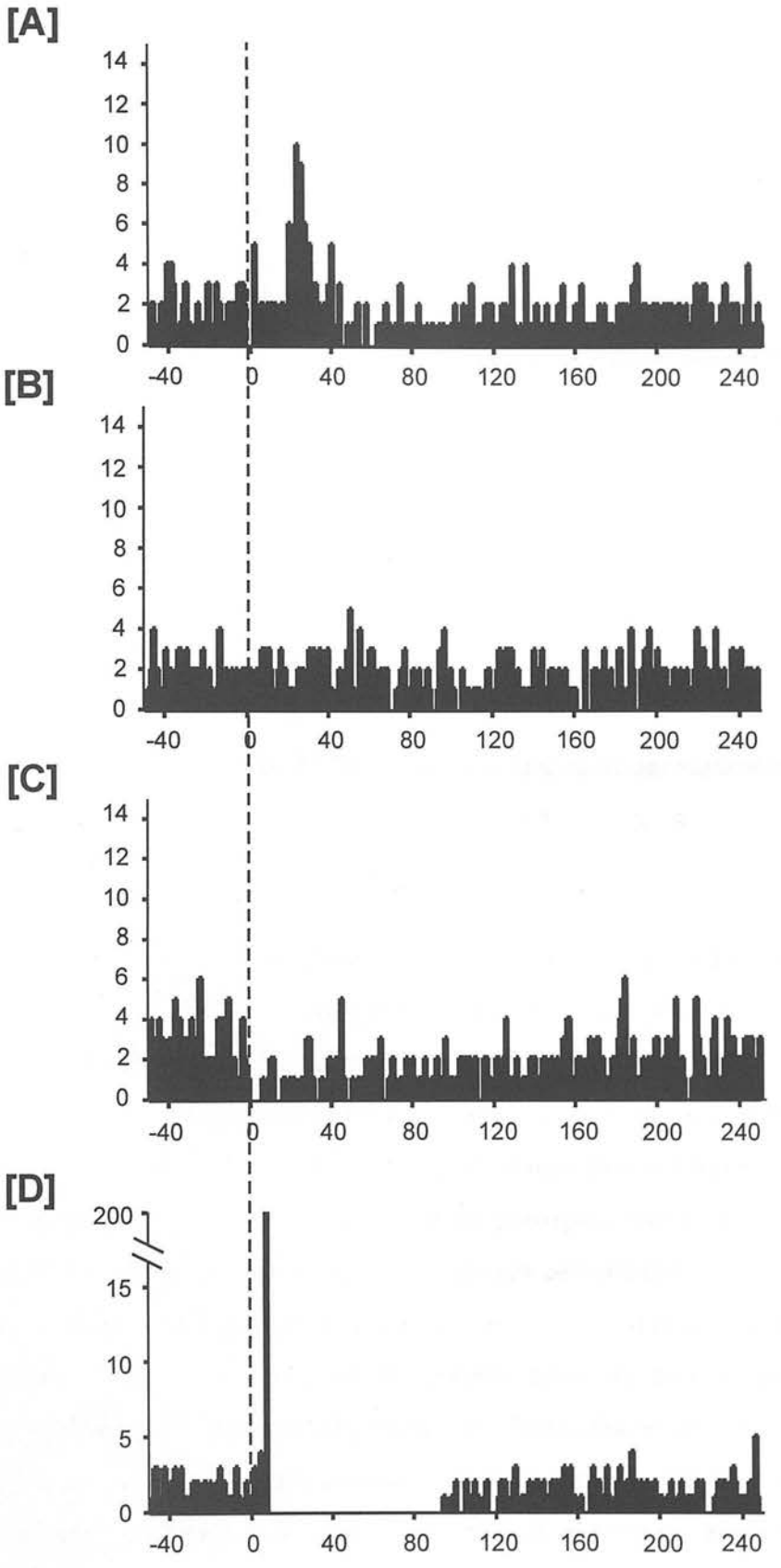
[A]
14
12
10
8
6
4
2
0
-40
0
40
80
120
160
200
240
[B]
14
12
10
8
6
4
2
0
-40
0
40
80
120
160
200
240
[C]
14
12
10
8
6
4
2
0
-40
0
40
80
120
160
200
240
[D]
200
15
10
5
0
-40
0
40
80
120
160
200
240

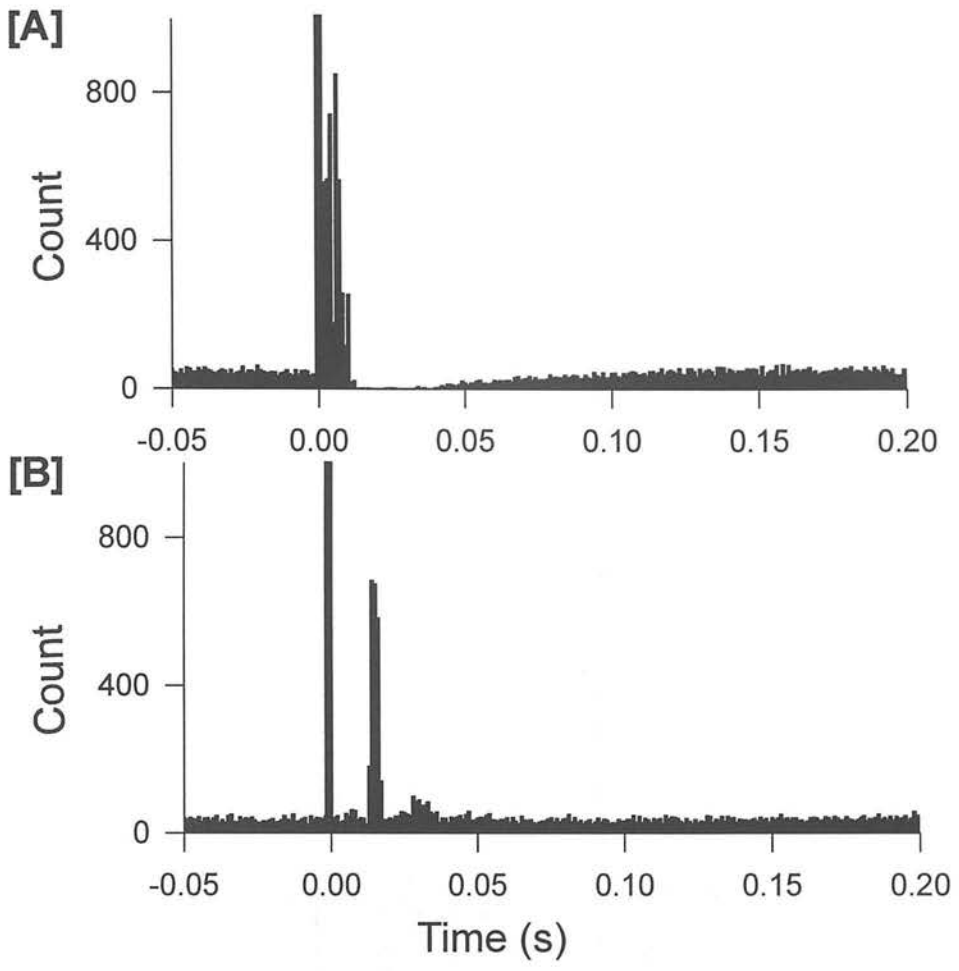

Figure 3.20. Shows the sum of the peri-stimulus time histograms constructed from individual mitral (n = 89) and granule cells (n = 39) prior to and following electrical stimulation of the LOT. The stimulation consisted of single, biphasic pulses (width of 0.1ms, amplitude of 0.3mA and a frequency of 0.5Hz). The histogram for mitral cells [A] shows a period of inhibition following stimulation of the LOT which encompasses the period of post-spike hyperpolarisation plus an additional inhibition from activation of the granule cell circuitry. The large counts in the bins shortly after the stimulus pulse are due to the variation in constant latency antidromic spikes. The histogram for granule cells [B] displays two periods of excitation following the stimulatory pulse. The first is due to orthodromic activation exhibited by five granule cells and the second period of excitation ties in with the post-stimulus inhibition of the mitral cells. In both histograms, black bars mask the stimulus artifacts.

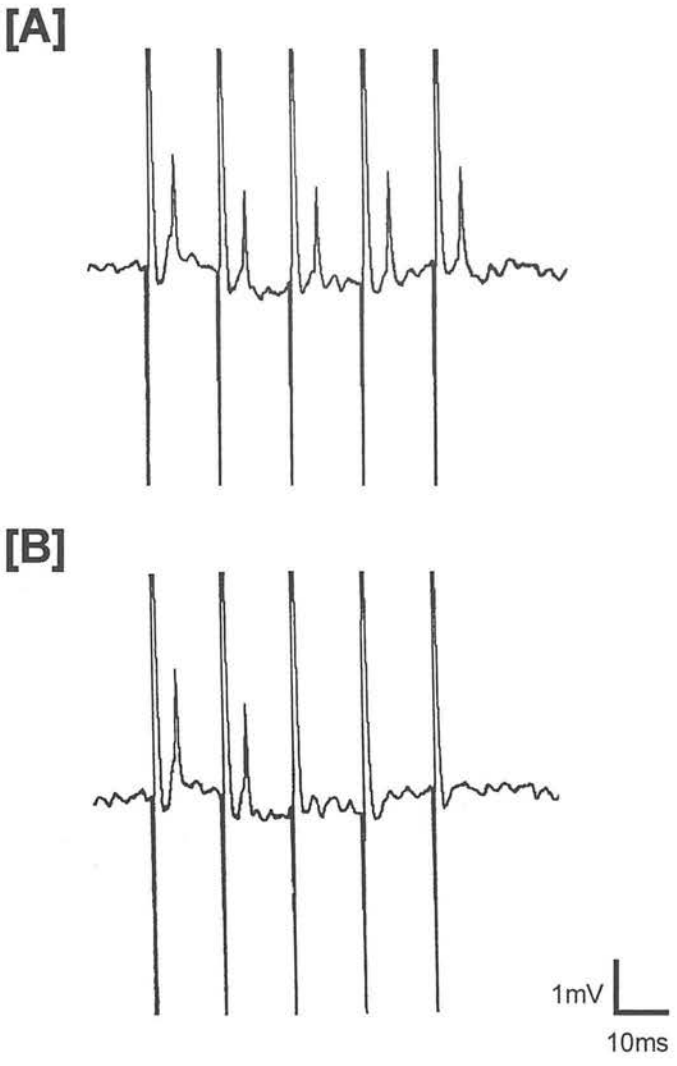

Figure 3.21. Oscilloscope reprints of the constant latency response of mitral cell antidromic spikes following stimulation of the LOT tract at differing intensities of stimulation. [A] At the threshold stimulus intensity (0.3mA) the antidromic spike follows each stimulus pulse however, when the intensity of stimulation is increased to 0.6mA there is a 60% failure of the antidromic spike [B].

Figure 3.22. Peri-stimulus histograms constructed from periods of mitral cell activity under [B] stimulation of the LOT and [C] constant-collision stimulation. The stimulation consisted of single, biphasic pulses (width of 0.1ms, amplitude of 0.3mA and a frequency of 0.5Hz). Constant-collision involves using spontaneous spikes as a trigger for the stimulator to deliver a pulse to the LOT. The ratemeter recording of mitral cell activity [A] shows that during the constant-collision protocol [C] the bursting nature of mitral cell firing is suppressed, and only returns once the stimulation is switched off. The peri-stimulus histograms show that stimulation of the LOT causes a period of inhibition in mitral cell firing [B], under constant-collision stimulation this period of inhibition is prolonged by approximately 5ms. This is due to the difference in arrival time of the stimulus pulse, in the constant-collision protocol the stimulus occurs after the spike leading to delayed activation of inhibitory collaterals relative to the time of the spike hence, there is a longer post-spike silence.

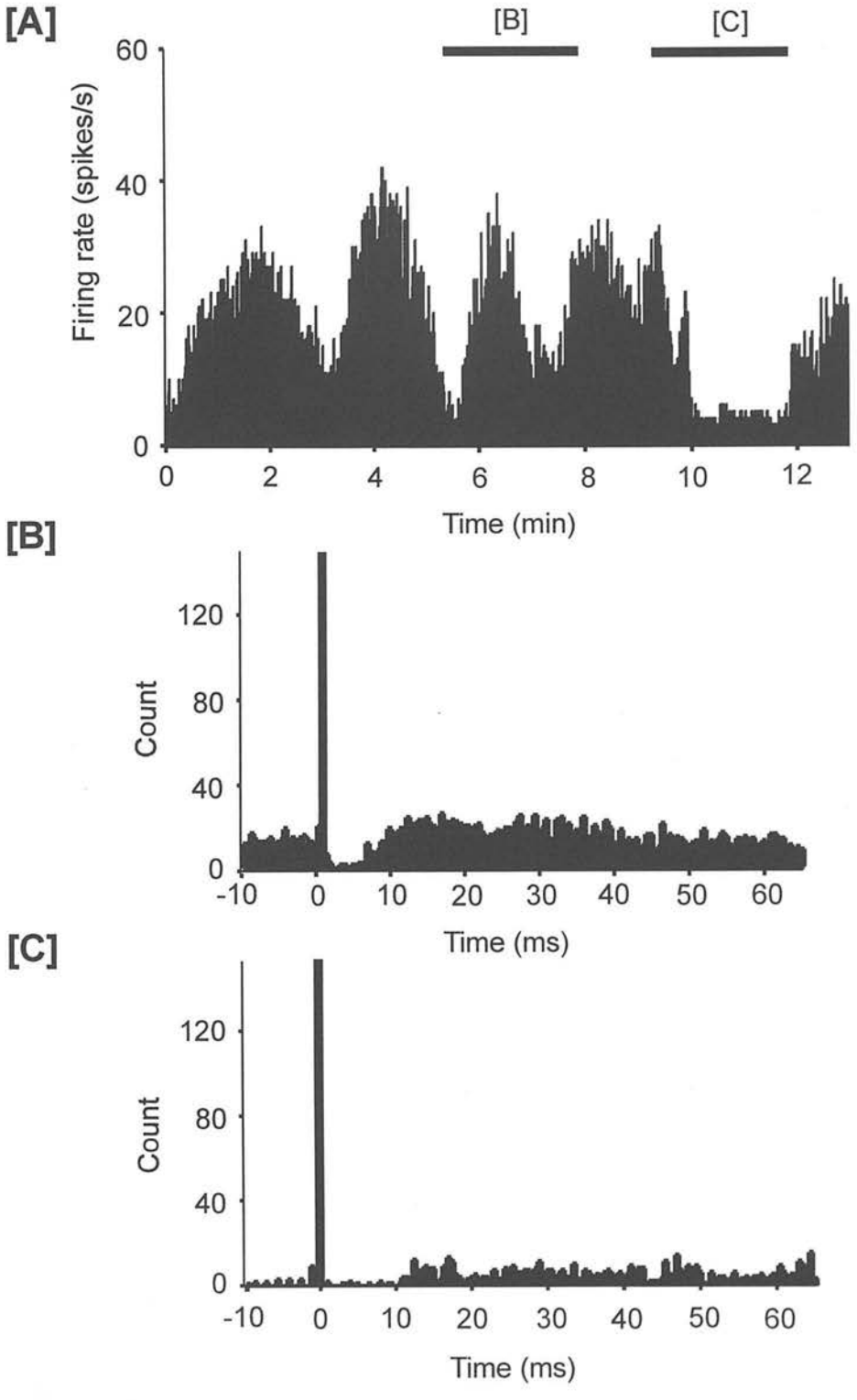
[A]
[B]
[C]
Firing rate (spikes/s)
60
40
20
0
0
2
4
6
8
10
12
Time (min)
[B]
Count
120
80
40
0
-10
0
10
20
30
40
50
60
Time (ms)
[C]
Count
120
80
40
0
-10
0
10
20
30
40
50
60
Time (ms)

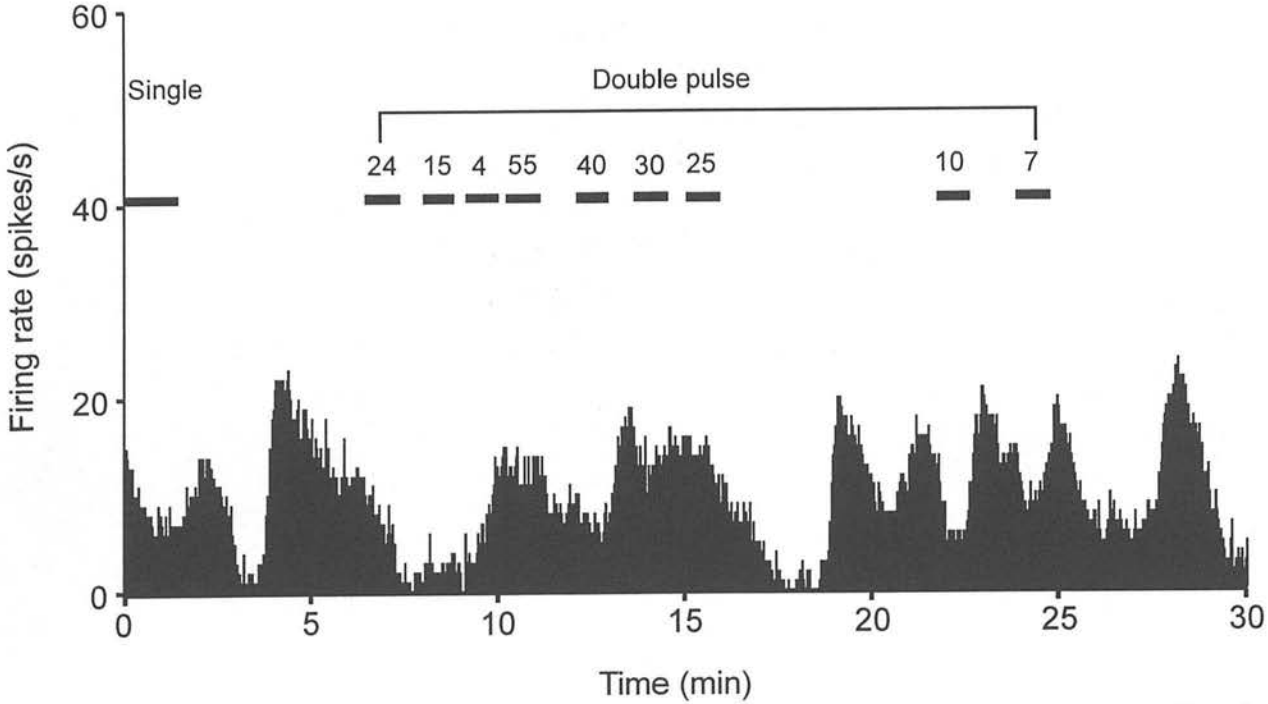

Figure 3.23. Demonstration of the effect on the mitral cell constant latency response of antidromically stimulating the LOT using a double-pulse protocol. Above, is the ratemeter recording of mitral cell activity with the periods of stimulation denoted by black bars and the stimulus inter-pulse gap (ms) indicated. Below, are the peri-stimulus histograms for each inter-pulse gap used the dashed lines represent the stimulus artefact and the black bars are the antidromic spikes. Notice that with an inter-pulse gap of 7-24ms the spike in response to the second pulse occasionally fails with total failure occurring at 15ms. With inter-pulse gaps of 25-55ms there is no failure in the antidromic response.

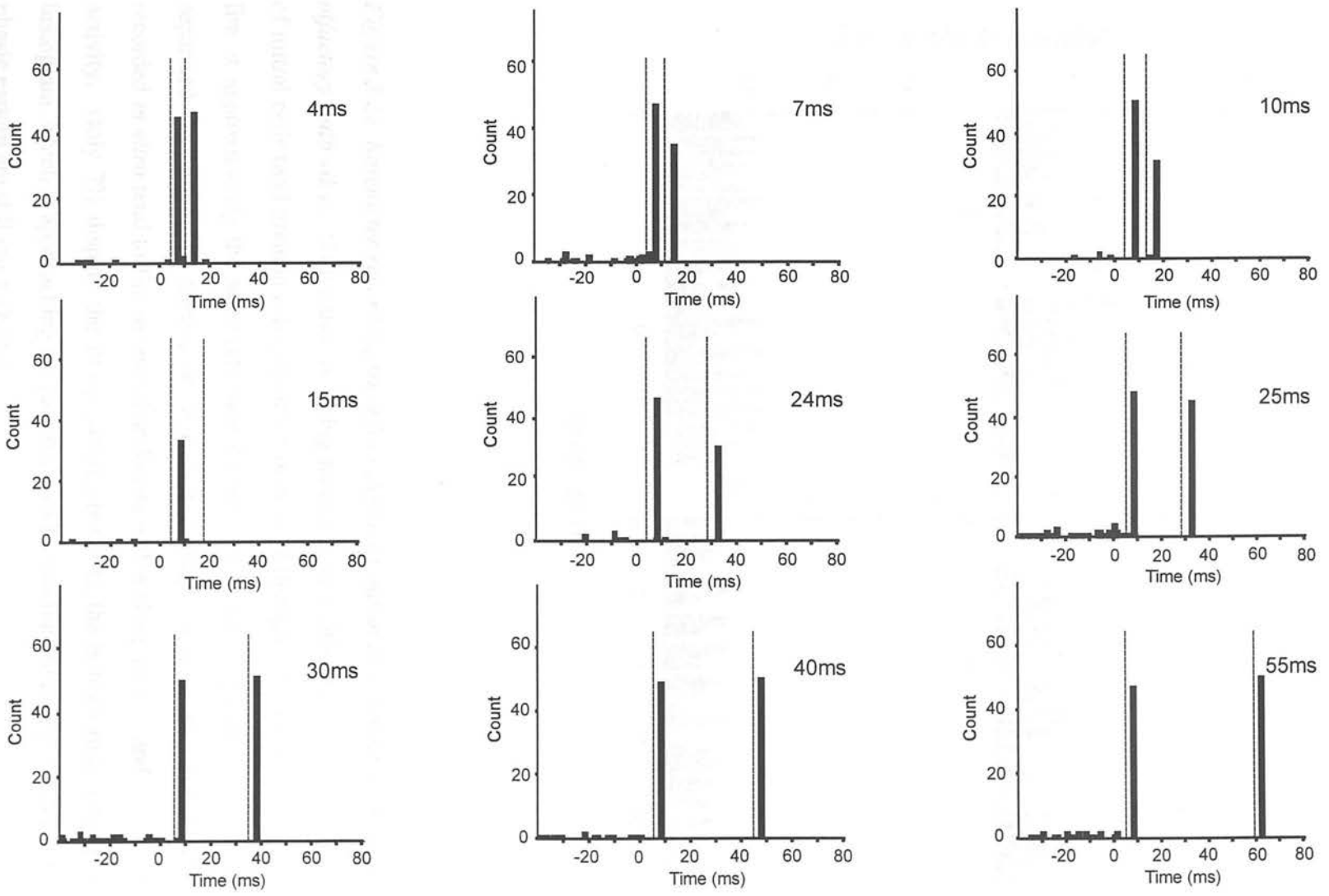
4ms
7ms
10ms
15ms
24ms
25ms
30ms
40ms
55ms
Count
Time (ms)
0
20
40
60
-20
0
20
40
60
80

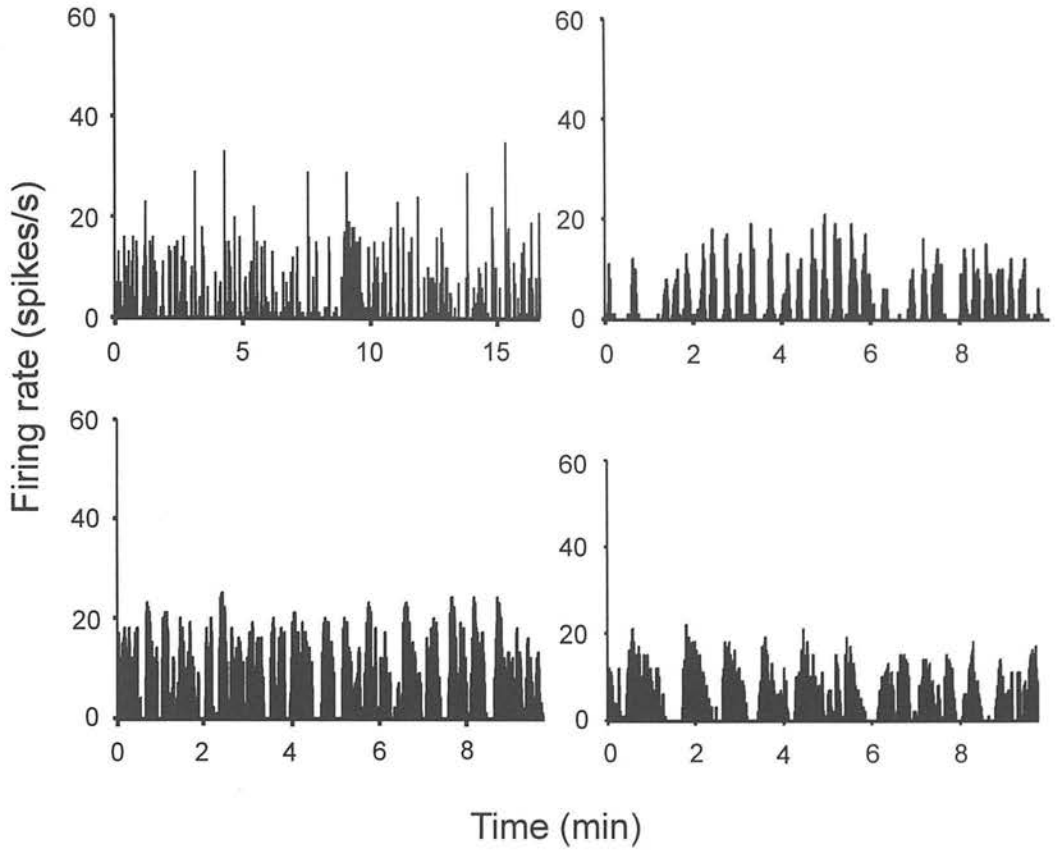

Figure 3.24. Ratemeter recording from four different mitral cells recorded from an olfactory bulb slice. Notice that the firing pattern is very different from recordings of mitral cells (and granule cells) recorded *in vivo*. Although cells recorded *in vitro* fire at approximately the same rate they do not exhibit the long bursts of activity separated by periods of silence or decreased activity. Instead the mitral cells recorded *in vitro* tend to fire in very short bursts with a sharp incline and decline of activity. Only 7% display the firing pattern shown in the bottom right ratemeter histogram, which is approaching the patterns seen *in vivo* but the time periods for the phasic pattern are still much shorter.

Figure 3.25. [A] Interspike interval histograms constructed from 5min periods of spontaneous activity of four different mitral cells recorded from olfactory bulb slices. [B] The hazard function of the mean interspike intervals for mitral cells (n = 45) recorded in vitro. The bimodal distribution displayed by mitral cells *in vivo* was not evident in the *in vitro* recordings; interspike interval distributions showed a longer modal interval compared to the cells recorded *in vivo*. The hazard function is also very different from plots constructed from *in vivo* recordings, the period of post-spike hyperpolarisation is longer lasting in cells recorded *in vitro* and there is no period of depolarisation as the probability of cell firing does not rise above the plateau level. A further difference is the probability of firing reaches a plateau at a higher firing rate than in cells recorded *in vivo*, indicating that the cells are more active in the olfactory bulb slice. Error bars represent the standard error of the mean.

[A]

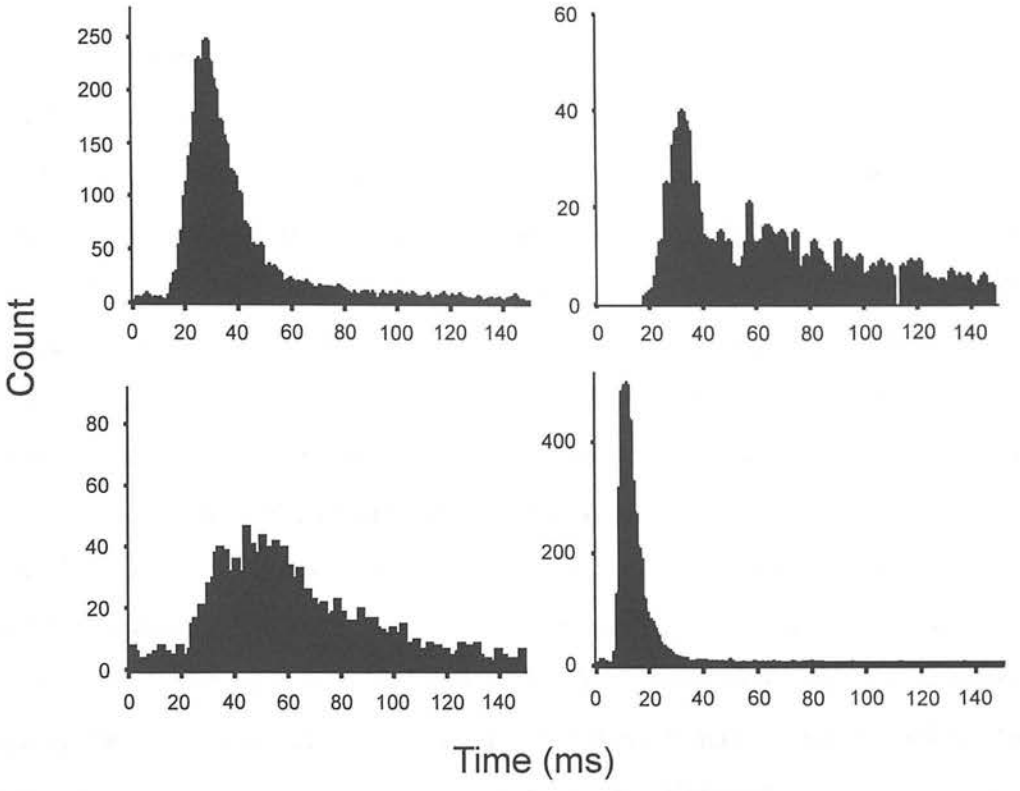

[B]

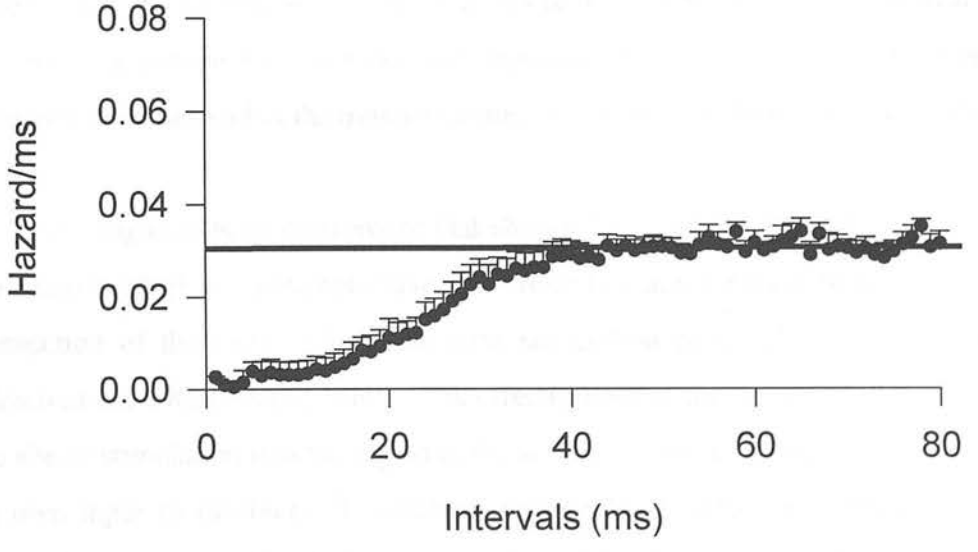

3.4 DISCUSSION

3.4.1 Stimulation site

The physiological approach to the study of mitral cells has taken advantage of the fact that the mitral cell axons gather to form the lateral olfactory tract. A single shock to the LOT sets up a volley of impulses that invade the mitral cells in the antidromic direction. Since the mitral cell bodies lie in a thin layer at the deep border of the external plexiform layer, an antidromic unitary spike recorded at that layer permits unequivocal identification of the recorded unit as a mitral cell. During experimental recording the unitary spikes emerge out of a background of summed extracellular field potentials. The depth of recorded units has been determined by correlating these field potentials with the histological layers of the bulb (Phillips *et al.*, 1963). The advantage of this method of depth determination is that it is instantly made at the time of experimentation. Evoked field potentials were used in the present study to differentiate between layers of the olfactory bulb and the field potentials recorded (fig. 3.3) are consistent with those described by Phillips *et al.* (1963). The field potential for each layer has been divided into three components on the basis of current sources/sinks and represent the excitation and inhibition of olfactory neurones within the mitral-granule cell circuitry, Rall and Shepherd (1968).

Investigators have been aware that shocks delivered to the LOT may activate the centrifugal fibres. Attempts have been made to eliminate these fibres by chronic transection of the LOT, with subsequent stimulation proximal to the transection (Green at al., 1962; Nicoll, 1969). The effectiveness of this is doubtful, as it forces the site of stimulation into the region of the accessory olfactory nucleus, which sends its own input to the bulb. In addition, retrograde effects on the mitral cells are unavoidable. None of the lesioning procedures have been reported to have obvious effects on the properties of unitary or summed potentials in the bulb when evoked from the LOT. Selective activation of different parts of the LOT also gives no evidence for a contribution from the centrifugal fibres. If the centrifugal fibres are

excitatory to the granule cell gemmules, as the anatomical evidence indicates (Price and Powell, 1970a) they would be expected to have a depolarising action on the gemmules. Since the mitral cell dendrites provide for a massive depolarisation of the granule gemmules, this might explain why the centrifugal contribution has not been evident.

The position of the stimulating electrode in electrophysiology experiments discussed in this thesis was 3.2mm anterior to bregma; at this distance from the olfactory bulb it is unlikely that the stimulatory pulse caused direct electrical activation by spread of the current pulse. (The latency of invasion of antidromic spikes recorded in SON neurones following stimulation of the neural stalk is decreased by 0.5ms when the stimulus intensity is doubled; corresponding to an increase in the radius spread of only about 0.1mm in this system (Dyball and Leng, 1991)). Furthermore, at this location the electrode is also far away from regions of the forebrain that send afferents directly to the olfactory bulb, such as the olfactory tubercle and the anterior olfactory nucleus. However, we cannot exclude the possibility that centrifugal fibres from the diagonal band, which run adjacent to the LOT were stimulated in our experiments. The afferents from the diagonal band are a combination of cholinergic and GABAergic fibres and terminate on granule cell spines in the granule and internal plexiform layers. As discussed above they act to depolarise granule cells similar to the action of mitral cells and hence, their influence is probably overshadowed by the massive input from the mitral cells following antidromic activation.

Evoked field potentials were used in conjunction with the collision test to determine if recordings were from antidromically-stimulated mitral cells. There were a small number of cells that displayed firing characteristics very similar to the mitral cells, but that did not respond to antidromic activation with a constant latency spike. There are two possible explanations for this; it may be due to the cells exhibiting

antidromic spikes with very short latencies that were subsequently obscured by the stimulus artefact. Alternatively, it may be that the stimulating electrode positioned over the LOT did not 'catch' all the fibres, consequently, not all the mitral cell axons would be activated resulting in the apparent failure of the antidromic spike.

3.4.2 Waveform

A proportion of the antidromic and spontaneous spikes recorded from mitral and granule cells displayed a distinctive 'notch' during the repolarising phase of the action potential. Similar complex waveforms have been observed in extracellular recordings from magnocellular neurones of the supraoptic and paraventricular nuclei Mason and Leng (1984). Mason and Leng (1984) noted that filtering of the signal could lead to distortion of the recorded waveform; to prevent this and to gain a more accurate description of the extracellular potentials the signal was recorded without filters. In all recordings made in the olfactory bulb filtering of the signal was kept to a minimum (low frequency cut-off, 500Hz; high frequency cut-off, wide band; 50Hz notch activated).

The shape of the mitral and granule cell waveform was the same in antidromically-evoked spikes as in spontaneous, orthodromic spikes this indicates that the waveform is derived from a single neurone rather than from two electrically coupled neurones. It also suggests that the second peak follows action potential invasion of the soma, rather than the axon. The overall mean duration of the action potential waveform recorded from SON neurones at 1/3 maximum height was 1.9 ± 0.17ms. By comparison, the mean duration of the 'notched' action potential waveform recorded from mitral cells in the olfactory bulb was 0.64 ± 0.11ms, much shorter than the waveforms observed in SON neurones. The second peak of the magnocellular waveforms occurred at the top of the repolarising phase and was often so prominent as to give the appearance that it was due to the superposition of two monophasic spikes this greatly increases the spike width. In contrast the waveform

of olfactory cells displayed a smaller 'notch' that generally occurred at the bottom of the repolarising phase.

The notched waveform was also seen in mitral cell spikes recorded from olfactory bulb slices. The 'notch' was seen to disappear upon bathing the slice in low Ca^{2+} medium and only returned once the bathing solution was replaced with standard medium. Further to the experiments performed *in vivo*, Mason and Leng (1984) investigated whether the notched peak of the SON neuronal spikes was related to specific ions or ion channels using the hypothalamic slice preparation. In most cases the spike displayed the complex waveform described *in vivo*. The notched component was abolished when external calcium (Ca^{2+}) concentration was lowered, but enhanced in magnitude and duration when barium ions (Ba^{2+}) were added to the bathing medium. It has been demonstrated in most mammalian cells studied that Ba^{2+} cross the calcium channel more effectively than Ca^{2+} itself (Hagiwara and Byerly, 1981). These results indicate that the notched component of the action potential is carried by Ca^{2+}. Ca^{2+}-dependent action potentials occur in a number of mammalian cells; including neurones of the inferior olive (Llinas and Yarom, 1983a and 1983b) and hippocampal neurones (Schwartzkroin and Slawsky, 1977). In light of the results from magnocellular cells it may be suggested that the 'notch' in the waveform of olfactory neurone spikes is also due to calcium currents. Mason and Leng (1984) noted that the occurrence of the second peak in extracellular spikes recorded *in vivo* was sensitive to electrode movement. Furthermore, the waveform recorded from intracellular electrodes *in vitro* did not show a distinctive second peak. Together these results suggest that the second component of the neuronal spikes is generated at a location other than the soma. It has been shown that by evoking a single action potential in the mitral cell calcium transients are observed in the primary and secondary dendrites as well as the soma and distal dendritic tuft (Bischofberger and Schild, 1995). It is possible therefore that the notched waveform in olfactory neurones is due to calcium currents in the distal dendrites.

3.4.3 Firing rates and discharge patterns

The spontaneous bursting discharge pattern displayed by olfactory bulb neurones has been only loosely described previously in the cat (Motokizawa and Ogawa, 1997), the rat (Yu *et al.*, 1993) and the pig (Reinhardt *et al.*, 1981). In the present study, from the analysis of extracellular recordings of mitral cell activity *in vivo,* it is proposed that the spontaneous discharge pattern of these cells is composed of three separate levels of bursting activity as illustrated by the auto-correlation plots of mitral cell spontaneous activity. This is the first in-depth report of the bursting nature exhibited by olfactory bulb mitral cells. The first and most noticeable level of bursting is the gross phasic pattern of mitral cell firing with periods of silence or quiescence between bursts of high activity. The second bursting pattern is thought to be as a result of a respiratory influence, the intermittent increases in firing rate occur at a frequency of approximately 1.5Hz which corresponds with the respiratory rate measured in anaesthetised animals. The final bursting pattern observed in this study is not exhibited by all mitral cells (57% of the mitral cells recorded), it is evident from the interspike interval histogram that some cells fire with two frequency modes; bimodal mitral cells. This is more clearly illustrated in instantaneous frequency distributions that show the high and low frequency modes are separate from each other and that there is often a delay before the high frequency mode is apparent.

3.4.3.1 Gross phasic pattern

Reinhardt *et al.*, (1981) describe the gross phasic element of mitral cell firing with similar burst lengths and inter-burst times as recorded in the present study. Yu *et al.* (1993) also described a phasic firing pattern but did not quantify the burst parameters. Both groups reported this phasic firing to be displayed by a percentage of the recorded mitral cells (29% and 70% respectively); the other cells were described as continuous firing, compared to the present study in which all mitral cells were described as discharging in a phasic pattern. The discrepancy may be due to the other groups ascribing a cell to be phasic only if it had very obvious periods of little

activity between bursts. However, in the present study, it was found that even if the 'background' activity was high there was still a phasic pattern of discharge superimposed on this and burst lengths and periods of quiescence could be measured. The periodicity of bursts in individual cells was surprisingly consistent, with little difference between burst lengths and inter-burst times.

The previous data shown by Reinhardt *et al* (1981) and Yu *et al* (1993) together with the interpretation of the results of the present study suggests that this gross, overall burst discharge pattern displayed by mitral/tufted cells is not critically influenced or controlled by respiration. This indicates that the phasic pattern originates in the heterogenous connections of individual mitral cells with local interneurones within the bulb. One possible explanation is that, during periods of high activity, the cells have been released from a powerful tonic inhibition.

The 'constant-collision' stimulation disrupted the phasic activity of mitral cells, since this stimulation protocol antidromically activates the neighbouring cells of the recorded cell but not the recorded cell itself, this protocol offers a demonstration of the influence surrounding cells have on the recorded unit. The present results indicate that the surrounding mitral cells have an inhibitory influence, since the bursting nature of the mitral cell was suppressed and only returned once the stimulus was removed. Furthermore, by doubling the intensity of the single pulse shock, thereby antidromically activating a greater proportion of mitral cells, it was shown that the antidromic spike of the recorded unit showed a 60% failure. Both results suggest that mitral cells experience strong lateral inhibition from surrounding mitral cells as well as reciprocal inhibition from the granule cell circuitry. The precise nature of this inhibitory effect is not clear, the extensive intrabulbar network of tufted cell collaterals may mediate it or alternatively the dendrites may release a transmitter that inhibits neighbouring mitral cells.

Simultaneous dual-recordings from two individual mitral cells show that there is limited correlation between the bursts of activity produced by mitral cells and this is consistent with the suggestion of lateral inhibition. However, synchronised activity in mitral cells before and during odourant stimulation has been shown to occur, simultaneous extracellular recordings from 'close' mitral cells (those separated by <40μm) reveal they have similar response profiles (Buonviso and Chaput, 1990) and temporal discharge patterns (Buonviso *et al.*, 1992). In the experiments described in this study the mitral cells observed in the dual recordings had much greater separation distances (>100μm) and this would explain the difference in the two sets of data. Together, these results indicate that active mitral cells form a core of excitation surrounded by a field of inhibition. Since only 45% of close mitral cells are connected to the same glomerulus, (Buonviso *et al.*, 1991), other factors besides common glomerular input probably influence the synchronised activity. A possible explanation for mitral cell synchronisation is that neighbouring mitral cells are coupled via gap junctions, as these intercellular channels can transmit electrical signals. There is evidence to suggest that the olfactory bulb may process olfactory information through radial columns of neurones; gap junctions between neurones are thought to form functional networks of cells exhibiting co-ordinated activity patterns Paternostro *et al.* (1995).

It was considered that the mitral cell phasic discharge pattern may be due, in part, to electroencephalographic (EEG) bursts that are generated throughout the cortex. EEG measurements made in the olfactory system (Eeckman and Freeman, 1990) show that there are sinusoidal bursts of electrical activity in the γ-range (30-100Hz). However, it is thought that none of the inputs to the olfactory bulb carries periodic signals in the γ-range and that the high frequency oscillations present in the olfactory system are generated locally, mediated by negative feedback from local interneurones (Eeckman and Freeman, 1990).

3.4.3.2 Bursting under a respiratory influence

The auto-correlation plots reveal that within each burst of mitral cell activity there are intermittent increases in firing rate and Fourier analysis of these histograms show that these occur with a frequency of 1.5Hz. This frequency is consistent with mitral cell activity being increased during the inspiratory phase of respiration since it was measured that rats maintained under urethane anaesthesia had respiration rates of approximately the same frequency. Onoda and Mori (1980) describe how the periodic increase in mitral cell activity is correlated to air intake, even in the absence of odour application and that the periodic activity disappeared when airflow through the nostril was bypassed. Previous data that conclude that mitral cell activity is not strongly influenced by respiration are discussing the gross phasic pattern which it has been concluded is not under respiratory control since the periods of activity and quiescence are too long to accommodate a respiratory drive.

3.4.3.3 Additional high frequency bursting in bimodal mitral cells

A proportion of the mitral cells recorded in this study displayed a bimodal interspike interval histogram indicating that these cells were firing at two different frequencies. Instantaneous frequency plots clearly show that the cell is firing at two distinct frequencies; a high frequency of firing (100-250Hz) and a lower frequency of firing of up to 100Hz. Furthermore, there is not only a clear separation of the two frequencies but at the onset of a burst there is a delay before the high frequency firing occurs. A bimodal distribution was also described by Motokizawa and Ogawa, (1997) however, the separation and delay in the two firing frequencies were not noticed as the instantaneous frequency plot was constructed from the interspike intervals and not the ratemeter recording as in this present study.

Hence, the present study provides the first account of this bursting behaviour exhibited by mitral cells. In bimodal mitral cells during a burst of activity the mean firing rate of the cell does not change, this indicates that as the high frequency firing

starts to show the slower firing frequency begins to fall away. Together with the fact that there is a delay before the high frequency firing is apparent is suggestive that the site of initiation of these two firing frequencies may be different and as site one becomes inhibited it leaves the way open for the second site to begin firing action potentials. Simultaneous dendritic and somatic whole-cell recordings from mitral cells have shown that the primary dendrites are capable of the active propagation of action potentials (Bischofberger and Jonas, 1997; Isaacson and Strowbridge, 1998). Furthermore, Chen *et al.* (1997) demonstrated that a proximal inhibitory input was able to shift the impulse origin from the soma to the distal dendrite and change the direction of impulse propagation in the dendrite from backward to forward. It is therefore postulated from the results of this present study that inhibition of the low frequency firing from the classical initiation site, close to the soma, enables a shift of initiation site to the distal dendrites that fire at the higher frequency. The source of inhibition close to the soma could be derived from the granule cell circuitry that exerts strong inhibitory effects over the output neurones.

3.4.4 Discharge patterns in vitro

The results from the *in vitro* recordings of mitral cells indicate that the mechanism for burst discharge production is diminished in the slice preparation. Chen and Shepherd (1997) characterised the membrane and synaptic properties of mitral cells in slices of rat olfactory bulb and found a low degree of spontaneous activity within the mitral cell layer. Nickell *et al.* (1996) also found a low level of spontaneously active mitral cells in their slice preparation. However, in the present study many spontaneous firing mitral cells were recorded and were found to fire at similar rates as recorded *in vivo*, yet the discharge pattern was very different. Only a small number of mitral cells displayed any sort of phasic firing pattern and even then the periods of activity and quiescence were markedly shorter than those recorded *in vivo*. This would suggest that either the cutting procedure in preparation of the slice removed a source necessary for the phasic drive or the conditions, in which the slices

were maintained, were detrimental to the 'normal' activity of olfactory neurones. As the secondary dendrites of mitral cells extend through a large fraction of the circumference of the olfactory bulb much of this system is unavoidably removed in the slice preparation and thereby greatly reduces the granule cell inhibition over mitral cells. Therefore the lack of phasic activity seen in the slice may be due to reduced input from the interneurone population.

3.4.5 Response to stimulation of the LOT

Mitral cells consistently showed an inhibitory response to antidromic stimulation of the LOT but cells recorded from the granule cell layer showed a variable response to the stimulation. Considering the dendrodendritic synapse that exists between the granule and mitral cell and since all mitral cells recorded responded to antidromic stimulation with a period of inhibition, one would expect this inhibition to be induced by the inhibitory action of the granule cell. Upon stimulation of the LOT the mitral cell would be activated and release glutamate onto the granule cell gemmules. This would lead to excitation of the granule cell and cause the release of GABA onto the mitral cell dendrites leading to inhibition of the mitral cell. Hence, one would expect to see an excitation of the granule cell following stimulation of the LOT.

One of the problems encountered in studying the physiology of interneurones in the granule cell layer is the presence of multiple cell types, none of which can be unequivocally identified by simple electrophysiological tests such as the antidromic activation criteria for mitral/tufted cells. Mori and Kishi (1982) showed, by using intracellular marking methods, that cells within the granule cell layer that exhibit paired LOT pulse suppression were granule cells and assumed those that do not were short-axon cells. The principal behind this method for identifying granule cells is based on the dendrodentritic synaptic interaction between mitral and granule cell dendrites. Stimulation of the LOT produces inhibition of mitral/tufted cells through

the dendrodendritic synapse. Because activation of granule cells is presumed to be through mitral/tufted dendrites, the ability to activate a granule cell during this IPSP is reduced by failure of spike invasion into the mitral cell dendrites.

However, since no clear criterion for electrophysiological identification of deep short-axon cells exists, it is not possible to rule out that some of the cells recorded in the granule cell layer were in fact short-axon cells. It must be noted however, that the great preponderance of granule cells in the granule cell layer makes it likely that in the present study recordings from the granule cell layer were from granule cells rather than the rarer short-axon cells.

Granule cells have been divided into several subtypes on both morphological (Orona *et al.*, 1983) and electrophysiological (Wellis and Scott, 1990) grounds. Additionally, subpopulations of mitral cells have been described (Orona *et al.*, 1984), and divided into two groups on the basis of the location of their dendritic ramifications within the external plexiform layer. This leads to a great diversity in the local circuitry of the olfactory bulb.

Concluding remark

We have made an in-depth study of the discharge patterns exhibited by the output neurones of the main olfactory bulb and have described for the first time a phasic firing pattern consisting of three levels of bursting behaviour and have suggested possible sources of origin of these bursts.

Chapter 4

The Expression of Fos Following Stimulation of the Lateral Olfactory Tract

4.1 INTRODUCTION

4.1.1 The immediate-early gene c-fos

Immediate-early gene expression has been extensively used for the functional mapping of neuronal activation (Morgan and Curran, 1991; Hoffman *et al.*, 1993). C-*fos* transcription can be induced in cells by a number of secondary messenger systems, including an increased concentration of intracellular Ca^{2+} following membrane depolarisation and influx through voltage-dependent calcium channels (Sheng *et al.*, 1990). Fos protein is transported to the nucleus (from the cytosol) where it forms a heterodimeric complex with Jun, the protein product of another immediate early gene, *c-jun*. The heterodimer binds specifically to a DNA regulatory sequence called the AP-1 biding site, and thereby can alter the transcription of other phenotype-specific target genes, (Curran and Franza, 1988; Morgan and Curran, 1989).

Sagar *et al* (1988) examined the expression of Fos within the rat brain following electrical stimulation of the hindlimb motor/sensory cortex. Fos staining was demonstrated within regions known from prior 2-deoxyglucose uptake experiments, to be metabolically activated by such stimulation. They suggested that Fos immunocytochemistry might provide a method to map the pattern of postsynaptic stimulation within the intact nervous system, with single cell resolution. Since Sagar *et al* (1988) published their findings, Fos expression has been extensively used for the functional anatomical mapping of neuronal activation.

It has been postulated that increased spike activity itself, rather than synaptic input, may be responsible for c-*fos* expression. This theory was addressed in an experiment by Luckman *et al.* (1994) in which the activation of vasopressin and oxytocin neurones of the hypothalamus was studied in the anaesthetised, lactating rat. To test the hypothesis, magnocellular neurones were stimulated by either the intracerebroventricular (*i.c.v.*) application of carbachol, a muscarinic receptor agonist

known to evoke both vasopressin and oxytocin release, hence a receptor-mediated action requiring post-synaptic activity. Alternatively the neurones were activated by antidromic stimulation of the pituitary stalk, an action that would result in spike activity without the influence of synaptic input.

They found a large increase in the number of Fos-positive nuclei in the supraoptic nucleus in brains that received an infusion of carbachol compared to control brains which received an infusion of physiological saline. However, there was no significant difference in the numbers of Fos-positive nuclei in the supraoptic nuclei between brains that had received antidromic stimulation and control rats that underwent surgery but did not receive any stimulation. This evidence strongly suggests that transynaptic activation is required for the full induction of c-*fos*.

4.1.2 Fos studies within the olfactory bulb

Several groups have employed *in situ* hybridisation of c-*fos* mRNA or the immunocytochemical localisation of the protein product, Fos, in the olfactory system. In the olfactory bulb the expression of c-*fos* mRNA has been mapped in response to brief exposure of specific odours (Guthrie *et al.*, 1993) and compared with the results from 2-deoxy-D-[^{14}C]glucose experiments.

In situ hybridisation analysis of odour-induced increases in c-*fos* mRNA expression was used to identify the types and spatial distributions of bulbar neurones activated by brief odours in the behaving rat. In rats removed from their home cages immediately before killing, hybridisation to c-*fos* mRNA was dense in olfactory structures, including the glomerular layer of the main olfactory bulb, the granule cell layer of the main and accessory bulbs and the cellular layers of the anterior olfactory nucleus and piriform cortex.

The possibility that high basal levels of c-*fos* mRNA in the olfactory bulb reflect continuous stimulation by ambient odours in the home cage was tested by maintaining rats in comparatively clean air for 30min before killing. Even though the environment was not specifically deodorised, hybridisation density in the olfactory bulbs of these rats was substantially less than in bulbs from paired littermates recently removed from the home cage. This result suggests that in alert rats, odours normally encountered in the environment stimulate c-*fos* expression by olfactory bulb neurones.

Under experimental conditions rats were maintained in clean air conditions for 30min before exposure to a specific odour (isoamyl acetate or peppermint) for a further 30min. Regional elevations in hybridisation to c-*fos* mRNA in the main olfactory bulb were observed and the distributions of these regions were different, though overlapping, for the two odour groups. Intense hybridisation is associated with (i) individually, spatially segregated glomeruli and (ii) underlying portions of the granule cell layer that extend well beyond the vertical zone defined by a single glomerulus. Autoradiographic grains were concentrated over small neurones surrounding individual glomeruli (the periglomerular interneurones) however cell labelling in the region of neighbouring glomeruli was absent. Underlying the activated glomeruli, grain density was also high over scattered neurones in the external plexiform layer and fewer neurones in the mitral cell layer. Based on size and distribution, these neurones are thought to be external/middle tufted cells and mitral/deep tufted cells respectively.

Dense hybridisation was also associated with large numbers of granule cells underlying activated glomeruli, with clearly defined boundaries between groups of granule cells. Although labelled neurones were present throughout the depth of the granule cell layer, densely labelled cells were more prevalent in superficial layers. It is noteworthy that superficial granule cells receive excitatory input (via reciprocal

dendrodendritic synapses) from the secondary dendrites of tufted cells in the external plexiform layer, many of which were labelled after odour presentation, whereas deeper granule cells are contacted primarily by mitral cells, fewer of which were labelled after odour presentation. This pattern of hybridisation was obtained in rats exposed to odours and was not seen in rats maintained in clean air. Densitometric analysis of film autoradiograms revealed that hybridisation densities in odour-stimulated regions of the glomerular and granule cell layers were 4.4- and 1.9-fold higher, respectively, than in non-activated portions of the same laminae.

Wilson *et al.* (1996) looked at the NMDA-receptor modulation of c-*fos* expression in the olfactory bulb. Mitral cell excitation of granule cells is thought to be mediated by both AMPA and NMDA glutamate receptors, the latter contributing to the prolongation of granule cell depolarisation. It was demonstrated by Guthrie *et al.* (1993) that the NMDA receptor antagonist MK-801 enhanced c-*fos* mRNA expression in mitral/tufted cells of awake rats given odour stimulation. In these experiments, the effect of NMDA receptor antagonists on c-*fos* expression was studied in urethane anaesthetised rats. Rats maintained in room air under urethane anaesthesia alone displayed low levels of c-*fos* mRNA hybridisation, cell labelling occurred in the granule and glomerular layers, with particularly high grain density over scattered mitral cells, a result not seen in the study conducted by Guthrie *et al.* (1993). Treatment with ketamine hydochloride (a non-competitive NMDA blocker) caused increased labelling in the mitral and granule cell layers compared to rats that received an anaesthetic dose only. Administration of the specific NMDA receptor antagonist, CGP39551, produced a further increase in mitral cell layer c-*fos* mRNA hybridisation, and a reduction of labelling in the granule cell layer. MK-801 (also a non-competitive NMDA blocker) again, produced a large increase in hybridisation in the mitral cell layer, resulting in dense labelling of virtually all mitral cells, while the incidence of well-labelled granule cells was negligible. Overall, cell labelling patterns reveal a negative correlation between hybridisation levels in the granule and

mitral cell layers; the less labelling seen in the granule cell layer, the more labelling seen in the mitral cell layer.

4.1.3 Retrograde tracer studies

A direct connection between the MOB and the supraoptic nucleus (SON) was first postulated by Scalia and Winans (1975). Following degeneration procedures, terminal fields in the area immediately ventral and lateral to the posterior portions of the SON were observed. Using neurophysin immunocytochemical labelling of the SON, the fine resolution of axon terminals and the dendritic zone of the SON were uncovered (Smithson *et al.*, 1989). It was realised that the dendrites extend ventrolaterally into periamygdaloid areas as well as the established projection anteroposteriorly. A combination of anterograde and retrograde tracer studies (Smithson *et al.*, 1992) supported the earlier findings of a direct connection from the MOB and AOB. Smithson *et al* (1992) reported that the LOT contains efferents from both the main and the accessory olfactory bulbs providing a direct connection to the ipsilateral SON, but not to the contralateral SON or the paraventricular nucleus.

A series of electrophysiological experiments were performed in the rat to look at the response of SON neurones to electrical stimulation of the LOT (Hatton and Yang, 1989). A slice (500-600μm) was prepared that consisted of the basal hypothalamus and ventral cortex extending several millimetres rostral to the SON. The stimulating electrode was placed in the LOT approximately 2mm rostral to the ipsilateral SON. Intracellular recordings from SON neurones following LOT stimulation reveal monosynaptic excitation in approximately equal numbers of oxytocin and vasopressin neurones. The inputs to and activation of oxytocin cells following LOT stimulation suggests a possible role for olfaction in the modulation of oxytocin release during suckling, parturition and maternal behaviour. Increased dye coupling between SON neurones in maternally behaving virgins and lactating rats following *in vitro* LOT stimulation (Hatton and Yang, 1990; Modney *et al.*, 1990)

suggest that olfactory input may be involved in the synchronisation of oxytocin cell bursting, thus facilitating the pulsatile release of oxytocin during parturition and milk let-down.

AIMS

The initial aim of this section of the project was to confirm the previously reported connection between the olfactory system and the magnocellular cells of the supraoptic nucleus (SON). Several reports have suggested a direct pathway connecting the main and accessory olfactory bulbs to the dendritic region of the SON using tracer techniques (Smithson *et al.*, 1989, 1992) and *in vitro* electrophysiology (Hatton and Yang, 1989). In the present study, retrograde labelling was combined with c-*fos* immunocytochemistry to look at the pathway between these two regions. Fos expression was used as a marker to observe the effects of stimulating the LOT, *in vivo*, on neuronal activity within the SON and other regions of the brain associated with the olfactory system. Having determined the rate and pattern of mitral cell discharge (Chapter 3) two stimulation protocols were used, both were strong stimuli applied in different formats. The first was a short burst at a high frequency to mimic an acute, strong output from the olfactory bulb; the second was a prolonged stimulation used to disrupt the output discharge pattern.

4.2 METHODS

4.2.1. Retrograde labelling

Rats were anaesthetised with 5% Halothane anaesthesia and positioned within a stereotaxic frame, throughout the procedure the rats were maintained under 2-3% Halothane. Injection sites were located by measuring co-ordinates from bregma (Paxinos and Watson, 1997) SON: 0.9mm posterior, 1.9mm lateral and 9.0mm dorsoventrally; anterior cortical amygdala: 3.8mm posterior, 4.0mm lateral and 9.0mm dorsoventrally. Each rat received a unilateral injection of Fluoro-Gold (FG) into either the SON or the amgydala region. A 1.0mm hole was made using a dental

drill (round 2 burr) and a guide cannula attached to the arm of the frame was lowered to the required depth.

A non-metallic syringe needle used for filling microelectrodes (MicroFil, World Precision instruments, Inc, USA) was attached to a 25µl Hamilton syringe containing the FG solution. The electrode filler had been cut so that it was just seen to exit the guide cannula, this was to prevent the tracer from being drawn up the cannula rather than being ejected into the brain tissue. The electrode filler was inserted into the guide cannula and the syringe clamped into position. A volume of 1µl FG was injected and then the guide cannula was withdrawn slowly over a period of 30min to minimise uptake of tracer by damaged fibres of passage. Once the guide cannula had been removed the wound was closed with 3-4 sutures (EP 2). Following surgery, rats were placed into a clean cage and quickly recovered from the anaesthetic. A survival time of 2-7 days is recommended for transport of the tracer (Fluorochome Inc.) after which five rats were used in the electrophysiology experiments described below, the remainder (n=5) were administered a lethal dose of pentobarbitone and perfused.

4.2.2. Surgical preparation

Experiments were performed on virgin female Sprague-Dawley rats (250-350g). The experiments involved non-recovery surgery however, the animals were anaesthetised with an injection of Sagatal (sodium pentobarbitone, 60mg/kg, i.p) rather than urethane. The tissue was to be processed for Fos immunocytochemistry following the completion of the electrophysiological experiment and urethane has been shown to induce the expression of Fos (Takayama *et al.*, 1994) which would give misleading results. The level of anaesthesia was monitored throughout the surgical procedure and supplementary doses administered as necessary. The rats were prepared for dorsal surgery, holes were drilled over both the left and right LOT (4.0mm lateral and 3.2mm anterior to bregma).

4.2.3 Experimental design

In experimental rats, a bipolar stainless steel electrode was lowered into the left LOT and the stimulator delivered a biphasic pulse of 1mA peak to peak with a width of 1ms at a frequency of either 50Hz for a period of 10min or 200Hz for a period of 10s. The electrode was then lowered into the right LOT and removed without stimulation. Initial experiments used the contralateral side to stimulation as an internal control. However, it was necessary to include a sham operated group to gain an insight into the control levels of Fos as the olfactory system contains bilateral connections. Thus, stimulation of the LOT would affect the contralateral as well as ipsilateral hemisphere. Therefore, in the sham operated group the stimulating electrode was lowered into both the right and left LOT but no current was applied on either side. The position of the stimulating electrodes in the right and left LOT was verified post-experimentally and the photomicrograph in figure 4.1 shows the passage of the electrodes through the brain towards the LOT.

The anaesthesia was maintained for 90min after the surgery (and stimulation if it was an experimental group); the rats then received an overdose of pentobarbitone and were transcardially perfused with a solution of 4% paraformaldehyde in 0.1M phosphate buffer (see section 2.6, General Materials and Methods). The brains were removed and a nick made in the left side of the brain to discriminate between experimental and control sides. This was difficult to achieve with the olfactory bulbs owing to their small size, so the rostral tip of the left (experimental) lobe was trimmed, so that it was slightly shorter than the right lobe. The brains were snap frozen and stored at -70°C until they were cut and processed for Fos immunocytochemistry. As a positive control for the induction and subsequent labelling of Fos protein, sections from a rat that had received an injection of hypertonic saline (i.p) were processed for Fos immunocytochemistry along with the experimental brain sections. Giovannelli *et al.* (1990) have shown that the osmotic stress related to hypertonic saline administration reliably induces a great number of

Fos-positive neurones in both the SON and the PVN. Therefore, once Fos was seen to have been labelled in these sections the visualisation reaction was terminated.

4.2.4 Data analysis and photomicrographs

The slides were coded by covering identification numbers with masking tape and assigned random numbers before quantification to prevent bias. Using a Leica microscope and camera system the number of Fos-positive nuclei in each brain region of interest, from both hemispheres, were counted. This was done under x20 objective in brightlight conditions. For each brain region, counts were made on at least 10 sections for each animal and the mean value (± S.E.M.) calculated. Statistical analysis was performed using the SigmaStat software package on a PC. Non-parametric or distribution-free tests were performed on ranks of the observations when the populations were not normal. To compare data within a group the Wilcoxon-Signed Rank test was used and to compare data between two independent groups the Mann-Whitney Rank Sum Test was used. Statistical significance was accepted when $p<0.05$. Asterisks above the bars in the histograms indicate there is a significant difference between values. Retrogradely labelled cells were viewed under a U.V light and filter, the number of cells labelled with Fluoro-Gold were counted for both the ipsilateral and contralateral lobes of the olfactory bulb. In rats that received an injection of tracer prior to stimulation of the LOT, the number of double labelled cells were counted as well as those that were filled with tracer alone and cells that were Fos-positive but not labelled with tracer. All coronal reconstructions are based on the Atlas of Paxinos and Watson, (1997) the location in relation to bregma is printed to the top right of each map.

Acknowledgement

Christine Fiddler (BSc Honours student) assisted in the processing of brain sections for Fos immunocytochemistry (n=10) and subsequent analysis.

Figure 4.1. Verification of the sites for stimulation, [A] the coronal reconstruction shows the location of the LOT and [B] the photomicrograph shows electrode tracts directed towards this position. The co-ordinate (mm anterior to bregma) is indicated in the top right of the section. The photomicrograph is a 52μm section; the tracts have been stained due to the presence of large amounts of endogenous peroxidase in this region of the section during the immunocytochemical processing for Fos. The schematic diagram shown in [C] illustrates the two different stimulation parameters that were used to stimulate the LOT; both were strong stimuli applied in a different pattern. The first stimulation parameter involved a short burst at a high frequency (200Hz, 10s) this was used to mimic an acute, strong output from the olfactory bulb and the second stimulation parameter was a prolonged stimulation, at a lower frequency to reduce the intensity of the stimulus applied, (50Hz, 10min) and aimed to disrupt the output pattern of the olfactory bulb.

[A]

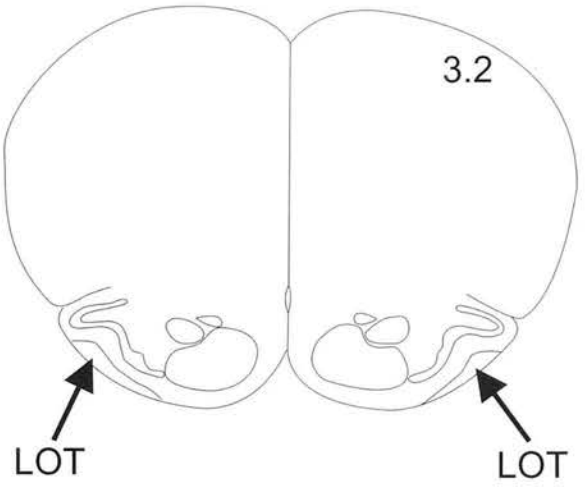

[B]

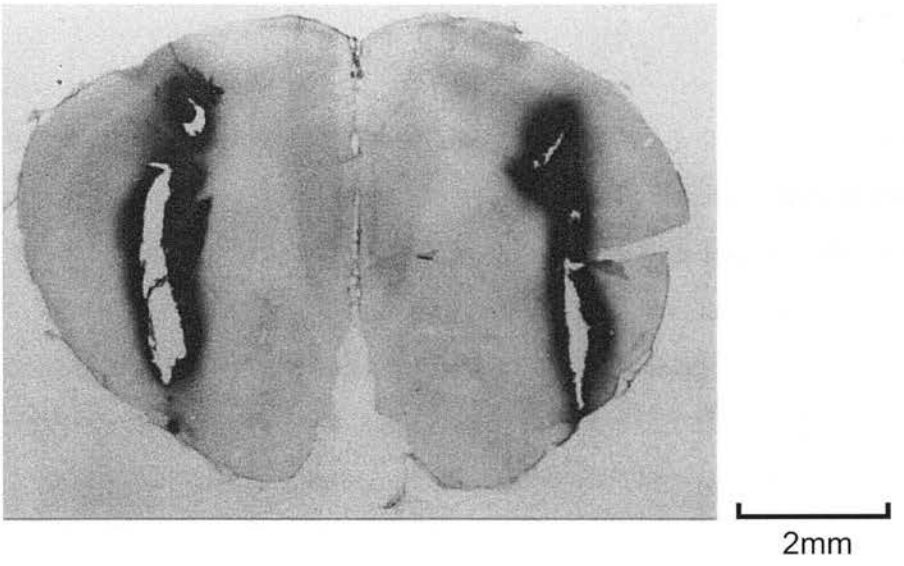

[C]

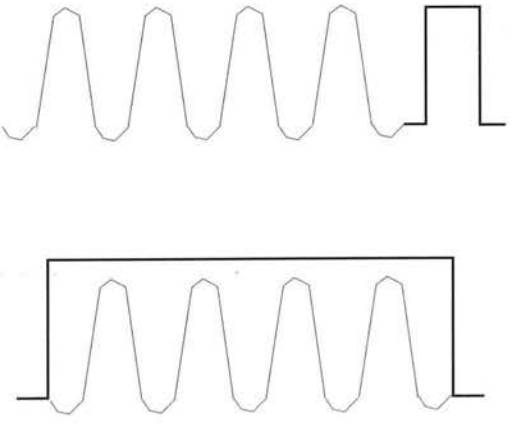

4.3 RESULTS

Following the prolonged stimulation of the LOT (n = 13) Fos-positive nuclei were found in several regions of the brain both ipsilateral and contralateral to the side of stimulation. The level of staining was compared with the other groups, sham operated (n = 4) and short pulse of stimulation (n = 4) for all regions in the olfactory bulb, cortex and brainstem. In each of the following figures the number of rats in the three different stimulation protocols remain the same: control (4), 50Hz/10min (13), and 200Hz/10s (4).

4.3.1 Main olfactory bulb - mitral cells

In the mitral cell layer of the main olfactory bulb (fig 4.2.) there was a high degree of Fos staining on the ipsilateral side following prolonged stimulation of the LOT. The mean number of Fos-positive nuclei counted for the ipsilateral side was 61.4 ± 4.1 nuclei/section which was significantly higher than the mean value for the contralateral side of 11.2 ± 1.9 nuclei/section ($p<0.0001$). The level of Fos staining following the prolonged stimulation was significantly higher ($p<0.001$) than that seen in control rats (ipsilateral, mean number of Fos-positive nuclei was 20.5 ± 1.7 nuclei/section) and following the short pulse (ipsilateral, 22.2 ± 2.4 nuclei/section). There was no significant difference between control rats and those that received the short pulse of stimulation furthermore, within each group there was no difference between ipsilateral and contralateral sides.

4.3.2 Main olfactory bulb - tufted and periglomerular cells

The number of activated tufted and periglomerular cells (fig 4.3) decreased following stimulation of the LOT in comparison to control rats. There were relatively few Fos-positive internal and middle tufted cells in all three groups. There was no significant difference between ipsilateral and contralateral sides for any cell type in any of the three experimental groups. In the case of internal tufted cells the only significant difference in the mean number of Fos-positive cells was between the

contralateral control (9.8 ± 0.8 nuclei/section) and the contralateral side during prolonged stimulation (4.9 ± 0.5 nuclei/section). The numbers of Fos-positive middle tufted cells fell from control levels of 16.9 ± 1.1 nuclei/section to 9.5 ± 1.3 nuclei/section in the short pulse group and 3.9 ± 0.7 nuclei/section in the prolonged group. A similar fall in numbers was seen for the Fos-positive external tufted cells and the periglomerular cells. Photomicrographs in figure 4.3C highlight the changes in cellular expression of Fos in mitral/tufted cells described above.

4.3.3 Main olfactory bulb - granule cell layer

The granule cell layer of the main olfactory bulb showed a high degree of staining for Fos. Granule cells were rarely seen in the medial section of the slice and more frequently located in the dorsal and ventral poles with no clear distinction between the deep and superficial layers of granule cells (fig. 4.4A). For each group there was no significant difference between the numbers of Fos-positive nuclei in the dorsal or ventral poles, furthermore there was no difference between ipsilateral and contralateral sides of the bulb (fig. 4.4B). There was no significant difference between the numbers of Fos-positive nuclei in the short pulse stimulation group (ipsilateral, dorsal pole: 35.5 ± 4.7 nuclei/section) compared to the control group (ipsilateral, dorsal pole: 34.5 ± 5.4 nuclei/section). There was an increase in Fos expression following prolonged stimulation of the LOT both ipsilaterally (increased to 85.7 ± 5.9 nuclei/section) and contralaterally (increased to 99.7 ± 13.4 nuclei/section) compared to control levels and the short-pulse group ($p<0.001$). The photomicrographs in figure 4.4C show the difference between the granule cell layer following prolonged-stimulation and sections from brains that were stimulated with a short pulse and control rats. The granule cell layer from the prolonged stimulation group has cells arranged in sheets that follow the contour of the bulb; the organisation of Fos-positive granule cells in the other two groups is more random.

4.3.4 Accessory olfactory bulb

Fos-positive nuclei were also seen in the accessory olfactory bulb (fig. 4.5). The layers of the accessory olfactory bulb are not as clearly organised as in the main olfactory bulb, but the mitral and granule cell layers are easily identifiable. In the granule cell layer there was no significant difference between ipsilateral and contralateral sides for any of the three experimental groups, neither was there a difference in levels of Fos staining between the control rats and the short-pulse stimulation group. There was a significant increase ($p<0.01$) in the number of Fos-positive nuclei in the granule cell layer of the accessory olfactory bulb following prolonged-stimulation (19.1 ± 2.1 nuclei/section) compared to control levels, (ipsilateral: 7.4 ± 3.2 nuclei/section). In the mitral cell layer there was no significant difference between ipsilateral and contralateral sides for the control and short-pulse groups, but in the prolonged group the ipsilateral side showed a higher number of Fos-positive nuclei (ipsilateral: 59.6 ± 4.8 nuclei/section, contralateral: 43.0 ± 2.9 nuclei/section) ($p<0.001$). Both the prolonged ($p<0.0001$) and short-pulse ($p<0.01$) stimulation groups showed a higher number of Fos-positive nuclei in the mitral cell layer compared to control rats (control: 13.5 ± 3.8 nuclei/section, prolonged group: 59.6 ± 4.8 nuclei/section, short pulse group: 44.1 ± 12.2 nuclei/section), there was no significant difference between the two stimulation groups.

4.3.5 Piriform cortex

Outwith the olfactory bulb, one of the most striking areas of staining for Fos protein was in the piriform cortex. Two different portions of the piriform cortex were counted. The first, most rostral, area of the piriform cortex counted is found at the level of the horizontal limb of the diagonal band (0.48mm anterior to bregma). At this point the piriform cortex forms an arch over the lateral olfactory tract and the number of Fos-positive nuclei that comprised this arch were counted (fig. 4.6). Fos-positive nuclei were only found in this area following prolonged stimulation of the

LOT and there was no significant difference between ipsilateral and contralateral sides, (ipsilateral: 70.3 ± 9.2 nuclei/section, contralateral: 59.6 ± 12.5 nuclei/section).

The second region of the piriform cortex in which Fos-positive nuclei were counted is located at the level of the SON (1.3mm posterior to bregma). The piriform cortex now runs in a band from the rhinal fissure to the ventral surface of the brain following the curvature of the lateral wall (fig. 4.7). The number of Fos-positive nuclei in this section of the piriform cortex was low in the control brains, with no difference between ipsilateral and contralateral sides (ipsilateral: 14.1 ± 3.6 nuclei/section). Again there was no significant difference between ipsilateral and contralateral sides for the prolonged stimulation group, but the number of Fos-positive nuclei following prolonged stimulation was significantly higher ($p<0.0001$) than in control rats (ipsilateral: 119.6 ± 18.2 nuclei/section). In the short-pulse stimulation group there were a greater number of Fos-positive profiles on the ipsilateral side ($p<0.0001$) (ipsilateral: 69.8 ± 21.6 nuclei/section; contralateral: 5.0 ± 2.1 nuclei/section). The level of staining following the short pulse stimulation was lower than after the prolonged stimulation ($p< 0.001$) but higher ipsilaterally (and lower contralaterally) than in control rats ($p<0.01$).

4.3.6 Hypothalamic nuclei

Other areas of the brain which expressed Fos following stimulation of the LOT were the paraventricular and supraoptic nuclei of the hypothalamus. There was no significant difference in the numbers of Fos-positive nuclei found in the ipsilateral and contralateral sides for either region. In the paraventricular nucleus (fig. 4.8) both the prolonged and short pulse stimulation significantly increased ($p<0.0001$) the number of Fos-positive nuclei above control levels (control: 0.8 ± 0.3 nuclei/section, prolonged: 17.2 ± 1.4 nuclei/section, short pulse: 7.3 ± 1.8 nuclei/section). The Fos-positive cells were predominantly located in the parvocellular region of the nucleus. In the SON (fig. 4.9) there were relatively few Fos-positive nuclei in all three

experimental groups. There was a small increase ($p<0.01$) in the number of Fos-positive nuclei in the ipsilateral side following prolonged stimulation compared to the ipsilateral side in control rats, (control: 10.4 ± 1.5 nuclei/section, prolonged group: 16.5 ± 1.1 nuclei/section) but there was no significant difference between the contralateral sides of the two groups. The short-pulse stimulus group was significantly lower, both ipsilaterally and contralaterally, than the prolonged-stimulation group ($p<0.0001$) but not significantly different from the control group.

The numbers of Fos-positive neurones in the SON and PVN of the hypertonic saline treated rat (n=1) were significantly higher than counts in the control group or either stimulation group. There was no significant difference between the two hemispheres for either region. In the SON the number of Fos-positive nuclei were 37.5 ± 3.2 and 37.8 ± 2.5 nuclei/section and in the PVN the number of Fos-positive nuclei were 32.6 ± 4.6 and 35.8 ± 2.8 nuclei/section. The results for the hypertonic saline rat are shown in the summary of results (fig. 4.10).

In the brainstem, a small number of Fos-positive nuclei were found in the locus coereulus, raphe nucleus and A1 region in control rats and following stimulation of the LOT but there was no significant difference between the groups.

4.3.7 Retrograde labelling

Following the microinjection of a 2% solution of Fluoro-Gold into the region of the SON (n = 5) labelled cells could be seen in the ipsilateral main and accessory olfactory bulbs but not the contralateral bulb. In the main olfactory bulb, labelled cells were located in the mitral and external plexiform layers, the latter of which were found in the deep sublaminae and not seen in the middle or external sublaminae of the external plexiform layer. These cells could therefore be described as either displaced mitral cells or deep tufted cells. In the histogram (fig 4.11B) these cells have been called tufted cells. A much greater proportion (approximately 75%) of

labelled cells were located within the mitral cell layer. In the accessory olfactory bulb the layers are not so distinct but the mitral cells were clearly labelled. No fluoresence was seen in the granule or glomerular cell layers of either the main or accessory olfactory bulbs. Retrograde labelling was not seen in any other brain region, including the piriform cortex, following injection of tracer into the SON region.

Following the injection of Fluoro-Gold into the region of the anterior cortical amgydala (n = 5) labelled cells were seen in the ipsilateral piriform cortex and the ipsilateral diagonal band (fig. 4.12). Injection into this area also resulted in a large number of labelled mitral cells in the ipsilateral main olfactory bulb, no labelling was seen in the contralateral olfactory bulb or the accessory olfactory bulb. The cytoplasm of some mitral cells became completely filled with Fluoro-Gold highlighting the characteristic pyramidal shape of their soma. Again, there was no fluorescence seen in the granule or glomerular cell layers of the main olfactory bulb. The animals in this group also underwent prolonged stimulation of the LOT. This induced Fos expression within the olfactory bulb and hence, a proportion of the retrogradely labelled cells was also labelled with Fos (fig. 4.12D). However, stimulation of the LOT did not induce Fos expression in the diagonal band or the amygdaloid nuclei.

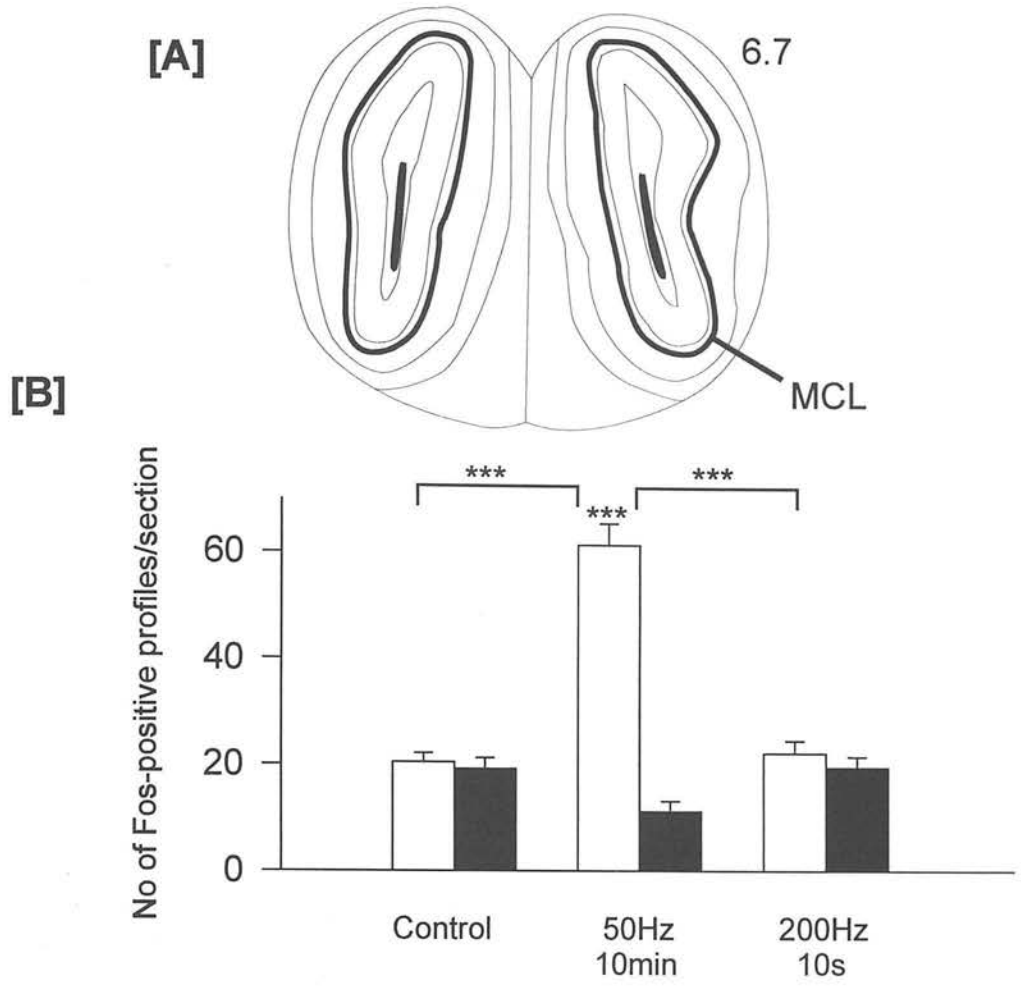

Figure 4.2. [A] Coronal reconstruction of the main olfactory bulb of the rat (6.7mm anterior to bregma). The mitral cell layer is highlighted by a thick black line. [B] The bar chart shows the number of Fos-positive nuclei located in the mitral cell layer under sham stimulated and following stimulation of the LOT at two different frequencies. Counts made in the ipsilateral side to stimulation are shown as open bars and counts made in the contralateral side as filled bars in the histogram [B]. There is a clear activation of mitral cells in the ipsilateral olfactory bulb during prolonged stimulation that is statistically different from the contralateral bulb and control group ***P<0.0001 (Mann-Whitney Rank Sum Test). There is no significant difference between the Fos counted in the short-pulse group and control group. Photomicrographs of cells in the mitral cell layer are shown in figure 4.3[C] along with the tufted cells and periglomerular cells. Abbreviations; MCL mitral cell layer.

Figure 4.3. [A] Coronal reconstruction of the main olfactory bulb (6.7mm anterior to bregma) indicates the position of the three types of tufted cell (Td internal; Td middle and; Td external) within the external plexiform layer. The position of periglomerular and short-axon cells is shown between the glomeruli. [B] Bar charts showing the number of Fos-positive nuclei counted in the glomerular and external plexiform layers. Over the page, [C] photomicrographs showing the expression of Fos in the tufted, periglomerular and mitral cells under the different stimulation parameters. Notice that there are relatively few Fos-positive profiles in the category of internal and middle tufted cells for all stimulation groups. Both stimulation parameters are seen to lower the number of activated tufted and periglomerular/short-axon cells relative to the control group. ***P<0.0001, **p<0.001, *p<0.01 (Mann-Whitney Rank Sum Test). Abbreviations: EPL, external plexiform layer; GCL, granule cell layer; MCL, mitral cell layer; PG, periglomerular cell; SA, short-axon cells; Td, tufted cell.

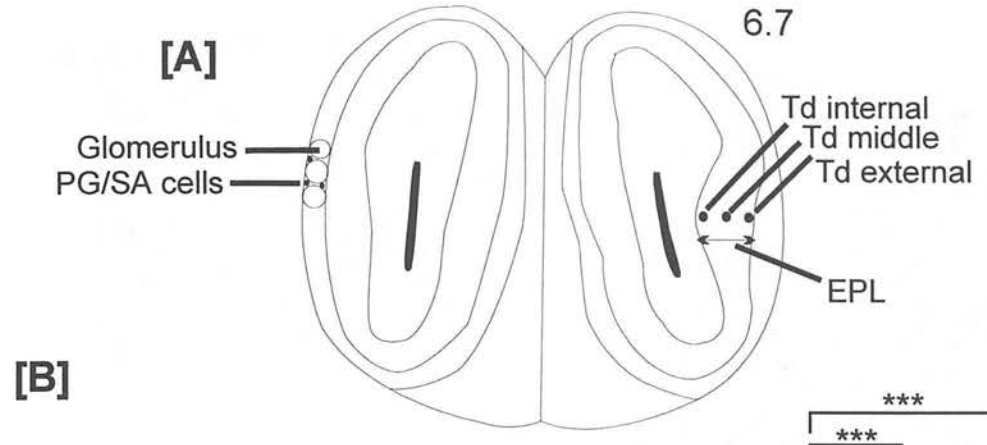
[A]
6.7
Glomerulus
PG/SA cells
Td internal
Td middle
Td external
EPL

[B]

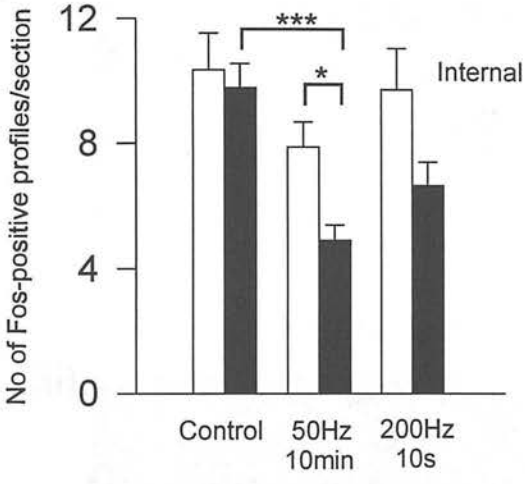
No of Fos-positive profiles/section
12
8
4
0
***
*
Internal
Control
50Hz 10min
200Hz 10s

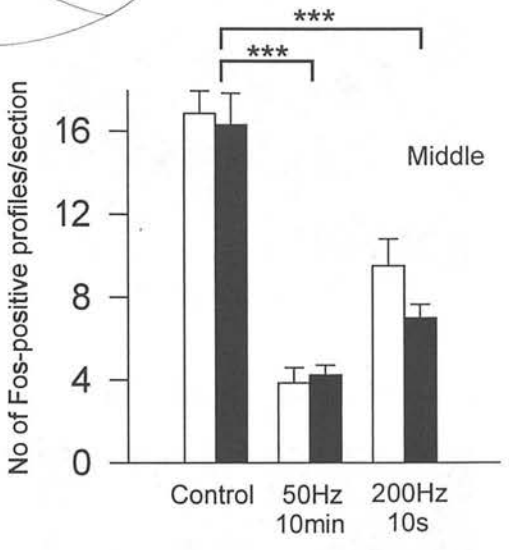
No of Fos-positive profiles/section
16
12
8
4
0
***
***
Middle
Control
50Hz 10min
200Hz 10s

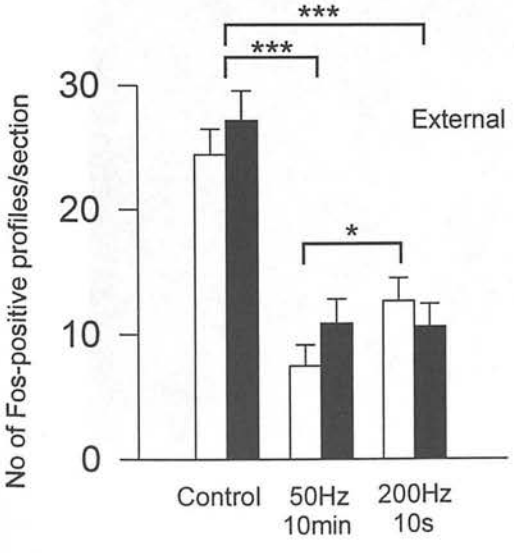
No of Fos-positive profiles/section
30
20
10
0
***
***
*
External
Control
50Hz 10min
200Hz 10s

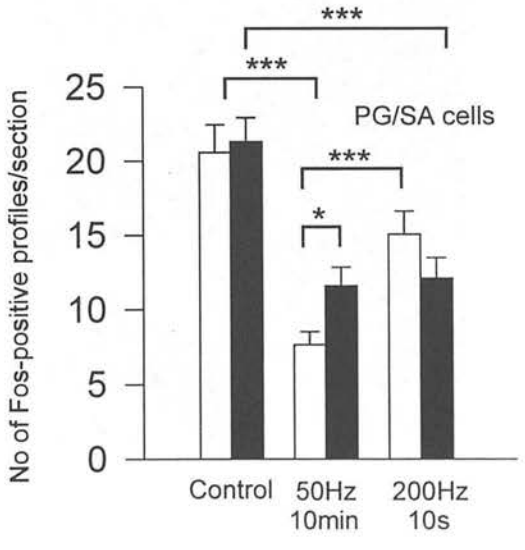
No of Fos-positive profiles/section
25
20
15
10
5
0
***
***
***
*
PG/SA cells
Control
50Hz 10min
200Hz 10s

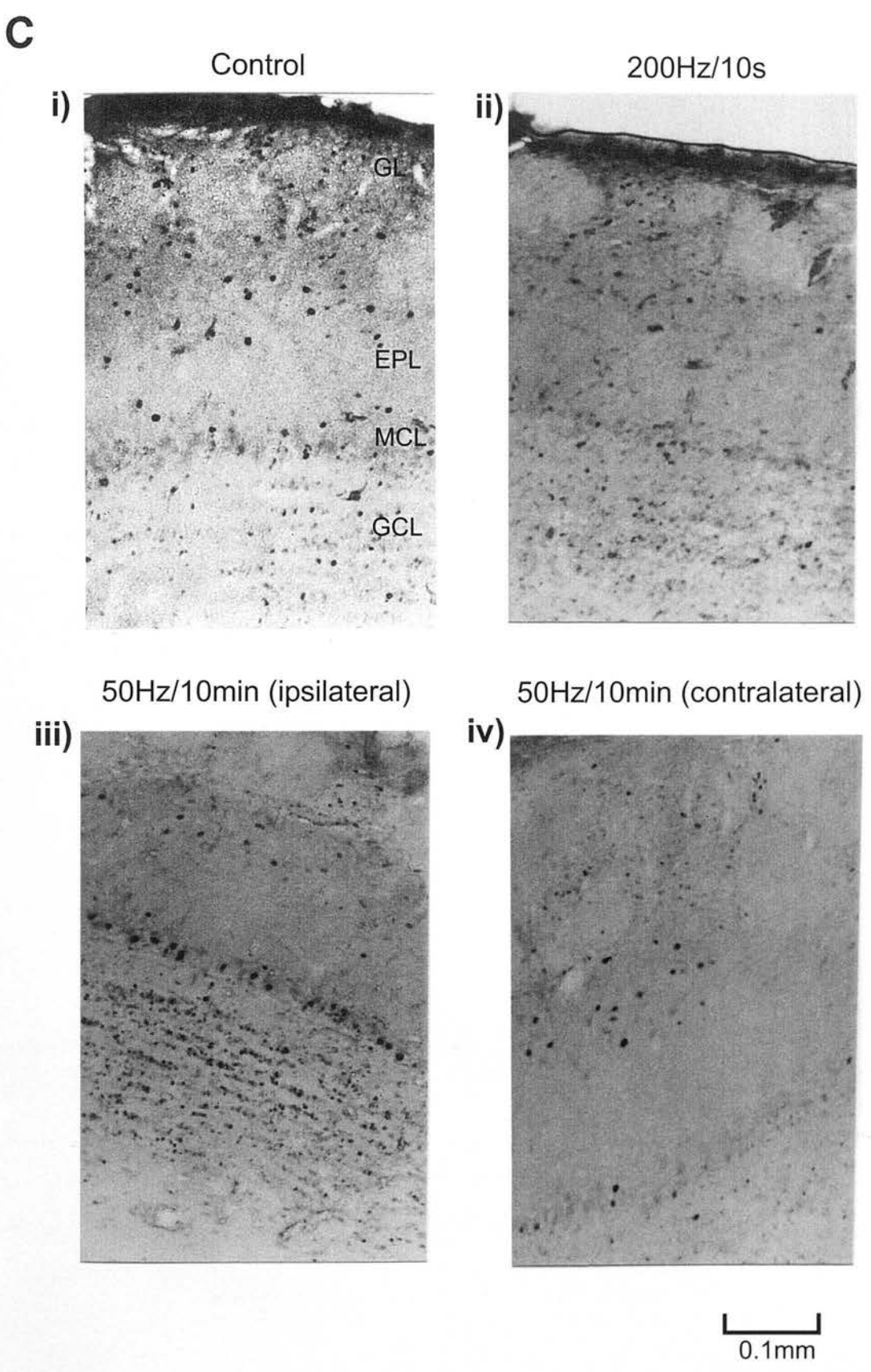
C
Control
200Hz/10s
i)
ii)
GL
EPL
MCL
GCL
50Hz/10min (ipsilateral)
50Hz/10min (contralateral)
iii)
iv)
0.1mm

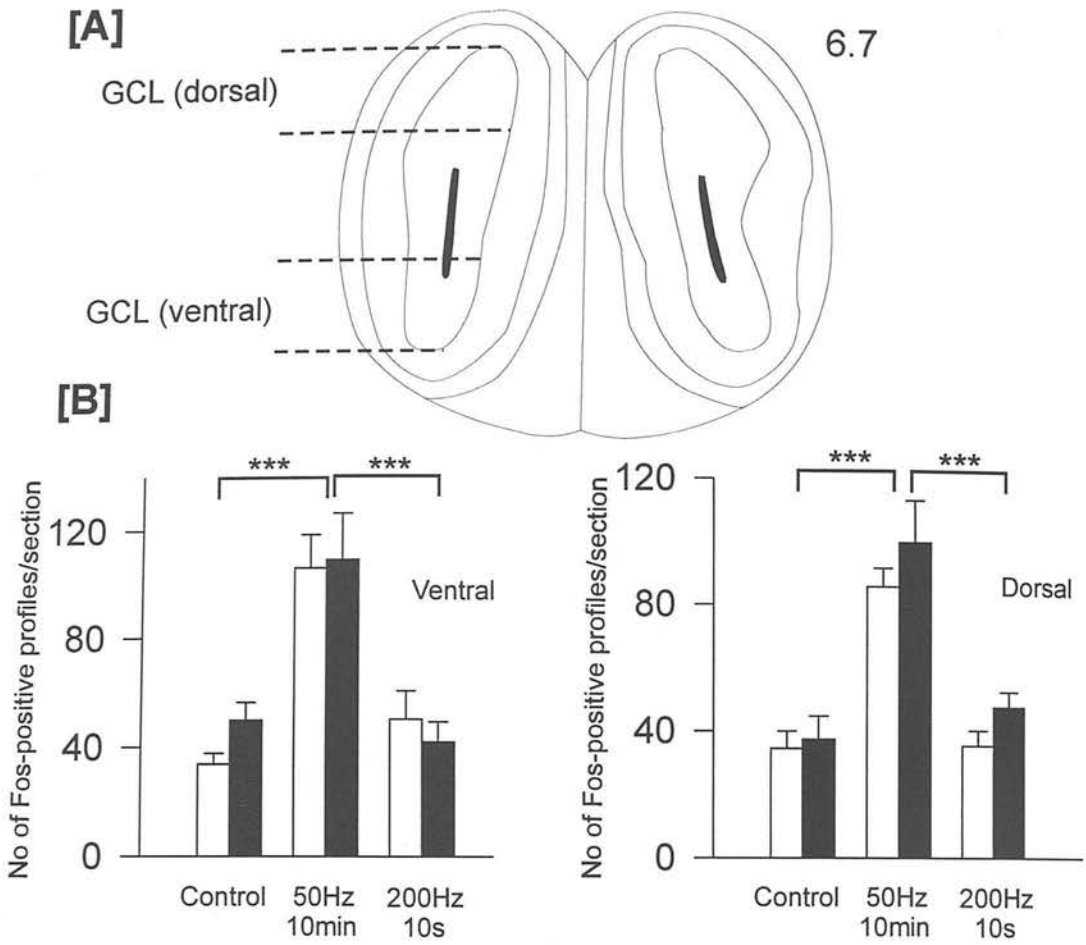

Figure 4.4. [A] Coronal reconstruction of the main olfactory bulb (6.7mm anterior to bregma) indicates the position of the granule cell layer and the area of this layer in which Fos-positive nuclei were counted. [B] Bar charts showing the number of Fos-positive nuclei counted in the dorsal and ventral surfaces of the granule cell layer. [C] Photomicrographs showing the density of Fos expression in the ipsilateral dorsal pole of the granule cell layer with the different stimulation parameters. Notice that levels of Fos expression in the granule cell layer did not differ greatly between the dorsal and ventral surfaces and there is no significant difference between ipsilateral and contralateral sides in the control group or either of the stimulation parameters. Higher levels of Fos were counted in the olfactory bulbs of the prolonged stimulation group. ***$p<0.0001$, **$p<0.001$, *$p<0.01$ (Mann-Whitney Rank Sum Test). Abbreviations; GCL, granule cell layer; MCL, mitral cell layer.

C

i) Control

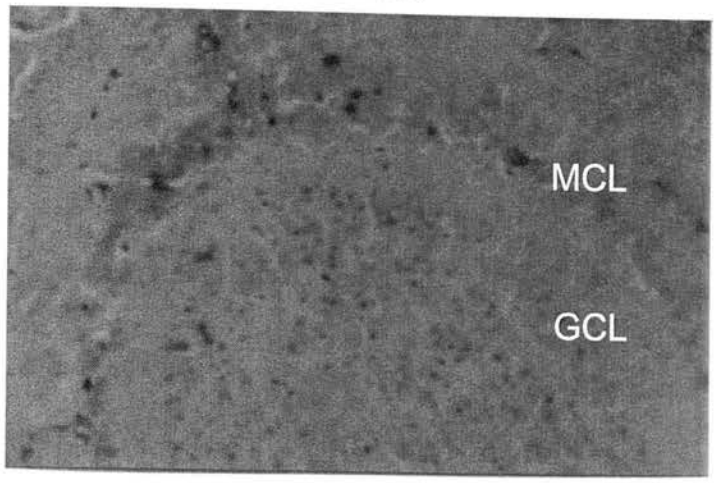

ii) 50Hz/10min

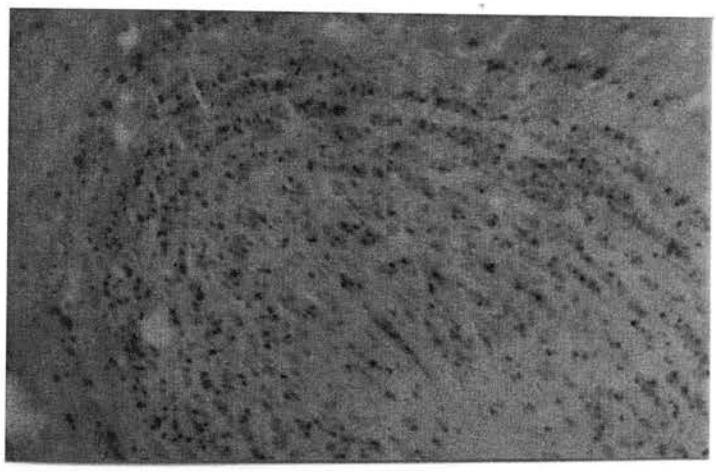

iii) 200Hz/10s

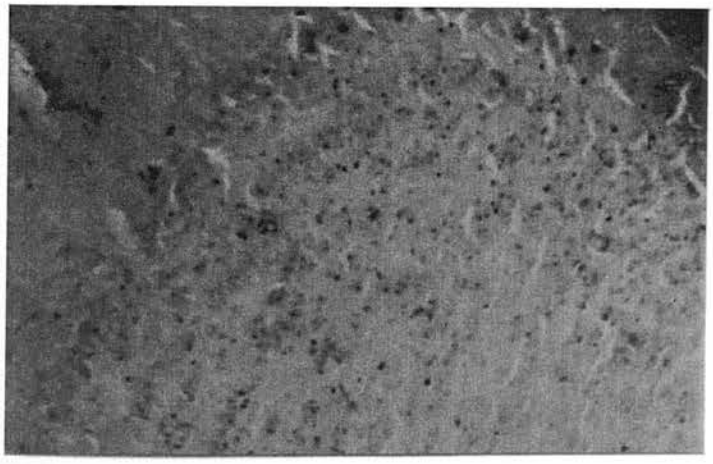

0.1mm

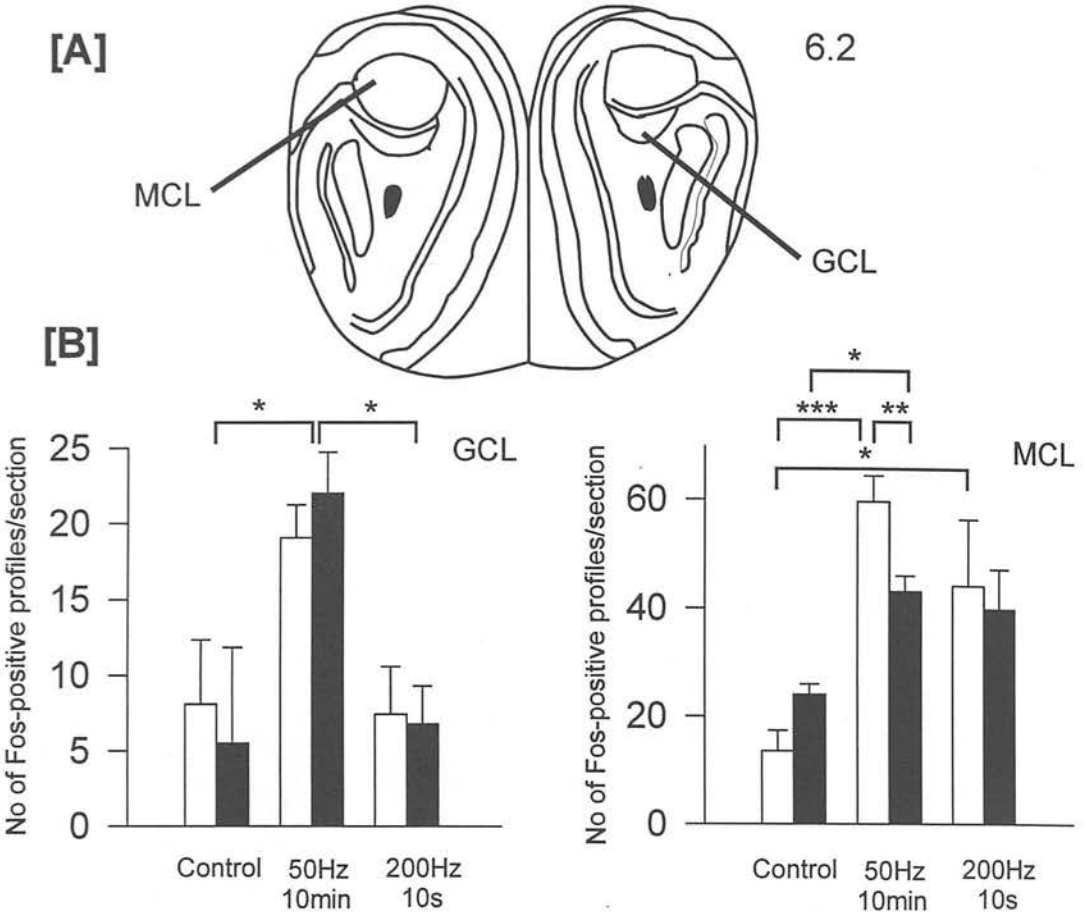

Figure 4.5. [A] Coronal reconstruction of the olfactory bulb (6.2mm anterior to bregma) indicates the region of the accessory olfactory bulb and the position of the granule and mitral cell layers within the accessory olfactory bulb. [B] Bar charts showing the number of Fos-positive nuclei counted in the mitral and granule cell layers in both the ipsilateral and contralateral accessory olfactory bulbs. [C] Photomicrographs showing the density of Fos expression in the accessory olfactory bulb under the different stimulation parameters. Notice that levels of Fos expression in the granule cell layer did not differ between ipsilateral and contralateral bulbs and only differed ($p<0.001$) in the mitral cell layer during the prolonged stimulation. There are higher levels of Fos in the mitral cell layer during both experimental groups compared to controls and the granule cell layer shows higher levels of Fos during the prolonged stimulation. ***$p<0.0001$, **$p<0.001$, *$p<0.01$ (Mann-Whitney Rank Sum Test). Abbreviations; GCL, granule cell layer; MCL, mitral cell layer.

C

Control

i)

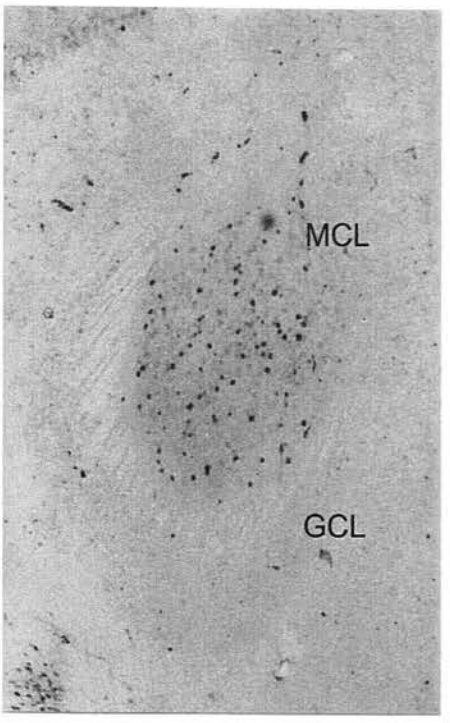

0.2mm

50Hz/10min

ii)

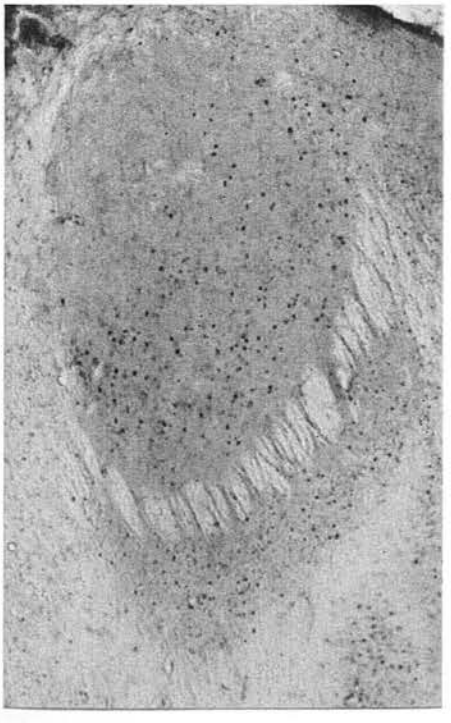

200Hz/10s

iii)

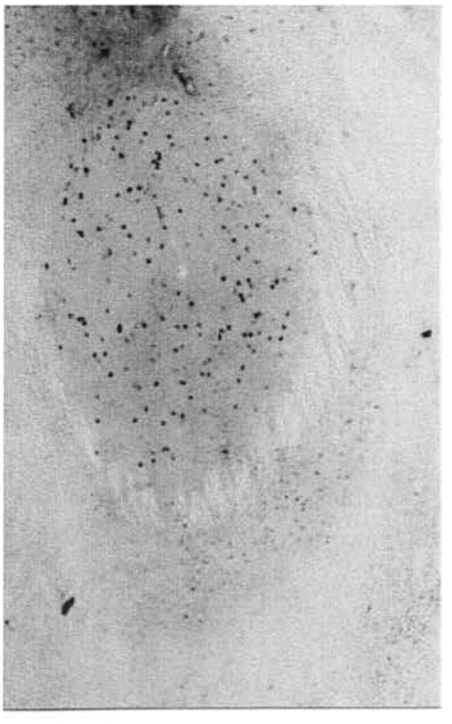

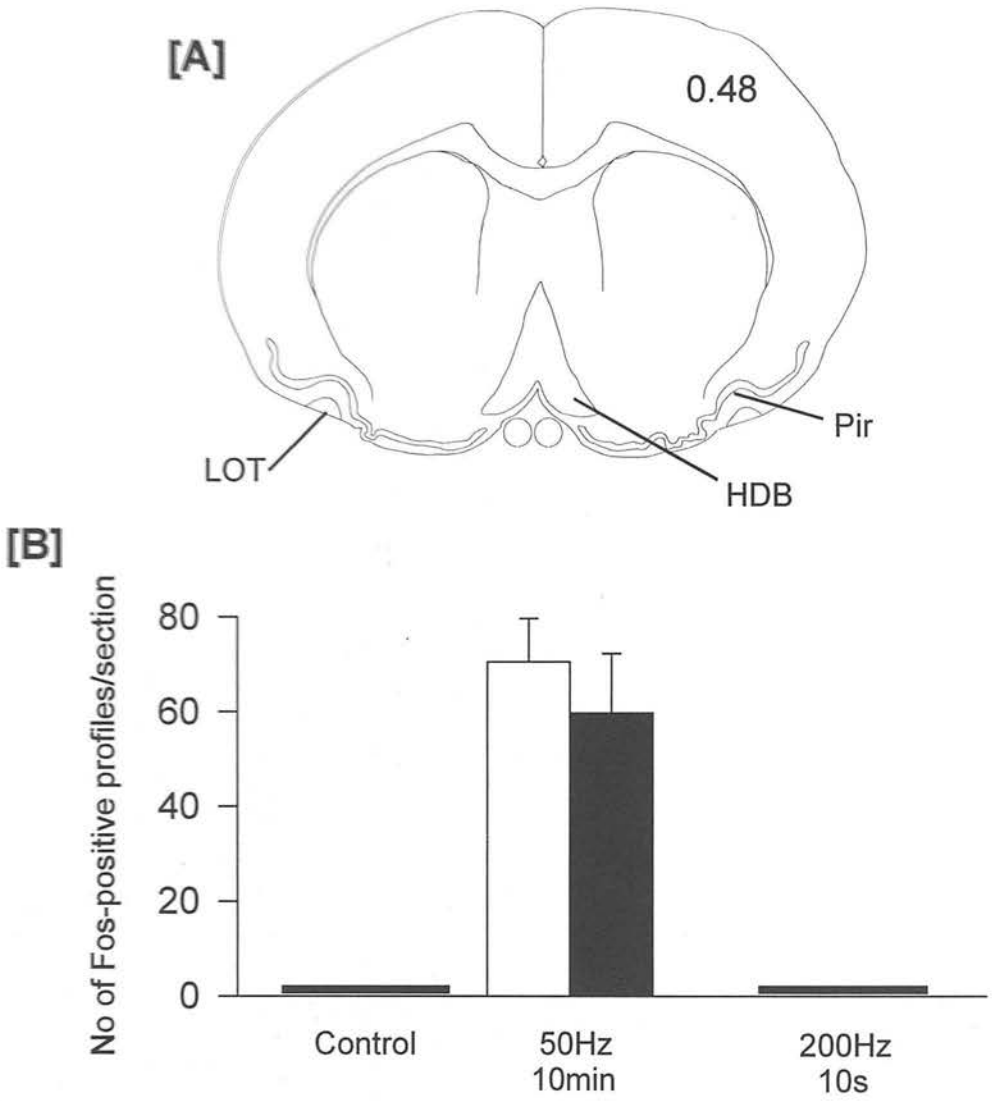

Figure 4.6. [A] Coronal reconstruction of the rat brain (0.48mm anterior to bregma) indicates the second region of the piriform cortex in which Fos-positive nuclei were counted. [B] Bar charts showing the number of Fos-positive nuclei counted in this section of the piriform cortex ipsilateral and contralateral to the side of stimulation. [C] Photomicrographs show the density of Fos expression in the piriform cortex under the different stimulation parameters. Notice that Fos-positive nuclei are only present in this part of the piriform cortex following a prolonged stimulation of the LOT. There is no significant difference between the ipsilateral and contralateral sides. Abbreviations; HDB, horizontal limb of the diagonal band; LOT, lateral olfactory tract; Pir, piriform cortex.

C

Control

i)

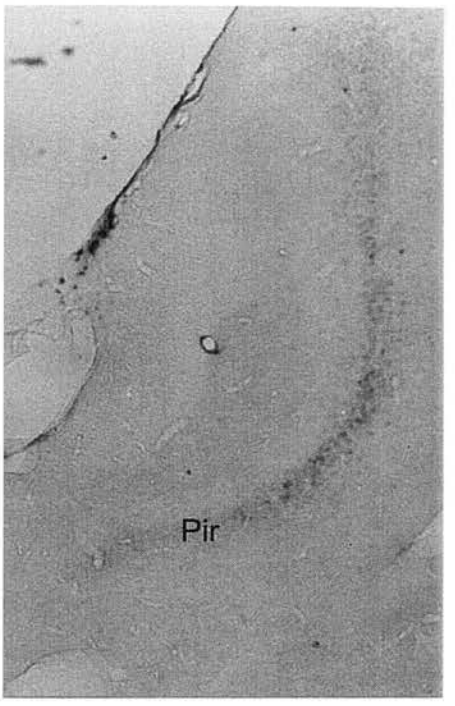

200Hz/10s

ii)

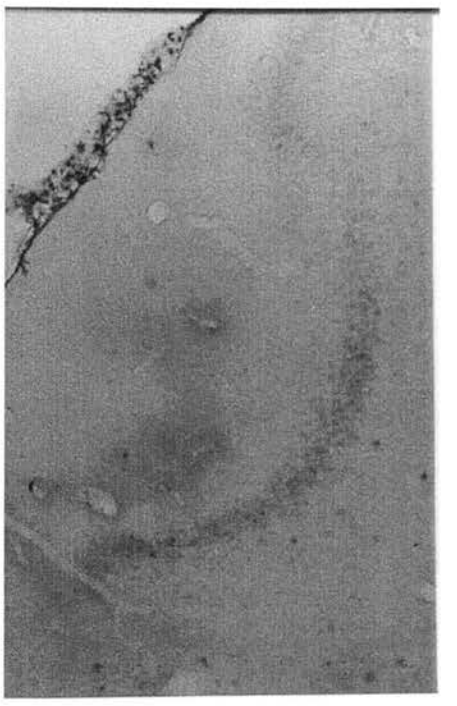

50Hz/10min

iii)

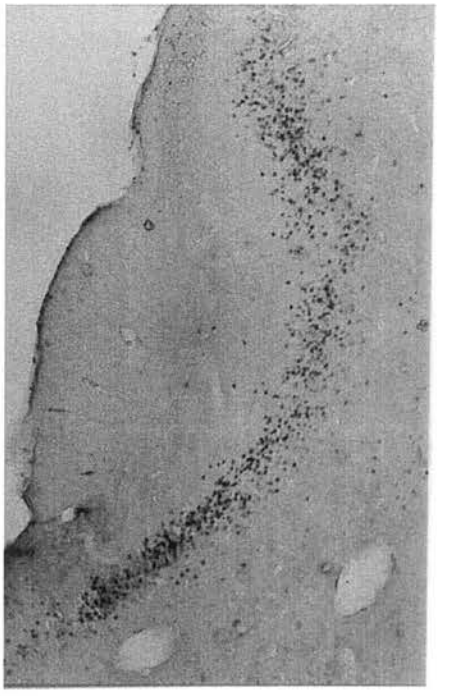

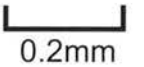

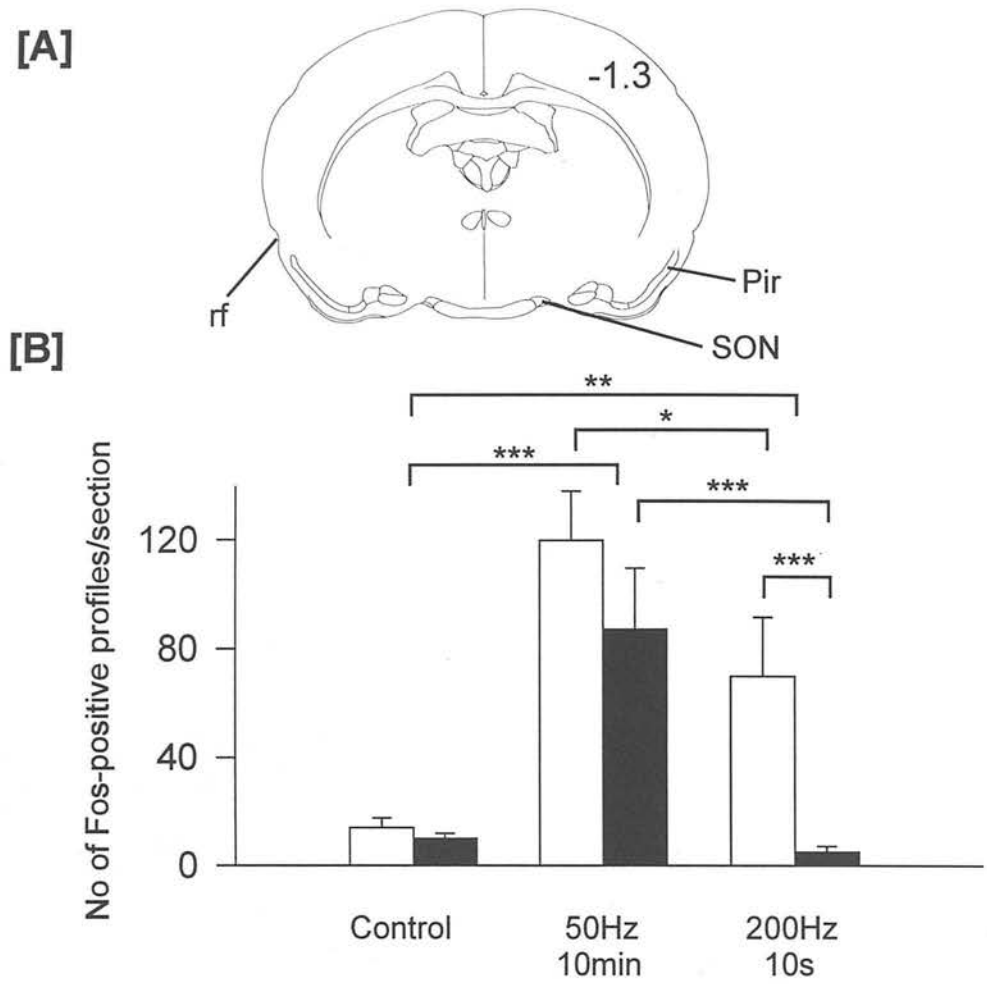

Figure 4.7. [A] Coronal reconstruction of the rat brain (1.3mm posterior to bregma) indicates the region of the piriform cortex in which Fos-positive nuclei were counted. [B] Bar charts showing the number of Fos-positive nuclei counted in this section of the piriform cortex in both the ipsilateral and contralateral hemispheres. [C] Photomicrographs showing the density of Fos expression in the piriform cortex under the different stimulation parameters. There was no significant difference between contralateral and ipsilateral sides in the control and prolonged stimulation groups, however there was a very clear difference in the number of Fos-positive nuclei between the two sides of the brain following short-pulse stimulation of the LOT. There is a clear difference between the levels of Fos in the ipsilateral sides of the stimulated groups and the control group. ***$p<0.001$, **$p<0.001$, *$p<0.01$ (Mann-Whitney Rank Sum Test). Abbreviations; Pir, piriform cortex; rf, rhinal fissure; SON, supraoptic nucleus.

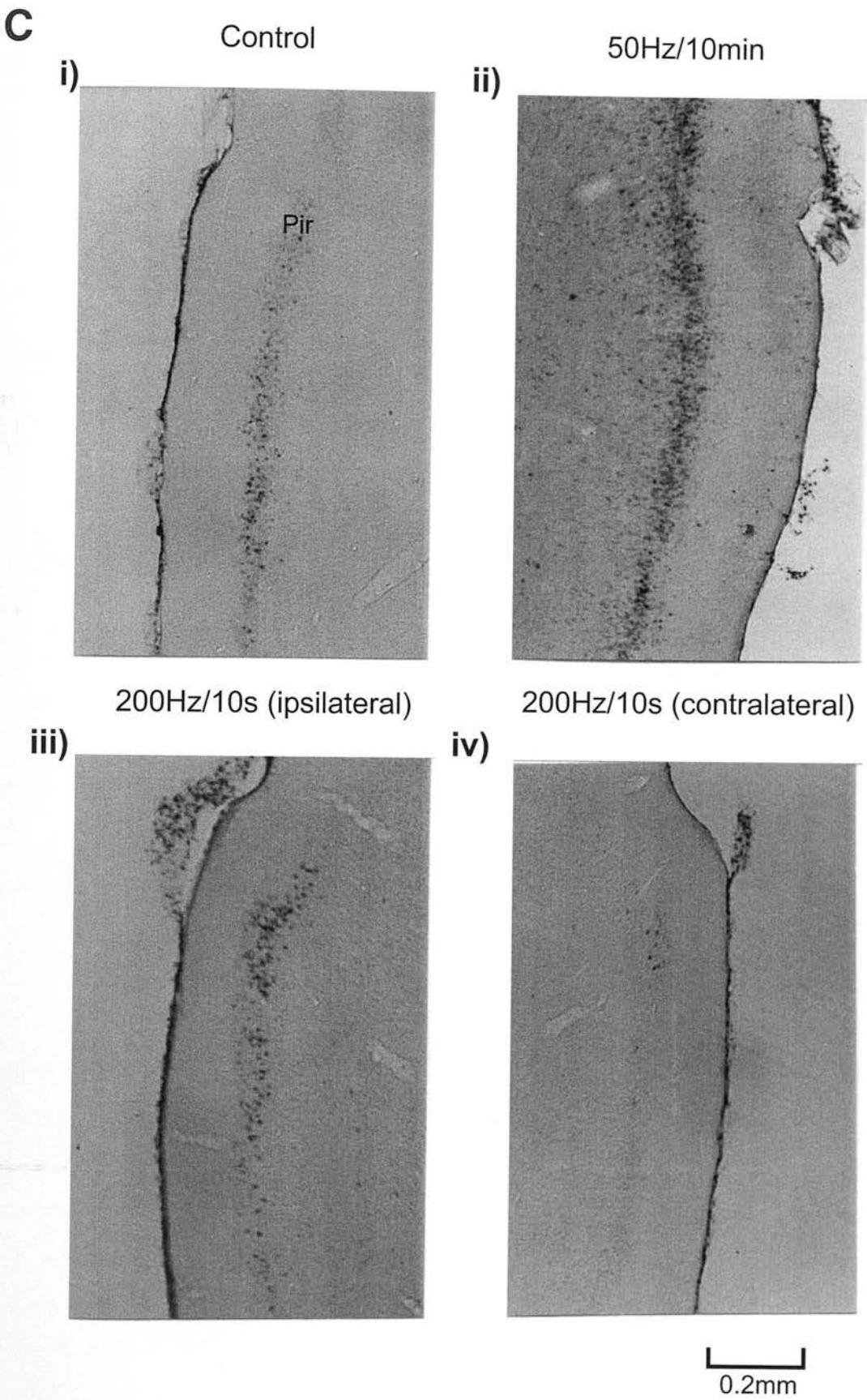
C
Control
i)
Pir
50Hz/10min
ii)
200Hz/10s (ipsilateral)
iii)
200Hz/10s (contralateral)
iv)
0.2mm

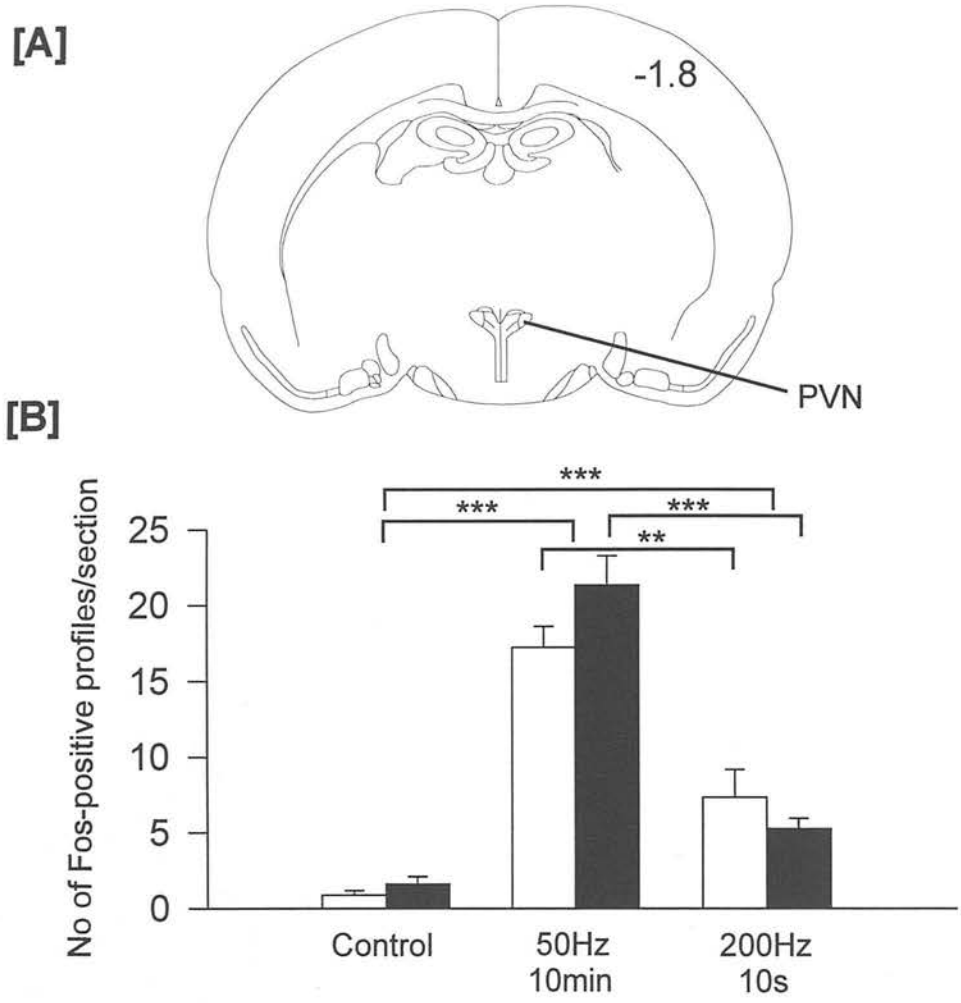

Figure 4.8. [A] Coronal reconstruction of the rat brain (1.8mm posterior to bregma) indicates the position of the paraventricular nucleus. [B] Bar chart showing the number of Fos-positive nuclei counted in the ipsilateral and contralateral PVN. [C] Photomicrographs showing the density of Fos expression in the PVN under the different stimulation parameters. Within each experimental group there is no significant difference between ipsilateral and contralateral sides however, there is a large increase in the number of Fos-positive nuclei following a prolonged stimulation of the LOT compared to controls. There is also a significant increase in Fos-positive cells following the short-pulse stimulation protocol. The Fos-positive cells are located in the medial (parvocellular) region of the PVN. ***$p<0.0001$, **$p<0.001$, *$p<0.01$ (Mann-Whitney Rank Sum Test). Abbreviations; PVN, paraventricular nucleus.

C

i)

Control

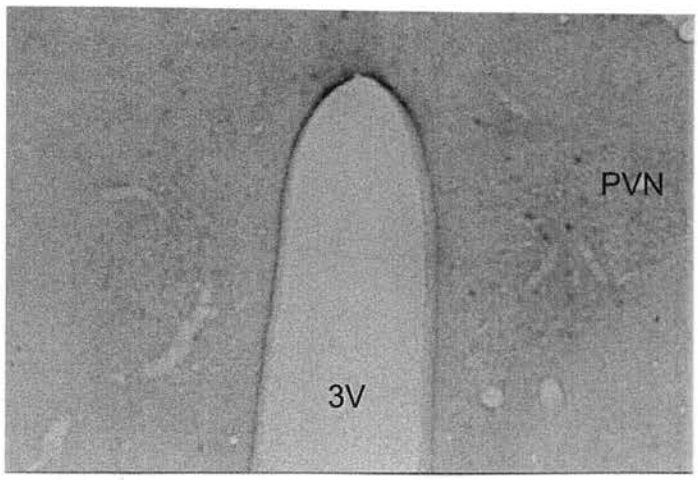

ii)

50Hz/10min

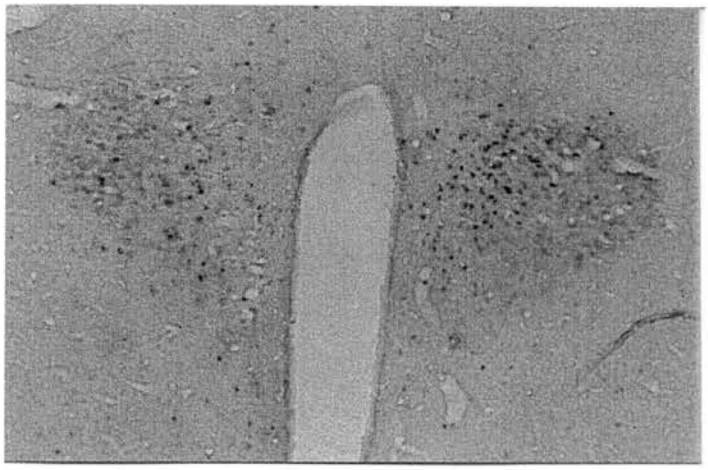

iii)

200Hz/10s

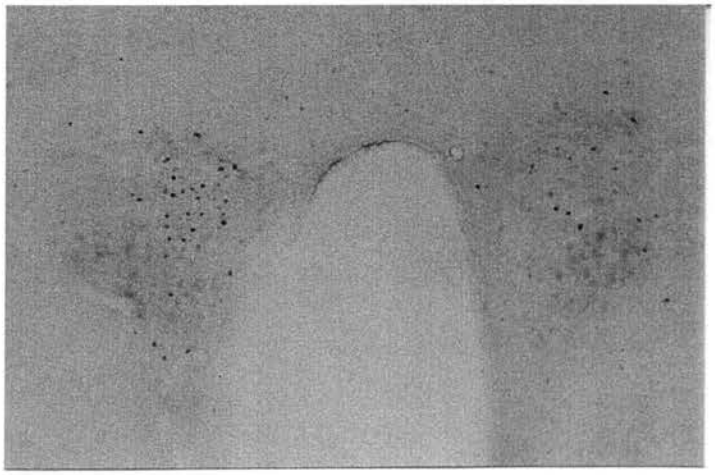

0.1mm

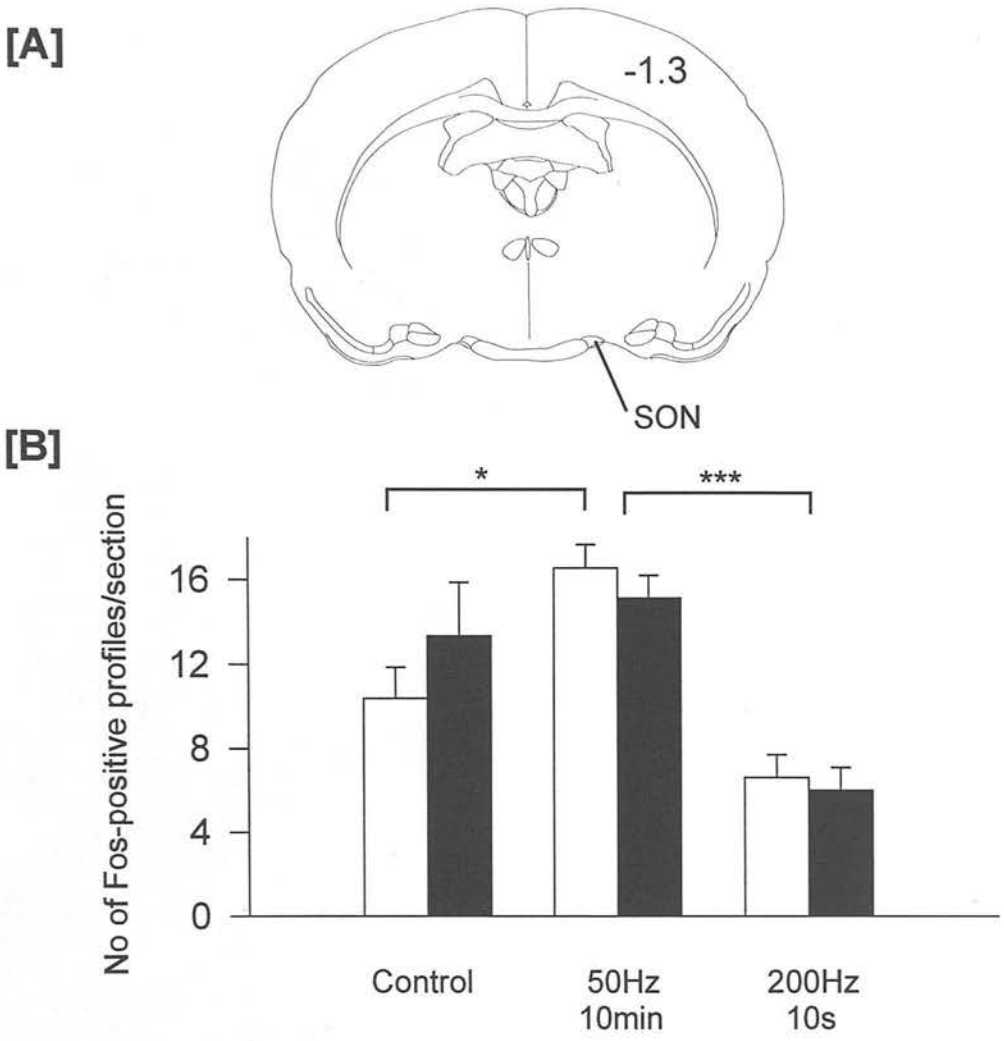

Figure 4.9. [A] Coronal reconstruction of the rat brain (1.3mm posterior to bregma) indicates the position of the supraoptic nucleus. [B] Bar chart shows the number of Fos-positive nuclei counted in the ipsilateral and contralateral SON. [C] Photomicrographs showing the density of Fos expression in the SON under the different stimulation parameters and in a section taken from a hypertonic saline treated rat. The number of Fos-positive profiles within the supraoptic nucleus of all groups was relatively low when compared to the levels of Fos that can be induced by hypertonic saline injected i.p. There is no significant difference between ipsilateral and contralateral for any of the stimulation parameters but a significant difference ($p<0.01$) was found between control levels and the prolonged stimulation group and also between the prolonged stimulation and short pulse stimulation groups

C

Control

i)

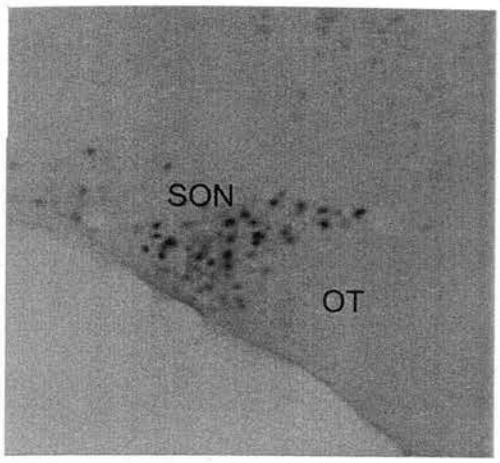

Hypertonic saline control

ii)

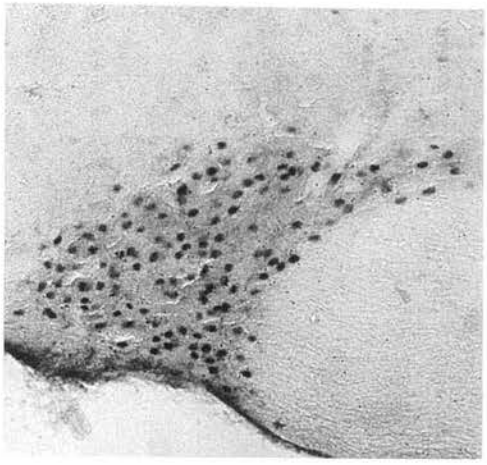

50Hz/10min

iii)

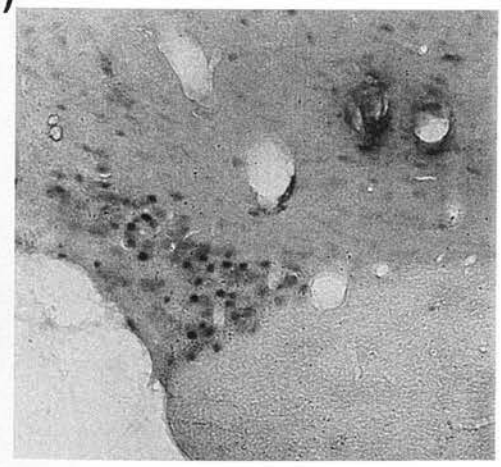

200Hz/10s

iv)

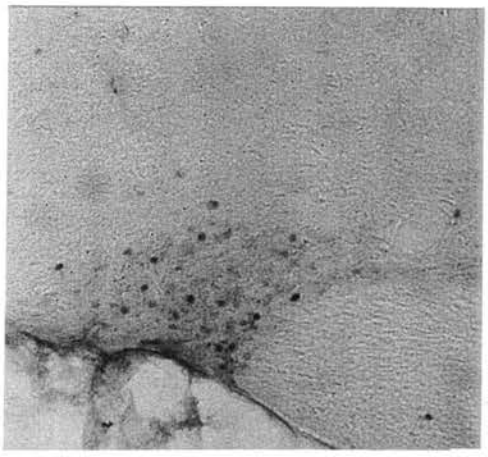

0.1mm

Figure 4.10. A summary of the results from the Fos study. In all the bar charts the control group comprises of 4 rats that received surgery but no stimulation. The prolonged stimulation (50Hz/10min) group consists of thirteen rats and the short-pulse stimulation (200Hz/10s) group consists of four rats. The ipsilateral side to stimulation is represented by open bars and the contralateral side by filled bars

- In the main olfactory bulb following antidromic activation of the LOT with a prolonged period of stimulation there is a large increase in the number of Fos-positive cells in the mitral cell layer of the ipsilateral bulb.
- Granule cells in the main olfactory bulb both ipsilaterally and contralaterally also shows a higher level of Fos staining following the prolonged stimulation.
- The middle tufted cells of the main olfactory bulb, which are output neurones of the olfactory bulb as well as the mitral cells, show a fall in the levels of Fos expression following both stimulation protocols compared to the control rats.
- In the rostral portion of the piriform cortex at the level of the horizontal limb of the diagonal band Fos is only expressed following the prolonged stimulation and is found both ipsilaterally and contralaterally.
- In the more caudal regions of the piriform cortex there is increased Fos expression following the prolonged stimulation ipsilateral and contralateral and following the short-pulse stimulation ipsilateral side only, compared to control levels.
- The supraoptic nucleus of the hypothalamus did not show high levels of Fos staining in any of the groups. A significant difference ($p<0.01$) was seen between the control and prolonged stimulation group but the increase in Fos was seen bilaterally. The level of Fos induced in the SON by hypertonic saline (i.p.) is shown for comparative purposes.
- In the paraventricular nucleus there were significantly higher levels of Fos following both prolonged and short-pulse stimulation compared to controls furthermore, there was significantly more Fos in the PVN following prolonged stimulation compared to the short-pulse stimulation. The level of Fos induced in the PVN by hypertonic saline (i.p.) is shown for comparative purposes.

Main olfactory bulb

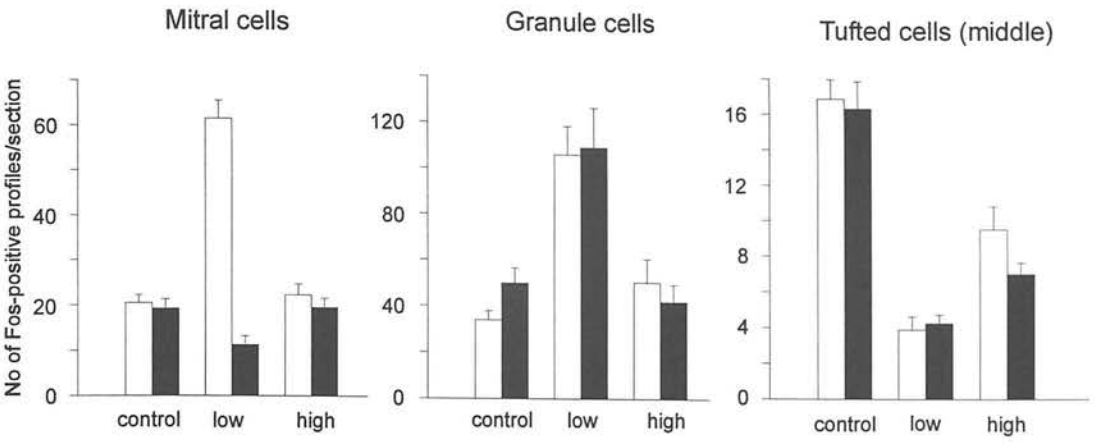

Piriform cortex

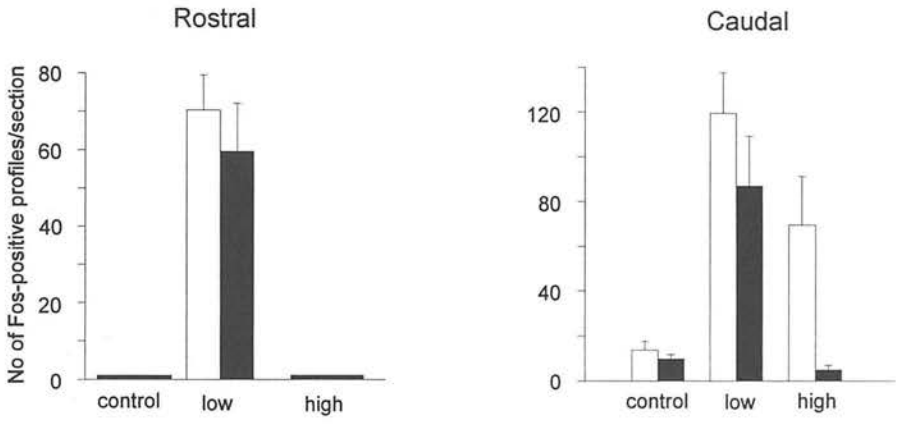

Hypothalamic nuclei

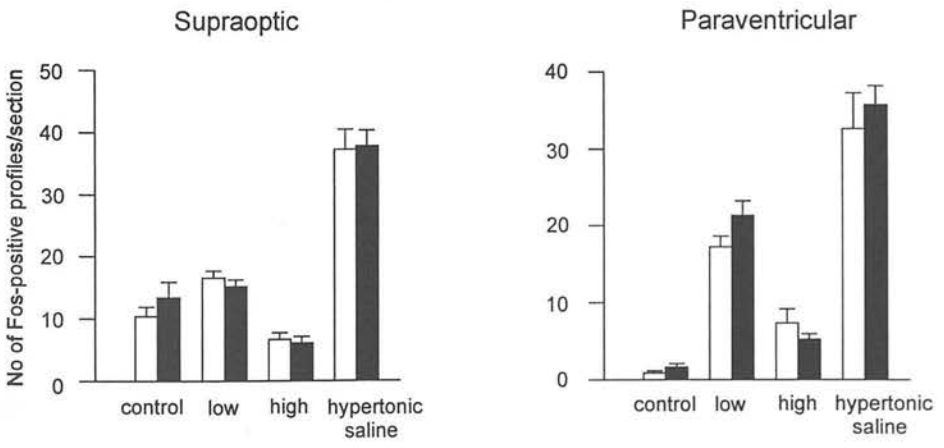

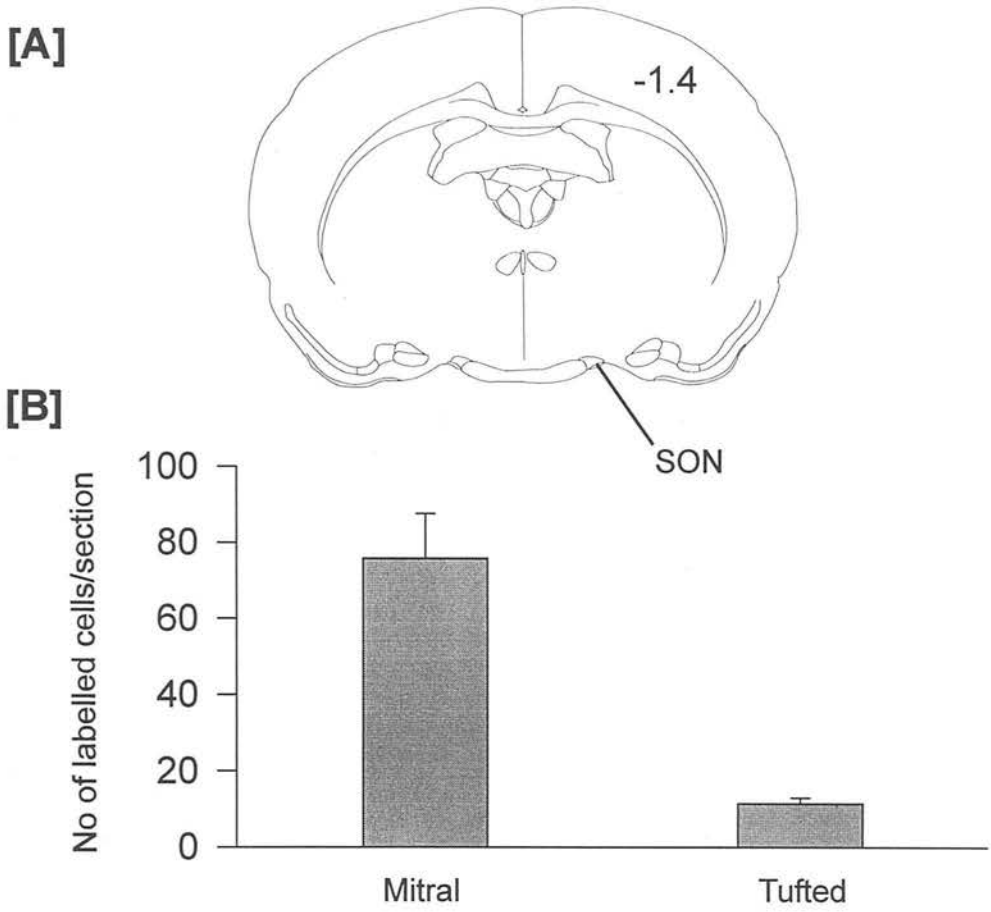

Figure 4.11. [A] Coronal reconstruction of the rat brain (1.3mm posterior to bregma) indicating the position of the supraoptic nucleus (SON) into which Fluoro-Gold was injected. [B] Bar chart showing the number of mitral and tufted cells in the main olfactory bulb ipsilateral to the injection that were retrogradely labelled with Fluoro-Gold. [C] Photomicrographs showing the injection site and labelled mitral and tufted cells. The injection of Fluoro-Gold filled the SON and spread dorsomedial from the SON. A much greater proportion of labelled cells (90%) were situated in the mitral cell layer. The tufted cells that were retrogradely labelled were generally found in the deep sublaminae of the external plexiform layer suggesting they were deep/middle tufted cells. No retrogradely labelled cells were found in the contralateral bulb or any other region of the brain. Abbreviations: EPL, external plexiform layer; GCL, granule cell layer; MCL, mitral cell layer; OT, optic tract; SON, supraoptic nucleus.

C

i)

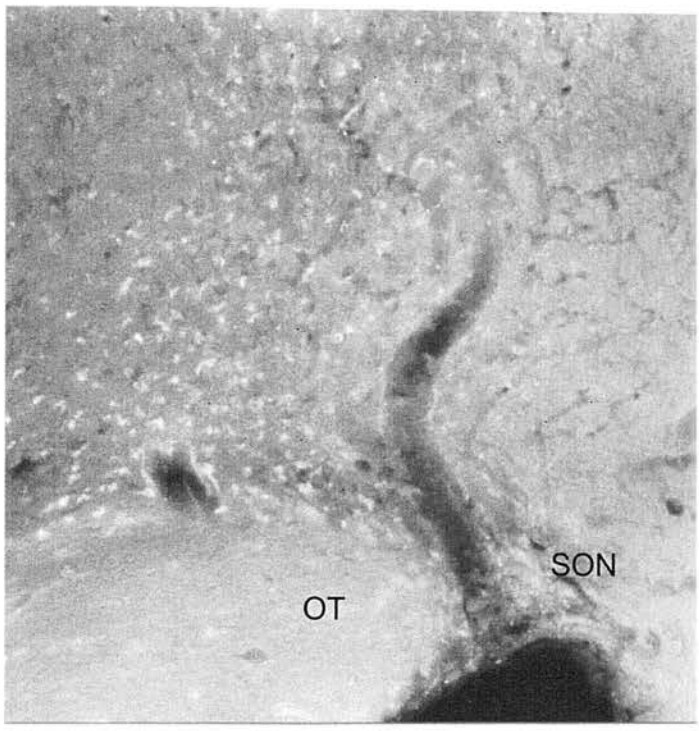

0.2mm

ii)

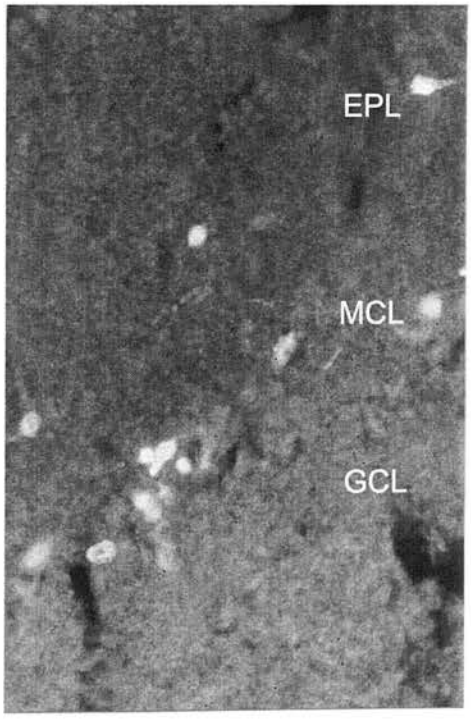

0.05mm

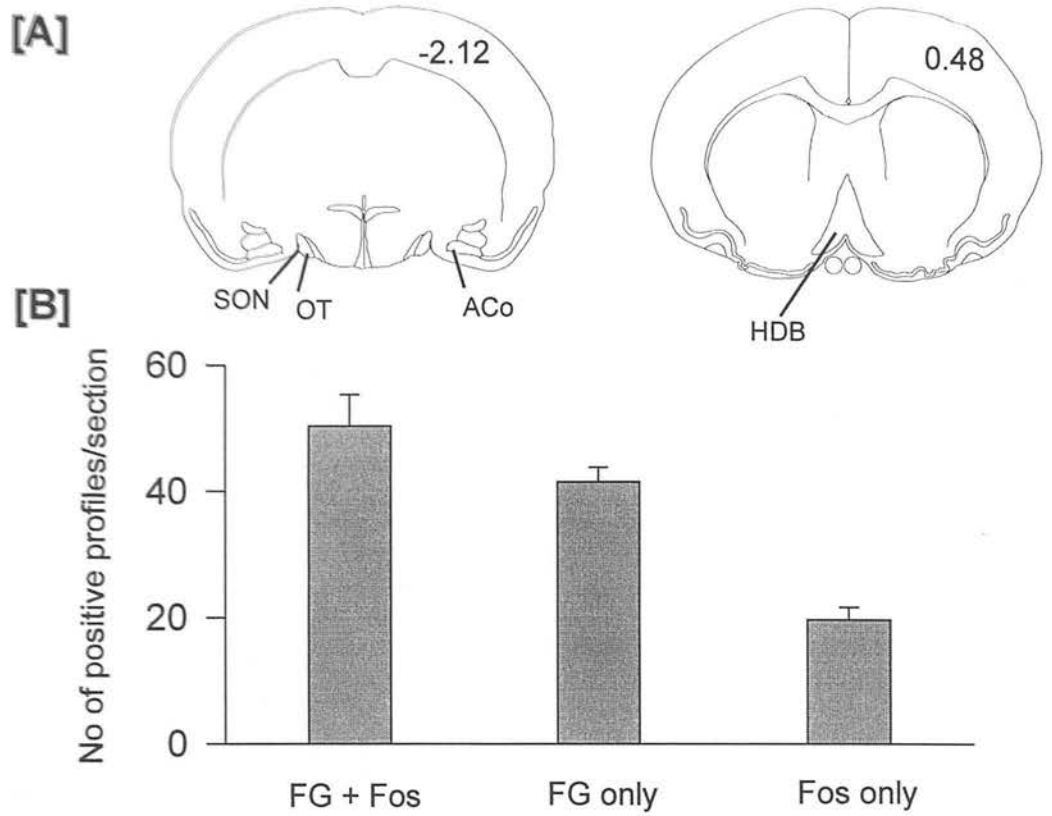

Figure 4.12. [A] Coronal reconstruction's of the rat brain (2.12mm posterior and 0.48mm anterior to bregma), indicating the position of the amygdala into which Fluoro-Gold was injected and the position of the horizontal limb of the diagonal band. [B] Bar chart showing the number of mitral cells in the main olfactory bulb ipsilateral to the injection that were retrogradely labelled with Fluoro-Gold and also the number of cells that were stained positive for Fos following prolonged stimulation of the LOT. [C] Photomicrographs showing (i) the injection site (ii) the cells in the HDB that were retrogradely labelled and over the page, [D] labelled mitral cells in the main olfactory bulb. Following the injection of Fluoro-Gold into the amygdala labelled cells were found in the ipsilateral HDB but no Fos was counted in this region following prolonged stimulation of the LOT. Retrogradely labelled cells were seen in the mitral cell layer of the ipsilateral main olfactory bulb and approximately 60% of these cells were activated by the stimulation. Abbreviations: ACo, Anterior cortical amygdaloid nucleus; EPL, external plexiform layer; GCL, granule cell layer; HDB, horizontal limb of the diagonal band; MCL, mitral cell layer; OT, optic tract; SON, supraoptic nucleus.

C

i)

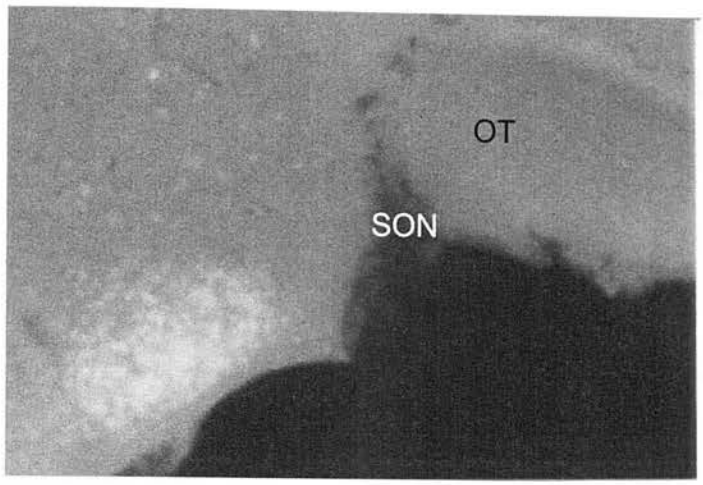

0.2mm

ii)

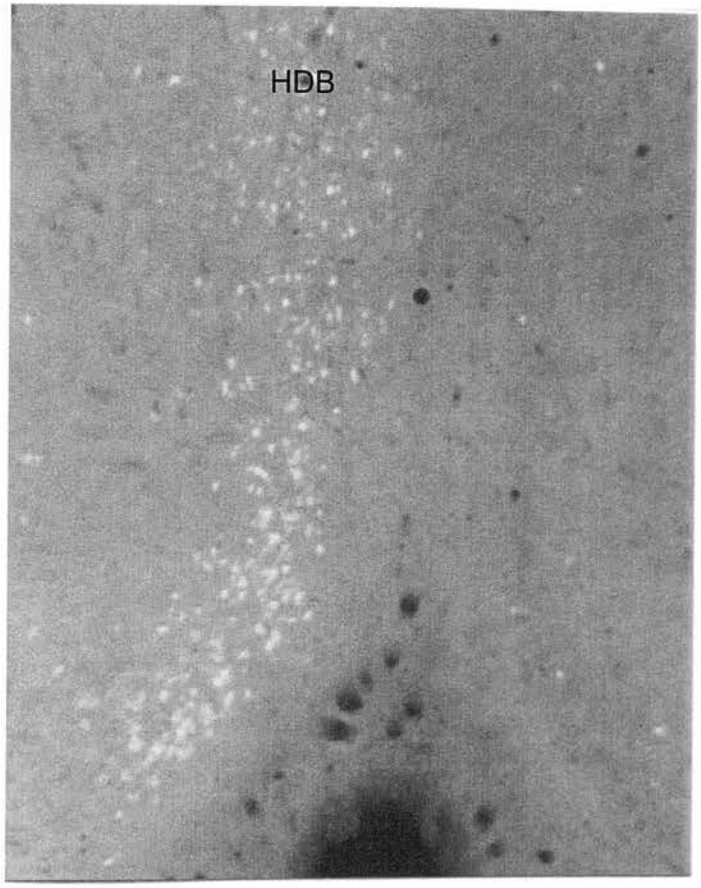

0.2mm

D

i)

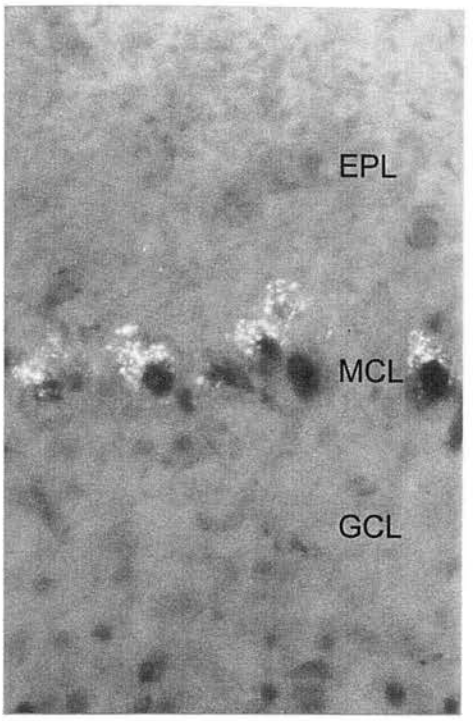

ii)

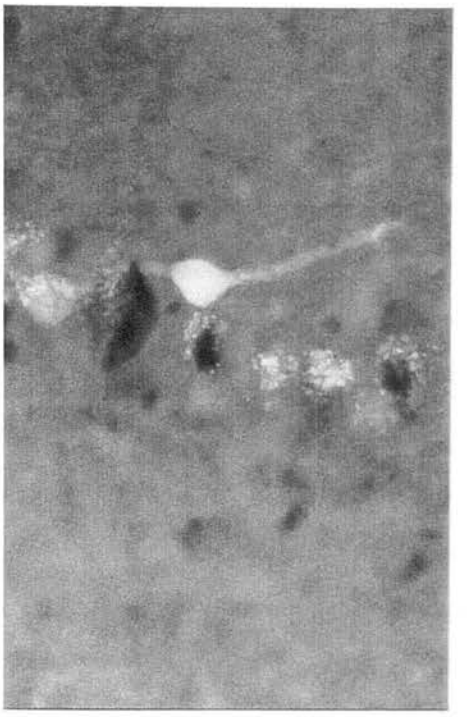

0.025mm

4.4 DISCUSSION

The initial objective of the Fos study was to confirm and expand present knowledge of the neural pathway between the olfactory bulb and the SON. Several groups have found a monosynaptic connection between these two systems using retrograde tracing techniques (Smithson *et al.*, 1989) and electrical stimulation of the LOT *in vitro* (Hatton and Yang, 1989). An advantage of Fos immunocytochemistry is that it is capable of labelling polysynaptically activated neurones, whereas tract-tracing methodologies demonstrate direct (monosynaptic) neuronal connections only.

4.4.1 Stimulation parameters

The different stimulation protocols followed to induce Fos expression in areas associated with the olfactory system were both strong stimuli. This was necessary so that the stimulus would have a greater effect than the spontaneous output of the olfactory bulb, since the results from Chapter 3 established that the mitral cells are capable of firing at high rates of discharge (up to 250Hz). Also, from the recordings of the spontaneous activity of mitral cells (Chapter 3) it was shown that mitral cells fire in a phasic discharge pattern, with periods of activity lasting on average two minutes with equal periods of silence or quiescence between these bursts of activity. Taking this into account a constant stimulation over a prolonged period of time was applied, to disrupt the spontaneous output pattern.

Young and Wilson (1999) demonstrated that mitral/tufted cell inhibition varies with LOT stimulus intensity. Increasing either stimulus intensity or stimulus frequency increased the duration of mitral/tufted cell spontaneous activity suppression. The enhanced suppression during 5Hz stimulation was immediately reversed by the onset of a slower 1Hz stimulation. The stimulation intensities used seem very low in comparison to the rates we have shown these cells capable of firing at. The suppression of mitral/tufted cells evoked by LOT stimulation is mediated primarily by dendrodendritic reciprocal synapses with GABAergic granule cells.

Mitral/tufted cells release glutamate from dendritic pre-synaptic terminals which evoke EPSPs in granule cell dendrites via NMDA and non-NMDA receptors (Isaacson and Strowbridge, 1998; Schoppa *et al.*, 1998). The NMDA component of granule cell excitation has been shown to underlie the intensity dependence of LOT evoked inhibition (Wilson *et al.*, 1996). This suggests that a shift in frequency of the stimulus is able to dramatically modify the extent of granule cell mediated inhibition.

4.4.2 Fos expression in the hypothalamic nuclei

The PVN contains both large (magnocellular) and small (parvocellular) neurones. There are eight subdivisions within the PVN, three of which are magnocellular and the rest are parvocellular (Swanson and Kuypers, 1980). The anterior and medial parts of the magnocellular divisions contain primarily oxytocin neurones. The posterior part of the PVN, the largest subdivision, consists of two distinct populations located in the medial and lateral areas (Hatton *et al.*, 1976). Oxytocin neurones are primarily found in the medial area, and vasopressin neurones in the lateral area. The SON contains only large (magnocellular) neurones: oxytocin neurones are mainly located posterodorsally and vasopressin neurones are mainly located posterodorsally (Swaab *et al.*, 1975).

Retrograde labelling studies in the present study as well as previous labelling studies have indicated there is a monosynaptic pathway between the olfactory bulb and the SON (Smithson *et al.*, 1992). However, in the present study the microinjection of the fluorescent tracer was only into the vicinity of the SON and not restricted to the nucleus. This means that fibres within the surrounding area as well as damaged fibres of passage are likely to have taken up the tracer, although every effort was made in order to limit the tracer being taken up by damaged fibres. Taking this into consideration the retrograde labelling results from the present study are not able to confirm the monosynaptic pathway between the olfactory bulb and the SON. The Fos studies showed that following prolonged stimulation of the lateral

olfactory tract there is a significant increase in Fos expression ($p<0.01$) compared to control levels. However, the increase in Fos expression is seen in both the ipsilateral and contralateral sides to stimulation so does not support the unilateral connection to the SON reported by Smithson *et al.*, 1992.

In addition to the anatomical data Hatton and Yang (1989) have performed electrophysiological recordings *in vitro* to test the hypothesis that there is a neural pathway between the olfactory bulb and the SON. Upon electrical stimulation of the LOT they found that cells within the SON responded with short latency excitatory responses supportive of a direct pathway from the olfactory bulb to the SON. The stimulation site in the *in vitro* slice was very close to the SON, which raises the possibility of current spread causing direct stimulation of the SON neurones. This is exacerbated by the fact that the SON dendritic zone has been found to extend ventrolaterally, thereby increasing the chances of direct stimulation.

The Fos results from the present study that involved stimulation of the LOT (*in vivo)* at a site far removed from the SON seems to cast a doubt over a unilateral neural pathway between the olfactory bulb and the SON. However, we must bear in mind several factors governing the expression of Fos before a definitive conclusion can be drawn. The rats in each group were all sacrificed 90 minutes following the stimulation which has been found to be the optimum time period for Fos expression using other stimulation protocols such as morphine withdrawal (Johnstone *et al.*, 2000). However, without looking at different time periods after the stimulation we cannot rule out the possibility that following stimulation of the olfactory system there is only a transient activation of SON neurones and that the Fos expression was 'missed'. Furthermore, the expression of Fos is a standard marker of cellular activity, however, other immediate early genes such as *c-jun* as well as other transcriptional factors maybe involved in altering the gene activity of the cell.

Smithson *et al.*, (1992) did not find a pathway between the olfactory bulb and the PVN, this is surprising since in the majority of cases projections to the magnocellular cells of the SON are also found to project to the magnocellular cells of the PVN (for review see Hatton, 1989). Since the anatomical studies had not shown a pathway to the PVN, Hatton and Yang (1989) did not address the issue of whether LOT stimulation affected the firing rate of cells within the PVN. However, the possible influence of the PVN over neurones on the olfactory bulb was looked at by Yu *et al.* (1996), they found that stimulation of the PVN resulted in the excitation of granule cells and inhibition of mitral cell firing. However, the latency of response was much too long to be accounted for by neural transmission alone, furthermore following unilateral transection of all centrifugal pathways to the olfactory bulb stimulation of the PVN gave the same responses. Yu *et al.* (1996) suggested that stimulation of the PVN resulted in oxytocin release into the CSF and that this is the route by which PVN oxytocin exerts its effect on bulbar neurones. In support of this idea it was shown that infusion of oxytocin (i.c.v.) reproduced the PVN-induced responses in mitral and granule cells Yu *et al.* (1996). This suggests that, in agreement with the anatomical studies, there is no neural pathway linking the olfactory bulb to the PVN. The increased Fos expression in the parvocellular region of the PVN in the present study is likely to represent a stress response, since it was seen contralaterally and it is the parvocellular cells that mediate responses to stress. The stimulation of the LOT may have stimulated areas associated with the stress response leading to activation of the cells in the PVN.

4.4.3 Fos labelling within the olfactory bulb

Following stimulation of the LOT, which results in the antidromic activation of the mitral cell we expected to induce Fos expression in the granule cells of the ipsilateral bulb through the synaptic connections between the mitral and granule cell; upon stimulation the mitral cells release glutamate that acts to excite the granule cells. We did not expect any increase in Fos expression in the mitral cell layer

because Fos induction in other systems requires a positive input i.e. synaptic activation of the cell.

4.4.3.1 Mitral cells

However, contrary to our predictions, Fos expression within the mitral cell layer of the ipsilateral MOB was significantly higher than control bulbs following the prolonged stimulation of the LOT. Mitral cells are inhibited immediately following their activation by olfactory afferents or by antidromic stimulation of the LOT. The reciprocal dendrodendritic inhibitory pathway that exists between mitral cells and first-order interneurones mediates this recurrent inhibition. Stimulation of mitral cells results in the synaptic activation, by the release of glutamate, of granule and periglomerular cells which in turn release GABA back onto the mitral cells resulting in synaptic inhibition. Therefore, the increased expression of Fos in the mitral cell layer is unexpected on two levels, firstly it is thought that Fos is not induced simply by increased spike activity but requires synaptic activation and secondly, it is inconsistent with the expectation of increased mitral cell inhibition during periods of high granule cell activity. The latter can probably be explained by the fact that the mitral cells were driven by intense antidromic stimulation which may 'overshadow' and saturate the granule cell inhibitory drive. However the first observation is more difficult to explain.

Fos expression can be induced by a number of second messenger systems, including an increase in intracellular Ca^{2+} following activation of voltage-dependent Ca^{2+} channels, Luckman *et al.*, (1994). It was hypothesised by Luckman *et al.* (1994) that spike activity itself, rather than synaptic input, might be responsible for Fos induction, if this was the case it would explain the expression of Fos within the mitral cell layer of the olfactory bulb following antidromic stimulation. To test this hypothesis Luckman *et al.* (1994) examined Fos expression within magnocellular neurones following a similar level of receptor-mediated and antidromic activation. It

was found that i.c.v. administration of the muscarinic agent carbachol, but not antidromic stimulation, resulted in Fos expression, indicating that transynaptic activation is required. If the findings obtained in the magnocellular system are applicable to other neuronal systems, then the demonstration of Fos expression within the ipsilateral granule cell layer upon antidromic stimulation of mitral cells is to be anticipated. However, the demonstration of Fos expression within the ipsilateral mitral cell layer following antidromic stimulation of the mitral cell axons was, given the results of Luckman *et al.*, (1994), not expected. It is important to emphasize that the failure of antidromic stimulation to induce Fos expression within magnocellular neurones may be specific and therefore not applicable to other neural systems.

The olfactory bulb receives a massive input of centrifugal afferent fibres. The locus coeruleus located within the brainstem is the major, if not sole, source of noradrenergic innervation of the telencephalon and a third of all locus coeruleus neurones have been shown to project to the olfactory bulb (Shipley *et al.*, 1995). Noradrenaline attenuates the inhibitory feedback onto mitral cells by a direct action on the inhibitory interneurones and therefore facilitates mitral cell firing (Jahr and Nicoll, 1982a). Fluorescence histochemistry studies have revealed that noradrenergic projections from the locus coeruleus enter the olfactory bulb through the medial olfactory tracts and will therefore be unaffected by lateral olfactory tract stimulation (Fallon and Moore, 1978). However, centrifugal fibres running alongside the LOT originating from the diagonal band (HDB) may be inadvertently stimulated during the stimulation of the LOT. GABAergic and cholinergic neurones have been identified within the centrifugal fibres arising from the HDB and retrograde tracing studies have revealed that they project to the ipsilateral MOB only (De Olmos *et al.*, 1978; Senut *et al.*, 1989). Stimulation of the HDB results in the inhibition of granule cells and the subsequent disinhibition and therefore excitation of mitral cells (Kunze *et al.*, 1991). Activation of this projection, which would occur upon electrical

stimulation of the LOT, may explain the induction of Fos within the mitral cell layer however, whether disinhibition rather than synaptic activation is capable of inducing Fos expression is not known. Furthermore, Fos-positive nuclei were observed within the MCL of the AOB which does not receive afferent inputs from the HDB therefore, activation of this projection as a possible explanation for Fos induction within the MCL is not applicable in this case.

NMDA antagonists effectively block stimulation induced immediate early gene expression by neurones in areas such as the hippocampal formation (Wisden *et al.*, 1990). However the application of MK-801 (a NMDA receptor antagonist) enhanced *c-fos* expression in mitral/tufted cells of the main olfactory bulb of the rat (Wilson et al., 1996). One possible explanation for this unexpected enhancement of *c-fos* expression is disinhibition. Disinhibition of mitral/tufted cells could occur through a reduction of the glutamatergic excitation of inhibitory granule cells following NMDA receptor blockade.

However, these experiments were conducted in urethane anaesthetised rats and it was discovered that rats maintained under urethane anaesthesia had a greater incidence of c-*fos* mRNA in mitral cells and much lower levels in the glomerular and granule layers, than had been previously reported in awake rats (Guthrie *et al.*, 1993). It may simply be that a reduction in granule cell activity causes the enhanced labelling of mitral cells, but a direct effect by urethane can not be ruled out.

The cellular locus of urethane action is not known, anaesthetics particularly urethane, have been shown to induce c-*fos* expression in several brain regions (Takayama *et al.*, 1994). Therefore caution must be taken in interpreting the results described above. In the present study we used pentobarbital anaesthesia rather than urethane in order to prevent such potentially misleading results. It is important to take into consideration the different anaesthetics used in the electrophysiology

experiments detailed in Chapter 3 (urethane) and the Fos study described in this chapter (pentobarbital). It is thought that urethane induces Fos expression (Takayama *et al.*, 1994) this suggests that it may increase the activity of recorded cells and may influence the firing patterns and frequencies described for olfactory neurones in Chapter 3. However, by recording field potentials in the olfactory bulb it was shown by Stewart and Scott (1976) that urethane did not alter the test response to a pair of pulses delivered to the lateral olfactory tract. Since the field potential represents the population activity of neurones within the olfactory bulb layers this would suggest that urethane is not having a significant affect on the discharge rate of olfactory neurones.

It may be that NMDA antagonist-induced changes in mitral cell c-*fos* expression do not solely reflect depolarisation. Although often indicative of recent depolarisation and calcium influx, neuronal c-*fos* expression can be induced by other stimuli and is subject to control by several different regulatory elements in the promoter region of the gene. Mutation of the Ca^{2+}/cAMP response element (Ca/CRE) reportedly produces an increase in constitutive levels of c-*fos* expression by mitral cells in one mutant mouse line, suggesting that c-*fos* expression need not reflect induction by Ca^{2+} in these cells (Robertson et al., 1995). Both mitral and granule cells express mRNAs encoding the subunits which comprise the NMDA receptor complex and interestingly, mitral and granule cells express different NMDA receptor subunits, suggesting that their responses to NMDA-acting drugs may be different (Watanabe et al., 1993). Therefore, NMDA antagonists may act directly to induce mitral cell c-*fos* expression via second messenger pathways that act on other upstream regulatory elements.

Finally, one further point to consider is that the expression of Fos in the mitral cell layer following antidromic stimulation may be due to the auto-excitation of mitral cells that has been proposed to occur (Aroniadou-Anderjaska *et al.*, 1999). If

this is correct then upon stimulation the glutamate released by the mitral cell could excite the parent mitral cell as well as neighbouring mitral cells and hence increase cell activity through a synaptically mediated event, leading to increased Fos expression. However, we cannot dismiss the fact that the antidromic stimulation of the output cells in the olfactory system resulting in increased spike activity, unlike in the magnocellular system, is capable of inducing Fos expression.

The contralateral mitral cell layer following prolonged stimulation shows less Fos than control levels and this is due to the bilateral effect of LOT stimulation. The mitral cells of the ipsilateral bulb project to the pars externa of the anterior olfactory nucleus, whose cells then project via the anterior commisure to the contralateral granule cell layer. Activation of these commissural pathways produces strong inhibitory effects on mitral/tufted cells in the contralateral bulb. It should be noted that the short-pulse stimulation did not produce the same response (the levels of Fos in both ipsilateral and contralateral bulbs under this stimulation protocol were not significantly different to levels seen in the control group) the reason for this is unclear.

4.4.3.2 Tufted cells

Following both protocols of stimulation of the LOT there was a reduced number of Fos-positive tufted cells compared to control brains. This is expected if the basal levels of Fos are high and stimulation of the LOT leads to decreased activity of output neurones. The middle and internal tufted cells are output neurones like the mitral cells (external tufted cells are classed as short-axon cells as they do not project into the LOT) and so are antidromically activated by LOT stimulation, but the two classes of output neurone do have certain differences in their connectivity.

The positions and lengths of mitral cell and tufted cell secondary dendrites could influence the degree of their interaction with the granule cell dendrites.

Synaptic inhibition is exerted on the secondary dendrites in the EPL via the dendritic spines of the granule cells. It has been shown that separate populations of granule cells innervate superficial versus deep regions of the EPL (Orona *et al.*, 1983). Different degrees of inhibition by these granule cell populations could account for the excitability differences between the output neurones (Schneider and Scott, 1983; Onoda and Mori, 1980); tufted cells have lower firing thresholds than mitral cells. Unlike Type I mitral cells, all classes of tufted cell and the type II mitral cells have extensive axonal collateralisation in the internal plexiform and granule cell layers. This may provide a second pathway for activating superficial granule cells in addition to the reciprocal synapse in the EPL. Furthermore, the cells with deep secondary dendrites (Type I mitral cells) have the longest secondary dendrites, the more superficial the cell is the shorter its secondary dendrites are. This indicates that cells with deeper dendrites have more surface area for granule cell contact and therefore, receive greater inhibitory drive.

Therefore the difference in Fos expression between the two types of output cell and the fall in Fos expression of the tufted cells after stimulation of the LOT may be somehow related to the difference in their interactions with the granule cell circuitry or their different projection patterns to the piriform cortex. Alternatively it could be due to different regulation of the c-*fos* gene within the two cell types. The regulatory effects of Fos heterodimers appear rather complex *in vivo*, ranging from activation to repression of transcription. Fos itself acts as a negative regulator of its own promoter, to repress transcription of the c-*fos* gene (Konig *et al.*, 1989; Sassone-Corsi *et al.*, 1988; Wilson and Treisman, 1988). Therefore, Fos expression in tufted cells may have been attenuated by autoregulation or alternatively some unknown mechanism has acted to prevent facilitation of the protein complex from the cytosol to the nucleus or promoted facilitation of the protein complex to another region of the cell.

4.4.3.3 Granule cells

As expected there was an increase in the number of Fos -positive profiles in the granule cell layer following stimulation of the LOT. This is due to the mitral cell releasing glutamate onto the dendritic spines of the granule cell resulting in granule cell excitation. There was no significant difference between the ipsilateral and contralateral bulbs in the number of Fos-positive profiles located within the granule cell layer and this is explained by the inter-bulbar connection through the anterior commissure. Mitral cell collaterals project to the anterior olfactory nucleus which then project, via the anterior commissure, and terminate within the granule cell layer of the contralateral bulb. This causes excitation of the contralateral granule cells and thereby increases Fos expression in the contralateral granule cell layer. Again the short-pulse stimulation was not effective in inducing Fos expression in the ipsilateral or contralateral granule cell layer.

4.4.4 The piriform cortex

The piriform cortex is also known as the primary olfactory cortex and is the first region to which the olfactory bulb sends its efferents for processing of olfactory information, so it is not surprising that Fos was expressed in this structure. It has been suggested that tufted and mitral cells have different projection patterns to the olfactory cortex (Haberly and Price, 1977). Mitral cells are retrogradely labelled from all parts of the olfactory cortex following the injection of horseradish peroxidase. However, the ratio of labelled tufted cells to mitral cells is greatly diminished as injections are made into caudal olfactory cortex regions, suggesting that the axons of tufted cells terminate in the rostral part of the olfactory cortex.

In the present study at the rostral level of the olfactory cortex Fos was only seen following prolonged stimulation of the LOT. This could be due to the activation of pyramidal neurones within the cortex by either mitral cells or tufted cells. The expression of Fos in both the ipsilateral and contralateral sides of the

rostral olfactory cortex is due to bilateral connections, via commissural fibres, between the two sides of the olfactory cortex. The caudal piriform cortex, which is thought to receive mostly mitral cell projections, shows increased Fos ipsilaterally and contralaterally following prolonged stimulation of the LOT, again, consistent with the activation of mitral cells ipsilaterally and the commissural fibres transmitting excitation to the contralateral olfactory cortex. There is a significant increase in Fos expressed in the ipsilateral, caudal olfactory cortex following short-pulse stimulation that is expected since the mitral cells are activated by the stimulation protocol although they do not express increased levels of Fos in this case.

Concluding remark

From the findings of this study it seems that the neural pathway between the olfactory bulb and the SON may be more complex than a simple unilateral, monosynaptic connection. This conclusion is based on the fact that stimulation of the LOT, that induced Fos expression in known olfactory areas, failed to induce an unilateral Fos response in the SON.

Chapter 5

The Response of Olfactory Bulb Neurones to Opioids

5.1 INTRODUCTION

5.1.1 Opioid actions during pregnancy and parturition

Russell *et al.* (1993) described two distinct opioid mechanisms that regulate the secretion of oxytocin. Both κ-and μ-receptors are located on the cell bodies and dendrites of oxytocin neurones, but only κ-receptors are found at the nerve terminals. Therefore, both μ- and κ-receptor agonists can act centrally to inhibit oxytocin neurones but only κ-receptor agonists can act at the secretory terminals (Bicknell *et al.*, 1988). Met-enkephalin, which is co-secreted with oxytocin, is a δ-receptor agonist, but extended forms of Met-enkephalin are active at neurohypophysial κ-receptors (Leng *et al.*, 1994). At the neural lobe, oxytocin secretion is restrained by co-secreted opioid peptides including dynorphin (released by both vasopressin and oxytocin terminals) and Met-enkephalin (released by oxytocin terminals), acting through κ-receptors (Leng *et al.*, 1994; Zhao *et al.*, 1988). This appears to be principally an auto-inhibitory mechanism. In mid-pregnancy, oxytocin secretion is powerfully restrained by this auto-inhibition (Douglas *et al.*, 1993; Russell *et al.*, 1995), which may contribute to the accumulation of oxytocin stores in the neural lobe in advance of parturition. By the end of pregnancy oxytocin nerve terminals become desensitised to endogenous opioid restraint, which may contribute to the high secretion of oxytocin during parturition. At this time, a separate endogenous opioid system, acting upon μ-receptors, actively restrains the electrical activity of oxytocin neurones (Douglas *et al.*, 1995; Russell *et al.*, 1995). Oxytocin release within the supraoptic and paraventricular nuclei is elevated during parturition as well as during suckling, but not during late pregnancy.

Oxytocin is important for the normal progress of parturition to increase the contractility of the uterus near term. High concentrations of progesterone are secreted from the corpus luteum during early pregnancy and this persists until shortly before the end of pregnancy. Progesterone acts to maintain uterine quiescence by decreasing uterine sensitivity to oxytocin (Burgess *et al.*, 1992). It has been shown

that in ovariectomised rats administration of progesterone inhibits the electrical activity of oxytocin neurones (Negoro *et al.*, 1973). Furthermore, Grazzinni *et al.* (1998) have shown that progesterone acts by inhibiting oxytocin binding to oxytocin receptors *in vitro*. During parturition bursts of activity of oxytocin neurones become highly synchronised and these bursts are correlated with abdominal contractions and the expulsion of pups in conscious rats (Summerlee, 1981). It is this pulsatile release of oxytocin from the pituitary gland as a consequence of bursting activity of oxytocin neurones that is important for advancing the progress of parturition.

Systemic and central administration of morphine, an opioid agonist, delays the course of established parturition, with the delay accompanied by reduced plasma oxytocin levels and overcome by treatment either with naloxone, a non-selective opioid antagonist, or by infusion of oxytocin (Bicknell *et al.*, 1988). The process of parturition is hastened by administration of naloxone. Thus, an endogenous opioid mechanism inhibiting oxytocin release appears to be active during late pregnancy, immediately before and during parturition. This mechanism does not operate earlier in pregnancy or during normal lactation and is not seen in virgin rats (Leng *et al.*, 1988).

5.1.2 Role of olfaction during parturition

At the time of parturition the mother expends great energy in sniffing and licking of the pups and olfactory cues from infants play an important role in enabling the inexperienced mother to recognise the offspring and facilitate the onset of maternal behaviour. The noradrenergic projections from the locus coeruleus play a major role in modulating olfactory responses at the time of parturition, depletion of olfactory bulb noradrenaline, by the microinfusion of the neurotoxin 6-hydroxy dopamine (6-OHDA), before parturition, results in the canabalism in primiparous but not multiparous mice (Dickinson and Keverne, 1988). This suggests that maternal experience aids the process of recognition, once the memory has been formed

noradrenaline is not required for its recall. The recognition of newly born infants is also well documented in the sheep, the mother ewe rapidly bonds with the newborn lamb and shows selective maternal care to her own offspring and will violently reject 'strange' lambs. This selective bond is based on the sense of smell, in particular the smell of amniotic fluid covering the lamb following parturition. Before giving birth pregnant ewes find the smell of amniotic fluid repulsive, but immediately after the feotal membranes have ruptured the ewe is attracted to the smell (Levy *et al.*, 1983). This reaction seems to rely heavily on olfactory cues, sheep in which the olfactory epithelium has been destroyed using zinc sulphate show no preference.

5.1.3 Mechanisms of opioid action

Endogenous opioid peptides and opiates like morphine exert their pharmacological and physiological effects on the target tissues by specifically binding to membrane-bound receptors. Several studies have used autoradiographical techniques to map the anatomical distribution of opiate receptors in the mammalian central nervous system (McLean *et al.*, 1986; Mansour *et al.*, 1988). Although there have been suggestions for as many as nine different receptor types, the three widely accepted opioid receptor types are referred to as: mu- (μ); delta- (δ) and; kappa- (κ). These receptors are members of the seven transmembrane domain G-protein-coupled receptor family.

Electrophysiological studies in various areas of the mammalian central nervous system have shown that activation of opioid receptors predominantly results in an inhibition of the neuronal firing of action potentials. In all systems, opioid receptors couple to their effector mechanisms through G proteins alone (Childers, 1991). At first it was thought that μ- and δ-receptors exerted their inhibitory actions through activation of inwardly-rectifying K^+ conductances whereas κ-receptors acted through inhibition of voltage-activated Ca^{2+} conductances. It is now understood that the effector mechanisms employed by each of the receptors is cell-type specific, because

μ-receptors are also able to inhibit voltage-activated Ca^{2+} conductances and κ-receptor activation can also activate inwardly-rectifying K^+ conductances (Grudt and Williams, 1995). In addition to activation/inhibition of ion channels, opioid effector mechanisms can also be mediated by second messenger systems such as inhibition of adenylyl cyclase (Childers, 1991) as well as activation of phospholipase C (Smart *et al.*, 1995).

In magnocellular neurosecretory cells the alteration in membrane conductances associated with action potential activity by opioids may modulate cellular excitability in several ways. By the pre-synaptic inhibition of afferent inputs, hyperpolarisation of the post-synaptic membrane through activation of K^+-channels and/or reduction of post-spike excitability by reducing depolarising after-potential amplitude by reducing Ca^{2+} entry (for review see, Brown *et al.*, 2000).

Following chronic i.c.v administration of morphine or U50, 488H (μ- and κ-receptor agonists respectively) oxytocin cells of the supraoptic nucleus develop tolerance to these opioids (Russell *et al.*, 1995; Brown *et al.*, 1998). This reflects a reduced sensitivity to inhibition by the receptor agonists, and in the case of morphine, may result from μ-receptor down-regulation (Sumner *et al.*, 1990). Morphine dependence involves changes in the cells such that they require the continued presence of morphine to function 'normally' this is revealed by a rebound hyper-excitation after withdrawal of morphine acutely by the administration of naloxone (synthetic antagonist). Many central neurones express μ-receptors (Mansour *et al.*, 1995) but few have been shown to exhibit morphine dependence (Nye and Nestler, 1996).

5.1.4 Location of opioid receptors in the olfactory system

McLean *et al.*, (1986) mapped the localisation of μ- and δ- sites in the diencephalon and telencephalon of the rat, [^{125}I]D-Ala^2-MePhe^4-Met(o)^5-ol-

enkephalin (FK) and [^{3}H]D-Ala^2-D-Leu^5-enkephalin (DADLE) was used to bind at μ- and δ- sites respectively. The sections were conterstained and analysed for correspondence of receptor distribution, marked by silver grains and underlying cytoarchitecture. In the main olfactory bulb, the μ-receptors (labelled by FK) and δ-receptors (labelled by DADLE) each had distinct distributions. Moderately dense FK binding was localised in the olfactory glomeruli and inner half of the external plexiform layer, binding was also found in the accessory olfactory bulb. In contrast, dense binding of DADLE was present only in the external plexiform layer of the main olfactory bulb; binding was absent in the glomeruli of the main bulb and throughout the accessory olfactory bulb. The mitral, internal plexiform, and internal granule cell layers showed low-to-moderate levels of FK and DADLE binding. Furthermore, both μ and δ sites were sparse in the piriform cortex, though FK binding was slightly enriched in the molecular layer.

FK binding sites are relatively enriched in the terminal zones of efferent projections arising from both main and accessory olfactory bulbs. These zones include the external plexiform layers of the anterior olfactory nucleus, the olfactory tubercle and medial and cortical nuclei of the amgydala. Thus μ-receptors are in position to modulate information in both primary and secondary olfactory relay synapses. In contrast, δ-receptors, although overlapping with the μ-receptors in the external plexiform layers of secondary structures, are not found in the terminal zones of primary olfactory inputs.

5.1.5 Mu-receptor isoforms

Recent research has revealed two μ-opioid receptor isoforms; rMOR1 and rMOR1B (Zimprich *et al.*, 1995a). The immunolocalisation of these two isoforms has been achieved in the central nervous system of the rat (Schulz *et al.*, 1998). The two isoforms only differ from each other in length and amino acid composition at the very end of their carboxy tails and they arise from alternative splicing of the

cytoplasmic tail of the rat μ-opioid receptor. Both isoforms bind μ-opioid receptor-selective agonists with similar high affinity, and they are equally effective in the inhibition of forskolin-induced cAMP formation. They are also both able to stimulate phospholipase C and to mobilise Ca^{2+} from intracellular stores to about the same extent (Zimprich *et al.*, 1995b). However, the two isoforms differ in their desensitisation characteristics in that rMOR1B seems to be more resistant to agonist-induced desensitisation of coupling to adenylate cyclase than rMOR1 (Zimprich *et al.*, 1995a).

Schulz *et al.* (1998) used isoform-specific peptide antibodies to rMOR1 and rMOR1B to determine their distribution in the rat CNS. Prominent MOR1-like immunoreactivity was abundant in many regions throughout the CNS revealing a distribution which was essentially identical to that previously reported by others (Arvidsson *et al.*, 1995). However, MOR1B-like immunoreactivity was restricted to the olfactory bulb, there were no overlapping regions between the MOR1-positive regions and MOR1B-positive areas within the bulbar laminae. In the main olfactory bulb MOR1-like immunoreactivity (MOR1-LI) was localised at the mitral cell and glomerular layers targeted to the perikarya of the mitral cells and periglomerular cells and their processes that ramify within glomeruli. MOR1-LI was also seen in the anterior olfactory nucleus; olfactory tubercle; accessory olfactory bulb and the piriform cortex.

MOR1B-like immunoreactivity (MOR1B-LI) was prominent in the external plexiform layer associated with the neuronal perikarya and the thick dendrites of mitral cells that were coursing upwards to ramify within the glomeruli. MOR1B-LI was not seen in granule cell bodies but the staining seen in the EPL may have been associated with the granular dendrites as well as those belonging to mitral cells. Unlike MOR1, MOR1B-LI was not seen in any other part of the olfactory system.

AIMS

In the introduction to this chapter the inhibitory action of opioids on the activity of oxytocin neurones was described. Morphine has been shown to disrupt the normal progress of parturition by its inhibition of oxytocin release by the magnocellular cells of the hypothalamic nuclei. It has been proposed that a neural connection exists between the supraoptic nucleus of the hypothalamus and the olfactory bulb (Smithson *et al.*, 1989,1992; Hatton and Yang, 1989) furthermore, it has been suggested that this pathway is active at the time of parturition Meddle *et al.* (1998). The olfactory bulb is rich in opioid receptors and terminations of Met-enkephalinergic centrifugal fibres that enter the bulb via the anterior commissure are found in the granule cell layer (Davis *et al.*, 1982). In addition there is also an element of dynorphin immunoreactivity found in the glomerular layer of the main olfactory bulb (Khachaturian *et al.*, 1982). There is a great deal of sniffing and licking of the pups as they are delivered and the olfactory system is highly active at the time of parturition and plays an important role in determining the onset of maternal behaviour expressed by the mother (Keverne, 1988). It was considered whether the disruption of parturition by morphine was in part due to disruption of olfactory output that may be directed towards the hypothalamic nuclei.

Upon chronic administration of morphine, oxytocin neurones become both tolerant to and dependent upon this opiate (Russell *et al.*, 1995). Tolerance is seen as a reduction in the effectiveness of morphine inhibition over time, while dependence is manifested as increased activity following withdrawal of morphine. Although many systems within the brain express the mu-receptor, few have been shown to develop morphine dependence (Nye and Nestler, 1996). With this in mind, olfactory neurones were tested for their ability to become tolerant and dependent upon morphine.

5.2 METHODS

5.2.1 Experimental design

5.2.1.1 Application of opioid agonists, in vivo

The basic surgical preparation is the same as described in previous chapters. On the day of experimentation, female Sprague-Dawley rats (300-350g) were anaesthetised with urethane (i.p. 1.25 ml/kg body weight) and a jugular cannula inserted. The rats were positioned in a stereotaxic frame and dorsal surgery was performed. The stimulating and recording electrodes were positioned in the LOT and olfactory bulb respectively.

The μ-receptor agonist morphine sulphate (MOR) was dissolved in 0.9% saline to give a stock solution of 2mg/ml. From this stock solution the following dilutions were made: 20μg/ml; 200μg/ml and 1mg/ml. In some experiments U50,488H ((±)-U-50488 hydrochloride, Tocris Cookson Ltd, UK) a kappa-receptor agonist was administered and the same range of dilutions were made. A stock solution (10mg/ml) of the universal antagonist naloxone (NLX) (Naloxone hydrochloride $2H_2O$, Tocris Cookson Ltd, UK) was also made and dilutions of 1mg/ml and 2mg/ml prepared. The solutions were contained in eppendorfs and stored at 4°C.

Once a mitral cell had been identified and a period of spontaneous and stimulated activity recorded, the dose of the selected drug was administered i.v. via the jugular cannula. The drug was washed through the cannula tubing by a bolus of 0.9% saline. A period of 10-15min was allowed between successive doses.

5.2.1.2 Morphine tolerant animals

Female Sprague-Dawley rats (with a minimum weight of 300g) were fitted with osmotic mimipumps which delivered increasing concentrations of MOR via an intracerebroventricular (i.c.v) cannula. This surgery was completed five days before the electrophysiology experiment. Rats were anaesthetised with urethane (i.p,

1.25g/kg body weight) and a jugular cannula inserted and dorsal surgery performed. In some cases the dental acrylic applied during placement of the i.c.v cannula covered bregma, in these instances the drill was used to remove the acrylic taking care not to drill through the surface of the skull. Once bregma had been located the co-ordinates for the placement of the recording electrode could be measured.

When a mitral cell had been found and identified a period of spontaneous activity was recorded before application of NLX. Doses of NLX were relatively high (1mg/kg and 5mg/kg body weight) due to the continuous infusion of high concentrations of MOR over the five day period. At the end of the experiment the rat was killed with an overdose (i.v) of pentobarbitone.

5.2.1.3 Application of morphine, in vitro

Female Sprague-Dawley rats (60-120g) were used in all the *in vitro* experiments. A horizontal slice (400μm) of the olfactory bulb was prepared and the slice was placed on the ramp of an interface chamber that allowed aerated and heated (33°C ± 0.2°C) aCSF to flow underneath the slice and vapour saturated gas to pass over the uppermost surface of the slice. The slice was left to incubate in these conditions for at least 1h before recording began.

The medium (aCSF) consisted of the following (in mM); NaCl 124, KCl 3, NaH_2PO_4 1.25, $CaCl_2$ 2, $MgSO_4$ 1.3, $NaHCO_3$ 26, and D(+)-glucose 10 (Chen and Shepherd, 1997). This contains approximately half the concentration of potassium ions than a standard recipe for aCSF. This was achieved by lowering the KCl concentration and replacing KH_2PO_4 with NaH_2PO_4. It was necessary to make this alteration since high potassium concentrations can cause epileptiform activity in cortical slices (McBain, 1995). A stock solution (10mM) of MOR was prepared and dilutions of 30μm and 10μm prepared immediately before use.

5.3 RESULTS

5.3.1 In vivo preparation

A total of twenty-three mitral cells and six cells from the granule cell layer were tested with opioid agonists and antagonists. In the mitral cell group all cells showed a phasic firing pattern; eleven showed silent periods between bursts of activity and twelve showed periods of reduced activity in-between bursts. In the control periods before drug application the length of bursts varied in the range 51.5 to 259.3s (mean ± S.E.M. = 109.5 ± 7.5s) and the interburst time varied between 27.4 to 351.9s (mean ± S.E.M. = 97.6 ± 10.7s). The firing rate of mitral cells during this control period was in the range 3.4 - 26.4 spikes/s (mean ± S.E.M. = 12.5 ± 1.4 spikes/s). Cells recorded from the granule cell layer showed firing rates in the range 4.4 to 15.7 spikes/s (mean ± S.E.M. = 8.9 ± 1.8 spikes/s) during the control period before drug application.

Following the administration of MOR (i.v.) at doses in the range 10μg/kg to 1mg/kg body weight, there were no immediate or obvious effects on the firing rate of mitral or granule cells (fig. 5.1). Furthermore, there was no difference in the response evoked by low or high doses of MOR. All figures show the response to 500μg/kg, since this is equivalent to the 10μM dose given *in vitro* and results can be compared. It also allows results to be compared with responses seen in oxytocin neurones to the same dose of MOR. Thus, in the olfactory bulb the application of 500μg/kg MOR did not seem to have a significant effect on neurone firing, an equivalent dose of MOR (i.v.) results in approximately 95% inhibition of firing rate in oxytocin neurones of the rat SON (Ludwig *et al.*, 1997). The firing rate of granule cells was not significantly lowered by the application of MOR (fig. 5.1) to between 3.5 and 7.6 spikes/s (mean ± S.E.M. = 5.3 ± 1.0 spikes/s). In the case of mitral cells the periodicity of bursts was not significantly altered: burst length was in the range 51.8 to 254.5s (mean ± S.E.M. = 108.5 ± 7.9s) and the interburst time was slightly, but not significantly shorter with a range 13.7 to 206.5s (mean ± S.E.M. = 75.5 ±

7.8s). The firing rate of mitral cells was in the range 3.1-16.7 spikes/s (mean ± S.E.M. = 8.1 ± 1.6 spikes/s), again not significantly different from control levels.

However, the interspike interval distributions reveals that for mitral cells that fired with two modes (n=9) the high frequency mode was greatly diminished in amplitude i.e. the number of events that occurred within this mode were far fewer. There is a significant fall in the high frequency peak ($p < 0.05$, Wilcoxon Signed Rank Test) yet the increase in the second mode is not significantly different from control levels. Mitral cells firing in one mode did not show a significant response to MOR. The hazard functions of both mitral cells that fire in one mode and two modes are shown in figure 5.2 and the difference between pre- and post-MOR plots is emphasised in the subtraction plots in figure 5.3.

Four of the six granule cells that were tested with opioid agonists were tested for a reversal of these effects by the application of the non-selective opioid receptor antagonist naloxone (NLX) (1mg/kg body weight) the two cells not tested were lost prematurely. NLX was also applied to nine mitral cells that had previously been tested with an agonist. As there had not been a significant effect by MOR on the firing rate and discharge patterns of mitral and granule cells the effect of NLX was also seen to be non-significant (fig. 5.1). The firing rate of mitral cells following the application of NLX was in the range 6.1 to 17.8 spikes/s (mean ± S.E.M. = 8.7 ± 1.5 spikes/s) and the firing rate of granule cells was in the range 6.3 to 12.7 spikes/s (mean ± S.E.M. = 7.6 ± 2.0 spike/s). The olfactory neurones were also tested with U50, 488H, a κ-receptor agonist. Results show that this second agonist did not have any affect on the firing rate or discharge pattern of mitral (n = 4) or granule cells (n = 3) figure 5.4 shows a representative mitral cell.

5.3.2 In vitro preparation.

As well as looking at how the firing pattern was changed by removing external influences we also looked to see how the application of MOR would affect the neurones in the slice preparation (n=17), using an *in vitro* preparation also has the advantage of enabling us to modify the external environment. The MOR was administered at two concentrations; 30μM and 10μM and there was found to be no difference in responses to the two different doses. The values for firing rates are given for the cells that received the 10μM dose so that results can be compared with the data from *in vivo* experiments as 10μM is approximately equivalent to 500g/kg taking into consideration that the *in vivo* dose is distributed 10ml per 100g body weight.

It has already been established in Chapter 3 that the firing rate of mitral cells is different *in vitro* to what we see *in vivo*. The effect of morphine is also different in that in some cases (n=10) it eliminated all cell firing. In these cells firing returned almost immediately upon the application of NLX, returning to basal levels (fig. 5.5). In other cells (n=7) MOR simply lowered the firing rate (fig. 5.5); in some of these cells (n=4) MOR prevents firing but the cell recovers before NLX is applied. The mean results for all mitral cells tested with 10μM MOR are as follows: before MOR administration the firing rate was in the range of 2.8 to 14.3 spikes/s (mean ± S.E.M. = 7.5 ±0.8 spikes/s. Following a dose of 10μM MOR the firing rates fell to 0.03 to 2.13 spikes/s (mean ± S.E.M. = 0.9 ± 0.6 spikes/s).

The mitral cells were then tested with a dose of NLX at the same dose as the MOR that was applied previously and resulted in the inhibition of firing. Following the application of 10μM NLX the firing rates increased, returning to pre-MOR rates, in the range 3.0 to 14.3 spikes/s (mean ± S.E.M. = 8.8 ± 2.7 spikes/s).

The effect of low Ca^{2+} was tested on the firing rate of mitral cells in the slice (the composition of the low Ca^{2+} medium is in Chapter: General Materials and Methods). The low Ca^{2+} medium was used to determine whether MOR exerted its effects by acting directly on the recorded cell via modulation of Ca^{2+} channels. However, we did not anticipate that upon application of the reduced Ca^{2+} medium mitral cell activity would be fully inhibited (fig. 5.6). Prior to the perfusion of the low Ca^{2+} medium the firing rate was in the range 2.8 to 14.3 spikes/s (mean ± S.E.M. = 7.5 ± 0.8 spikes/s). After introducing the low Ca^{2+} medium into the recording chamber the firing rate fell from basal levels to between 0.06 and 0.99 spikes/s (mean ± S.E.M. = 0.4 ± 0.16 spikes/s). Upon the re-perfusion of standard medium the firing rates increased again to 5.0 to 8.33 spikes/s (mean ± S.E.M. = 5.98 ± 0.93 spikes/s). When the mitral cells that exhibited the 'notched' waveform (11%) were tested with the low Ca^{2+} medium the notch was abolished and returned only once the low Ca^{2+}medium had been washed off.

5.3.3 Morphine tolerant animals

The oxytocin neurones of the SON are one of the few cell types that are capable of exhibiting dependence on MOR. The same protocol was used to attempt to induce morphine-tolerance and dependence in olfactory bulb neurones. Six rats were successfully implanted with the mini-osmotic pump used to deliver increasing concentrations of MOR over a 5-day period. From these rats the spontaneous activity of fifteen mitral cells was recorded and six of these cells were tested for a withdrawal response upon the application of NLX. Ratemeter recordings of mitral cell activity (fig. 5.7A) show that in these morphine-tolerant rats the cells fire with the same characteristics as mitral cells in morphine-naive rats.

The dose of NLX given (5mg/kg body weight) was higher than that applied to the morphine-naive rats in order to overcome the high concentrations of MOR that the rats had received over the 5 day period previous to the experiment. The effect of

NLX administration is shown in figure 5.7C. Mitral cells that fired in one mode as well as the bimodal mitral cells showed a significant increase in their firing rates however, the periodicity of the bursts were not significantly altered. Prior to NLX the mean firing rate was in the range 5.4 to 13.3 spikes/s (mean ± S.E.M. = 8.8 ± 1.8 spikes/s). The burst lengths were in the range 62.0 to 226.2s (mean ± S.E.M. = 126.7 ± 9.7s) and the inter-burst periods were in the range 39.9 to 390.2s (mean ± S.E.M. = 126.9 ± 17.2s). Following the administration of NLX (5mg/kg) to morphine-tolerant rats the firing rate of mitral cells significantly increased to within the range 10.9 to 17.3 spikes/s (mean ± S.E.M. = 14.1 ± 1.9 spikes/s), but the burst parameters did not significantly change. The burst lengths were in the range 53.7 to 158.8s (mean ± S.E.M. = 107.2 ± 7.8s) and the inter-burst time was in the range 23.8 to 390.2s (mean ± S.E.M. = 121.6 ± 27.3s).

Figure 5.1 Effects of the application of the μ-receptor agonist morphine (MOR) and the non-selective opioid antagonist naloxone (NLX) on the firing rate and discharge pattern of the olfactory bulb neurones. [A] Representative cells from the bimodal mitral cells (n=9) and granule cells (n=6). The systemic dose of MOR (500μg/kg) does not significantly lower the mean firing rate of either cell type furthermore, in the case of the phasically firing mitral cell MOR does not alter the periodicity of discharge activity. NLX (1mg/kg) does not have any significant affect on the firing rate of either cell type. [B]-[D] Interspike interval histograms constructed from 5min period of cell activity indicated by broken lines in the ratemeter recordings in [A]. The histograms for the bimodal mitral cell show that it is the first mode that is effected by MOR administration and this is not reversible.

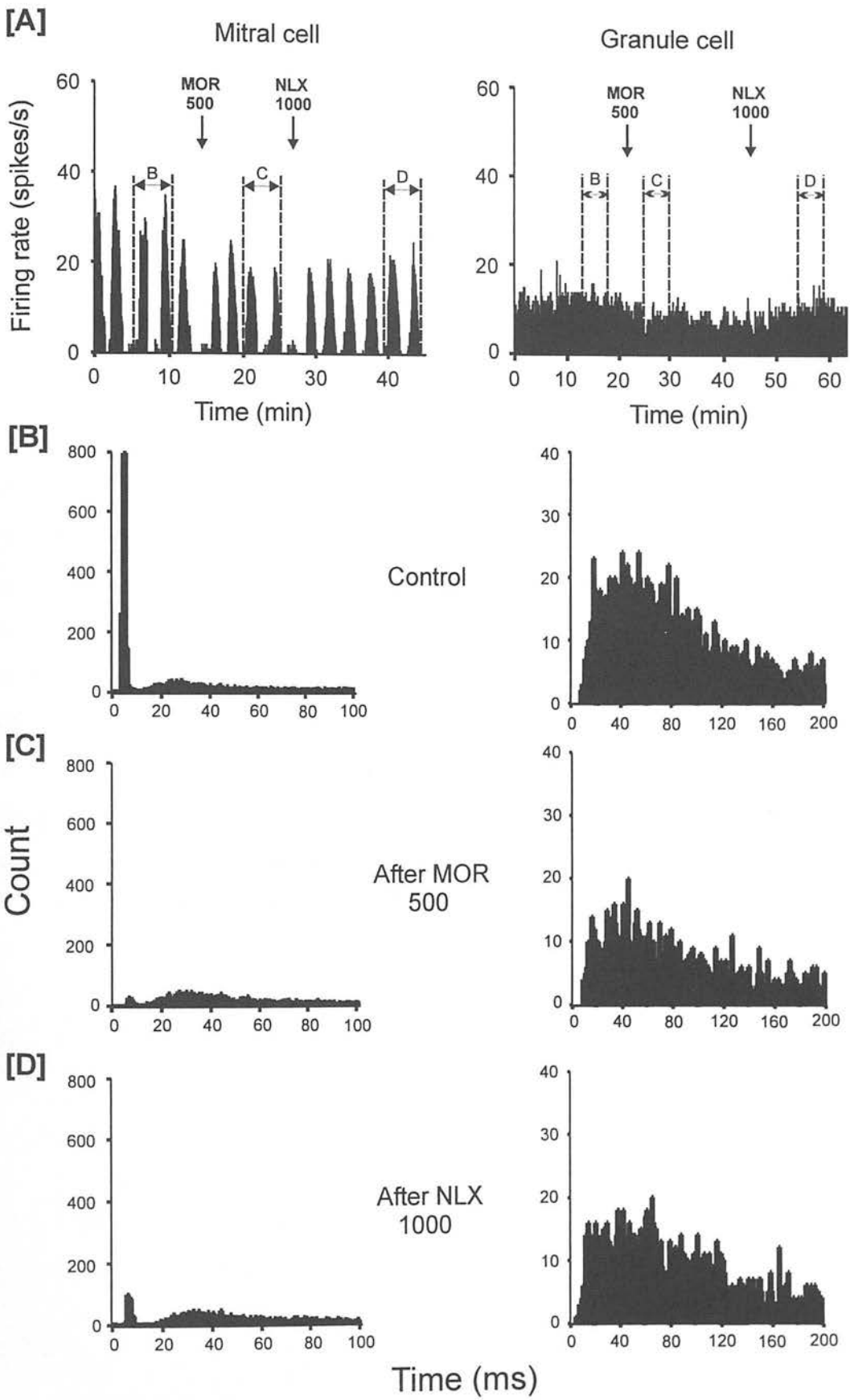
[A]
Mitral cell
Granule cell
Firing rate (spikes/s)
MOR 500
NLX 1000
B
C
D
Time (min)
[B]
Control
[C]
After MOR 500
[D]
After NLX 1000
Count
Time (ms)

Figure 5.2 Plots of the hazard functions of the mean interspike intervals for mitral cells that fire with [A] two modes (n = 9) and [B] one mode (n = 7) both before and after morphine (500μg/kg body weight) administration. Pre-MOR values are shown as filled circles and the post-MOR values are shown as open triangles in both graphs. Morphine clearly lowers the probability of the cell firing between 0 and 10ms in the bimodal mitral cells ($p<0.05$, Wilcoxon Signed Rank Test) and also slightly lowers the probability of firing 15-25ms after a spike, although this was not found to be significant. The graph for mitral cells that fire in one mode show that morphine acts to slightly increase the probability of the cell firing between 10 and 20ms but this was not found to be significantly different from pre-MOR values.

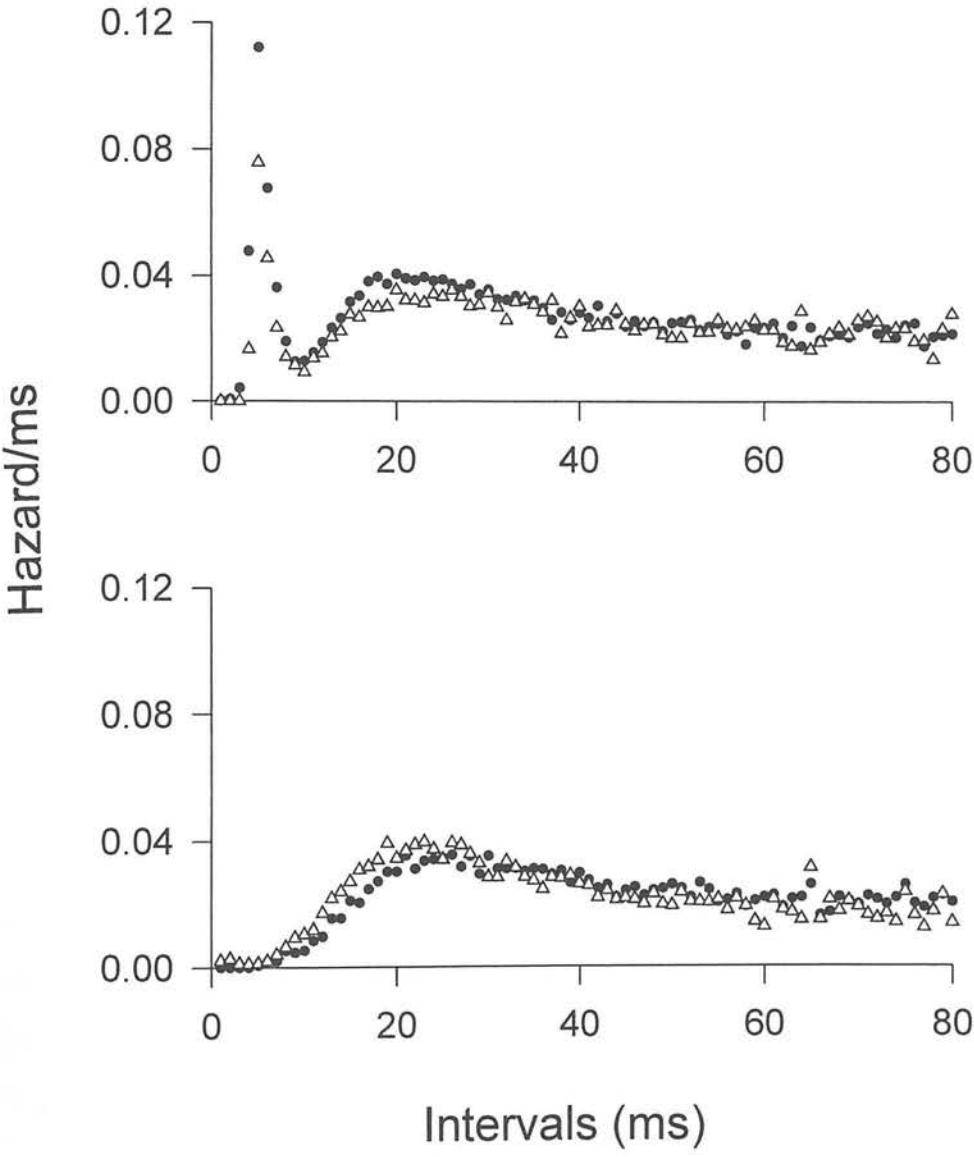
0.12
0.08
0.04
0.00
0
20
40
60
80
Hazard/ms
0.12
0.08
0.04
0.00
0
20
40
60
80
Intervals (ms)

Figure 5.3 Subtraction plots constructed from the hazard functions in the preceding figure. A line is drawn along the zero point, which indicates no change between pre- and post-MOR values. [A] Shows the result of subtracting post-MOR values from the pre-MOR values for the bimodal mitral cell group (n = 9) the positive values reflect a fall in the probability of firing, due to the post-MOR values being lower than in the control period. Notice there is very little difference between the two sets of values in the second mode indicating that morphine is having a greater influence over firing in the period up to 10ms after a spike. Furthermore, MOR is having no effect on intervals greater than 40ms which was established in Chapter 3 to be the period at which the hazard plot reaches a plateau indicating the spike has no influence over cell firing. This would suggest that MOR effects the cell membrane so as to reduce the first depolarising after-potential, rather than affecting synaptically mediated contacts i.e. the granule cell circuitry. [B] Shows that in mitral cells firing with only one mode morphine has little effect on the probability of subsequent firing of action potentials after a spike, with all values located close to the zero line. Together the subtraction plots suggest that MOR is selectively exerting an inhibitory influence on the high frequency component of the mitral cell firing pattern and not affecting the longer intervals.

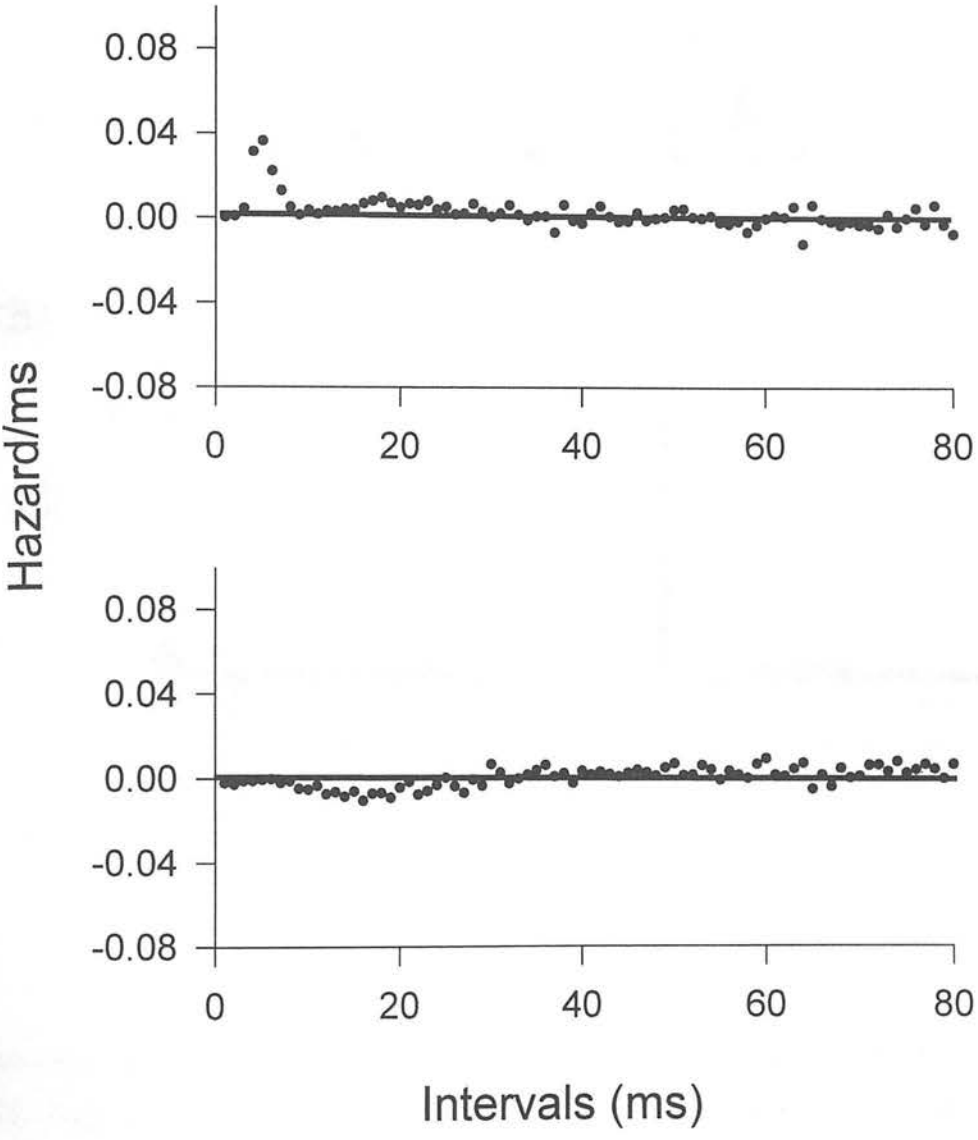
Hazard/ms
0.08
0.04
0.00
-0.04
-0.08
0
20
40
60
80
0.08
0.04
0.00
-0.04
-0.08
0
20
40
60
80
Intervals (ms)

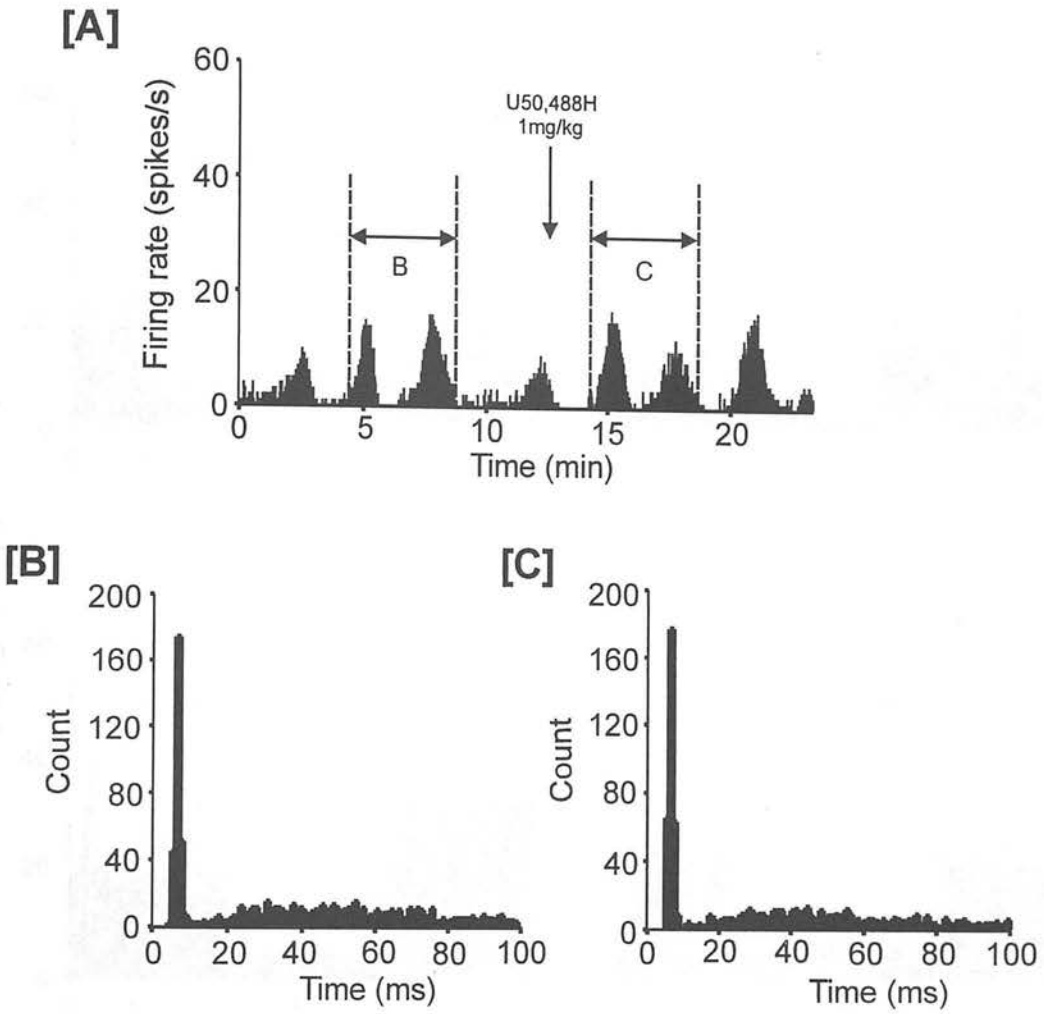

Figure 5.4 [A] A representative mitral cell recording illustrating the effects of U50, 488H (1mg/kg) upon mitral cell firing without prior administration of MOR. The application of U50 does not affect the firing rate or pattern of mitral cell discharge. There is no change in the interspike interval distribution constructed from 5min periods of mitral cell activity before [B] and after U50 administration, indicating that this agonist does not have any affect on the firing rate or discharge pattern of olfactory bulb mitral cells.

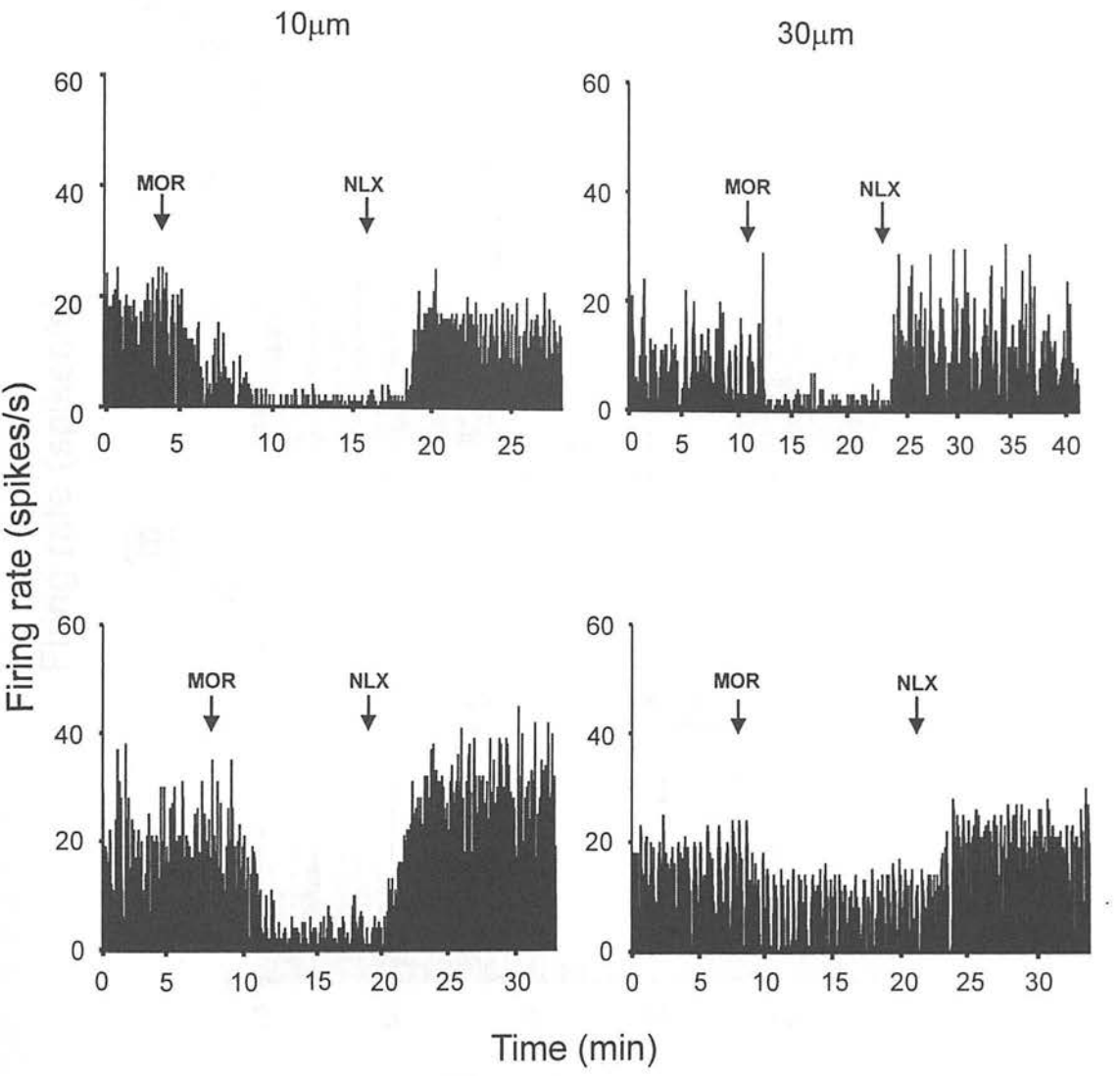

Figure 5.5 The effects of MOR on the firing rate of mitral cells was also studied in vitro (at a dose of 30μm, n=13; and 10μm, n=4). In the olfactory bulb slice perfusion of a 10μm MOR solution is the equivalent of the 500mg/kg MOR dose applied *in vivo* furthermore, the higher dose (30μm) produced the same results. In the olfactory bulb slice mitral cells show a varied response to MOR; MOR was seen to eliminate the spontaneous activity of mitral cells (n=10) and in others it significantly reduced the firing rate (n=7). The depression of mitral cell firing by MOR was reversed by the perfusion of NLX (at an equal dose to the MOR applied) in all recordings. Some of the mitral cells (n=4) showed recovery from the MOR dose before NLX was applied.

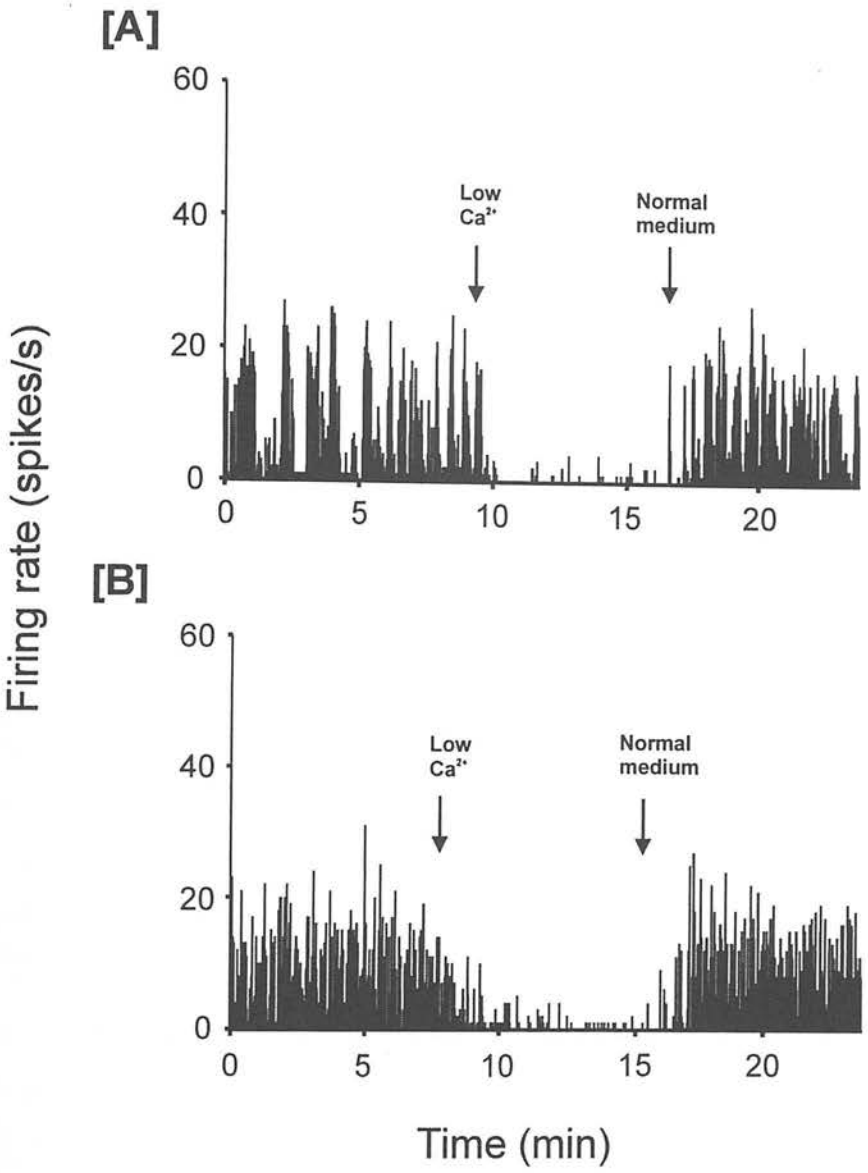

Figure 5.6 Ratemeter histograms to show the affect on mitral cell firing of perfusing the olfactory bulb slice with a low Ca^{2+} medium (n=6). The application of a medium containing a low concentration of Ca^{2+} has an immediate, inhibitory effect on the spontaneous activity of all mitral cells tested. The cell returns to its basal firing rate only when standard medium replaces the low Ca^{2+} medium.

Figure 5.7 [A] Ratemeter records from two different mitral cells in morphine-tolerant rats (n=6) to show the effect of NLX administration and to determine whether the output cells of the olfactory system were capable of developing morphine-dependence as evidenced by a hyper-excitation morphine withdrawal response. Interspike interval histograms constructed from 5min period of cell activity [B] before NLX application and [C] after NLX (5mg/kg). The mitral cells display only a moderate response to the application of NLX, the firing rate is increased (but not to the degree of hyperexcitation) and the periodicity and burst length are not altered indicating that mitral cells do not develop morphine-dependence.

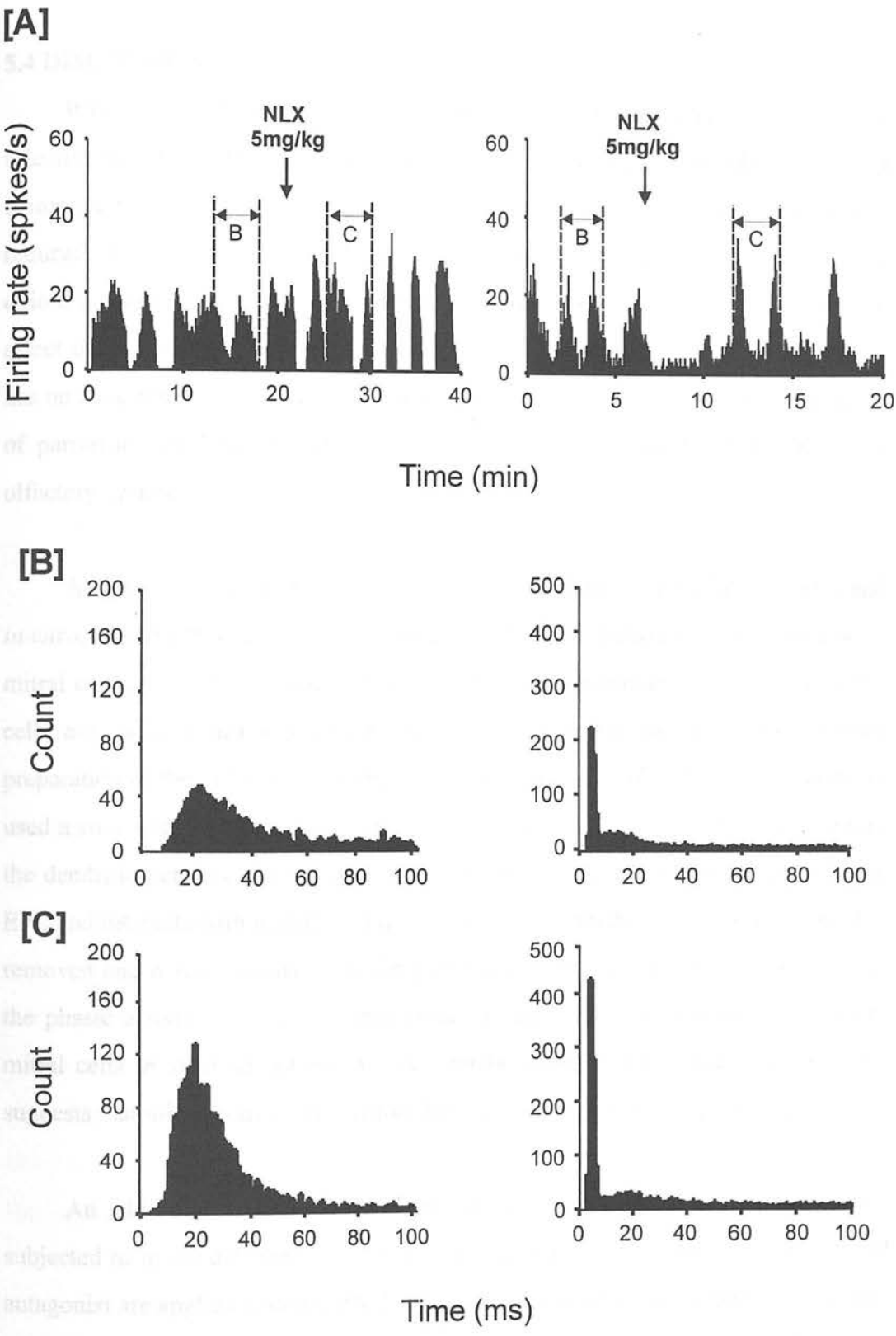
[A]
NLX
5mg/kg
B
C
Firing rate (spikes/s)
Time (min)
[B]
Count
[C]
Count
Time (ms)

5.4 DISCUSSION

It is clear from the results in the present study that MOR has a subtle and yet selective inhibitory affect on the discharge pattern of bimodal mitral cells. The mean firing rate is not significantly lowered but the high frequency component is markedly reduced and this effect is not reversed upon the application of the non-selective opioid antagonist, naloxone. Furthermore, the inhibitory action of MOR does not affect the periodicity of mitral cell phasic activity. These subtle effects that MOR has on the output discharge of the olfactory bulb strongly suggests that the disruption of parturition by MOR is not mediated, even in part, by MOR inhibition of the olfactory system.

A difference was seen between the response of mitral cells to MOR *in vivo* and *in vitro*, this might be explained by considering the contribution to tonic inhibition of mitral cell activity by granule cells in the different preparations. *In vivo* the mitral cells are under a heavy tonic inhibition however, in the cutting process during preparation of the olfactory bulb slice, even in a relatively thick horizontal slice (we used a slice with a thickness of 400μm), it is impossible to avoid removing much of the dendritic network of the mitral cells that extends for very large distances in the EPL and interacts with granule cell dendrites. Hence, much of the inhibitory input is removed and it was established in Chapter 3 that mitral cells *in vitro* do not display the phasic activity that is so characteristic of mitral cells *in vivo* and furthermore mitral cells *in vitro* do not exhibit the bimodal firing patterns seen *in vivo*. This suggests that mitral activity in olfactory bulb slices is severely compromised.

An additional concern is the doses of agonist and antagonist the cells were subjected to in the different preparations. In the *in vivo* preparation the agonist and antagonist are applied systemically through an intravenous cannula, with this method of application it is difficult to determine the concentration of drug that actually exerts an effect on the bulbar neurones. In the *in vitro* preparation the agonist and

antagonist were applied through the perfusion tubing of the recording chamber which is a more direct method of application. This may be why we see such an immediate and dramatic response to morphine and are able to reverse the inhibition with the application of naloxone in the *in vitro* preparation. Therefore, the neurones in the *in vivo* preparation may have effectively received a reduced dose and this might explain why we see such a reduced and irreversible response to morphine. A solution to this problem would be to apply morphine in a more direct way in the *in vivo* preparation. This would prove to be technically difficult but may be achieved by lowering a second electrode into the region of the recording electrode and ejecting a known concentration of morphine/naloxone.

It was proposed in Chapter 3 that the high frequency firing seen in mitral cells recorded *in vivo* originated at the dendrites and started to fire as the initiation site at the soma was inhibited. Hence, the *in vivo* MOR results would lead us to believe that MOR is acting at the dendrites to inhibit the high frequency firing component however, in the *in vitro* results mitral cells do not display the high frequency mode and yet MOR seems to have a greater effect on inhibiting the firing rate of mitral cells. If much of the interneurone network is lost in the slice preparation then the inhibition exerted at the soma would be considerably less and this may be why the high frequency firing is not seen, the soma is not inhibited thereby preventing the dendrites from initiating action potentials, but this does not answer the question as to where MOR acts. It may be the case that MOR acts to modulate the mitral cell discharge pattern by interacting with the granule cell, but this is an area in which more work needs to be done in order to fully understand the significance of inhibiting the high frequency firing of the mitral cell.

Very few data are available in the literature concerning the action of exogenous opioids on olfactory bulb neurones. Perez *et al.* (1989) looked at the modulatory influences of the mu-opioid agonist morphine and the kappa agonist U-50, 488H on

evoked field potentials from the main olfactory bulb in response to orthodromic stimulation of the olfactory nerve. Topically administered morphine (at a low dose of 100nM) upon the main olfactory bulb dorsal surface produced a naloxone-sensitive depression of the late component of the response without modifying the early one. Whilst topical administration of U50, 488H eliminated both the early and the late components however, naloxone (applied at a dose of 2mg/kg, i.v. for both agonists) did not antagonise U50, 488H effects. Interpretation of the components of orthodromically evoked field potentials (Freeman, 1972) suggest that the early component represents the synchronous excitation of granule cells through activation of mitral/tufted neurones, whereas the later components are thought to represent the reciprocal interactions between the output neurones and the granule cells. Hence, these results indicate that mu- and kappa-opioid agonists may modulate sensory transmission at the level of second-order neurones of the olfactory pathway, the mitral/tufted cells. This is consistent with the anatomical studies that show mu-binding sites in the external plexiform layer of the olfactory bulb to be in the position to modulate the activity of the mitral cells that are the main output neurones of the olfactory bulb (McLean *et al.*, 1986).

Concluding remark

The hypothesis that morphine inhibition of oxytocin release by magnocellular cells of the SON leading to disruption in the normal progression of parturition is in part mediated by inhibition in the olfactory system has been found not to be plausible. The effects of morphine on the discharge output from the olfactory bulb is minimal, the periodicity and firing rate are not significantly altered. Morphine has been found to have a subtle effect on the firing pattern of olfactory neurones in that it selectively inhibits the fast firing component exhibited by a proportion of mitral cells. Furthermore, morphine-tolerant rats do not display a withdrawal response indicating that the mitral cells do not develop morphine dependence.

Chapter 6

General Discussion

The experiments described in this thesis were designed first to confirm the proposed neural pathway between the olfactory bulb and the supraoptic nucleus and second to test the hypothesis of whether morphine which has been shown to disrupt the progression of parturition by inhibiting release of oxytocin from the hypothalamic nuclei exerts this inhibitory influence in part by inhibiting the output of the olfactory system. The olfactory system has been shown to play an active role in determining the onset of maternal behaviour and is required for the successful recognition of the young at the time of parturition.

Previously it has been reported that the mitral/tufted cells of the main and accessory olfactory bulbs send efferents to the ipsilateral supraoptic nucleus. This has been demonstrated using both anatomical tract tracing methods (Smithson *et al.*, 1992) and electrophysiological activation of SON neurones following stimulation of the LOT, *in vitro*. In order to study the proposed neural pathway between the olfactory bulb and the SON we stimulated the LOT *in vivo* and used the expression of Fos protein as an indication of neuronal activity induced by the stimulus (Chapter 4). Before we applied a stimulus to the LOT in an attempt to activate SON neurones we felt it was necessary to first understand the discharge output of the olfactory bulb. This was achieved by making extracellular recordings of unit activity from the output cells of the main olfactory bulb and since the activity of the output neurones is under considerable influence from local interneurones, recordings of these were also made (Chapter 3). It was established that output from the olfactory bulb had a phasic discharge pattern with the constituent bursts lasting for 1-2min with approximately equal periods of silence or quiescence between the bursts of activity. Furthermore, the rate of spontaneous discharge shown by these cells was surprisingly high.

Pathway between the olfactory system and the hypothalamic nuclei

Having established the output pattern from the olfactory bulb and the rate of spontaneous discharge we stimulated the LOT accordingly. Two stimulation protocols were applied, one to mimic a strong surge of olfactory output and the other to disrupt the 'normal' pattern of olfactory output. Results were not as we had hypothesised, we had expected to find an unilateral increase in Fos expression in the SON to be consistent with the observations made by Smithson *et al.* (1992) and Hatton *et al.* (1989) however, following the stimulation of the LOT under both stimulating protocols there was a significant difference in the level of Fos staining in both the ipsilateral and contralateral SON. This raises the possibility that the proposed unilateral, monosynaptic connection between the SON and olfactory bulb is more complex than at first thought.

As a consequence of this study we found a rather surprising result in that the antidromic activation of the output cells of the olfactory bulb led to increased Fos expression by these cells (Chapter 4). It has been previously thought that the induction of Fos requires synaptic activation rather than simply increased spike activity. For the olfactory bulb, at least, this does not seem to hold true and this may be unique to the olfactory bulb mitral cells.

Discharge patterns of olfactory neurones

A wealth of information has been gathered on the synaptic actions and inhibitory circuits of the olfactory bulb but surprisingly little has been reported on the discharge patterns of the bulbar neurones. We have conducted an in depth study of the phasic activity exhibited by mitral cells and discovered that there are three levels of bursting displayed at different timescales, superimposed on one another. The most obvious phasic activity is what I have termed the gross pattern of activity, this is seen in all mitral cells and can be either distinct bursts of activity clearly separated by periods of silence or bursts of increased activity against a high background activity

but with clear periods of quiescence between the bursts. This phasic activity was not seen in the granule cell recordings. The periodicity of this pattern is much too long to be accounted for by a respiratory drive and is more likely to originate from the oscillatory nature of the synaptic connections between the mitral and granule cell reciprocal synapse. However, both the granule and mitral cells displayed a rhythmic activity under the influence of respiration but this was within the overall discharge pattern. The third type of bursting pattern found was only displayed by a proportion of the mitral cells, which we have termed 'bimodal' mitral cells on the account of them having two modes of firing; a high frequency firing in the range 100-250Hz and a lower rate of firing in the range 0-100Hz. Analysis of the instantaneous frequency of these cells showed a very interesting feature, the high frequency firing did not come into effect until approximately 30 seconds after the start of the burst. Since it has been shown that mitral cells are capable of back-propagation along their dendrites and furthermore, that the site of action potential initiation can be shifted to the dendritic compartment, it was postulated that the high frequency firing was from a dendritic source. This is the first report of such activity in the mitral cells and demands further attention to elucidate the precise nature of this high frequency mode of firing.

Influence of opiates in the olfactory system

It has been mentioned in the text of Chapter 5 that the administration of MOR delays the normal progression of parturition by inhibiting oxytocin release from the magnocellular cells of the SON. The olfactory system was considered as a potential target for inhibition by MOR at the time of parturition as the olfactory bulb is highly active at this time and is a determinant for the 'normal' expression of maternal behaviour. However, we found that the inhibitory effects of MOR in the olfactory system are relatively weak when compared to the effects seen in the SON and were therefore not capable of any significant affect on the delay of parturition evoked by MOR. We did see a subtle effect of MOR on the high frequency firing described

above. The administration of MOR led to the selective inhibition of the high frequency firing that was not naloxone-reversible. Very little has been studied concerning the actions of opiates in the olfactory bulb and is an area which requires further research.

Overall, the results from this thesis demonstrate that the cells of the olfactory bulb are involved in sophisticated interactions with each other through both intra- and inter-bulbar neural circuits and this leads to a complex discharge output from the olfactory bulb and the emerging dendritic properties of the mitral cells is a field of research that should be investigated more closely.

PUBLICATIONS

Jayne Bramley and Gareth Leng (1998). Effects of morphine on the firing rate of olfactory bulb mitral cells. European Journal of Neuroscience, 10 (Suppl.10), 298, 116.29P

Jayne Bramley and Gareth Leng (1999). Firing patterns of olfactory bulb mitral cells. Journal of Physiology Proceedings, 520, 51P

OTHER PRESENTATION

(included in meeting abstract book)

J. Bramley, C. Fiddler, A. Douglas and G. Leng. Expression of Fos positive nuclei in the rat brain following electrical stimulation of the lateral olfactory tract *in vivo*. Poster presentation at the XXVIIth Meeting of Experimental Neuroendocrinology Society in Lille, France, September 2-5, 1998.

Firing patterns of olfactory bulb mitral cells

Jayne Bramley and Gareth Leng

Department of Biomedical Sciences, University Medical School, Edinburgh EH8 9AG

The primary dendrites of mitral cells synapse with the olfactory nerve and their axons form the lateral olfactory tract (LOT), making the mitral cell the first relay neurone in the olfactory system. The olfactory bulb (OB) has a highly organized structure and provides a relatively simple system in which to study synaptic interactions between dendrites. The mitral cell has large, branching, secondary dendrites that interact with neighbouring mitral cells and local interneurones. These dendritic interactions lead to lateral and reciprocal inhibition, which may be important in the generation of the firing pattern typical of mitral cells. This study looks at the characteristic patterns of mitral cell firing and compares extracellular recordings obtained from *in vivo* and *in vitro* preparations.

Female Sprague–Dawley rats (250–300 g) were anaesthetized with urethane (I.P. 1·25 g kg^{-1} body weight) for all the *in vivo* experiments. A bipolar stimulating electrode was positioned stereotaxically over the LOT to allow antidromic identification of mitral cells. The ipsilateral OB was exposed for the placement of the recording electrode in the mitral cell layer (MCL). The activities of 61 mitral cells were recorded. Of these, 90% displayed a marked, slow, cyclic firing pattern, with peaks of activity at 30–50 spikes s^{-1} occurring with a period of 200–400 s. During the peaks of activity, analysis of interspike intervals revealed two clear modes, one reflecting high-frequency clusters of spikes occurring at an interval range of 4–8 ms, the other reflecting intervals between spikes ranging from 10 to 60 ms. This pattern of firing was not seen in the granule cells. Simultaneous recordings of pairs of mitral cells show there is a weak correlation of burst activity between mitral cells. This suggests the rhythmic firing pattern is not due entirely to an external influence.

For *in vitro* experiments, rats (50–100 g) were anaesthetized with halothane before decapitation and removal of the brain tissue. Olfactory slices were cut in the horizontal plane at a thickness of 400 μm. The slices were left to incubate in oxygenated medium for 1 h before recording began. In comparison with *in vivo* experiments, there were fewer spontaneously active mitral cells. Those that did show spontaneous activity fired in the range 15–20 spikes s^{-1}. They did not fire in the same slow, cyclic fashion as they did *in vivo*, and analysis of interspike intervals did not reveal two modes of firing.

In conclusion, *in vivo* data show mitral cells fire in a characteristic pattern that seems to be generated locally within the bulb. There is a difference in the firing patterns recorded from *in vivo* and *in vitro* preparations. This could be due to the loss of mitral cell dendritic branches when making the slice.

116.29 EFFECTS OF MORPHINE ON THE FIRING RATE OF OLFACTORY BULB MITRAL CELLS

Jayne Bramley* and Gareth Leng Dept of Physiology, University Medical School, Edinburgh, EH8 9AG, U.K

Axons of mitral cells form the lateral olfactory tract (LOT), an efferent projection connecting the olfactory bulb (OB) to regions such as the hypothalamus, amygdala and hippocampus. In order to study the *in vivo* firing characteristics of mitral cells, extracellular recordings were made from single neurones in urethane-anaesthetised female Sprague-Dawley rats. Modulation of mitral cell activity by opioid agonists was also investigated by the intra venous administration of morphine (10, 100, and 500μg/kg). A stimulating electrode was positioned stereotaxically over the LOT to allow antidromic identification of mitral cells. The ipsilateral OB was exposed for placement of the recording electrode in the mitral cell layer. In this preparation, mitral cells discharge characteristically with a marked, slow, cyclic pattern, with peaks of activity at 30-50 spikes/s occuring with a period of 200-400s. During the peaks of activity, analysis of interspike intervals revealed two clear modes, one reflecting high frequency clusters of spikes occuring at intervals of 4-8ms, the other reflecting intervals between clusters of 10-60ms. Following application of morphine there was a consistent, selective suppression of the high frequency clustering of cells.

Bibliography

ADLER, E.M., AUGUSTINE, G.J., DUFFY, S.N. & CHARLTON, M.P. (1991). Alien intracellular calcium chelators attenuate neurotransmitter release at the squid giant synapse. *J.Neurosci.* **11(6)**, 1496-5077.

ADRIAN, E.D. (1950). On the electrical activity of the mammalian olfactory bulb. *Electroencephalogr.Clin.Neurophysiol.* **2**, 377-388.

ANTON, P.S., GRANGER, R. & LYNCH, G. (1993). Simulated dendritic spines influence reciprocal synaptic strengths and lateral inhibition in the olfactory bulb. *Brain Res.* **628 (1-2)**, 157-655.

ARANEDA, S., GAMRANI, H., FONT, C., CALAS, A., PUJOL, J.F. & BOBILLIER, P. (1980). Retrograde axonal transport following injection of [3H]-serotonin into the olfactory bulb. II. Radioautographic study. *Brain Res.* **196 (2)**, 417-427.

ARMSTRONG, W.E., WARACH, S., HATTON, G.I. & MCNEILL, T.H. (1980). Subnuclei in the rat hypothalamic paraventriculer nucleus: A cytoarchitectual, horseradish peroxidase and immunocytochemical analysis. *Neurosci.* **5**, 1931-1958.

ARMSTRONG, W.E., SCHOLER, J. & MCNEILL, T.H. (1982). Immunocytochemical, Golgi and electron microscopic characterization of putative dendrites in the ventral glial lamina of the rat supraoptic nucleus. *Neurosci.* **7**, 679-694.

ARMSTRONG, W.E. (1995). Morphological and electrophysiological classification of hypothalamic supraoptic neurons. [Review] [388 refs]. *Prog.Neurobiol.* **47 (4-5)**, 291-339.

ARONIADOU-ANDERJASKA, V., ENNIS, M. & SHIPLEY, M.T. (1999). Dendrodendritic recurrent excitation in mitral cells of the rat olfactory bulb. *J Neurophysiol.* **82 (1)**, 489-494.

ARVIDSSON, U., RIEDL, M., CHAKRABARTI, S., LEE, J.-H., NAKANO, A.H., DADO, R., LOH, H., LAW, P.-Y., WESSENDORF, M. & ELDE, R. (1995). Distribution and targeting of a mu-opioid receptor (MOR1) in brain and spinal cord. *J.Neurosci.* **15**, 3328-3341.

AUSTIN, L., RECASENS, M. & MANDEL, P. (1979). GABA in the olfactory bulb and olfactory nucleus of the rat: the distribution of gamma-aminobutyric acid, glutamic acid decarboxylase, GABA transaminase and succinate semialdehyde dehydrogenase. *J Neurochem.* **32 (5)**, 1473-1477.

AVERY, R.B. & JOHNSTON, D. (1996). Multiple channel types contribute to the low-voltage-activated calcium current in hippocampal CA3 pyramidal neurons. *J Neurosci.* **16 (18)**, 5567-5582.

BAIR, W., KOCH, C., NEWSOME, W. & BRITTEN, K. (1994). Power spectrum analysis of bursting cells in area MT in the behaving monkey. *J Neurosci.* **14 (5 Pt 1)**, 2870-2892.

BAKER, H., KAWANO, T., MARGOLIS, F.L. & JOH, T.H. (1983). Transneuronal regulation of tyrosine hydroxylase expression in the olfactory bulb of mouse and rat. *J.Neurosci.* **3**, 69-78.

BARKER, J.L., CRAYTON, J.W. & NICOLL, R.A. (1971). Noradrenaline and acetylcholine responses of supraoptic neurosecretory cells. *J Physiol.(Lond)* **218 (1)**, 19-32.

BARTOLOMEI, J.C. & GREER, C.A. (1998). The organization of piriform cortex and the lateral olfactory tract following the loss of mitral cells in PCD mice. *Exp Neurol 1998 Dec;154(2):537-50* **154 (2)**, 537-550.

BAUMGARTEN, R., BLOOM, F.E., OLIVER, A.P. & SALMOIRAGHI, G.C. (1963). Response of individual olfactory nerve cells to microelectrophoretically administered chemical substances. *Pflügers Arch.ges.Physiol.* **277**, 125-140.

BERKOWICZ, D.A., TROMBLEY, P.Q. & SHEPHERD, G.M. (1994). Evidence for glutamate as the olfactory receptor cell neurotransmitter. *J Neurophysiol.* **71 (6)**, 2557-2561.

BICKNELL, R.J., LENG, G., LINCOLN, D.W. & RUSSELL, J.A. (1988). Naloxone excites oxytocin neurones in the supraoptic nucleus of lactating rats after chronic morphine treatment. *J.Physiol.* **396**, 297-317.

BICKNELL, R.J., LENG, G., RUSSELL, J.A., DYER, R.G., MANSFIELD, S. & ZHAO, B.G. (1988). Hypothalamic opioid mechanisms controlling oxytocin neurones during parturition. *Brain Res.Bull.* **20**, 743-749.

BISCHOFBERGER, J. & SCHILD, D. (1995). Different spatial patterns of [Ca2+] increase caused by N- and L-type Ca2+ channel activation in frog olfactory bulb neurones. *J Physiol (Lond)* **487 (Pt 2)**, 305-317.

BISCHOFBERGER, J. & JONAS, P. (1997). Action potential propagation into the presynaptic dendrites of rat mitral cells. *J Physiol.(Lond)* **504 (Pt 2)**, 359-365.

BLOOM, F.E., COSTA, E. & SALMOIRAGHI, G.C. (1964). Analysis of individual rabbit olfactory bulb neuron responses to the microelectrophoresis of acetylcholine, norepinephrine and serotonin synergists and antagonists. *J.Pharmac.exp.Ther.* **146**, 16-23.

BLOOM, F.E., HOFFER, B.J. & SIGGINS, G.R. (1971). Studies on norepinephrine-containing afferents to Purkinje cells of art cerebellum. I. Localization of the fibers and their synapses. *Brain Res.* **25 (3)**, 501-521.

BOEKHOFF, I., TAREILUS, E., STROTMANN, J. & BREER, H. (1990). Rapid activation of alternative second messenger pathways in olfactory cilia from rats by different odorants. *EMBO J* **9(8)**, 2453-2488.

BRADFORD, H.F. & RICHARDS, C.D. (1976). Specific release of endogenous glutamate from piriform cortex stimulated in vitro. *Brain Res.* **105 (1)**, 168-172.

BREER, H., BOEKHOFF, I. & TAREILUS, E. (1990). Rapid kinetics of second messenger formation in olfactory transduction. *Nature* **345**, 65-68.

BRENELLS, A.B. (1974). Spontaneous and neurally evoked release of labelled noradrenaline from rabbit olfactory bulbs *in vitro*. *J.Physiol., Lond.* **240**, 279-293.

BRENNAN, P., KABA, H. & KEVERNE, E.B. (1990). Olfactory recognition: a simple memory system. *Science* **250**, 1223-1226.

BRENNAN, P. & KEVERNE, B. (1997). Neural mechanisms of mammalian olfactory learning. *Prog.Neurobiol.* **51**, 457-481.

BROADWELL, R.D. (1975). Olfactory relationships of the telencephalon and diencephalon in the rabbit. II. An autoradiographic and horseradish peroxidase study of the efferent connections of the anterior olfactory nucleus. *J.comp.Neurol.* **164**, 389-410.

BROADWELL, R.D. & JACOBOWITZ, D.M. (1976). Olfactroy relationships of the telencephalon and diencephalon in the rabbit-III. The ipsilateral centrifugal fibers to the olfactory bulbar and retrobulbar formations. *J.comp.Neurol.* **170**, 321-346.

BROCK, L.G., COOMBS, J.S. & ECCLES, J.C. (1953). Intracellular recording from antidromically activated motorneurones. *J.Physiol.* **122**, 429-461.

BROWN, C.H., LUDWIG, M. & LENG, G. (1998). Kappa-opioid regulation of neuronal activity in the rat supraoptic nucleus *in vivo*. *J.Neurosci.* **18**, 9480-9488.

BROWN, C.H., RUSSELL, J.A. & LENG, G. (2000). Opioid modulation of magnocellular neurosecretory cell activity. *Neurosci.Res.* **36**, 97-120.

BRUCE, H. (1959). An exteroceptive block to pregnancy in the mouse. *Nature* **184**, 105

BRUNJES, P.C. (1994). Unilateral naris closure and olfactory system development. *Brain Res.Rev.* **19**, 146-160.

BUCK, L. & AXEL, R. (1991). A novel multigene family may encode odorant receptors: a molecular basis for odor recognition. *Cell* **65 (1)**, 175-187.

BUFLER, J., ZUFALL, F., FRANKE, C. & HATT, H. (1992). Patch-clamp recordings of spiking and nonspiking interneurons from rabbit olfactory bulb slices: GABA- and other transmitter receptors. *J Comp Physiol [A]* **170 (2)**, 153-159.

BUFLER, J., ZUFALL, F., FRANKE, C. & HATT, H. (1992). Patch-clamp recordings of spiking and nonspiking interneurons from rabbit olfactory bulb slices: membrane properties and ionic currents. *J Comp Physiol [A]* **170 (2)**, 145-152.

BUFLER, J., OPITZ, T. & HATT, H. (1993). Electrophysiological and morphological properties of granule cells: patch-clamp recordings of newborn rabbit olfactory bulb slices. *Neurosci Lett.* **161 (2)**, 129-132.

BUONVISO, N. & CHAPUT, M.A. (1990). Response similarity to odors in olfactory bulb output cells presumed to be connected to the same glomerulus: electrophysiological study using simultaneous single-unit recordings. *J.Neurophysiol.* **63 (3)**, 447-454.

BUONVISO, N., CHAPUT, M.A. & SCOTT, J.W. (1991). Mitral cell-to-glomerulus connectivity: an HRP study of the orientation of mitral cell apical dendrites. *J.comp.Neurol.* **307 (1)**, 57-64.

BUONVISO, N., CHAPUT, M.A. & BERTHOMMIER, F. (1992). Temporal pattern analyses in pairs of neighboring mitral cells. *J.Neurophysiol.* **68 (2)**, 417-424.

BUONVISO, N., CHAPUT, M.A. & BERTHOMMIER, F. (1996). Similarity of granular-induced inhibitory periods in pairs of neighboring mitral/tufted cells. *J.Neurophysiol.* **76 (4)**, 2393-2401.

BURD, G.D., DAVIS, B.J. & MACRIDES, F. (1982). Ultrastructural identification of substance P immunoreactive neurons in the main olfactory bulb of the hamster. *Neuroscience* **7**, 2697-2704.

BURGESS, K.M., JENKIN, G., RALPH, M.M. & THORBURN, G.D. (1992). Effect of the antiprogestin RU486 on uterine sensitivity to oxytocin in ewes in late pregnancy. *J.Endocrinology* **134**, 353-360.

CALAMANDREI, G., WILKINSON, L.S. & KEVERNE, E.B. (1992). Olfactory recognition of infants in laboratory mice: role of noradrenergic mechanisms. *Physiology & Behavior* **52 (5)**, 901-907.

CASABONA, G., CATANIA, M.V., STORTO, M., FERRARIS, N., PERROTEAU, I., FASOLO, A., NICOLETTI, F. & BOVOLIN, P. (1998). Deafferentation up-regulates the expression of the mGlu1a metabotropic glutamate receptor protein in the olfatory bulb. *Eur.J.Neurosci.* **10**, 771-776.

CECCATELLI, S., VILLAR, M.J., GOLDSTEIN, M. & HOKFELT, T. (1989). Expression of c-fos immunoreactivity in transmitter-characterized neurones after stress. *Proc.Natl.Acad.Sci.U S A* **86**, 9569-9573.

CHEN, W.R. & SHEPHERD, G.M. (1997). Membrane and synaptic properties of mitral cells in slices of rat olfactory bulb. *Brain Research* **745**, 189-196.

CHEN, W.R., MIDTGAARD, J. & SHEPHERD, G.M. (1997). Forward and backward propagation of dendritic impulses and their synaptic control in mitral cells. *Science* **278**, 463-467.

CHILDERS, S.R. (1991). Opioid receptor-coupled second messenger systems. *Life Sci.* **48**, 1991-2003.

COHEN, D.R. & CURRAN, T. (1989). The stucture and function of the fos proto-oncogene. *Crit.Rev.Oncog.* **1**, 65-88.

COOMBS, J.S., ECCLES, J.C. & FATT, P. (1955). The electrical properties of the motorneurone membrane. *J.Physiol.* **130**, 291-325.

COOMBS, J.S., CURTIS, D.R. & ECCLES, J.C. (1957). The interpretation of spike potentials of motorneurones. *J.Physiol.* **139**, 198-231.

COTMAN, C.W. & IVERSON, L.L. (1987). Excitatory amino acids in the brain-focus on NMDA receptors. *Trends Neurosci.* 7, 263-265.

CURRAN, T. & FRANZA, B.R.J. (1988). Fos and Jun: the AP-1 connection. *Cell* **55**, 395-397.

DAHLSTRÖM, A. & FUXE, K. (1964). Evidence for the existence of monoamine containing neurons in the central nervous system-I. Demonstration of monoamines in the cell bodies of brain stem neurones. *Acta.physiol.scand.* **62, Suppl. 232**, 1-55.

DAHLSTRÖM, A., FUXE, K., OLSON, L. & UNGERSTEDT, U. (1965). On the distribution and possible function of monoamine nerve terminals in the olfactory bulb of the rabbit. *Life Sci.* **4**, 2071-2074.

DAVIS, B.J., MACRIDES, F., YOUNGS, W.M., SCHNEIDER, S.P. & ROSENE, D.L. (1978). Efferents and centrifugal afferents of the main and accessory olfactory bulbs in the hamster. *Brain Res.Bull.* **3**, 59-72.

DAVIS, B.J. & MACRIDES, F. (1981). The organization of centrifugal projections from the anterior olfactory nucleus, ventral hippocampal rudiment, and piriform cortex to the main olfactory bulb in the hamster: an autoradiographic study. *J.comp.Neurol.* **203**, 475-493.

DAVIS, B.J., BURD, G.D. & MACRIDES, F. (1982). Localization of methionine-enkephalin, substance P and somatostatin immunoreactivities in the main olfactory bulb of the hamster. *J.comp.Neurol.* **204**, 377-383.

DELFS, J.M., KONG, H., MESTEK, A., CHEN, Y., YU, L., REISINE, T. & CHESSELET, M.-F. (1994). Expression of mu opioid receptor mRNA in rat brain. *J.comp.Neurol.* **345**, 46-68.

DEOLMOS, J., HARDY, H. & HEIMER, L. (1978). The afferent connections of the main and the accessory olfactory bulb formations in the rat: and experimental HRP-study. *J.comp.Neurol.* **181**, 213-244.

DESMAISONS, D., VINCENT, J.D. & LLEDO, P.M. (1999). Control of action potential timing by intrinsic subthreshold oscillations in olfactory bulb output neurons. *J.Neurosci.* **19**, 10727-10737.

DICKINSON, C. & KEVERNE, E.B. (1988). Importance of noradrenergic mechanisms in the olfactory bulbs for the maternal behaviour of mice. *Physiology & Behavior* **43 (3)**, 313-316.

DOUGLAS, A.J., DYE, S., LENG, G., RUSSELL, J.A. & BICKNELL, R.J. (1993). Endogenous opioid regulation of oxytocin secretion through pregnancy in the rat. *J.Neuroendocrinology* **5**, 307-314.

DOUGLAS, A.J., NEUMANN, I., MEEREN, H.K., LENG, G., JOHNSTONE, L.E., MUNRO, G. & RUSSELL, J.A. (1995). Central endogenous opioid inhibition of supraoptic oxytocin neurons in pregnant rats. *Journal of Neuroscience* **15 (7 Pt 1)**, 5049-5057.

DRAGUNOW, M., GOULDING, M., FAULL, R.L., RALPH, R., MEE, E. & FRITH, R. (1990). Induction of c-fos mRNA and protein in neurons and glia after traumatic brain injury: pharmacological characteristics. *Exp.Neurol.* **107**, 236-248.

DUCHAMP-VIRET, P. & DUCHAMP, A. (1993). GABAergic control of odour-induced activity in the frog olfactory bulb: possible GABAergic modulation of granule cell inhibitory action [published erratum appears in Neuroscience 1994 Jan;58(2):337-40]. *Neuroscience* **56 (4)**, 905-914.

DUNLAP, K., LUEBKE, J.I. & TURNER, T.J. (1995). Exocytotic Ca2+ channels in mammalian central neurons. *Trends Neurosci.* **18 (2)**, 89-98.

ECCLES, J.C. (1957). *The Physiology of Nerve Cells*. Baltimore: John Hopkins.

EECKMAN, F.H. & FREEMAN, W.J. (1990). Correlations between unit firing and EEG in the rat olfactory system. *Brain Res.* **528 (2)**, 238-244.

ELAAGOUBY, A., RAVEL, N. & GERVAIS, R. (1991). Cholinergic modulation of excitability in the rat olfactory bulb: effect of local application of cholinergic agents on evoked field potentials. *Neuroscience* **45 (3)**, 653-662.

ENNIS, M., ZIMMER, L.A. & SHIPLEY, M.T. (1996). Olfactory nerve stimulation activates rat mitral cells via NMDA and non-NMDA receptors in vitro. *Neuroreport* **7**, 989-992.

EZEH, P.I., WELLIS, D.P. & SCOTT, J.W. (1993). Organization of inhibition in the rat olfactory bulb external plexiform layer. *J.Neurophysiol.* **70 (1)**, 263-274.

EZEH, P.I., DAVIS, L.M. & SCOTT, J.W. (1995). Regional distribution of rat electroolfactogram. *J.Neurophysiol.* **73 (6)**, 2207-2220.

FABER, T., JOERGES, J. & MENZEL, R. (1999). Associative learning modifies neural representations of odors in the insect brain [see comments]. *Nat.Neurosci.* **2 (1)**, 74-78.

FALLON, J.H. & MOORE, R.Y. (1978). Catecholamine innervation of the basal forebrain. III. olfactory bulb, anterior olfactory nucleus, olfactory tubercle and piriform cortex. *J.comp.Neurol.* **180**, 533-544.

FENELON, V.S., POULAIN, D.A. & THEODOSIS, D.T. (1993). Oxytocin neuron activation and Fos expression: a quantitative immunocytochemical analysis of the effect of lactation, parturition, osmotic and cardiovascular stimulation. *Neurosci.* **53**, 77-89.

FENELON, V.S. & HERBISON, A.E. (1996). Plasticity in $GABA_A$ receptor subunit mRNA expression by hypothalamic magnocellular neurones in the adult rat. *J.Neurosci.* **16**, 4872-4880.

FERRARIS, N., PERROTEAU, I., DEMARCHIS, S., FASOLO, A. & BOVOLIN, P. (1997). Glutamatergic deafferentation of olfactory bulb modulates the expression of mGluR1a mRNA. *Neuroreport* **8 (8)**, 1949-1953.

FINGER, T.E. & SILVER, W.L. (1987). *Neurobiology of Taste and Smell.* John Wiley & Sons.

FINLEY, J.C.W., MADERDRUT, J.L., ROGER, L.J. & PETRUSZ, P. (1981). The immunocytochemical localization of somatostatin-containing neurons in the rat central nervous system. *Neuroscience* **6**, 2173-2192.

FREEMAN, W.J. (1972). Depth recording of averaged evoked potential of olfactory bulb. *Journal of Neurophysiology* **35 (6)**, 780-796.

FREEMAN, W.J. (1975). *Mass action in the Nervous System.* New York: Academic Press.

FRIEDRICH, R.W. & KORSCHING, S.I. (1996). Representation of odorant information by spatial afferent activity patterns in the zebrafish olfactory bulb. *Soc.Neurosci.Abstr.* **22**, 1072

FUORTES, M.G.F., FRANK, K. & BECKER, M.C. (1957). Steps in the production of motorneuron spikes. *J.gen.Physiol.* **40**, 735-752.

GARCIA-DIAZ, D.E., JIMENEZ-MONTUFAR, L.L., GUEVARA-AGUILAR, R., WAYNER, M.J. & ARMSTRONG, D.L. (1988). Olfactory and visceral projections to the nucleus of the solitary tract. *Physiol Behav* **44 (4-5)**, 619-624.

GIOVANNELLI, L., SHIROMANI, P.J., JIRIKOWSKI, G.F. & BLOOM, F.E. (1990). Oxytocin neurons in the rat hypothalamus exhibit c-fos immunoreactivity upon osmotic stress. *Brain Res.* **531**, 299-303.

GIOVANNELLI, L., SHIROMANI, P.J., JIRIKOWSKI, G.F. & BLOOM, F.E. (1992). Expression of c-fos protein by immunohistochemically identified oxytocin neurones in the rat hypothalamus upon osmotic stimulation. *Brain Res.* **588**, 41-48.

GODFREY, D.A., ROSS, C.D., CARTER, J.A., LOWRY, O.H. & MATCHINSKY, F.M. (1980). Effect of intervening lesions on amino acid distributions in rat olfactory cortex and olfactory bulb. *J.Histochem.Cytochem.* **28**, 1157-1169.

GONZALEZ-ESTRADA, M.T. & FREEMAN, W.J. (1980). Effects of carnosine on olfactory bulb EEG, evoked potentials and DC potentials. *Brain Res.* **202 (2)**, 373-386.

GRAY, C.M., KOENIG, P., ENGEL, A.K. & SINGER, W. (1989). Oscillatory responses in cat visual cortex exhibited inter-columnar synchronization which reflects global stimulus properties. *Nature.* **338**, 334-337.

GRAZIADEI, P.P. & MONTI, G.G. (1979). Neurogenesis and neuron regeneration in the olfactory system of mammals. III. Deafferentation and reinnervation of the olfactory bulb following section of the fila olfactoria in rat. *J Neurocytol.* **9 (2)**, 145-162.

GRAZZINI, E., GULLION, G., MOUILLAC, B. & ZINGG, H.H. (1998). Inhibition of oxytocin receptor function by direct binding of progesterone. *Nature* **392**, 509-512.

GREEN, J.D., MANCIA, M. & VON BAUMGARTEN, R. (1962). Recurrent inhibition in the olfactory bulb I. Effects of antidromic stimulation of the lateral olfactory tract. *J.Neurophysiol.* **25**, 467-488.

GREER, C.A. (1987). Golgi analyses of dendritic organization among denervated olfactory bulb granule cells. *J.comp.Neurol.* **257 (3)**, 442-452.

GRUDT, T.J. & WILLIAMS, J.T. (1995). Opioid receptors and the regulation of ion conductances. *Rev.Neurosci.* **6**, 279-286.

GUEVARA-GUZMAN, R., GARCIA-DIAZ, D.E., SOLANO-FLORES, L.P., WAYNER, M.J. & ARMSTRONG, D.L. (1991). Role of the paraventricular nucleus in the projection from the nucleus of the solitary tract to the olfactory bulb. *Brain Res.Bull.* **27 (3-4)**, 447-450.

GUTHRIE, K.M., ANDERSON, A.J., LEON, M. & GALL, C. (1993). Odor-induced increases in c-fos mRNA expression reveal an anatomical "unit" for odor processing in olfactory bulb. *Proc.Natl.Acad.Sci.U S A* **90 (8)**, 3329-3333.

HABERLY, L.B. & PRICE, J.L. (1977). The axonal projection patterns of the mitral and tufted cells of the olfactory bulb in the rat. *Brain Res.* **129 (1)**, 152-157.

HAGIWARA, S. & BYERLY, L. (1981). Calcium channel. *Ann.Rev.Neurosci.* **4**, 69-125.

HALARIS, A.E., JONES, B.E. & MOORE, R.Y. (1976). Axonal transport in serotonin neurons of the midbrain raphe. *Brain Res.* **107 (3)**, 555-574.

HALASZ, N., LJUNGDAHL, A., HOKFELT, T., JOHANSSON, O., GOLDSTEIN, M., PARK, D. & BIBERFELD, P. (1977). Transmitter histochemistry of the rat olfactory bulb. I. Immunohistochemical localization of monoamine synthesizing enzymes. Support for intrabulbar, periglomerular dopamine neurons. *Brain Res.* **126 (3)**, 455-474.

HALASZ, N., LJUNGDAHL, A. & HOKFELT, T. (1978). Transmitter histochemistry of the rat olfactory bulb. II. Fluorescence histochemical, autoradiographic and electron microscopic localization of monoamines. *Brain Res.* **154 (2)**, 253-271.

HALASZ, N. & SHEPHERD, G.M. (1983). Neurochemistry of the vertebrate olfactory bulb. *Neuroscience* **10 (3)**, 579-619.

HALÁSZ, N., PARRY, D.M., BLACKETT, N.M., LJUNGDAHL, Å. & HÖKFELT, T. (1981). (^{3}H) γ-aminobutyrate autoradiography of the rat olfactory bulb: hypothetical grain analysis of the distribution of silver grains. *Neuroscience* **6**, 473-479.

HAMAMURA, M., NUNEZ, D.J., LENG, G., EMSON, P.C. & KIYAMA, H. (1992). c-fos may code for a common transcription factor within the hypothalamic neural circuits involved in osmoregulation. *Brain Res.* **572**, 42-51.

HANEY, M. & MICZEK, K.A. (1989). Morphine effects on maternal aggression, pup care and analgesia in mice. *Psychopharmacology* **98 (1)**, 68-74.

HATTON, G.I., HUTTON, U.E., HOBLITZELL, E.R. & ARMSTRONG, W.E. (1976). Morphological evidence for two populations of magnocellular elements in the rat paraventricular nucleus. *Brain Res.* **108**, 187-193.

HATTON, G.I. & YANG, Q.Z. (1989). Supraoptic nucleus afferents from the main olfactory bulb--II. Intracellularly recorded responses to lateral olfactory tract stimulation in rat brain slices. *Neuroscience* **31 (2)**, 289-297.

HATTON, G.I. (1990). Emerging concepts of structure-function dynamics in adult brain: the hypothalamo-neurohypophysial system. [Review] [551 refs]. *Progress in Neurobiology* **34 (6)**, 437-504.

HATTON, G.I. & YANG, Q.Z. (1990). Activation of excitatory amino acid inputs to supraoptic neurons. I. Induced increases in dye-coupling in lactating, but not virgin or male rats. *Brain Res.* **513 (2)**, 264-269.

HERKENHAM, M. & PERT, C.B. (1982). Light microscopic localization of brain opiate receptors: a general autoradiographic method which preserves tissue quality. *J.Neurochem* **2**, 1129-1149.

HIRSCH, J.D. & MARGOLIS, F.L. (1980). Influence of unilateral olfactory bulbectomy on opiate and other binding sites in the contralateral bulb. *Brain Res.* **199 (1)**, 39-47.

HOFFMAN, G.E., DAVIS, B.J. & MACRIDES, F. (1979). LHRH perikarya send axons to the olfactory bulb in the hamster. *Soc.Neurosci.Abs.* **5**, 528

HOFFMAN, G.E., SMITH, M.S. & VERBALIS, J.G. (1993). c-Fos and related immediate early gene products as markers of activity in neuroendocrine systems [Review]. *Frontiers in neuroendocrinology* **14**, 173-213.

HÖKFELT, T., KELLERTH, J.O., NILSSON, G. & PERNOW, B. (1975). Substance P: localization in the central nervous system and in some primary sensory neurones. *Science N.Y* **190**, 889-890.

INAGAKI, S., SENBA, E., SHIOSAKA, S., TAKAGI, H., KAWAI, Y., TAKATSUKI, K., SAKANAKA, M., MATSUZAKI, T. & TOHYAMA, M. (1981). Regional distribution of substance P-like immunoreactivity in the frog brain and spinal cord: immunohistochemical analysis. *J.comp.Neurol.* **201**, 243-254.

INAGAKI, S., SAKANAKA, M., SHIOSAKA, S., SENBA, E., TAKATSUKI, K., KAWAI, Y., MINAGAWA, H., TOHYAMA, M. & TAKAGI, H. (1982). Ontogeny of substance P-containing neuron system of the rat: immunohistochemical analysis-I. Forebrain and upper brain stem. *Neuroscience* **7**, 251-277.

ISAACSON, J.S. & STROWBRIDGE, B.W. (1998). Olfactory reciprocal synapses: dendritic signaling in the CNS. *Neuron* **20 (4)**, 749-761.

JACKOWSKI, A., PARNAVELAS, J.G. & LIEBERMAN, A.R. (1978). The reciprocal synapse in the external plexiform layer of the mammalian olfactory bulb. *Brain Res.* **159 (1)**, 17-28.

JAHR, C.E. & NICOLL, R.A. (1982). Noradrenergic modulation of dendrodendritic inhibition in the olfactory bulb. *Nature* **297**, 227-229.

JAHR, C.E. & NICOLL, R.A. (1982). An intracellular analysis of dendrodendritic inhibition in the turtle in vitro olfactory bulb. *J.Physiol.(Lond)* **326**, 213-234.

JENNES, L. & STUMPF, W.E. (1980). LHRH-systems in the brain of the golden hamster. *Cell Tissue Res.* **209**, 239-256.

JIA, C., CHEN, W.R. & SHEPHERD, G.M. (1999). Synaptic organization and neurotransmitters in the rat accessory olfactory bulb. *J.Neurophysiol.* **81 (1)**, 345-355.

JIANG, M.R., GRIFF, E.R., ENNIS, M., ZIMMER, L.A. & SHIPLEY, M.T. (1996). Activation of locus coeruleus enhances the responses of olfactory bulb mitral cells to weak olfactory nerve input. *J.Neurosci.* **16**, 6319-6329.

JOHNSTON, D., MAGEE, J.C., COLBERT, C.M. & CRISTIE, B.R. (1996). Active properties of neuronal dendrites. *Annu Rev Neurosci 1996;19:165-86* **19**, 165-186.

JOHNSTONE, L.E., BROWN, C.B., MEEREN, H.K.M., VUIJST, C.L., BROOKS, P.J., LENG, G. & RUSSELL, J.A. (2000). Local morphine withdrawal increases *c-fos* gene, Fos protein, and oxytocin gene expression in hypothalamic magnocellular neurosecretory cells. *J. Neuroendocrinology*. **20 (3)**, 1272-1280.

JOURDAN, F. (1982). Spatial dimension in olfactory coding: a representation of the 2- deoxyglucose patterns of glomerular labeling in the olfactory bulb. *Brain Res.* **240 (2)**, 341-344.

KABA, H., ROSSER, A. & KEVERNE, B. (1989). Neural basis of olfactory memory in the context of pregnancy block. *Neuroscience* **32 (3)**, 657-662.

KABA, H., HAYASHI, Y., HIGUCHI, T. & NAKANISHI, S. (1994). Induction of an olfactory memory by the activation of a metabotropic glutamate receptor. *Science* **265**, 262-264.

KANDEL, E.R., SPENCER, W.A. & BRINLEY JR, F.J. (1961). Electrophysiology of hippocampal neurons I. Sequential invasion and synaptic organization. *J.Neurophysiol.* **24**, 225-242.

KANDEL, E.R. & SPENCER, W.A. (1961). Electrophysiology of hippocampal neurons II. After-potentials and repetitive firing. *J.Neurophysiol.* **24**, 243-259.

KASHIWADANI, H., SASAKI, Y.F., UCHIDA, N. & MORI, K. (1999). Synchronized oscillatory discharges of mitral/tufted cells with different molecular receptive ranges in the rabbit olfactory bulb. *J Neurophysiol 1999 Oct;82(4):1786-92* **82 (4)**, 1786-1792.

KENDRICK, K.M., LEVY, F. & KEVERNE, E.B. (1992). Changes in the sensory processing of olfactory signals induced by birth in sleep. *Science* **256**, 833-836.

KEVERNE, E.B. & DE LA RIVA, C. (1982). Pheromones in mice: reciprocal interaction between the nose and brain. *Nature* **296**, 148-150.

KEVERNE, E.B. (1988). Central mechanisms underlying the neural and neuroendocrine determinants of maternal behaviour. [Review] *Psychoneuroendocrinology* **13 (1-2)**, 127-141.

KEVERNE, E.B., LEVY, F., GUEVARA-GUZMAN, R. & KENDRICK, K.M. (1993). Influence of birth and maternal experience on olfactory bulb neurotransmitter release. *Neuroscience* **56 (3)**, 557-565.

KEVERNE, E.B. (1995). Olfactory learning. [Review] *Current Opinion in Neurobiology* **5 (4)**, 482-488.

KEVERNE, E.B. (1999). The vomeronasal organ. *Science* **286**, 716-720.

KEVETTER, G.A. & WINANS, S.S. (1981a). Connections of the corticomedial amygdala in the golden hamster. II. Efferents of the "olfactory amygdala". *J.comp.Neurol.* **197 (1)**, 99-111.

KEVETTER, G.A. & WINANS, S.S. (1981b). Connections of the corticomedial amygdala in the golden hamster. I. Efferents of the "vomeronasal amygdala". *J.comp.Neurol.* **197 (1)**, 81-98.

KOELLE, G.B. (1954). The histochemical localization of cholinesterases in the central nervous system of the rat. *J.comp.Neurol* **100**, 211-235.

KOLUNIE, J.M. & STERN, J.M. (1995). Maternal aggression in rats: effects of olfactory bulbectomy, ZnSO4- induced anosmia, and vomeronasal organ removal. *Horm.Behav.* **29 (4)**, 492-518.

KONIG, H., PONTA, H., RAHMSDORF, U., BUSCHER, M., SCHONTHAL, A., RAHMSDORF, H.J. & HERRLICH, P. (1989). Autoregulation of Fos: the dyad symmetry element as the major target of repression. *EMBO J.* **8**, 2559-2566.

KOSAKA, K., TOIDA, K., MARGOLIS, F.L. & KOSAKA, T. (1997). Chemically defined neuron groups and their subpopulations in the glomerular layer of the rat main olfactory bulb--II. Prominent differences in the intraglomerular dendritic arborization and their relationship to olfactory nerve terminals. *Neuroscience* **76 (3)**, 775-786.

KRIEGER, J. & BREER, H. (1999). Olfactory reception in invertebrates. *Science* **286**, 720-723.

KUNZE, W.A., SHAFTON, A.D., KEMM, R.E. & MCKENZIE, J.S. (1991). Effect of stimulating the nucleus of the horizontal limb of the diagonal band on single unit activity in the olfactory bulb. *Neuroscience* **40 (1)**, 21-27.

KUNZE, W.A., SHAFTON, A.D., KEMM, R.E. & MCKENZIE, J.S. (1992). Olfactory bulb output neurons excited from a basal forebrain magnocellular nucleus. *Brain Res.* **583 (1-2)**, 327-331.

KUNZE, W.A., SHAFTON, A.D., KEM, R.E. & MCKENZIE, J.S. (1992). Intracellular responses of olfactory bulb granule cells to stimulating the horizontal diagonal band nucleus. *Neuroscience* **48 (2)**, 363-369.

LANCET, D., GREER, C.A., KAUER, J.S. & SHEPHERD, G.M. (1982). Mapping of odor-related neuronal activity in the olfactory bulb by high- resolution 2-deoxyglucose autoradiography. *Proc.Natl.Acad.Sci.U S A* **79 (2)**, 670-674.

LAURENT, G. & DAVIDOWITZ, H. (1994). Encoding of olfactory information with oscillating neural assemblies. *Science* **265**, 1872-1875.

LAURENT, G. (1999). A systems perspective on early olfactory coding. *Science* **286**, 723-728.

LENG, G., MANSFIELD, S., BICKNELL, R.J., BLACKBURN, R.E., BROWN, D., CHAPMAN, C., DYER, R.G., HOLLINGSWORTH, S., SHIBUKI, K., YATES, J.O. & WAY, S. (1988). Endogenous opioid actions and effects of environmental disturbance on patrurition and oxttocin secretion in rats. *J.Reprod.Fert.* **84**, 345-356.

LENG, G., BICKNELL, R.J., BROWN, D., BOWDEN, C., CHAPMAN, C. & RUSSELL, J.A. (1994). Stimulus-induced depletion of pro-enkephalins, oxytocin and vasopressin and pro-enkephalin interaction with posterior pituitary hormone release *in vitro*. *Neuroendocrinology* **1**, 35-46.

LESTIENNE, R. & TUCKWELL, H.C. (1998). The significance of precisely replicating patterns in mammalian CNS spike trains. *Neuroscience* **82 (2)**, 315-336.

LESTIENNE, R., TUCKWELL, H.C., CHALANSONNET, M. & CHAPUT, M. (1999). Repeating triplets of spikes and oscillations in the mitral cell discharges of freely breathing rats. *Eur.J.Neurosci.* **11 (9)**, 3185-3193.

LEVY, F., POINDRON, P. & LE NEINDRE, P. (1983). Attraction and repulsion by amniotic fluids and their olfactory control in the ewe around parturition. *Physiology & Behavior* **31 (5)**, 687-692.

LEVY, F., DREIFUSS, J.J., DUBOIS-DAUPHIN, M., BERTI, M., BARBERIS, C. & TRIBOLLET, E. (1992). Autoradiographic detection of vasopressin binding sites, but not of oxytocin binding sites, in the sheep olfactory bulb. *Brain Res.* **595 (1)**, 154-158.

LEVY, F., KENDRICK, K.M., GOODE, J.A., GUEVARA-GUZMAN, R. & KEVERNE, E.B. (1995). Oxytocin and vasopressin release in the olfactory bulb of parturient ewes: changes with maternal experience and effects on acetylcholine, gamma-aminobutyric acid, glutamate and noradrenaline release. *Brain Res.* **669 (2)**, 197-206.

LICHT, G. & MEREDITH, M. (1985). Convergence of olfactory and vomeronasal pathways in the amygdala. *Chemical Senses* **10 (3)**, 459-460.

LJUNGDAHL, Å., HÖKFELT, T. & NILSSON, E. (1978). Distribution of substance P-like immunoreactivity in the central nervous system of the rat-I. Cell bodies and nerve terminals. *Neuroscience* **3**, 861-943.

LLINAS, R. & YAROM, Y. (1983). Electrophysiology of mammalian inferior olivary neurones in vitro. Different types of voltage-dependent ionic conductances. *J.Physiol.(Lond)* **315**, 549-567.

LLINAS, R. & YAROM, Y. (1983). Properties and distribution of ionic conductances generating electroresponsiveness of mammalian inferior olivary neurones in vitro. *J.Physiol.(Lond)* **315**, 569-584.

LLOYD-THOMAS, A. & KEVERNE, E.B. (1982). Role of the brain and accessory olfactory system in the block to pregnancy in mice. *Neuroscience* **7 (4)**, 907-913.

LUCKMAN, S.M., ANTONIJEVIC, I., LENG, G., DYE, S., DOUGLAS, A.J., RUSSELL, J.A. & BICKNELL, R.J. (1993). The maintenance of normal parturition in the rat requires neurohypophysial oxytocin. *J.Neuroendocrinology* **5**, 7-12.

LUCKMAN, S.M., DYBALL, R.E. & LENG, G. (1994). Induction of c-fos expression in hypothalamic magnocellular neurons requires synaptic activation and not simply increased spike activity. *J.Neurosci.* **14 (8)**, 4825-4830.

LUCKMAN, S.M. (1995). Fos expression within regions of the preoptic area, hypothalamus and brainstem during pregnancy and parturition. *Brain Res.* **669 (1)**, 115-124.

LUDWIG, M., BROWN, C.H., RUSSELL, J.A. & LENG, G. (1997). Local opioid inhibition and morphine dependence of supraoptic nucleus oxytocin neurones in the rat *in vivo*. *J.Physiol.* **505**, 145-152.

MACLEOD, K. & LAURENT, G. (1996). Distinct mechanisms for synchronization and temporal patterning of odor- encoding neural assemblies. *Science* **274**, 976-979.

MACLEOD, K., BACKER, A. & LAURENT, G. (1998). Who reads temporal information contained across synchronized and oscillatory spike trains? *Nature* **395**, 693-698.

MACLEOD, N.K. & STRAUGHAN, D.W. (1979). Responses of olfactory bulb neurones to the dipeptide carnosine. *Exp.Brain Res.* **34 (1)**, 183-188.

MACRIDES, F. & SCHNEIDER, S.P. (1982). Laminar organization of mitral and tufted cells in the main olfactory bulb of the adult hamster. *J.comp.Neurol.* **208**, 419-430.

MALIOSO, M.-L., MARQUEZE-POUEY, B., KUHSE, J. & BETZ, H. (1991). Widespread expression of glycine receptor subunit mRNAs in the adult and developing rat brain. *EMBO J.* **10**, 2401-2409.

MANSOUR, A., KHACHATURIAN, H., LEWIS, M.E., AKIL, H. & WATSON, S.J. (1988). Anatomy of CNS opioid receptors. [Review] [54 refs]. *Trends in Neurosciences* **11 (7)**, 308-314.

MANSOUR, A., FOX, C.A., BURKE, S., AKIL, H. & WATSON, S.J. (1995). Immunohistochemical localization of the cloned mu opioid receptor in the rat CNS. *J.Comp.Neuroanat.* **8**, 283-305.

MARGOLIS, F. (1972). A brain protein unique to the olfactory bulb. *Proc.natn Acad.Sci.U.S.A* **69**, 1221-1224.

MARGOLIS, F., KAWANO, T. & GRILLO, M. (1986). Ontogeny of carnosine, olfactory marker protein and neurotransmitter enzymes in the olfactory bulb and olfactory mucosa of the rat. In *Ontogeny of Olfaction*, ed. BREIPOHL, W., pp. 107-116. Berlin: Springer-Verlag.

MARGOLIS, F.L. (1974). Carnosine in the primary olfactory pathway. *Science* **184**, 909-911.

MARGOLIS, F.L., ROBERTS, N., FERRIERO, D. & FELDMAN, J. (1974). Denervation in the primary olfactory pathway of mice: biochemical and morphological effects. *Brain Res.* **81 (3)**, 469-483.

MARGOLIS, F.L. (1981). *Biochemistry of Taste and Olfaction.* New York: Acad. Press.

MASON, W.T. & LENG, G. (1984). Complex action potential waveform recorded from supraoptic and paraventricular neurones of the rat: Evidence for sodium and calcium spike components at different membrane sites. *Exp.Brain Res.* **56**, 135-143.

MATHEWS, D.F. (1972). Response patterns of single units in the olfactory bulb of the rat to odor. *Brain Res.* **47 (2)**, 389-400.

MATSUI, S. & YAMAMOTO, C. (1975). Release of radioactive glutamic acid from thin sections of guinea-pig olfactory cortex in vitro. *J.Neurochem.* **24 (2)**, 245-250.

MCBAIN, C.J. (1995). Hippocampal inhibitory neuron activity in the elevated potassium model of epilepsy [corrected and republished with original paging, article originally printed in J Neurophysiol 1994 Dec;72(6):2853-63]. *J.Neurophysiol.* **73 (2)**, 2853-2863.

MCLEAN, S., ROTHMAN, R.B. & HERKENHAM, M. (1986). Autoradiographic localization of mu- and delta-opiate receptors in the forebrain of the rat. *Brain Res.* **378 (1)**, 49-60.

MCLENNAN, H. (1971). The pharmacology of inhibition of mitral cells in the olfactory bulb. *Brain Res.* **29 (2)**, 177-184.

MEDDLE, S.L., SELVARAJAH, J.R., RUSSELL, J.A., BICKNELL, R.J. & LENG, G. (1998). Identification of a direct neuronal pathway from the olfactory bulb to the supraoptic nucleus that becomes activated at parturition in the rat. *J.Endocrinol.* **156 Suppl.**, P184

MEISAMI, E. (1976). Effects of olfactory deprivation on postnatal growth of the rat olfactory bulb utilizing a new method for production of neonatal anosmia. *Brain Res.* **107**, 437-444.

MODNEY, B.K., YANG, Q.Z. & HATTON, G.I. (1990). Activation of excitatory amino acid inputs to supraoptic neurons. II. Increased dye-coupling in maternally behaving virgin rats. *Brain Res.* **513 (2)**, 270-273.

MODNEY, B.K. & HATTON, G.I. (1994). Maternal behaviors: evidence that they feed back to alter brain morphology and function. [Review] [23 refs]. *Acta Paediatrica Supp.* **397**, 29-32.

MOMBAERTS, P., WANG, F., DULAC, C., CHAO, S.K., NEMES, A., MENDELSOHN, M., EDMONDSON, J. & AXEL, R. (1996). Visualizing an olfactory sensory map. *Cell* **87**, 675-686.

MOMBAERTS, P. (1999). Seven-transmembrane proteins as odorant and chemosensory receptors. *Science* **286**, 707-711.

MONTI, G.G. (1983). Experimental studies on the olfactory marker protein. III. The olfactory marker protein in the olfactory neuroepithelium lacking connections with the forebrain. *Brain Res* **262 (2)**, 303-308.

MORGAN, J.I. & CURRAN, T. (1989). Stimulus-transcription coupling in neurons: role of cellular immediate-early genes. *Trends Neurosci.* **12 (11)**, 459-462.

MORGAN, J.I. & CURRAN, T. (1991). Stimulus-transcription coupling in the nervous system: involvement of the inducible proto-oncogenes fos and jun. *Ann.Rev.Neurosci.* **14**, 421-451.

MORI, K. & TAKAGI, S.F. (1975). Spike generation in the mitral cell dendrite of the rabbit olfactory bulb. *Brain Res.* **100 (3)**, 685-689.

MORI, K. & TAKAGI, S.F. (1978). An intracellular study of dendrodendritic inhibitory synapses on mitral cells in the rabbit olfactory bulb. *J.Physiol.(Lond)* **279**, 569-588.

MORI, K. & SHEPHERD, G.M. (1979). Synaptic excitation and long-lasting inhibition of mitral cells in the in vitro turtle olfactory bulb. *Brain Res.* **172 (1)**, 155-159.

MORI, K., NOWYCKY, M.C. & SHEPHERD, G.M. (1981). Analysis of a long-duration inhibitory potential in mitral cells in the isolated turtle olfactory bulb. *J.Physiol.(Lond)* **314**, 311-320.

MORI, K., NOWYCKY, M.C. & SHEPHERD, G.M. (1981). Analysis of synaptic potentials in mitral cells in the isolated turtle olfactory bulb. *J.Physiol.(Lond)* **314**, 295-309.

MORI, K., NOWYCKY, M.C. & SHEPHERD, G.M. (1981). Electrophysiological analysis of mitral cells in the isolated turtle olfactory bulb. *J.Physiol.(Lond)* **314**, 281-294.

MORI, K. & KISHI, K. (1982). The morphology and physiology of the granule cells in the rabbit olfactory bulb revealed by intracellular recording and HRP injection. *Brain Res.* **247 (1)**, 129-133.

MORI, K., KISHI, K. & OJIMA, H. (1983). Distribution of dendrites of mitral, displaced mitral, and granule cells in the rabbit olfactory bulb. *J.comp.Neurol.* **226**, 339-355.

MORI, K. (1987). Membrane and synaptic properties of identified neurons in the olfactory bulb. *Prog.Neurobiol.* **29**, 274-320.

MORI, K., MATAGA, N. & IMAMURA, K. (1992). Differential specificities of single mitral cells in rabbit olfactory bulb for a homologous series of fatty acid odor molecules. *J.Neurophysiol.* **67**, 786-789.

MORI, K., NAGAO, H. & YOSHIHARA, Y. (1999). The olfactory bulb: Coding and processing of odour molecule information. *Science* **286**, 711-715.

MOTOKIZAWA, F. (1996). Odor representation and discrimination in mitral/tufted cells of the rat olfactory bulb. *Exp.Brain Res.* **112 (1)**, 24-34.

MOTOKIZAWA, F. & OGAWA, Y. (1997). Discharge properties of mitral/tufted cells in the olfactory bulb of cats. *Brain Res.* **763 (2)**, 285-287.

MOULY, A.M., ELAAGOUBY, A. & RAVEL, N. (1995). A study of the effects of noradrenaline in the rat olfactory bulb using evoked field potential response. *Brain Res.* **681 (1-2)**, 47-57.

MUNARO, N.I., DOTTI, C. & TALEISNIK, S. (1986). Glutamic acid decarboxylase activity in the hypothalamus of the rat: effect of estrogens. *Advances in Biochemical Psychopharmacology* **42**, 201-207.

MUNARO, N.I. (1990). Maternal behavior: glutamic acid decarboxylase activity in the olfactory bulb of the rat. *Pharmacol.Biochem.Behav.* **36 (1)**, 81-84.

NADI, N.S., HIRSCH, J.D. & MARGOLIS, F.L. (1980). Laminar distribution of putative neurotransmitter amino accids and ligand binding sites in the dog olfactory bulb. *J.Neurochem.* **34**, 138-146.

NAKAMURA, T. & GOLD, G.H. (1987). A cyclic nucleotide-gated conductance in olfactory receptor cilia. *Nature* **325**, 442-444.

NAKASHIMA, M., MORI, K. & TAKAGI, S.F. (1978). Centrifugal influence on olfactory bulb activity in the rabbit. *Brain Res.* **154 (2)**, 301-306.

NEGORO, H., VISESSUWAN, S. & HOLLAND, R.C. (1973). Unit activity in the paraventricular nucleus of female rats at different stages of the reproductive cycle and after ovariectomy, with or without oestrogen or progesterone treatment. *J.Endocrinology* **59**, 545-558.

NICKELL, W.T. & SHIPLEY, M.T. (1988). Neurophysiology of magnocellular forebrain inputs to the olfactory bulb in the rat: frequency potentiation of field potentials and inhibition of output neurons. *J.Neurosci.* **8 (12)**, 4492-4502.

NICKELL, W.T. & SHIPLEY, M.T. (1993). Evidence for presynaptic inhibition of the olfactory commissural pathway by cholinergic agonists and stimulation of the nucleus of the diagonal band. *J.Neurosci.* **13 (2)**, 650-659.

NICKELL, W.T., SHIPLEY, M.T. & BEHBEHANI, M.M. (1996). Orthodromic synaptic activation of rat olfactory bulb mitral cells in isolated slices. *Brain Res.Bull.* **39 (1)**, 57-62.

NICOLL, R.A. (1969). Inhibitory mechanisms in the rabbit olfactory bulb: dendrodendritic mechanisms. *Brain Res.* **14**, 157-172.

NICOLL, R.A. (1970). GABA and dendrdendritic inhibition in the olfactory bulb. *Pharmacologist* **12**, 236

NICOLL, R.A. (1971). Pharmacological evidence for GABA as the transmitter in granule cell inhibition in the olfactory bulb. *Brain Res.* **35 (1)**, 137-149.

NICOLL, R.A., ALGER, B.E. & JAHR, C.E. (1980). Peptides as putative excitatory neurotransmitters: carnosine, enkephalin, substance P and TRH. *Proc.R Soc.Lond B Biol.Sci.* **210**, 133-149.

NICOLL, R.A. & JAHR, C.E. (1982). Self-excitation of olfactory bulb neurones. *Nature* **296**, 441-444.

NOWYCKY, M.C., MORI, K. & SHEPHERD, G.M. (1981). GABAergic mechanisms of dendrodendritic synapses in isolated turtle olfactory bulb. *J.Neurophysiol.* **46 (3)**, 639-648.

NOWYCKY, M.C., MORI, K. & SHEPHERD, G.M. (1981). Blockade of synaptic inhibition reveals long-lasting synaptic excitation in isolated turtle olfactory bulb. *J.Neurophysiol.* **46 (3)**, 649-658.

NYE, H.E. & NESTLER, E.J. (1996). Induction of chronic Fos-related antigens in rat brain by chronic morphine administration. *Mol.Pharmacol.* **49**, 636-645.

OKUTANI, F., KABA, H., TAKAHASHI, S. & SETO, K. (1998). The biphasic effects of locus coeruleus noradrenergic activation on dendrodendritic inhibition in the rat olfactory bulb. *Brain Res.* **783 (2)**, 272-279.

ONODA, N. & MORI, K. (1980). Depth distribution of temporal firing patterns in olfactory bulb related to air-intake cycles. *J.Neurophysiol.* **44 (1)**, 29-39.

ORONA, E., SCOTT, J.W. & RAINER, E.C. (1983). Different granule cell populations innervate superficial and deep regions of the external plexiform layer in rat olfactory bulb. *J.comp.Neurol.* **217 (2)**, 227-237.

ORONA, E., RAINER, E.C. & SCOTT, J.W. (1984). Dendritic and axonal organization of mitral and tufted cells in the rat olfactory bulb. *J.comp.Neurol.* **226 (3)**, 346-356.

PACE, U., HANSKI, E., SALOMON, Y. & LANCET, D. (1985). Odorant-sensitive adenylate cyclase may mediate olfactory reception. *Nature* **316**, 255-258.

PANHUBER, H., LAING, D.G., WILLCOX, M.E., EAGLESON, G.K. & PITTMAN, E.A. (1985). The distribution of the size and number of mitral cells in the olfactory bulb of the rat. *J.Anat.* **140 (Pt 2)**, 297-308.

PATERNOSTRO, M.A., REYHER, C.K. & BRUNJES, P.C. (1995). Intracellular injections of lucifer yellow into lightly fixed mitral cells reveal neuronal dye-coupling in the developing rat olfactory bulb [published erratum appears in Brain Res Dev Brain Res 1995 Apr 18;85(2):303]. *Brain Res.Dev.Brain Res.* **84 (1)**, 1-10.

PAXINOS, G. & WATSON, C. (1997). *The Rat Brain in Stereotaxic Coordinates*. Academic Press.

PHILLIPS, C.G., POWELL, T.P. & SHEPHERD, G.M. (1963). Responses of mitral cells to stimulation of the lateral olfactory tract in the rabbit. *J.Physiol.* **168**, 65-88.

PHILLIPS, H.S., HOSTETTER, G., KERDELHUE, B. & KOZLOWSKI, G.P. (1980). Immunocytochemical olcalization of LHRH in central olfactory pathways of hamster. *Brain Res.* **193**, 574-579.

PHILPOT, B.D., FOSTER, T.C. & BRUNJES, P.C. (1997). Mitral/tufted cell activity is attenuated and becomes uncoupled from respiration following naris closure. *J.Neurobiol.* **33 (4)** , 374-386.

PHILPOT, B.D., LYDERS, E.M. & BRUNJES, P.C. (1998). The NMDA receptor participates in respiration-related mitral cell synchrony. *Exp.Brain Res.* **118 (2)**, 205-209.

PINCHING, A.J. & POWELL, T.P. (1971). The neuropil of the glomeruli of the olfactory bulb. *J.Cell Sci.* **9 (2)**, 347-377.

PINCHING, A.J. & POWELL, T.P. (1971). The neuron types of the glomerular layer of the olfactory bulb. *J.Cell Sci.* **9 (2)**, 305-345.

PINCHING, A.J. & POWELL, T.P. (1972). The termination of centrifugal fibres in the glomerular layer of the olfactory bulb. *J.Cell Sci.* **10 (3)**, 621-635.

POWELL, T.P.S. & COWAN, W.M. (1963). Centrifugal fibres in the lateral olfactory tract. *Nature* **199**, 1296-1297.

PRICE, J.L. (1968). The termination of centrifugal fibers in the olfactory bulb. *Brain Res.* 7, 483-486.

PRICE, J.L. & POWELL, T.P. (1970). The synaptology of the granule cells of the olfactory bulb. *J.Cell Sci.* **7 (1)**, 125-155.

PRICE, J.L. & POWELL, T.P. (1970). The morphology of the granule cells of the olfactory bulb. *J.Cell Sci.* **7 (1)**, 91-123.

PRICE, J.L. & POWELL, T.P. (1970). The mitral and short axon cells of the olfactory bulb. *J.Cell Sci.* **7 (3)**, 631-651.

RALL, W., SHEPHERD, G.M., REESE, T.S. & BRIGHTMAN, M.W. (1966). Dendrodendritic synaptic pathway for inhibition in the olfactory bulb. *Exp.Neurol.* **14 (1)**, 44-56.

RALL, W. & SHEPHERD, G.M. (1968). Theoretical reconstruction of field potentials and dendrodendritic synaptic interactions in olfactory bulb. *J.Neurophysiol.* **31 (6)**, 884-915.

RANDALL, A.D. & TSIEN, R.W. (1997). Contrasting biophysical and pharmacological properties of T-type and R- type calcium channels. *Neuropharmacology* **36 (7)**, 879-893.

REINHARDT, W., KONDA, N., MACLEOD, N. & ELLENDORFF, F. (1981). Electrophysiology of olfacto-limbic-hypothalamic connections in the pig. *Exp.Brain Res.* **43 (1)**, 1-10.

RIBAK, C.E., VAUGHN, J.E., SAITO, K., BARBER, R. & ROBERTS, E. (1977). Glutamate decarboxylase localization in neurons of the olfactory bulb. *Brain Res.* **126 (1)**, 1-18.

RIBAK, C.E., VAUGHN, J.E. & BARBER, R.P. (1981). Immunocytochemical localization of GABAergic neurones at the electron microscopical level. *Histochem.J.* **13 (4)**, 555-582.

ROBERTSON, L.M., KERPPOLA, T.K., VENDRELL, M., LUK, D., SMEYNE, R.J., BOCCHIARO, C., MORGAN, J.I. & CURRAN, T. (1995). Regulation of c-fos expression in

transgenic mice requires muliplt interdependent transcription control elements. *Neuron* **14**, 241-252.

RODIECK, R.W., KIANG, N.Y.S. & GERSTEIN, G.L. (1962). Some quantitative methods for the study of spontaneous activity of single neurones. *Biophysical J.* **2**, 351-368.

ROSPARS, J.P. & LANSKY, P. (1993). Stochastic model neuron without resetting of dendritic potential: application to the olfactory system. *Biol.Cybern.* **69 (4)**, 283-294.

ROSPARS, J.P., LANSKY, P., VAILLANT, J., DUCHAMP-VIRET, P. & DUCHAMP, A. (1994). Spontaneous activity of first- and second-order neurons in the frog olfactory system. *Brain Res.* **662 (1-2)**, 31-44.

ROSSER, A.E. & KEVERNE, E.B. (1985). The importance of central noradrenergic neurones in the formation of an olfactory memory in the prevention of pregnancy block. *Neuroscience* **15 (4)**, 1141-1147.

ROTTER, A., BIRDSALL, N.J.M., BURGEN, A.S.V., FIELD, P.M., HULME, E.C. & RAISMAN, G. (1977). Muscarinic receptors in the central nervous system of the rat. I. Technique for autoradiographic localisation of the binding of [3H] propylbenzilylcholine mustard and its distribution in the forebrain. *Brain Res.Rev.* **1**, 141-165.

RUSSELL, J.A., COOMBES, J.E., LENG, G. & BICKNELL, R.J. (1993). Morphine tolerance and inhibition of oxytoocin secetion by kappa-opioids acting on the rat neurohypophysis. *J.Physiol.* **469**, 365-386.

RUSSELL, J.A., LENG, G. & BICKNELL, R.J. (1995). Opioid tolerance and dependence in the magnocellular oxytocin system: a physiological mechanism?. [Review]. *Exp.Physiol.* **80 (3)**, 307-340.

SAGAR, S.M., SHARP, F.R. & CURRAN, T. (1988). Expression of c-fos protein in brain: metabolic mapping at the cellular level. *Science* **240**, 1328-1331.

SASSOE-POGNETTO, M., CANTINO, D., PANZANELLI, P., VERDUN, d.C., GIUSTETTO, M., MARGOLIS, F.L., DE BIASI, S. & FASOLO, A. (1993). Presynaptic co-localization of carnosine and glutamate in olfactory neurones. *Neuroreport* **5 (1)**, 7-10.

SASSONE-CORSI, P., SISSON, J.C. & VERMA, I.M. (1988). Transcriptional autoregulation of the proto-oncogene fos. *Nature* **334**, 314-319.

SCALIA, F. & WINANS, S.S. (1975). The differential projections of the olfactory bulb and accessory olfactory bulb in mammals. *J.comp.Neurol.* **161 (1)**, 31-55.

SCHNEIDER, S.P. & MACRIDES, F. (1978). Laminar distributions of interneurons in the main olfactory bulb of the adult hamster. *Brain Res.Bull.* **3**, 73-82.

SCHNEIDER, S.P. & SCOTT, J.W. (1983). Orthodromic response properties of rat olfactory bulb mitral and tufted cells correlate with their projection patterns. *J.Neurophysiol.* **50 (2)**, 358-378.

SCHOPPA, N.E., KINZIE, J.M., SAHARA, Y., SERGERSON, T.P. & WESTBROOK, G.L. (1998). Dendrodendritic inhibition in the olfactory bulb is driven by NMDA receptors. *J.Neurosci.* **18**, 6790-6802.

SCHULZ, S., SCHREFF, M., KOCH, T., ZIMPRICH, A., GRAMSCH, C., ELDE, R. & HOLLT, V. (1998). Immunolocalization of two mu-opioid receptor isoforms (MOR1 and MOR1B) in the rat central nervous system. *Neuroscience* **82 (2)**, 613-622.

SCHWARTZKROIN, P.A. & SLAWSKY, M. (1977). Probable calcium spikes in hippocampal neurones. *Brain Res.* **135**, 157-161.

SCOTT, J.W. & AARON, D.D. (1977). Averaged induced waves in the olfactory bulb of the rat during odor stimulation. *Exp.Neurol.* **55 (Pt 3)**, 654-665.

SCOTT, J.W., MCBRIDE, R.L. & SCHNEIDER, S.P. (1980). The organization of projections from the olfactory bulb to the piriform cortex and olfactory tubercle in the rat. *J.comp.Neurol.* **194 (3)**, 519-534.

SCOTT, J.W. (1981). Electrophysiological identification of mitral and tufted cells and distributions of their axons in olfactory system of the rat. *J.Neurophysiol.* **46 (5)**, 918-931.

SCOTT, J.W., RANIER, E.C., PEMBERTON, J.L., ORONA, E. & MOURADIAN, L.E. (1985). Pattern of rat olfactory bulb mitral and tufted cell connections to the anterior olfactory nucleus pars externa. *J.comp.Neurol.* **242 (3)**, 415-424.

SENUT, M.C., MENETREY, D. & LAMOUR, Y. (1989). Cholinergic and peptide projections from the medial septum and the nucleus of the diagonal band of Broca to dorsal hippocampus, cingulate cortex and olfactory bulb: A combined wheatgerm agglutinin-apohorseradish peroxidase-gold immunohistochemical study. *Neurosci.* **30**, 385-403.

SHARP, F.R., KAUER, J.S. & SHEPHERD, G.M. (1975). Local sites of activity-related glucose metabolism in rat olfactory bulb during olfactory stimulation. *Brain Res.* **98 (3)**, 596-600.

SHARP, F.R., KAUER, J.S. & SHEPHERD, G.M. (1977). Laminar analysis of 2-deoxyglucose uptake in olfactory bulb and olfactory cortex of rabbit and rat. *J.Neurophysiol.* **40 (4)**, 800-813.

SHARP, F.R., SAGAR, S.M., HICKS, K., LOWENSTEIN, D. & HISANAGA, K. (1991). c-fos mRNA, Fos and Fos-related antigen induction by hypertonic saline and stress. *J.Neurosci.* **11**, 2321-2331.

SHEN, G.Y., CHEN, W.R., MIDTGAARD, J., SHEPHERD, G.M. & HINES, M.L. (1999). Computational analysis of action potential initiation in mitral cell soma and dendrites based on dual patch recordings. *J.Neurophysiol.* **82 (6)**, 3006-3020.

SHENG, M., MCFADDEN, G. & GREENBERG, M.E. (1990). Membrane depolarisation and calciun induce c-fos transcription vai phosphorylation of transcription factort CREB. *Neuron* **4**, 571-582.

SHEPHERD, G.M. (1963). Responses of mitral cells to olfactory nerve volleys in the rabbit. *J.Physiol.* **168**, 89-100.

SHEPHERD, G.M. (1963). Neuronal systems controlling mitral cell excitability. *J.Physiol.* **168**, 101-117.

SHEPHERD, G.M. (1971). Physiological evidence for dendrodendritic synaptic interactions in the rabbits olfactory glomerulus. *Brain Res.* **32**, 212-217.

SHEPHERD, G.M. (1972). Synaptic organization of the mammalian olfactory bulb. *Physiol.Rev.* **52 (4)** , 864-917.

SHEPHERD, G.M. & BRAYTON, R.K. (1979). Computer simulation of a dendrodendritic synaptic circuit for self- and lateral-inhibition in the olfactory bulb. *Brain Res.* **175 (2)**, 377-382.

SHEPHERD, G.M. & GREER, C.A. (1998). *The synaptic organisation of the brain.* Oxford University Press.

SHIPLEY, M.T., HALLORAN, F.J. & DE LA TORRE, J. (1985). Surprisingly rich projection from locus coeruleus to the olfactory bulb in the rat. *Brain Res.* **329 (1-2)**, 294-299.

SHIPLEY, M.T. & ENNIS, M. (1996). Functional organization of olfactory system. *J.Neurobiol.* **30 (1)**, 123-176.

SHU, S., JU, G. & FAN, L. (1988). The glucose oxidase-DAB-nickel method in peroxidase histochemistry of the nervous system. *Neurosci.Lett.* **85**, 169-171.

SHUTE, C.C. & LEWIS, P.R. (1967). The ascending cholinergic reticular system: neocortical, olfactory and subcortical projections. *Brain* **90 (3)**, 497-520.

SINGER, M.S., SHEPHERD, G.M. & GREER, C.A. (1995). Olfactory receptors guide axons [letter]. *Nature* **377**, 19-20.

SKLAR, P.B., ANHOLT, R.R. & SNYDER, S.H. (1986). The odorant-sensitive adenylate cyclase of olfactory receptor cells. Differential stimulation by distinct classes of odorants. *J.Biol.Chem.* **261 (33)**, 15538-15543.

SMART, D., SMITH, G. & LAMBERT, D.G. (1995). Mu-opioids activate phospholipase C in SH-SY5Y human neuroblastoma cells via calcium-channel opening. *Biochem.J.* **305**, 577-581.

SMITHSON, K.G., WEISS, M.L. & HATTON, G.I. (1989). Supraoptic nucleus afferents from the main olfactory bulb--I. Anatomical evidence from anterograde and retrograde tracers in rat. *Neuroscience* **31 (2)**, 277-287.

SMITHSON, K.G., WEISS, M.L. & HATTON, G.I. (1992). Supraoptic nucleus afferents from the accessory olfactory bulb: evidence from anterograde and retrograde tract tracing in the rat. *Brain Res.Bull.* **29 (2)**, 209-220.

SPENCER, W.A. & KANDEL, E.R. (1961). Electrophysiology of hippocampal neurons IV. Fast prepotentials. *J.Neurophysiol.* **24**, 272-285.

STERNBERGER, L.A. (1986). *The unlabeled antibody peroxidase-antiperoxidase (PAP) method.* John Wiley & Sons.

STEWART, W.B. & SCOTT, J.W. (1976). Anesthetic-dependent field potential interactions in the olfactory bulb. *Brain Res.* **103 (3)**, 487-499.

STEWART, W.B., KAUER, J.S. & SHEPHERD, G.M. (1979). Functional organization of rat olfactory bulb analysed by the 2- deoxyglucose method. *J.comp.Neurol.* **185 (4)**, 715-734.

STORM, J.F. (1988). Temporal integration by a slowly inactivating K+ current in hippocampal neurons. *Nature* **336**, 379-381.

STRUBLE, R.G. & WALTERS, C.P. (1982). Light microscope differentiation of two populations of rat olfactory bulb granule cells. *Brain Res.* **236 (2)**, 237-251.

STUART, G., SPRUSTON, N., SAKMANN, B. & HAUSSER, M. (1997). Action potential initiation and backpropagation in neurons of the mammalian CNS. *Trends Neurosci.* **20 (3)**, 125-131.

STUART, G.J. & SAKMANN, B. (1994). Active propagation of somatic action potentials into neocortical pyramidal cell dendrites. *Nature* **367**, 69-72.

SUMMERLEE, A.S. (1981). Extracellular recordings from oxytocin neurones during the expulsive phase of birth in unanaesthetized rats. *J.Physiol.(Lond)* **321**, 1-9.

SUMNER, B.E., COOMBES, J.E., PUMFORD, K.M. & RUSSELL, J.A. (1990). Opioid receptor subtypes in the supraoptic nucleus and posterior pituitary gland of morphine-tolerant rats. *Neurosci.* **37**, 635-645.

SWAAB, D.F., NIJVELDT, F. & POOL, C.W. (1975). Distribution of oxytocin and vasopressin in the rat suproptic and paraventricular nucleus. *J.Endocrinol.* **67**, 461-462.

SWANSON, L.W. & KUYPERS, H.G. (1980). The paraventricular nucleus of the hypothalamus: cytoarchitectonic subdivisions and organisation of projections to the pituitary, dorsal vagal complex and spinal cord as demonstrated by retrograde fluorescence double-labeling methods. *J.comp.Neurol.* **194**, 555-570.

TAKAYAMA, K., SUZUKI, T. & MIURA, M. (1994). The comparison of effects of various anesthetics on expression of Fos protein in the rat brain. *Neurosci.Lett.* **176**, 59-62.

TEICHER, M.H., STEWART, W.B., KAUER, J.S. & SHEPHERD, G.M. (1980). Suckling pheromone stimulation of a modified glomerular region in the developing rat olfactory bulb revealed by the 2-deoxyglucose method. *Brain Res.* **194 (2)**, 530-535.

TONOSAKI, K. & SHIBUYA, T. (1979). Action of some drugs on gecko olfactory bulb mitral cell responses to odor stimulation. *Brain Res.* **167**, 180-184.

TRELOAR, H., WALTERS, E., MARGOLIS, F. & KEY, B. (1996). Olfactory glomeruli are innervated by more than one distinct subset of primary sensory olfactory neurons in mice. *J.comp.Neurol.* **367 (4)**, 550-562.

TROMBLEY, P.Q. (1992). Norepinephrine inhibits calcium currents and EPSPs via a G-protein-coupled mechanism in olfactory bulb neurons. *J.Neurosci.* **12 (10)**, 3992-3998.

TROMBLEY, P.Q. & SHEPHERD, G.M. (1993). Synaptic transmission and modulation in the olfactory bulb. *Curr.Opin.Neurobiol.* **3 (4)**, 540-547.

TROMBLEY, P.Q. & SHEPHERD, G.M. (1994). Glycine exerts potent inhibitory actions on mammalian olfactory bulb neurons. *J.Neurophysiol.* **71 (2)**, 761-767.

TURNER, R.W., MEYERS, D.E., RICHARDSON, T.L. & BARKER, J.L. (1991). The site for initiation of action potential discharge over the somatodendritic axis of rat hippocampal CA1 pyramidal neurons. *J.Neurosci.* **11 (7)**, 2270-2280.

VAN DEN POL, A.N. & GORCS, T. (1988). Glycine and glycine receptor immunoreactivity in brain and spinal cord. *J.Neurosci.* **8 (2)**, 472-492.

VAN DEN POL, A.N. (1995). Presynaptic metabotropic glutamate receptors in adult and developing neurons: autoexcitation in the olfactory bulb. *J.comp.Neurol.* **359 (2)**, 253-271.

VON BAUMGARTEN, R., GREEN, J.D. & MANCIA, M. (1962). Recurrent inhibition in the olfactory bulb II. Effects of antidromicstimulation of commisural fibers. *J.Nerophysiol.* **25**, 489-500.

WALDOW, U., NOWYCKY, M.C. & SHEPHERD, G.M. (1981). Evoked potential and single unit responses to olfactory nerve volleys in the isolated turtle olfactory bulb. *Brain Res.* **211 (2)**, 267-283.

WANG, F., NEMES, A., MENDELSOHN, M. & AXEL, R. (1998). Odorant receptors govern the formation of a precise topographic map. *Cell* **93 (1)**, 47-60.

WANG, X., MCKENZIE, J.S. & KEMM, R.E. (1996). Whole cell calcium currents in acutely isolated olfactory bulb output neurons of the rat. *J.Neurophysiol.* **75 (3)**, 1138-1151.

WANG, X.J. (1993). Ionic basis for intrinsic 40 Hz neuronal oscillations [published erratum appears in Neuroreport 1994 Jan 12;5(4):531]. *Neuroreport* **5 (3)**, 221-224.

WANG, X.Y., MCKENZIE, J.S. & KEMM, R.E. (1996). Whole-cell K+ currents in identified olfactory bulb output neurones of rats. *J.Physiol.(Lond)* **490 (Pt 1)**, 63-77.

WATANABE, M., INOUE, Y., SAKIMURA, K. & MISHINA, M. (1993). Distinct distributions of five N-methyl-D-aspartate receptor channel subunit mRNAs in the forebrain. *J.comp.Neurol.* **338**, 377-390.

WELLIS, D.P. & SCOTT, J.W. (1987). Intracellular recordings of odor-induced responses in the rat olfactory bulb. *Chem.Senses* **12**, 707

WELLIS, D.P., SCOTT, J.W. & HARRISON, T.A. (1989). Discrimination among odorants by single neurons of the rat olfactory bulb. *J.Neurophysiol.* **61 (6)**, 1161-1177.

WELLIS, D.P. & SCOTT, J.W. (1990). Intracellular responses of identified rat olfactory bulb interneurons to electrical and odor stimulation. *J.Neurophysiol.* **64 (3)**, 932-947.

WENK, H., MEYER, U. & BIGL, V. (1977). Centrifugal cholinergic connections in the olfactory system of rats. *Neuroscience* **2 (5)**, 797-800.

WESTECKER, M.E. (1969). The time course of facilitation and inhibition in the olfactory bulb, investigated with double pulse stimulation of the lateral olfactory tract. *Brain Res.* **16 (2)**, 527-529.

WHITE, J., HAMILTON, K.A., NEFF, S.R. & KAUER, J.S. (1992). Emergent properties of odor information coding in a representational model of the salamander olfactory bulb. *J.Neurosci.* **12**, 1772-1780.

WILSON, D.A. & LEON, M. (1987). Evidence of lateral synaptic interactions in olfactory bulb output cell responses to odors. *Brain Res.* **417 (1)**, 175-180.

WILSON, D.A., SULLIVAN, R.M., GALL, C.M. & GUTHRIE, K.M. (1996). NMDA-receptor modulation of lateral inhibition and c-fos expression in olfactory bulb. *Brain Res.* **719 (1-2)**, 62-71.

WILSON, D.A. (1998). Habituation of odor responses in the rat anterior piriform cortex. *J.Neurophysiol.* **79 (3)**, 1425-1440.

WILSON, T. & TREISMAN, R. (1988). Fos C-terminal mutations block down-regulation of c-fos transcription following serum stimulation. *EMBO J.* **7**, 4193-4202.

WISDEN, W., ERRINGTON, M.L., WILLIAMS, S., DUNNET, S.B., WATERS, C., HITCHCOCK, D., EVANS, G., BLISS, T.V.P. & HUNT, S.P. (1990). Differential expression of immediate-early genes in the hippocampus and spinal cord. *Neuron* **4**, 603-614.

XIONG, J.-J. & HATTON, G.I. (1996). Differential responses of oxytocin and vasopressin neurones to the osmotic and stressful components of hypertonic saline injections: A Fos protein double labeling study. *Brain Res.* **719**, 143-153.

YAMAMOTO, C., YAMAMOTO, T. & IWAMA, K. (1963). The inhibitory systems in the olfactory bulb studied by intracellular recording. *J.Neurophysiol.* **26**, 403-415.

YAMAMOTO, C. & MATSUI, S. (1976). Effect of stimulation of excitatory nerve tract on release of glutamic acid from olfactory cortex slices *in vitro*. *J.Neurochem.* **26**, 487-491.

YANG, Q.Z., SMITHSON, K.G. & HATTON, G.I. (1995). NMDA and non-NMDA receptors on rat supraoptic nucleus neurons activated monosynaptically by olfactory afferents. *Brain Res.* **680 (1-2)**, 207-216.

YOKOI, M., MORI, K. & NAKANISHI, S. (1995). Refinement of odor molecule tuning by dendrodendritic synaptic inhibition in the olfactory bulb. *Proc.Natl.Acad.Sci.U.S.A* **92 (8)**, 3371-3375.

YOUNG, T.A. & WILSON, D.A. (1999). Frequency-dependent modulation of inhibition in the rat olfactory bulb. *Neurosci.Lett.* **276 (1)**, 65-67.

YU, G.Z., KABA, H., SAITO, H. & SETO, K. (1993). Heterogeneous characteristics of mitral cells in the rat olfactory bulb. *Brain Res.Bull.* **31 (6)**, 701-706.

YU, G.Z., KABA, H., OKUTANI, F., TAKAHASHI, S., HIGUCHI, T. & SETO, K. (1996). The action of oxytocin originating in the hypothalamic paraventricular nucleus on mitral and granule cells in the rat main olfactory bulb. *Neuroscience* **72 (4)**, 1073-1082.

ZHAO, B.G., CHAPMAN, C. & BICKNELL, R.J. (1988). Functional kappa-opioid receptors on oxytocin and vasopressin nerve terminals isolated from the rat neurohypophysis. *Brain Res.* **462**, 62-66.

ZIMPRICH, A., SIMON, T. & HOLLT, V. (1995). Transfected rat mu opioid receptors (rMOR1 and rMOR1B) stimulate phospholipase C and Ca2+ mobilization. *Neuroreport* **7**, 54-56.

ZIMPRICH, A., SIMON, T. & HOLLT, V. (1995). Cloning and expression of an isoform of the rat mu opioid receptor (rMOR1B) which differs in agonist induced desensitization from rMOR1. *Fedn.Eur.Biochem.Socs.Lett.* **359**, 142-146.